The Dissertation Committee for Shannan Lee Rossi Certifies that this is the approved version of the following dissertation:

Identification and Characterization of Cell-Adapted Mutations in West Nile Virus and Replicons

Committee:

Peter W. Mason, Ph.D., Supervisor

Scott Weaver, Ph.D.

Robert Tesh, M.D.

Ilya Frolov, Ph.D.

Charles Rice, Ph.D.

_____

Dean, Graduate School

Identification and Characterization of Cell-Adapted Mutations in West Nile Virus and Replicons

by

Shannan Lee Rossi, B.S.

Dissertation

Presented to the Faculty of the Graduate School of

The University of Texas Medical Branch

in Partial Fulfillment

of the Requirements

for the Degree of

Doctor of Philosophy

The University of Texas Medical Branch

May, 2008

Dedication

I dedicate this work to all those people who made me who I am.

Many people have entered into my life during my time here at UTMB. Some have also left. The one who has stayed through it all, the joy and the tears, is you Stacy. You've become part of my family and where always there, no matter how critical or silly the reason. I feel blessed to find a friend like you. Mom and Dad think so too! I'd like to thank my parents and grandparents who gave me the support to start, continue and finish graduate school. You have always encouraged me to achieve all that I can with grace and integrity. You have taught me that a strong work ethic, determination and sacrifice are necessary to attain my dreams and that adversity and challenge only make me a stronger individual. I could not have made it this far without your love and encouragement. For all the aforementioned reasons, I am forever grateful to you all. To John and Jenn, I say thank for you making me laugh and keeping me grounded. When I needed to take my mind off science, you were always there with a joke or available for a trip down memory lane.

Nik. You are my rock. Your strength gave me the motivation to continue and the determination to finish. More importantly, you allowed me to be myself and reminded me that just because my time was consumed by science didn't mean my life needed to be.

Grandma, I know you're always with me. I dedicate my dissertation to you.

Acknowledgements

I would like to acknowledge all the people who helped make this work possible.

All of the past and present members of the Mason lab have contributed to this work, either directly by helping with experiments or indirectly by supporting me with a joke or a smile. I especially thank the co-authors of my manuscripts, Qizu Zhao, Vivian O'Donnell, Rafik Fayzulin, Nathan Dewsbury and Nigel Bourne. You helped me design and conduct the experiments and proofread the manuscripts. Felicia and Doug, you helped make the time happier and pass a little quicker in between incubations.

I would also like to recognize members of the graduate school, namely Dorian Coppenhaver, Norbert Herzog, Kley Hughes and Steve Higgs, who were always there to listen. Graduate school would not have been the same if not for your guidance.

And finally to my mentor, Peter, for your patience and perseverance. I appreciate how difficult it is to train a young scientist and the effort has not gone unnoticed.

Several training grants have provided the funding that supported my research. I was supported from the NIH T32 training grants from FY2004 (AI 7526) and FY2005 (AI 060549-01) and the McLaughlin Endowment Fund Grant from FY 2006 and 2007.

Identification and Characterization of Cell-Adapted Mutations in West Nile Virus and Replicons

Publication No._____

Shannan L. Rossi, Ph.D.

The University of Texas Medical Branch, 2007

Supervisor: Peter W. Mason

Flavivirus persistence in cell culture is achieved by altering the interaction between the viral genome and the host cell. To identify some of the factors that contribute to a persistent West Nile virus (WNV) infection, WNV subgenomic replicon (WNR) genomes were modified to contain neomycin phosphotransferase (antibiotic-resistance) gene and cells that persistently harbored this WNR were selected for using G418. There were many changes to the genomes harvested from WNR-bearing cell cultures compared to the parental genome, perhaps the most striking was the prevalence of NS2A mutations. WNR and WNV genomes harboring these mutations replicated more poorly than wt WNR or WNV genomes *in vitro*. These NS2A mutant genomes, as well as a genome with a large deletion in the 3' UTR, were highly attenuated Swiss-Webster outbred mice. Low levels of IFN were produced from cells infected with NS2A or 3' UTR deletion WNR genomes compared to wt WNR genomes. Since the WNR and WNV cannot efficiently replicate, little stress is placed on the cell during replication, resulting in minimal engagement of the cell's stress and apoptotic responses and a noncytopathic

infection. As a result, little cytopathic effect and apoptotic death were observed in cells infected with NS2A or 3' UTR deletion WNR mutants compared to cells infected with wt WNR genomes. This lack of death may have been attributed to low levels of CHOP, a pro-apoptotic protein that is induced during endoplasmic reticulum stress. Taken together, these data support the hypothesis that WNR and WNV genomes that replicate poorly do not efficiently produce signs of their replication that can be recognized by the cell and place little stress upon the cell, resulting in an attenuated noncytopathic, persistent infection.

Table of Contents

List of Tables xv

List of Figures xvi

CHAPTER 1: INTRODUCTION **1**

Family Flaviviridae 1

Genus Hepacivirus 2

Genus Pestivirus 3

Genus Flavivirus 4

Genome structure 5

Functions of flavivirus proteins 8

The structural proteins and virion properties 8

The nonstructural proteins 11

Flavivirus intracellular life cycle 14

Arbovirus-Host Cell Interactions: Innate Immunity 16

Insect and insect cells 17

Mammalian cells 19

West Nile Virus History 22

It all started in 1937 22

WNV outbreaks 23

Taxonomy 26

West Nile Virus Transmission 29

Natural modes of transmission 29

Mosquito transmission 30

Non-vectored transmission 33

Artificial modes of transmission 34

West Nile Virus Pathogenesis 35
Avians 36
Rodents 37
Mice 37
Hamsters 39
Non-human primates 39
Humans 40
West Nile Virus Persistence 41
Impetus for this Research 44
CHAPTER 2: GENERATION AND CHARACTERIZATION OF REPLICON-BEARING CELLS **46**
Abstract 46
Introduction 47
Replicon cDNA clones 47
WNV replicon-bearing cell lines 48
Genome adaptation to cells in culture 49
Rationale 51
Materials and Methods 51
Construction of the West Nile virus replicon genome 51
Cell lines used and their maintenance 52
Identifying cell-adapted mutations 53
Engineering selected cell-adapted mutations into the parental WNR 54
Large-scale plasmid preparations by cesium chloride gradients 56
In vitro transcription of WNR RNA 57
Electroporation of cells 57
Testing Colony Formation Efficiency (CFE) 58
Generating replicon-bering cells 59
Immunohistochemistry 60

Results 60
Some cell types are permissive to persistent WNR genome replication 61
WNR phenotype in replicon-bearing cells 62
The WNR genome selected during generation of WNR-bearing cell lines 64
Replicon genomes from antibiotic-resistant replicon-bearing cell clones encode a variety mutations 65
Specific NS2A and NS3 mutations increase the ability of replicons to persistently infect Huh7 cells 67
NS2A mutant WNR produce low levels of WNV antigen 69
Discussion 70
CHAPTER 3: GENOMES ENCODING CELL-ADAPTED MUTATIONS ARE ATTENUATED *IN VITRO* **78**
Abstract 78
Introduction 79
Full-length infectious cDNA clones 79
Virus-like particles 80
VLP packaging cell lines 82
Rationale 83
Materials and Methods 83
Generating mutant WNR and WNV cDNA clones 83
Generating virus-like particles (VLPs) 84
Focus-formation assay 84
Flow cytometry to detect eGFP fluorescence in VLP-infected Cells 84
Construction of the West Nile virus full-lentgh infectious clone genome 85
Generating virus stocks 86
Sequencing virus pools 87
VLP and virus titrations 87

Results 88
Cell-adapted mutations reduce genome replication 88
Viruses encoding cell-adapted mutations replicate poorly *in vitro* 91
Discussion 94
CHAPTER 4: WNV ENCODING CELL-ADAPTED MUTATIONS ARE ATTENUATED IN MICE **98**
Abstract 98
Introduction 98
Rationale 100
Materials and Methods 101
Determining of 50% lethal dose in adult mice 101
Neutralization (PRNT80) assay 102
Quantifying viremia in WNV-infected adult mice 102
Determining neurovirulence in suckling mice 103
Sequencing viruses from moribund/dead adult mice 103
Sequencing brain homogenates from adult mice 103
Sequencing brain homogenates from suckling mice 105
Results 106
Viruses encoding cell-adapted mutations are attenuated *in vivo* 106
NS2A D73H WNV reversion to the wt genotype resulted in mouse mortality 113
NS2A D73H is neurovirulent in suckling mice 115
NS2A D73H WNV produces a low level viremia in mice 117

Discussion 118

CHAPTER 5: CELLS EXPRESSING ATTENUATED REPLICONS PRODUCE LOW LEVELS OF IFN AND AVOID APOPTOSIS 123

Abstract 123

Introduction 124

Flaviviruses and the innate immune response 124

ER stress 125

Apoptosis 127

The relationship between ER stress and apoptosis 129

Flavivirus infection induces ER stress and apoptosis 131

Rationale 132

Immunofluorescence assay (IFA) 132

Acquiring images 133

IFN bioassay 133

Detection of IFN activity in WNV-infected adult mice 134

Generation of VLP^{HS} 135

Determining IFN produced from VLP^{HS}-infected cells 135

VLP sensitivity to IFN pretreatment 136

Measuring cell viability (MTT Assay) 136

Detecting apoptotic cells by TUNEL assay 137

Western blots 138

Statistical analyses 139

Mice infected with NS2A D73H WNV produced less IFN than mice infected with wt WNV 140

Wt VLP^{HS} induce more IFN than mutant VLP^{HS} 141

Mutant and wt VLP^{HS} are equally sensitive to IFN 143

Replicons with cell-adapted mutations cause little CPE 144

Cells infected with wt VLP^{HS} undergo apoptosis 146

CHOP is induced in wt VLP^{HS}-infected cells 148

Discussion 150

CHAPTER 6: CONCLUSIONS AND FUTURE DIRECTIONS **154**

Summary 154

A model of WNV persistence..... 156

Implications and discussion..... 157

REFERENCES **163**

APPENDIX **193**

Abbreviations 193

Glossary 196

VITA **198**

List of Tables

Table 1: Colony formation efficiency of wt WNR in multiple cell types.....62
Table 2: Colony formation efficiency of mutant WNR genomes in Huh7 cells.....68
Table 3: RTPCR primers used to amplify WNV harvested from moribund mouse brain.....105
Table 4: LD_{50} values for mutant and wt WNVs in Swiss-Webster adult mice.....111
Table 5: Anti-WNV PRNT80 titers from mice that survived infection with mutant and wt WNV at 100 and 1000 ffu doses.....112
Table 6: Summary of the genotype of viruses extracted from moribund/dead mouse brains infected with 100 ffu of virus.....114
Table 7: List of sequencing primers used.....197

List of Figures

Figure 1: Flavivirus genome structure 6
Figure 2: WNV virion structure..... 10
Figure 3: Intracellular flavivirus life cycle..... 15
Figure 4: The intracellular innate immune response in mammalian cells 21
Figure 5: Location of WNV outbreaks 24
Figure 6: Phylogenetic tree of WNV lineages..... 28
Figure 7: Transmission cycle of WNV 30
Figure 8: Replicon and Full Length Infectious cDNA Construction..... 52
Figure 9: Diagram of how CFE was determined..... 58
Figure 10: Phenotype of the WNR within WNR-bearing BHK cells..... 63
Figure 11: Position of mutations identified in WNR-bearing cells 65
Figure 12: Cell-adapted NS2A mutations are present in the WNR genomes in replicon-bearing cells 67
Figure 13: IHC staining of WNR-transfected Huh7 cells..... 70
Figure 14: Model of the NS2A protein within the ER membrane..... 75
Figure 15: eGFP fluorescence from transient VLP-infected Vero cells 90
Figure 16: WNV antigen-positive foci..... 92
Figure 17: Wt and NS2A mutant WNV growth curves..... 93
Figure 18: Survival curve of adult Swiss-Webster mice infected with 1 ffu of mutant and wt WNV 107
Figure 19: Survival curve of adult Swiss-Webster mice infected with 10 ffu of mutant and wt WNV 108
Figure 20: Survival curve of adult Swiss-Webster mice infected with 100 ffu of mutant and wt WNV 109
Figure 21: Survival curve of adult Swiss-Webster mice infected with 1000 ffu of mutant and wt WNV 110
Figure 22: Survival Curve for Suckling Mice: NS2A D73H WNV vs. wt WNV..... 116
Figure 23: Viremia detected in NS2A D73H- and wt WNV-infected mice 117
Figure 24: IFN levels in NS2A D73H and wt WNV-infected mice..... 141
Figure 25: IFN produced from VLP^{HS}-infected cell lines..... 142
Figure 26: VLP^{HS} sensitivity to IFNβ pretreatment..... 144
Figure 27: Cells infected with cell-adapted VLPs cause little CPE 145
Figure 28: Wt VLP^{HS} infection induces apoptosis..... 147
Figure 29: Western blot detecting CHOP induction..... 148
Figure 30: Wt VLP^{HS} induces CHOP expression 150
Figure 31: Overview of the mechanism of persistence in replication-deficient WNV infection..... 157
Figure 32: Replicon Genomes 196

CHAPTER 1: INTRODUCTION[1]

Many viruses within the genus *Flavivirus* cause significant morbidity and mortality to vertebrates every year. These viruses have been the subjects of intense study for more than one hundred years. To combat the diseases caused by several of these viruses, countermeasures such as vaccines have been successfully created and are available for human use. However, diseases caused by other viruses in this family are still a threat for millions of people worldwide. Due to their widespread geographic distribution and medical importance, these viruses are likely to be the subjects of intensive research for decades to come.

Family Flaviviridae

The Flaviviridae family contains over 70 viruses that are responsible for a broad spectrum of symptoms including malaise, hemorrhage, fever, encephalitis, arthritis, liver necrosis and cancer, and infect a wide range of vertebrate and invertebrate hosts (Lindenbach and Rice, 2001). Despite their differences, these viruses share a similar genome organization. These viruses have a single-stranded RNA (ssRNA) genome of positive-sense polarity. The 5' end of the genome is either capped (a post-transcriptional modification that is required for translation) or folds into a conformational (tertiary) structure to function as an internal ribosome entry site (IRES). Unlike many other positive-stranded RNA viruses, members of the Flaviviridae family do not have 3' polyadenylated tails. There is one open reading frame (ORF) within the RNA genome from which a polyprotein is translated. This polyprotein is cleaved by viral and cellular proteases into the individual viral proteins. The spherical virions produced during infection are 30-80 nm in diameter and contain a lipid bilayer that originates from the

[1]Portions of this chapter have been published in Figure Virology. This journal grants copyright permission as long as proper citation is given: **Rossi, S.L.** and Mason, P.M. Persistent Infections of Mammals and Mammalian Cell Cultures with West Nile Virus. Future Virology, 3(1): 25-34.

host cell. Three genera comprise this family: *Hepacivirus*, *Pestivirus* and *Flavivirus*. The members within these families are categorized based on genome, antigen and nucleotide similarity.

GENUS HEPACIVIRUS

Hepatitis C virus (HCV) is the only member of the *Hepacivirus* genus (Lindenbach and Rice, 2001). HCV causes human disease and is most commonly transmitted person-to-person via infected bodily fluids (Major, Rehermann, and Feinstone, 2001). It is estimated that 2.2% of the world's population is infected with HCV (2004), and the majority of these infections are persistent. Many persistently infected patients will develop chronic hepatitis, which could lead to more severe outcomes including cirrhosis and cancer (Lindenbach and Rice, 2001). Despite the precautionary measures taken such as screening blood and organ donations, and the availability of antiviral drugs like interferon (IFN) and ribavirin, HCV continues to be a problem (Cornberg and Manna, 2006). Moreover, there is a large economic burden associated with caring for and treating HCV-infected patients (Shah and Wong, 2006).

The HCV genome is approximately 9.6 kilobases in length. The ORF is flanked on both ends by non-coding or untranslated regions (UTR). The 5' UTR functions as an IRES and allows the open-reading frame to be translated in the absence of a cap molecule (Lindenbach and Rice, 2001). Ten viral proteins are translated from the genome. The structural proteins, C, E1 and E2, form the virion. Nonstructural (NS) proteins include p7, NS2, NS3, NS4A, NS4B, NS5A and NS5B (Lindenbach and Rice, 2001). The NS proteins act as viral protease, helicase and polymerase, but the functions of many NS proteins are still unknown or not fully characterized. Only recently have reports described the ability of this virus to grow in cell culture (Lindenbach et al., 2005; Wakita et al., 2005; Zhong et al., 2005), which was heralded as a breakthrough in the field.

GENUS PESTIVIRUS

The pestiviruses are a group of viruses that primarily infect animals and cause diseases with a variety of signs and manifestations (Lindenbach and Rice, 2001). Genus members include border disease virus (BDV), bovine viral diarrhea viruses (BVDV-1 and BVDV-2) and classical swine fever virus (CSFV, previously known as hog cholera virus) (van Regenmortel et al., 2000). BVDV can cause acute infections in cows, and persistently infected newborns can become carriers of the virus (Murphy et al., 1999). BDV produces a congenital disorder in lambs (Murphy et al., 1999). CSFV causes an acute febrile illness characterized by diarrhea in swine (Murphy et al., 1999). There is a large economic impact from outbreaks of these viruses in herds, but monetary and livestock losses can be minimized using quarantine and/or vaccination (Murphy et al., 1999).

The pestivirus genome is similar to the hepacivirus genome. Before HCV could be grown in cell culture, pestiviruses were used as a model for HCV infection (Lindenbach and Rice, 2001). However, there are notable differences in the genome between pestiviruses and hepaciviruses. The average pestivirus genome is approximately 12 kilobases in length. The first translated protein is N^{pro}, which is auto-catalytically cleaved from the rest of the translated polyprotein, and is not required for genome replication (Lindenbach and Rice, 2001). Structural proteins include C, E^{rns}, E1 and E2; like HCV, C, E1 and E2 form the virion skeleton, but the function of E^{rns} is not fully characterized (Lindenbach and Rice, 2001). The NS2-3 proteins function as a complex that acts as the viral protease. Noncytopathic BVDV capable of persistently infecting cow fetus *in utero* has an uncleaved NS2-3 protein (Lindenbach and Rice, 2001). If alterations to the BVDV genome lead to the cleavage of the NS2-3 protein to form NS3, then the virus becomes cytopathic (Lindenbach and Rice, 2001). The functions of the remaining nonstructural proteins appear to be similar to their HCV counterparts (Lindenbach and Rice, 2001).

GENUS FLAVIVIRUS

The flaviviruses are aptly named after the yellow skin color (jaundice) and eyes of patients infected with the prototypic member of this genus, yellow fever virus (YFV). Viruses that comprise this genus infect a variety of vertebrates and invertebrates. Human disease, ranging from subclinical infections to hemorrhage and encephalitis, has been associated with over half of the known flaviviruses (van Regenmortel et al., 2000). Several of these viruses have a worldwide geographic distribution and multiple flaviviruses often co-exist in the same geographic region. Historically, YFV epidemics caused panic and disrupted societies (Monath, 1985). Some of that fear was calmed when an effective vaccine (17D YFV) was developed by serial passage of the virulent Asibi strain in embryonic chick tissues, which led to the accumulation of several attenuating mutations (Theiler and Smith, 1937). 17D YFV is considered one of the safest and most effective viral vaccines. As a result, the worldwide burden of YFV infections has been significantly reduced. Vaccines also exist for the diseases caused by Japanese encephalitis virus (JEV) and tick-borne encephalitis virus (TBEV). However, no vaccines or effective antiviral treatments exist for diseases caused by other flaviviruses, including dengue virus (DENV) and West Nile virus (WNV). DENV (serotypes 1-4) are endemic to sub-tropical and tropical climates, including many countries in Central and South America, Africa and Asia. Unexposed human populations traveling to 'exotic' locations where these viruses are endemic further amplify this burden. International travel and/or trade might have been the route by which WNV was introduced from the Middle East into North America (Lanciotti et al., 1999). Within the first seven transmission seasons (1999-2006) in the US, WNV was responsible for ~24,000 cases and almost 1000 deaths in humans, as reported to the Centers for Disease Control (http://www.cdc.gov/ncidod/dvbid/westnile/indexhtm). WNV is now endemic in North America.

The *Flavivirus* genus is distinguished from the other genera in the family Flaviviridae by the use of multiple vertebrate and invertebrate hosts for their transmission in nature. Some viruses have evolved to require hematophagous arthropods (arboviruses) for their maintenance in nature. These viruses actively replicate and proliferate in the

arthropod and are transmitted to naïve vertebrate hosts when the arthropod takes a bloodmeal. Members of the genus flavivirus are further divided based on their mode of transmission in nature: mosquito-borne, tick-borne or non-vectored. Non-vectored flaviviruses are maintained in nature either by no arthropod vector or by an arthropod that has yet to be identified. Mosquitoes are the most common flavivirus vectors. Mosquito-borne viruses include Alfuy, Banzi, Bouboui, Bussuquara, dengue, Edge Hill, Ilheus, Israel turkey meningitis, JEV, Jugra, Kokobera, Kunjin, Murray Valley encephalitis, Rocio, Sepik, St. Louis encephalitis, Usutu, Wesselsbron, WNV, YFV, and Zika viruses (Karabatsos, 1985). Flaviviruses that use ticks as part of their transmission cycle include Absettarov, Gadgets Gully, Hanzalova, Hypr, Kadam, Karshi, Kumlinge, Kyasanur Forest, Langat, louping ill, Omsk hemorrhagic fever, Powassan, and Russian spring-summer encephalitis viruses (Karabatsos, 1985). Non-vectored flaviviruses include Apoi, Aroa, Batu Cave, Bukalasa bat, Cacipacore, Carey Island, Cowbone Ridge, Dakar bat, Entebbe bat, Iguape, Jutiapa, Modoc, Montana myotis luekoencephalitis, Negishi, Phnom Penh bat, Potiskum, Rio Bravo, Saboya, Sal Vieja, San Perlita, and Sokuluk and Yokose viruses (Kuno et al., 1998).

Genome structure

Flaviviruses have a single-stranded RNA genome of approximately 11 kilobases in length with 5' and 3' UTRs flanking the single open reading frame. However, the structure of the flavivirus genome differs greatly from hepaciviruses and pestiviruses genomes. Unlike the 5' UTR of hepaci- and pestiviral genomes, the flavivirus 5' UTR does not form an IRES structure, and instead requires a m^7Gppp5'A cap for translation (Wengler, Wengler, and Gross, 1978). The 3' end of the genome is not polyadenylated (Wengler, Wengler, and Gross, 1978). The first complete description of the flaviviral genome organization came in 1985 when YFV was reported (Rice et al., 1985). A summary of these findings is shown in Figure 1.

Figure 1: Flavivirus genome structure

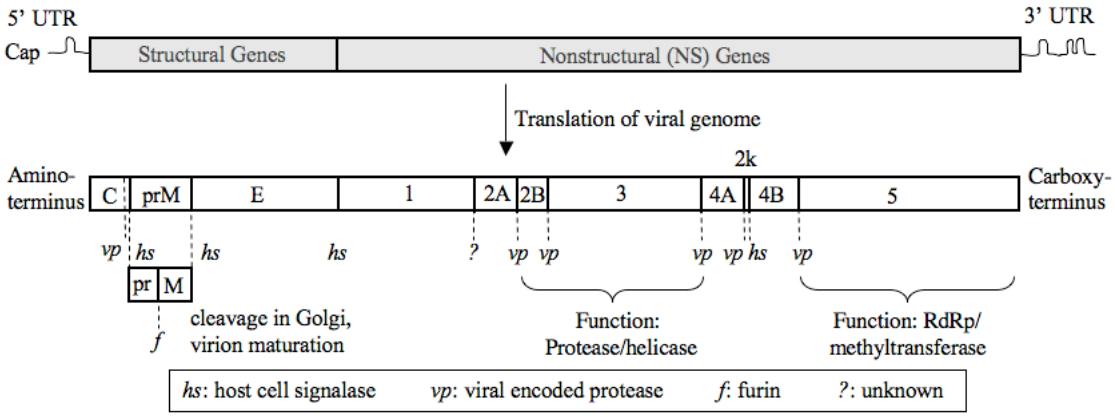

Figure 1: The order of elements and genes within the flaviviral genome. Image was inspired by Field's Virology (Lindenbach and Rice, 2001).

The three structural genes are located in the 5'-proximal third of the genome, followed by the seven NS genes in the distal two-thirds of the genome. The structural genes encode for proteins that are necessary for virion production; capsid (C), membrane (which is translated as a precursor protein, prM, and cleaved by furin to form the functional membrane protein, M) and envelope (E). The NS genes are translated and cleaved to produce the proteins NS1, NS2A, NS2B, NS3, NS4A, NS4B and NS5. These genes directly follow each other and are non-overlapping.

The initial hypothesis that these viral proteins were translated from multiple initiation sites within the flavivirus genome (Westaway, 1977) was not supported by the sequence analysis of YFV (Rice et al., 1985). It is currently accepted that the ORF is translated into one long polyprotein (Rice et al., 1985), which is co- and post-translationally cleaved to yield all 11 flaviviral proteins (Lindenbach and Rice, 2001). Many of these viral proteins are generated from a cleavage event catalyzed by the viral polymerase, whereas others are mediated by a host cell signalase (see Figure 1) (Lindenbach and Rice, 2001). The putative protease that mediates the cleavage between NS1 and NS2A proteins is hypothesized to be an endoplasmic reticulum (ER) membrane-bound protein (Falgout and Markoff, 1995). The final viral protein cleavage occurs in the

prM protein. Here, the host cell protein furin cleaves the prM protein to mature M protein (see life cycle for details). The functions of viral proteins are described in detail in the following sections.

Conformational structures formed in the 5' and 3' UTR are critical to the virus life cycle. The flavivirus 5' UTR is only about 100 nucleotides in length, but folds into a stable secondary structure (Brinton and Dispoto, 1988). The nucleotide sequence in the 5' UTR is not conserved among the flaviviruses, but the secondary structures they form are, suggesting that these structures are functionally necessary (Brinton and Dispoto, 1988). Deletions within the 5' UTR conserved stem-loop structure result in non-viable viruses, whereas viruses with deletions to the shorter stem or loop regions reduced genome replication and plaque size or had no effect (Cahour et al., 1995).

The 3' UTR is several hundred nucleotides in length and has considerable RNA secondary structure. Like the 5' UTR, the secondary structures but not the nucleotide sequence of the 3' UTR, are highly conserved among all flaviviruses (Chambers et al., 1990). The last ~100 nucleotides within mosquito-borne flaviviruses form a thermodynamically stable hairpin loop structure, called the 3'-SL (Chambers et al., 1990). The 3'-SL has been hypothesized to be involved in genome replication since viral (Chen et al., 1997; Tan et al., 1996) and host cell (Blackwell and Brinton, 1995; Blackwell and Brinton, 1997; De Nova-Ocampo, Villegas-Sepulveda, and del Angel, 2002; Garcia-Montalvo, Medina, and del Angel, 2004) proteins have been shown to bind to this region. Also within the 3' UTR, there are several conserved (CS and RCS) sequences, including CS1 and CS2 regions. Genome replication occurs when there is complementary base pairing between the 5' and 3' UTRs and proteins assemble to form the replication complex (see below). The cyclization domain consists of 8 nucleotides with the C gene and the CS1 region that are highly conserved and due to their directly complementary to each other, base pair to form thermodynamically stable secondary "panhandle" structures (Hahn et al., 1987). Deletion of the CS1 region resulted in a nonviable dengue virus (Men et al., 1996).

Functions of flavivirus proteins

The structural proteins and virion properties

The first viral protein to be translated is the C protein. The C-prM peptide spans the endoplasmic reticulum (ER) membrane due to a stretch of hydrophobic amino acids in the amino-terminus of the prM peptide, resulting in the C-containing portion of the peptide in the cytoplasm and the prM-containing portion in the ER lumen (Amberg et al., 1994; Markoff, 1989; Ruiz-Linares et al., 1989). The C protein is cleaved from prM by two coordinated cleavage events between these viral proteins: the NS2B-3 viral protease cleaves the C protein in the cytoplasm to form the carboxy terminus of C and a host cell-encoded protease cleaves within the ER lumen to release the amino terminus of prM (Amberg et al., 1994; Amberg and Rice, 1999; Lee et al., 2000). The cleaved C protein is approximately 11 kilodaltons (kD) in mass and contains positively charged basic amino acid residues that cluster at the amino- and carboxy-termini (Lindenbach and Rice, 2001). These net-positive charges may mediate the interaction between C protein and the negatively charged viral genomic RNA. Many C proteins interact with each other to form a 'cage like structure' around a single viral RNA molecule to form the nucleocapsid core, which is found in the center of the viral particle as shown in Figure 2 (Kuhn et al., 2002; Lobigs and Lee, 2004; Mukhopadhyay et al., 2003; Zhang et al., 2003). Deletion studies in TBEV and YFV have also revealed that regions of C can be removed and virions can still be formed, but some deletions result in viruses produced lower titers in culture than the wt TBEV (Kofler, Heinz, and Mandl, 2002) or YFV (Patkar et al., 2007).

The outer layer of the virion is comprised of the other two structural proteins, M and E. The M precursor protein, prM, is translated directly after the C protein and is approximately 26 kD in mass. PrM contains transmembrane domains that anchor the protein into the lipid bilayer of the ER. PrM and E proteins form heterodimers, allowing prM to serve as the required scaffold for proper E protein folding (Lorenz et al., 2002). Simultaneous synthesis of both prM and E proteins are required for the correct folding of the E protein (Konishi and Mason, 1993). After the immature virion is formed, prM is

cleaved into pr and M (see life cycle below). The amino-terminal pr portion of the protein is released from the cell after cleavage and is not associated with the mature virion particle (Murray, Aaskov, and Wright, 1993). The M protein remains embedded into the lipid bilayer of the virion.

The E protein covers the entire surface of the virion, and mediates the binding of the virion to cells. E is approximately 50 kD in mass and like the prM protein, E contains transmembrane domains that anchor the protein to the ER membrane (Zhang et al., 2003). Multiple disulfide bridges between cysteine residues help retain the structure of the E protein (Murray, Aaskov, and Wright, 1993). The E protein is also glycosylated (Winkler, Heinz, and Kunz, 1987). The presence or absence of N-linked glycosylation on the E protein is a determinant of WNV virulence (Beasley et al., 2005; Shirato et al., 2004) and affect virion assembly (Hanna et al., 2005). The crystal structure of E from TBEV (Rey et al., 1995) shows that the E tertiary structure folds into three domains: domain I forms the central portion of the protein, domain II contains the fusion peptide at the tip of the protein and domain III is an immunoglobulin-like domain. A loosely structured hinge region allows for conformational changes required during the fusion step in the life cycle (Mukhopadhyay, Kuhn, and Rossmann, 2005).

The structures of a couple of flavivirus virions have been elucidated based on cryoelectron microscopy and image reconstruction methods. In the center of the virion particle is the nucleocapsid, which contains the genomic RNA surrounded by a relatively unstructured clustering of multiple C proteins (Kuhn et al., 2002). The nucleocapsid is engulfed by the lipid bilayer that is derived from the ER, which contains the prM/E heterodimers. The immature particle contains trimeric spikes, each consisting of a prM/E heterodimers, in icosahedral symmetry (Zhang et al., 2003). In this conformation, the prM protein covers the fusion peptide present on the E protein (Zhang et al., 2003), thereby preventing premature fusion within the cell (Elshuber et al., 2003; Guirakhoo et al., 1991). The virion maturation process is described in detail in the life cycle section below. Unlike the immature virion, the surface of the mature flavivirus virion is relatively smooth, especially when compared to virions of other viral families like the Togaviridae

(Schlesinger and Schlesinger, 2001) or the Coronaviridae (Lai and Holmes, 2001). There are no prominent projections or spikes protruding from mature flavivirus virions. The WNV virion, which looks similar to the cryo-EM-generated images of DENV (Kuhn et al., 2002), is shown in Figure 2 (Mukhopadhyay et al., 2003). Dimers of E proteins are found in a head-to-tail conformation and in the virion are found in a "herring-bone" pattern lying parallel to the lipid bilayer (Rey et al., 1995) and coat the entire surface of the virion (Kuhn et al., 2002; Mukhopadhyay et al., 2003).

Figure 2: WNV virion structure

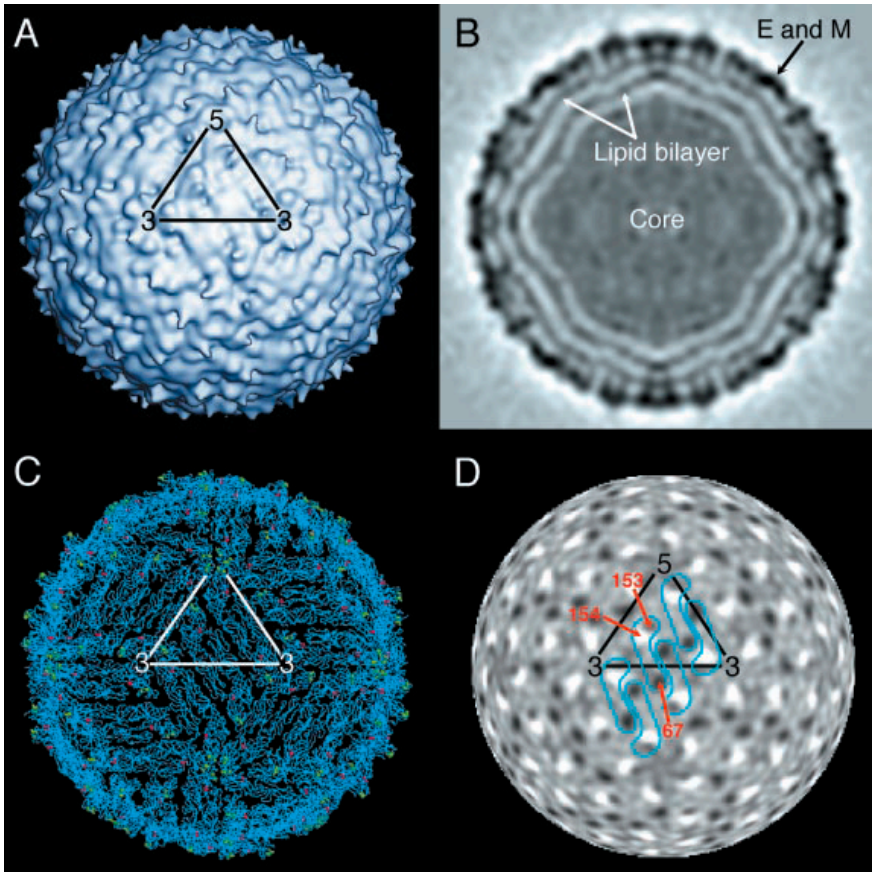

Figure 2: The structure of the WNV mature virion was determined by cyro-electron microscopy with a resolution of 17 Angstroms. Panel A shows the surface structure. A cross section through the virion particle shows the different electron-dense layers is shown in Panel B. Panel C show the stick representation of the E proteins and their structure with respect to each other. Panel D shows the density differences between

DENV and WNV virions. The location of E dimers is depicted in blue. Image reprinted with permission (Mukhopadhyay et al., 2003).

The nonstructural proteins

The first translated nonstructural protein is NS1. This glycoprotein is approximately 46 kD in mass and exists in several forms: full-length and truncated, monomer and dimer, intra- and extra-cellular (Blitvich et al., 1999; Smith and Wright, 1985). NS1 is required for genome replication and co-localizes with the genome replication complex and double-stranded (dsRNA) (Mackenzie, Jones, and Young, 1996; Westaway et al., 1997b). Some mutations to NS1 result in reduction of genome replication (Hall et al., 1999; Muylaert, Galler, and Rice, 1997), while other mutations or deletions are lethal (Lindenbach and Rice, 1997; Muylaert, Galler, and Rice, 1997).

The role of secreted and cell surface-associated NS1 is not fully characterized and their role in flavivirus pathogenesis are unclear. NS1 is found within the serum of patients acutely infected with WNV (Macdonald et al., 2005) and DENV (Alcon et al., 2002) and can be used as a marker to identify infection. Enhanced pathogenesis of DENV infection may be due in part due to cross-reactive anti-NS1 antibodies that bind to uninfected endothelial cells (Falconar, 1997) and trigger apoptosis, which may result in vascular leakage seen during dengue hemorrhagic fever (Lin et al., 2002). Additionally, secreted NS1 is preferentially endocytosed by liver cells and NS1-treated hepatocytes in culture produce higher virus titers upon infection than untreated hepatocytes (Alcon-LePoder et al., 2005). On the other hand, NS1 is immunogenic and antibodies generated against NS1 or vaccines based on NS1 production are protective (Costa et al., 2007; Fleeton et al., 1999; Lin et al., 1998; Wu et al., 2003). This protection may be mediated in part by cells of the immune system targeting host cells with NS1 on their surface for degredation via Fc-γ receptor-mediated phagocytosis (Chung et al., 2007). The host defense complement system, which forms the membrane-attack complex responsible for lysing cells, is inhibited by WNV NS1 protein upon binding to a complement regulatory protein factor H (Chung et al., 2006).

NS2A is a small (25 kD) hydrophobic protein. The function of NS2A is not fully characterized, but this viral protein is involved in viral RNA replication complex and virion assembly and may be involved in regulating the host cell's IFN response. NS2A has been shown to bind to the 3' UTR and several other NS proteins (Mackenzie et al., 1998). A cleavage site recognized by the NS2B/3 viral protease within the NS2A protein produces a truncated NS2A (NS2Aα) (Nestorowicz, Chambers, and Rice, 1994). Blocking cleavage at this site also blocks the generation of infectious virus (Kummerer and Rice, 2002). Interestingly, NS2A has also been linked with the ability to suppress the mammalian host cell's IFN response (Liu et al., 2004; Liu et al., 2006; Munoz-Jordan et al., 2003). This last point will be discussed in detail in Chapter 5.

The viral serine protease is comprised of a complex between NS2B and NS3. The small (~14 kD) hydrophobic, membrane-associated NS2B protein is a required cofactor for the serine protease activity of NS3. The hydrophobic domain of NS2B is dispensable with respect to enzymatic functionality, but the central portion of the protein is required (Chambers et al., 1993). Alanine substitutions for several individual amino acids in this central portion severely impacted or abolished NS2B/3 protease activity (Droll, Krishna Murthy, and Chambers, 2000; Lin et al., 2007; Niyomrattanakit et al., 2004). Unlike the previous two viral proteins, NS3 is a large (70 kD) hydrophilic protein that has no direct associations with cellular membranes. The amino-terminal portion of the protein harbors the serine protease catalytic triad (for YFV: H53, N77, S138), and in conjunction with NS2B, performs the necessary viral protease functions required for cleavage of the polyprotein. The sites on the viral polyprotein cleaved by the NS2B/3 complex are summarized in Figure 1.

Helicase activity in the carboxy-terminal portion of NS3 is hypothesized to help unwind secondary RNA structures or the growing RNA strand from the template RNA during replication (Lindenbach and Rice, 2001). NS3 has been found to associate with the 3' UTR of viral RNA and has significant homology to other known helicases. Helicase activity requires host-provided NPT to provide the energy required for this reaction. NS3 may help prime the viral RNA 5' end for capping by NS5 (Wengler and

Wengler, 1993). Moreover, NS5 may stimulate the non-protease enzymatic activities of NS3 (Yon et al., 2005).

NS4A and NS4B are two additional small hydrophobic membrane-bound proteins, approximately 16 and 27 kD, respectively. Like NS2A, both NS4A and NS4B have shown the ability to modulate the IFN response *in vitro* (Munoz-Jordan et al., 2003). However, the effects of NS4B were greater than either NS2A or NS4A and so this protein has been examined in further detail in several systems (Evans and Seeger, 2007; Munoz-Jordan et al., 2005). NS4A was found to colocalize with dsRNA, and like NS2A, is thought to help anchor the viral replication complex to the membrane (Mackenzie et al., 1998). The distribution of NS4B in the cell is more widespread; it has been found on cellular membranes and potentially in the nucleus (Westaway et al., 1997a). NS4B is further modified by a cleavage, which produces a small peptide (2k) and a smaller form of NS4B, and this cleavage may play a role in the proliferation of intracellular membranes (Roosendaal et al., 2006). NS4B may also function as a regulator of genome replication since it has been shown to dissociate NS3 from ssRNA (Umareddy et al., 2006). NS4B protein has also been shown to help modulate the ability of flavivirus infected mammalian cells to respond to interferon (IFN) (Evans and Seeger, 2007; Munoz-Jordan et al., 2005; Munoz-Jordan et al., 2003).

NS5 is a large (approximately 100 kD) hydrophilic viral protein that serves as the viral RNA-dependent RNA-polymerase (RdRp) and methyltransferase (Lindenbach and Rice, 2001). The classical GDD sequence (Gly-Asp-Asp) common to polyermases is located in the middle of the NS5 linear peptide. Mutating this GDD motif ablates the ability of the genome to replicate and has been used as a control virus to teasing part genome translation and transcription as translation is unaffected in these mutants. The 5' end of the viral genome is methylated by NS5. Post-translational modifications of NS5 include phosphorylation, but the purpose of this modification is unclear, but may be involved in regulating viral protein interactions or subcellular locations. Like NS4B, NS5 can also interfere with IFN-stimulated signaling in flavivirus infected mammalian cells

(Best et al., 2005; Lin et al., 2006; Park et al., 2007; Werme, Wigerius, and Johansson, 2007).

Flavivirus intracellular life cycle

The major events in the flavivirus infection life cycle within the cell are shown in Figure 3. Flaviviruses are thought to enter the cell by receptor-mediated endocytosis into coated pits (Gollins and Porterfield, 1985). Due to the wide variety of cell types flaviviruses can infect, including both vertebrate and invertebrate cells, the receptor must either be ubiquitous or multiple receptors may be utilized. Passing flaviviruses repeatedly *in vitro* or deliberate genetic modification can lead to the ability of the passaged viruses to bind to 'unnatural receptors' such as heparan sulfate (HS), which increases the virion's infectivity for many cell types (Gilfoy and Mason, 2007; Lee and Lobigs, 2000). Once the virion is engulfed into an intracellular endocytic vesicle, a pH-dependent conformational change in the virion coincident with an irreversible rearrangement of the E protein to expose the fusion loop, results in the release of the nucleocapsid into the cytoplasm (Gollins and Porterfield, 1986; Heinz et al., 1994). Once the nucleocapsid is released from the virion, the host cell machinery can translate the genomic RNA. The positive-strand genomic RNA is infectious and serves as a template for translation by the cellular machinery. Translation is cap-dependent, although reports have indicated that under some conditions, flaviviral genomes can be translated in a cap-independent manner (Edgil, Polacek, and Harris, 2006).

Figure 3: Intracellular flavivirus life cycle

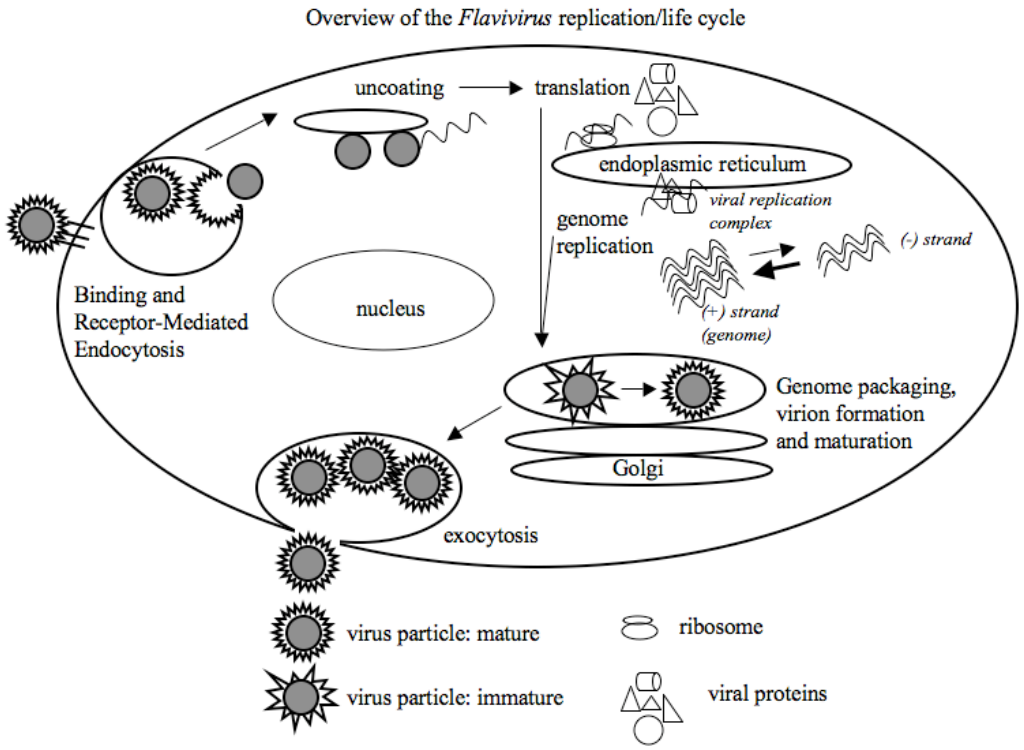

Figure 3: The lifecycle of flaviviruses, from virion binding and entry to exocytosis. Image was inspired from Field's Virology (Lindenbach and Rice, 2001).

Genome replication occurs at the replication complex, which occurs on intracellular virus-induced membranes called vesicle packets (VPs), and comprised of NS proteins (Mackenzie, Jones, and Young, 1996; Mackenzie et al., 1998; Westaway et al., 1997b). Host proteins may be involved as well. NS5 is thought to bind to the genomic RNA at the 3' end, followed by NS2A, NS3 and NS4A. NS2A and NS4A anchor the newly formed complex to intracellular membrane (Mackenzie, 2005; Mackenzie et al., 1998). The membrane invaginates, forming the VP, which is protected from cytoplasmic factors (Mackenzie, 2005). NS1 is recruited to the replication complex by its interaction with the membrane-bound NS4B protein (Lindenbach and Rice, 1999). The RdRp function of NS5 is responsible for RNA transcription. Minus-stranded RNA is dependent upon NS1 and transcribed quickly after infection (Lindenbach and Rice, 1997). More

genomic RNA is present during infection than minus-strand RNA (which serves as the template for genomic strand transcription) and the presence of both strands results in the generation of dsRNA (Cleaves, Ryan, and Schlesinger, 1981). DsRNA is recognized by the cell as a marker of infection and is described in detail in Chapter 5.

Multiple membrane structures, including convoluted membranes, paracrystalline arrays and the ER, are generated or expanded during a flavivirus infection (Mackenzie et al., 1998; Westaway et al., 1997b). These membranes serve as venues for the translation and proteolytic cleavages, as described previously. Genomic RNA is encapsidated by multiple copies of the C protein to form the nucleocapsid. Due to the cytoplasmic position of the nucleocapsid and the directionality of prM and E within the ER membrane, particles are believed to form when the nucleocapsid 'buds' into the lumen of the ER, thereby generating the immature virion (Figure 3). Interestingly, prM and E self-assemble into subviral particles (SVPs), which are particles devoid of C protein and viral RNA (Konishi, Fujii, and Mason, 2001; Konishi et al., 1991; Mason et al., 1991; Schalich et al., 1996). The virions are transported through the secretory pathway en route to the cell membrane (Mackenzie and Westaway, 2001). Furin, a proteolytic enzyme located in the trans-Golgi network, cleaves the prM to transform the immature particle to the mature (and infectious) M-containing virion (Stadler et al., 1997). Upon cleavage, M and E heterodimers dissociate. This cleavage event exposes the fusion loops on the E proteins, thereby allowing the mature particle to fuse upon endocytosis and acidification.

Particles are exocytosed from the cell to complete the life cycle. Immature particles are found gathered in vesicles near the plasma membrane and are released when this vesicle fuses to the plasma membrane (Mackenzie and Westaway, 2001). Cell lysis is not required for the release of flavivirus particles from the infected cell.

Arbovirus-Host Cell Interactions: Innate Immunity

The ability of a host to detect and combat an infection is critical to the host's survival. Some responses are broad and quickly engaged (innate immunity) while other

responses are highly specific, slowly engaged and require an immunological memory (adaptive immunity). The innate immune response is an anti-pathogenic response that has been described in plants, invertebrates and vertebrates, which offers no immunological memory of its own, but can be quickly engaged upon stimulation. Oftentimes, the innate immune response is critical to controlling the pathogen early during infection and helps to shape the course of the adaptive immune response. Although the adaptive immune response is important for flavivirus immunity, this response will not be discussed in detail here.

INSECT AND INSECT CELLS

The innate immune response in insect cells has been extensively studied in the insect model (fruit fly) *Drosophila melanogaster*. The two main antimicrobial signaling pathways have been studied following bacterial and fungal infections: the Toll pathway is engaged following recognition of Gram-positive bacteria and fungi while the immune deficiency (IMD) pathway is stimulated by Gram-negative bacteria recognition (Ferrandon et al., 2007). The working model for the identification of pathogens involves the recognition of pathogen-associated molecular patterns (PAMPs) on the invading microbe by soluble pattern-recognition receptors (PRRs) in the fly's open circulatory system (hemolymph). Upon detection of the PAMP by the PRR, the PRR stimulates the proteolytic cleavage of a variety of proteins, including the cytokine Spaetzle (Ferrandon et al., 2007). Spaetzle is expressed in an inactive pro-protein form and upon cleavage, associates with and activates Toll protein (Ferrandon et al., 2007; Weber et al., 2003). Toll signaling results in the production of the antimicrobial peptide, Drosomycin. The IMD pathway does not involve Toll, but establishes a signaling cascade following the stimulation of peptidoglycan-recogntition protein-LC, resulting in the downstream activation of the Relish transcription factor (NFκB homolog, described below) and the transcription of the antibactieral protein, Diptericin (Ferrandon et al., 2007).

Recently, some homologs to these Drosophila proteins have been identified in mosquitoes but the Toll and IMD pathways in mosquitoes have not been fully studied

(Bian et al., 2005; Luna et al., 2002; Shin, Bian, and Raikhel, 2006). However, the antimicrobial peptides produced in the mosquito, which are both constitutively expressed or produced in response to infection, have been examined in detail. The innate immune response in mosquito cells consists of a variety of peptides including cecropins, defensins, and transferrins have anti-pathogenic functions mainly against bacteria and multicellular parasites (Lowenberger, 2001). Melanization, a process by which pigmented melanin molecules envelops a pathogen, is another important defense mechanism employed by mosquitoes for combating pathogens (Beerntsen, James, and Christensen, 2000; Christensen et al., 2005). Little is known or has been described, however, about the innate immune response of the mosquito upon viral infection.

There are also many anti-pathogenic responses that are not traditionally considered to be part of the innate immune response, including posttranslational gene-silencing (PTGS) and heat shock proteins (Hsp). PTGS is naturally induced by dsRNA to control the level of specific intracellular (target) RNA molecules by a process called RNA interference (RNAi) (Fire et al., 1998). Most of the understanding of how RNAi functioned in invertebrates was gained from early experiments conducted in *Caenorhabditis elegans* and *Drosophila melanogaster*. Briefly, dsRNA is cleaved into small (21-25 nucleotides in length) segments with a short overhang on the 3' end (creating silencing RNA or siRNA) by a host cell RNase called Dicer. The cleaved siRNAs then associate with Argonaute proteins to form the RNA-induced silencing complex (RISC) (Sanchez-Vargas et al., 2004). This complex can bind to the target RNA by complementary base-pairing between the siRNA and the target RNA, which primes the target RNA for degredation by RISC (Sanchez-Vargas et al., 2004).

PTGS has been exploited as a mechanism to control arboviral infections in the mosquito host. Silencing a member of the RISC complex, Argonaute2, in *Anopheles (An.) gambiae* mosquitoes resulted in a higher titer of the alphavirus (family *Togaviridae*) O'nyong-nyong (ONNV) than untreated, ONNV-infected mosquitoes, indicating that PTGS (RNAi) helped to control ONNV infection in the mosquito (Keene et al., 2004). The target virus RNA can also be blocked by introducing dsRNA specific for that virus

into the mosquito or the mosquito cell line. Recombinant Sindbis viruses (SINV, alphavirus, family Togaviridae) that expressed portions of the DENV or YFV genomes under a second artificially generated subgenomic promoter rendered *Aedes (Ae.) aegypti* mosquitoes or C6/36 cells (*Ae. albopictus* mosquito cell line) resistant to DENV or JFV infection by PTGS (Adelman et al., 2001; Blair, Adelman, and Olson, 2000; Higgs et al., 1998; Olson et al., 1996). A decrease in the number of Semliki Forest virus (SFV, alphavirus, family *Togaviridae*) or DENV-infected C6/36 cells was observed in cultures treated with viral sequence-specific dsRNA compared to untreated SFV or DENV-infected cells (Caplen et al., 2002). It is likely that the RNAi mechanism is important for naturally helping to control flavivirus infections in mosquitoes, but this mechanism appears to be even more effective when experimentally supplemented with additional target dsRNA. To exploit this observation, transgenic mosquitoes expressing RNAi-triggering targets have been engineered to create a DENV-resistant mosquito populations in the hopes of preventing the transmission and spread of DENV (Olson et al., 2002; Travanty et al., 2004).

Hsps are a highly conserved family of proteins found in both prokaryotes and eukaryotes that are both constitutively expressed and induced upon certain stimuli (Arya, Mallik, and Lakhotia, 2007; Daugaard, Rohde, and Jaattela, 2007). The Hsp70 family has been extensively studied and its member proteins function as chaperone and anti-apoptotic proteins (Arya, Mallik, and Lakhotia, 2007). Silencing a member of the Hsp70 family, heat shock protein cognate 70B (Hsc70B) in *An. gambiae* mosquitoes resulted in both increased death and increased titers of ONNV in ONNV-infected mosquitoes (Sim et al., 2005). These results suggest that some constitutively expressed chaperone proteins are important in controlling arbovirus infections in mosquitoes.

MAMMALIAN CELLS

The antiviral responses in mammalian cells have been studied in greater detail than in mosquito cells. In mammalian cells, multiple and often redundant pathways are engaged during viral infection that are aimed at eliminating or reducing the harmful

effects of the virus (Figure 4). During replication, there are numerous interactions between the flavivirus and the host cell that can be deleterious to the cell and cytopathic effect is seen in many WNV-infected mammalian cell lines. In order for the cell to successfully combat infection and mount an effective antiviral response, the virus must first be detected. This detection is based on the cells ability to recognize PAMPs that are produced during the virus's life cycle. In the case of viruses with positive-sense RNA genomes, the PAMPs include RNA molecules with abnormal structures (5' triphosphate moieties or dsRNA) and/or viral RNA molecules present in unnatural locations (endosomal compartments). Cells recognize these RNAs via PRR proteins. DsRNA can be recognized by Toll-like receptor 3 (TLR3) (Alexopoulou et al., 2001), the RNA helicases, retinoic acid inducible gene-1 (RIG-I) and melanoma differentiation antigen 5 (mda5) (Andrejeva et al., 2004; Kato et al., 2006; Yoneyama et al., 2004) and the cellular protein kinase R (PKR) (Clemens, 1997; Gilfoy and Mason, 2007). It is interesting to note that TLRs in vertebrate cells can directly recognize PRRs where as Toll proteins in invertebrate cells cannot. Recently, reports have indicated that RNA molecules with exposed 5' triphosphate groups can be recognized by RIG-I (Hornung et al., 2006; Pichlmair et al., 2006; Plumet et al., 2007). SsRNA is recognized by TLR7/8 (Diebold et al., 2004).

PRRs signal through downstream molecules to elicit a specific antiviral response. TLR3 is present within endocytic vesicles (Takeda and Akira, 2005). When the dsRNA ligand binds to TLR3, signaling occurs through the adaptor molecule TRIF [TIR domain-containing adaptor inducing IFN (Oshiumi et al., 2003; Yamamoto et al., 2002)], which in turns activates the kinases IKK-ε (IκB kinase-ε) and TBK-1 (TANK-binding-kinase-1) (Fitzgerald et al., 2003). These kinases phosphorylate IRF3 (interferon-regulatory factor 3) (Fitzgerald et al., 2003), leading to its dimerization and translocation into the nucleus where it drives the transcription of IFN α and IFN β (Fitzgerald et al., 2003). RIG-I/mda5 also activates IRF3 via the adaptor molecules IPS-1/VISA/MAVs/Cardif (Kawai et al., 2005; Meylan et al., 2005; Seth et al., 2005; Xu et al., 2005). Both RIG-I/mda5 and PRK can activate NFκB, which translocates to the nucleus and promotes IFNβ transcription

(Hiscott et al., 2006). The interactions between flavivirus genomes and the innate immune response are described in Chapter 5.

Figure 4: The intracellular innate immune response in mammalian cells

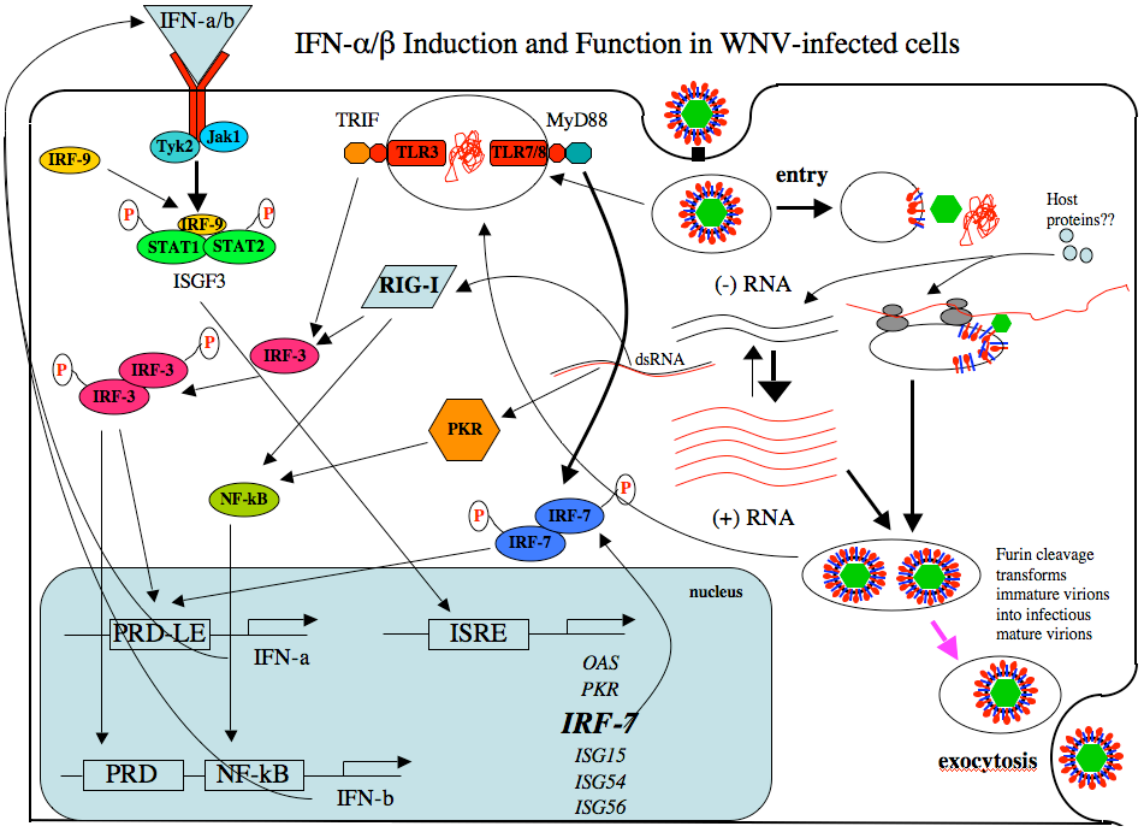

Figure 4: A generalized schematic diagram of the intracellular innate immune response. Upon WNV infection, the genome is translated and transcribed, generating PAMPs, which ultimately lead to the production of type I IFN. IFN can be recognized by cells with an IFNα/β receptor, which stimulates the production of ISGs.

IFNα and IFNβ are potent antiviral compounds that elicit a quick and nonspecific response to combat infection. IFN functions by establishing a signal cascade downstream of the IFNα/β receptor following binding to IFN. Tyk2 and Jak1 are phosphorylated upon ligand binding to the IFNα/β receptor, which results in the recruitment of STAT1 and STAT2 molecules. STATs 1 and 2, in conjunction with IRF-9, form the ISGF3 complex, which is capable of binding to the interferon-stimulation response element

(ISRE) promoter to drive the transcription of interferon-stimulated genes (ISG) (Horvath et al., 1996; Stark et al., 1998). ISGs include proteins like oligo-adenylate synthetase (OAS), protein kinase R (PKR), IRF7 and ISGs 15, 54 and 56.

West Nile Virus History

WNV is a mosquito-borne flavivirus that has been placed in the media spotlight in recent years. WNV, as well as the Australian strain Kunjin virus (KUNV), have historically been viewed as viruses with limited pathogenic capabilities (Gubler, 2007; Hall et al., 2002). However, an outbreak of human encephalitis and a large number of avian deaths in New York (NY) City in 1999 sparked fear in the U.S. population and invigorated studies to better understand the ecology, epidemiology and molecular virology of WNV. It is important that these studies be continued since WNV is now considered endemic in North America, as it is in other parts of the world, as shown in Figure 5.

IT ALL STARTED IN 1937

The first WNV isolate was made in 1937 from a 37-year-old woman suffering from a febrile illness during a field study to identify cases of YFV infection in Uganda (Smithburn et al., 1940). The patient denied being ill although her temperature was recorded at 100.6°F. Little else is known about her illness since she was unwilling to provide any information about her condition.

Most mice (90%) inoculated in the brain (intracranial: i.c.) with the patient's serum died. Their brains were harvested, homogenized and injected i.c. of naïve mice, who then also succumb to infection, indicating that this new agent was transmissible. The virus was also pathogenic in mice by the intranasal (i.n.) and intraperitoneal (i.p.) routes. This isolate caused disease (fever and encephalitis) in rhesus monkeys injected i.c or i.n., but only fever without signs of illness in moneys infected intravenously. Interestingly, rabbits, guinea pigs and hedgehogs injected i.c., i.n. or i.p. failed to show signs of disease.

Antibodies against WNV were produced in rabbits, guinea pigs and monkeys that survived infection. Additionally, the patient from which this isolate was made also had neutralizing antibodies in her serum 3 months after the initial blood draw.

WNV OUTBREAKS

Relatively few WNV outbreaks have been recorded between 1930 and the early 1990s, but when epidemics were detected, they were generally associated with mild or no symptoms in human populations and were not associated with disease in equines or avians (Hayes, 2001). Epidemics were noted in Egypt and Israel in the early 1950s with a few hundred human cases between them, reporting mostly febrile illness and scattered cases of neurologic disease, but not death (Murgue et al., 2001). The exception was an outbreak in France in 1962 that was characterized by encephalitis and mortality in horses (Joubert et al., 1967). As a result, WNV was not considered to be an important human pathogen. During this time period, many species of birds were found to have anti-WNV antibodies, but no mortality was observed in these populations (McIntosh et al., 1976). The initiation of some epidemics has been associated by heavy rainfall, which generate large mosquito populations (usually the *Culex* (*Cx.*) subgenus) capable of transmitting WNV (Hall et al., 2002; McIntosh et al., 1976). These "summer fevers" were generally short-lived and tended to end when cold weather disrupted mosquito-feeding behavior (Goldblum, Sterk, and Jasinskaklingberg, 1957).

Figure 5: Location of WNV outbreaks

Figure 5: The stars denote the locations of WNV outbreaks. The blue star shows the location of the original WNV isolate. Figure reprinted with permission (Gubler, 2007).

WNV was reclassified as an important human pathogen in the 1990s when more virulent infections became and caused severe human neurologic disease and death. There were small outbreaks recorded in Algeria (1994), Morocco (1996), Tunisia (1997), Italy (1998) and France (2000) that were associated with significant equine and human morbidity and mortality (Murgue et al., 2001). Outbreaks in Romania, Israel and Russia in the mid to late 1990s were well documented and uncharacteristically fatal for humans compared to the aforementioned outbreaks, with a large number of neurologic diseases and death.

In the summer of 1996, an outbreak of WNV in Romania resulted in several hundred cases of fever and neurological diseases (Tsai et al., 1998). Large percentages of domesticated chickens (41% of those analyzed) were also infected, but no cases of equine infection were recorded. Mosquito pools, including mosquitoes from seven taxa with an overwhelming percentage of the species being *Cx. pipiens*, resulted in only one viral isolate (Savage et al., 1999). This isolate grouped phylogencially with other lineage Ia

viruses (see Taxomony below), and was most similar to previous isolates from sub-Saharan Africa, suggesting that the virus responsible for this outbreak was of African origin.

In 1998, high morbidity and mortality were observed in flocks of geese and storks in Israel due to WNV infection, which were not observed in previously infected avian populations (Malkinson et al., 2002). The following years (1999-2000) brought over 400 human cases of disease and 29 deaths in Israel (Bin et al., 2001). Viruses isolated from this outbreak closely resembled viruses circulating in New York in 1999 and viruses from the Romanian (1997) and Russian (1999) outbreaks (Bin et al., 2001).

An outbreak in the Volgograd region in Russia in 1999 resulted in over 800 patients who sought medical treatment for symptoms of fever or neurological illness and of these, approximately half were attributed to WNV infection (Platonov et al., 2001). Isolated viruses showed similar nucleotide similarity to viruses isolated from Romania (1996), Kenya (1998) and Senegal (1993) and were therefore grouped in lineage Ia (Platonov et al., 2001). *Culex* mosquitoes (*Cx. pipiens* and *Cx. modestus*) are hypothesized to be the primary vectors during this outbreak (Fyodorova et al., 2006).

In 1999, the virus was found for the first time in North America. The epicenter of the outbreak was in the Queens Burough of New York City. A seroprevelance study of infected avian species revealed that within Queens and the surrounding area, approximately one third of the wild-caught birds tested positive for anti-WNV antibodies (Komar et al., 2001). Additionally, necropsies from birds at the Bronx Zoo indicated that these infections produced severe pathology (Anonymous, 1999). Wild-caught mosquitoes that tested positive for WNV included *Ae. vexans* and *Cx. pipiens* (http://www.cdc.gov/ncidod/dvbid/westnile/mosquitospecies.htm). The virus overwintered and produced additional infections in the warm months of 2000 that spread to neighboring states, producing human diseases in Connecticut and New Jersey and non-human infections (avian, animal or mosquito) as far south as North Carolina (http://www.cdc.gov/ncidod/dvbid/westnile/Mapsactivity/surv&control00Maps.htm). In 2002-3, the virus had spread to most of the continuous 48 states, producing over 13,000

human confirmed cases of disease with several hundred fatalities (http://www.cdc.gov/ncidod/dvbid/westnile/surv&controlCaseCount02_detailed.htm) (http://www.cdc.gov/ncidod/dvbid/westnile/surv&controlCaseCount03_detailed.htm). By the end of the 2006 transmission season in the U.S., over 24,000 cases and over 1000 deaths were reported to the CDC (http://www.cdc.gov/ncidod/dvbid/westnile/index.htm). Currently, WNV is endemic in North, Central and South America (Granwehr et al., 2004b; Komar and Clark, 2006).

TAXONOMY

The first evidence to suggest differences among the WNV isolates came from hemagluttination and antibody-binding assays (Hammam and Price, 1966). In recent years, sequencing has become the standard for determining the relationships between viruses. Nucleotide sequence analyses, either using partial or whole genome sequences, suggest that there are 5 WNV lineages, as shown in Figure 6 (Bondre et al., 2007). Lineage I is comprised of viruses geographically distributed worldwide. Under this newly described system, lineage I is divided into two clades: linage Ia (clade a) contains WNV from Europe, Africa and North America, and lineage Ib (clade b) is made up of KUNV. Lineage II viruses only contain African isolates (Lanciotti et al., 2002; Lanciotti et al., 1999). Lineage III is made of a single isolate from the Czech Republic named Rabensburg virus (Bakonyi et al., 2005). Isolates from the Caucasus Mountain valley and additional Indian isolates create lineages IV and V, respectively (Bondre et al., 2007). Previous publications proposed 3 lineages of WNV (Berthet et al., 1997; Lanciotti et al., 2002; Lanciotti et al., 1999). Here, lineage I viruses were subdivided into three clades (a, b and c). Lineage Ia and b contained the same viruses as described above, and clade 1c was comprised of viruses collected in the 1950's from India (Lanciotti et al., 2002). It appears under the new system, the lineage Ic viruses are now classified as lineage V.

There is a correlation between lineage and disease severity in humans. In general, lineage I viruses (with the potential exception of KUNV and some African strains) tend to cause severe human neurologic diseases and death. Lineage II viruses are generally

associated with a mild, self-limiting febrile illness. The newly described lineages III, IV and V have not been well characterized or are comprised of only one viral isolate, so general statements about the diseases they cause cannot be made at this time.

Figure 6: Phylogenetic tree of WNV lineages

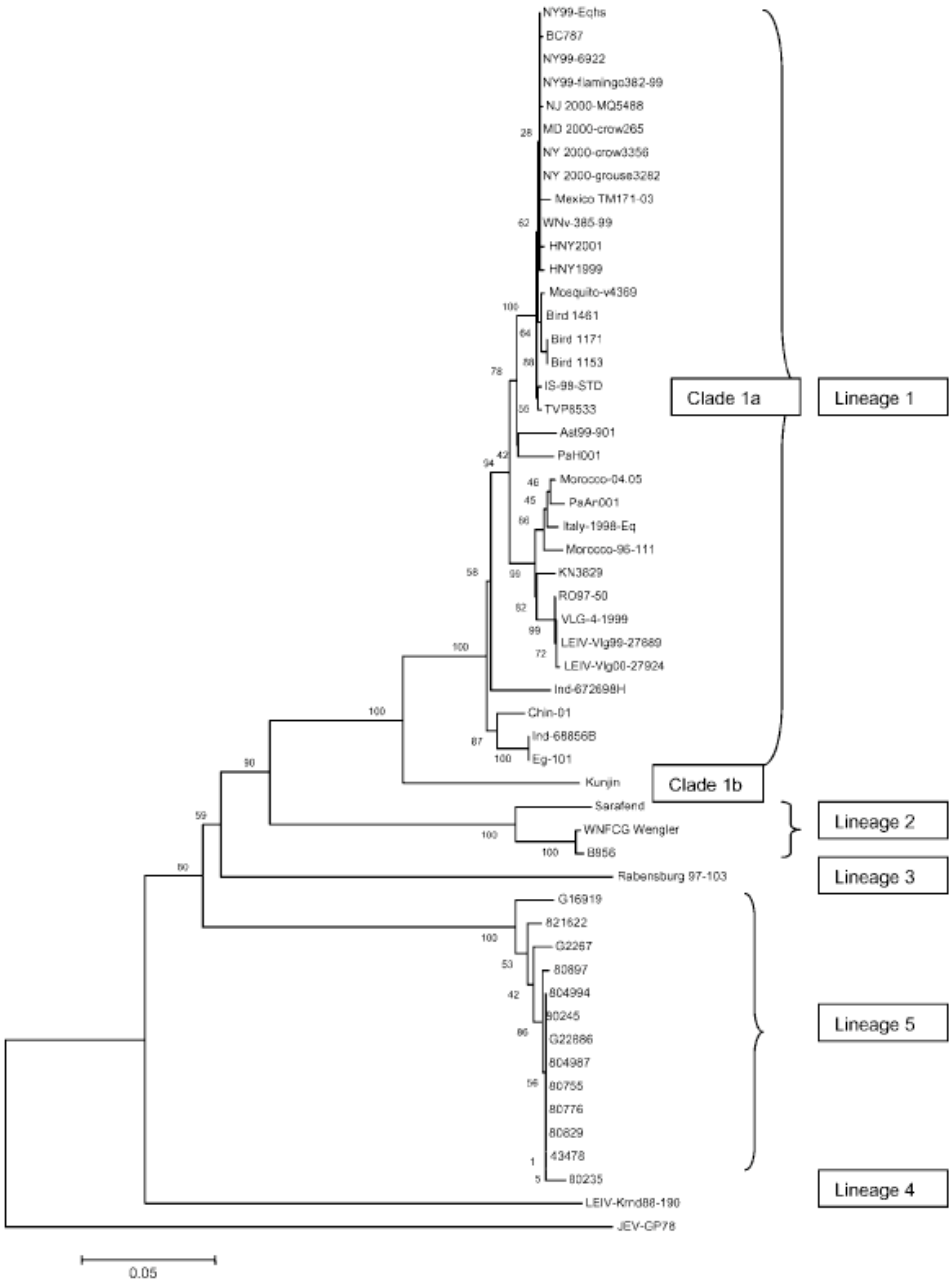

Figure 6: A phylogenetic tree based on neighbor-joining (Jukes-Cantor distance formula) based on 921 nucleotides within the C-prM-E genes using JEV as an outgroup. Bootstrap values were based on 1000 replicates. Figure from (Bondre et al., 2007), reprinted with permission.

West Nile Virus Transmission

NATURAL MODES OF TRANSMISSION

The transmission cycle of WNV in nature is primarily between birds and mosquitoes, as shown in Figure 7. Birds are required for the stable maintenance of the virus in nature since some species produce high titer viremias upon infection and have a quick generation time (many naïve animals born each year). A mosquito feeding upon a viremic bird becomes infected when the virus infects the cells lining the mosquito's digestive organ, the midgut. From there, the infection disseminates to infect multiple organs, including the salivary glands where the virus is amplified and secreted with saliva into a host upon the next bloodmeal. If this host was naïve to WNV, the newly infected bird becomes viremic. The level of viremia is species-specific, but some avian species can produce titers up to 10^{10} pfu/ml (Komar et al., 2003). These titers easily infect a naïve feeding mosquito, whom after a period of time (extrinsic incubation period), can transmit the virus upon the next bloodmeal. Interestingly, experimental infections of rodents such as hamsters (Xiao et al., 2001), cottontail rabbits (Tiawsirisup et al., 2005), squirrels (Root et al., 2006) and chipmunks (Platt et al., 2007), which produce viremias (averaging $1x10^{4-5}$ pfu/ml or $TCID_{50}$/ml serum) that are sufficient to infect naïve mosquitoes and may contribute to WNV transmission in nature. Moreover, transmission of WNV to naïve mosquitoes co-feeding with infected mosquitoes (non-viremic transmission) on a naïve rodent has been demonstrated in the laboratory (Higgs et al., 2005). In some instances, however, an infection can be spread from bird-to-bird (or vertebrate-to-vertebrate) or from mosquito-to-mosquito. These routes of infection are less common and their importance to the maintenance of the virus in nature is unclear.

Unlike several other arboviruses, WNV infection does not appear to be restricted to a single species or group of vertebrates. In fact, WNV infections have been documented in reptiles like snakes (Klenk and Komar, 2003; Steinman et al., 2006) and alligators (Miller et al., 2003) and one species of amphibian (Klenk and Komar, 2003).

WNV infections have been documented in numerous species of avians and mammals. With the exception of a few (as noted above), many of these species including humans are considered incidental or "dead-end" hosts since the levels of viremia are low and thought not to be sufficient to infect a feeding naive mosquito.

Figure 7: Transmission cycle of WNV

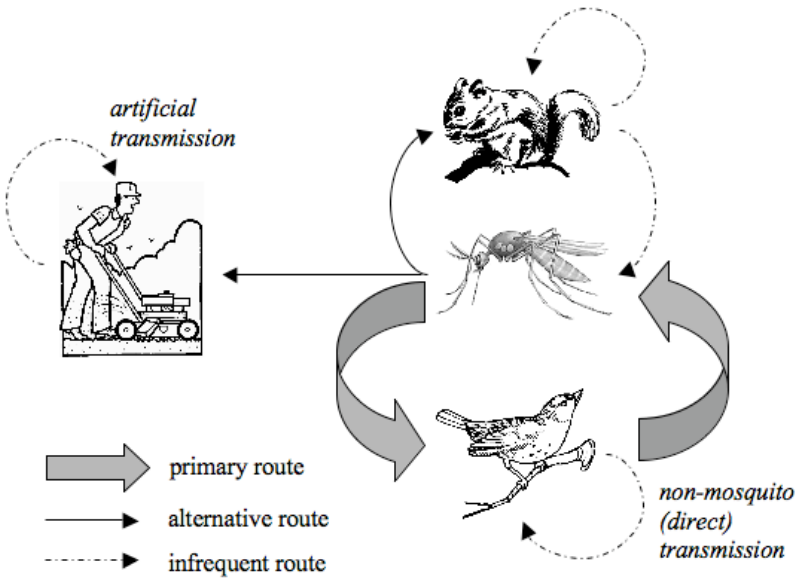

Figure 7: The transmission cycle for WNV is primarily between birds and mosquitoes (mosquito transmission), but may also be transmitted at lower frequencies directly between vertebrates (non-mosquito transmission) or be transmitted as a result of human activities (artificial transmission).

Mosquito transmission

The most common route of WNV infection in mosquitoes is by imbibing a bloodmeal from an infected vertebrate host. The blood enters the mosquito's digestive organ, the midgut. The virus exits infected midgut cells on the basal side where it accesses the hemocoel, the body cavity that contains fluids that bathe the organs in the mosquito open circulatory system. Once in the hemocoel, the infection spreads (disseminates) to many secondary organs including the salivary glands (Girard, Klingler,

and Higgs, 2004). Many investigators also inject virus directly into the mosquito's thorax to bypass the midgut, which speeds up the course of virus dissemination to the salivary glands. Infection in the salivary glands was first detected on day 5 post infection (pi) after an oral feed, but virus wasn't detected in the acinar cavity (contains the saliva to be deposited in the host during a bloodmeal) until day 8 pi (Girard, Klingler, and Higgs, 2004). Eight days after the infected bloodmeal, the mosquito can transmit the virus to a naïve vertebrate when she next feeds. When the mosquito takes a bloodmeal, she probes throughout the dermis until she finds a suitable location, all the while depositing saliva and virus into the host. *In vitro* assays (capillary tube and blood droplet feeding) indicate that the mosquitoes deposit 10^{1}-10^{4} pfu (Styer, Bernard, and Kramer, 2006; Vanlandingham et al., 2004). *In vivo* assays (based upon the mosquito feeding on an ear or tail of a living host) estimated higher deposition titers of 10^{4}-10^{6} pfu, depending on the mosquito species (Styer et al., 2007). *Cx. pipiens* and *Cx. tarsalis*, the mosquitoes species implied to be critical in the transmission of WNV in the U.S., inoculated $10^{5.9}$-$10^{6.1}$ pfu and $10^{4.3}$-10^{5} pfu, respectively (Styer et al., 2007). Interestingly, a small amount was detected in the blood directly after feeding and this deposition may influence the kinetics of viral pathogenesis in the host (Styer et al., 2007).

Vertical transmission (usually transovarial transmission from mother to offspring) of WNV has been demonstrated in both the laboratory (Baqar et al., 1993; Reisen et al., 2006; Tesh, 1980) and in nature (Miller et al., 2000), but the importance of this mode of transmission in the overall transmission of WNV is unclear. Non-vertebrate transmission may be more important for maintaining WNV during the years when mosquito populations are low or for overwintering the virus.

Mosquito transmission is influenced by several factors. Mosquitoes live for a relatively short period of time in nature (up to ~ 1 month) and therefore, naïve mosquitoes are rapidly being produced. The species of mosquito also has a great impact on transmission since some mosquitoes are more permissive to infection and feeding behaviors may tend to favor certain species of vertebrate. Although many species of mosquito have tested positive for WNV infection in nature (Karabatsos,

1985)(http://www.cdc.gov/ncidod/dvbid/westnile/mosquitospecies.htm), members of the *Culex* genus were the most common captured mosquito to be repeatedly found positive for WNV in several outbreaks (Bernard et al., 2001; McIntosh et al., 1976; Savage et al., 1999; Taylor et al., 1956). In Texas, *Ae. aegypti, Ae. albopictus and Cx. p. quinquefasciatus* have all been implicated as competent vectors of WNV transmission (Vanlandingham et al., 2007). *Ae. aegypti* and *Ae. albopictus* are preferential anthropophilic feeders (Vanlandingham et al., 2007), while the *Cx. pipiens* are opportunistic and will feed on many species of both avian and mammalian hosts (Molaei et al., 2007). This promiscuous feeding may contribute to the wide number of avian and mammalian species found to be infected with WNV in nature. Additionally, the strain of the circulating virus can influence the kinetics of transmission. The NY99 strain has been replaced in nature with the new dominant genotype, WN02 (Ebel et al., 2004) (Davis et al., 2005). Viruses within the WN02 genotype have a 4-day shorter extrinsic incubation period in *Culex* mosquitoes (*Cx. pipiens* and *Cx. tarsalis*) than NY99, which may be due to a more rapid dissemination from the midgut (Ebel et al., 2004; Moudy et al., 2007).

Not much is known about the effect WNV infection has on the mosquito. There appears to be no detrimental effect of infection upon the mosquito as a whole. However, experimentally infected *Cx. pipiens quinquefasciatus* mosquitoes show damage at the cellular level (Girard et al., 2007). Cells in the midgut are infected 2 days post infection [dpi] after infection via a bloodmeal (Girard, Klingler, and Higgs, 2004) and these were identified as the first cells to be infected after feeding (Scholle et al., 2004). Apoptosis, or programmed cell death, was observed in midgut cells of mosquitoes that were refractory to disseminated WNV infection, suggesting that apoptosis prevented WNV from entering the heomcoel in these mosquitoes (Vaidyanathan and Scott, 2006). Extensive intracellular membrane proliferation is detected in infected salivary gland cells (Girard et al., 2007), which is consistent with ultrastructural studies conducted on mammalian cells. Long-term mosquito infection (21 dpi and older) leads to cytopathic effect and apoptosis in salivary gland cells, as well as slightly lower WNV titers than found for acutely infected mosquitoes in the saliva (Girard et al., 2007). The percentage of saliva samples

containing WNV also decreased with long-term infection. This suggests that the ability of the mosquito to transmit virus declines with age.

Non-vectored transmission

Experimental evidence indicates that WNV can be transmitted to a naïve vertebrate host without the mosquito vector. A raptor that died of an acute WNV infection in the middle of the winter in the absence of feeding mosquitoes suggested that transmission could occur via ingestion of virally infected prey (Garmendia et al., 2000). This observation has been supported by experimental infections. Several studies have indicated that ingestion of WNV-infected animals or WNV in solution can result in infection. Efficient oral transmission of a Nigerian WNV isolate was demonstrated in experimentally infected mice; virus was detected in the brain, lung, intestine, kidney, liver and blood and 80% of infected mice succumb to infection (Odelola and Oduye, 1977). Although these studies clearly demonstrated the ability to orally transmit WNV, the titers found in the ingested material, like the titers produced during an acute viremic state of infection, were high. It is unclear how efficiently lower titers would be transmitted by ingestion.

Direct contact between infected and naïve vertebrates can also result in WNV transmission. Geese housed in physical contact of experimentally infected geese were capable of being infected by WNV Isr98 (Banet-Noach, Simanov, and Malkinson, 2003) or the WNV strain 9/99 North American lineage Ia isolate (Swayne et al., 2001). Five out of seven crows housed with direct contact to WNV NY99-infected cagemates died of infection (McLean et al., 2001). Direct horizontal transmission of WNV NY99 has also been observed in Black-billed Magpies, Blue Jays and Ring-billed gulls (Komar et al., 2003). The ability of WNV to spread directly between birds through contact is supported by the presence of virus in oral and cloacal swabs in birds experimentally infected with WNV NY99 (Komar et al., 2003), suggesting the virus may be orally transmitted between cagemates.

Direct WNV transmission has not been experimentally demonstrated for mammals, but there is ample evidence of virus shedding. Viral RNA was present in oral, urine and fecal samples from experimentally infected fox squirrels during the first 12 days after infection of a lineage Ia WNV (Root et al., 2006). Similarly, WNV was isolated from oral and rectal swabs and from the urine of experimentally infected Eastern chipmunks on day 3 pi (Platt et al., 2007). Viral antigen was detected in the kidneys and virus was present in the urine of experimentally infected hamsters weeks after infection (Tesh et al., 2005; Tonry et al., 2005b; Xiao et al., 2001). Sixty percent of experimentally infected hamsters periodically shed infectious virus in their urine for over 230 days with an average titer on positive days of over 1,000 pfu/ml, suggesting the capacity to transmit the virus to a naïve host without the intermediate mosquito vector throughout the 8-month period (Tesh et al., 2005). However, naïve hamsters housed with WNV-infected cagements failed to shown evidence of infection (R.B. Tesh, unpublished data), suggesting that the rate of horizontal transmission in hamsters may be lower than the rates observed for birds.

The non-vectored flaviviruses, including Modoc virus (MODV), are assumed to be transmitted and maintained in nature without an arthropod vector (Burke and Monath, 2001). Attempts to infect mosquitoes with MODV have been unsuccessful (Johnson, 1967). Shedding virus in the urine (viruria) is a likely mechanism for the maintenance of MODV in nature (Davis and Hardy, 1974; Johnson, 1970). Horizontal transmission of MODV between rodents has been demonstrated with mixed success; oral transmission has been demonstrated in laboratory mice (Johnson, 1967), but naive deer mice (Davis, Hardy, and Reeves, 1974) or hamsters (Davis and Hardy, 1974) rarely became infected from their infected cagemates. Vertical transmission of MODV has not been convincingly demonstrated (Davis and Hardy, 1974; Davis, Hardy, and Reeves, 1974).

ARTIFICIAL MODES OF TRANSMISSION

Human WNV infections transmitted through unnatural routes have been documented and measures to prevent the spread of WNV via these routes have been

implemented. During the first few years after the introduction of WNV into North America, a small proportion of naïve patients became infected with WNV via blood and/or organs from infected donors (Anonymous, 2002; Biggerstaff and Petersen, 2003; Petersen and Marfin, 2002). This problem is evident based on the large percentage of infected yet seemingly healthy people (~80%) who could be viremic at the time of donation. In 2003, routine screening of blood donations was instituted in the US to identify contaminated specimens. Since 2005, there have been no documented cases of WNV transmission via blood transfusion (Stramer, 2007). However, shortly after this article was published, a potential case of blood transfusion acquired fatal WNV infection in 2006 was reported (Anonymous, 2007), highlighting the continued (albeit rare) risk of transmitting WNV infection via blood. Interestingly, the social benefit of unscreened organ donation has been shown by one manuscript to outweigh the need to ensure that all organs are free of WNV due to the percentage of false-positive samples detected during screening (Kiberd and Forward, 2004). Organs from donors that have no neurologic symptoms or recent febrile illness are considered safe for transplantation and are screened at the hospital's choice (http://www.optn.org/news/newsDetail.asp?id=303).

West Nile Virus Pathogenesis

Most pathogenesis studies have been performed under experimental conditions using a well-defined WNV stock at a previously quantitated titer. While these types of highly controlled experiments are critical to our understanding of flavivirus pathogenesis, some studies may not accurately reflect the events seen in nature. Most infections are performed using doses that would mimic those administered by a mosquito (see above): 10^2-10^5 pfu. These doses are sometimes also chosen since they will reproducibly produce disease. The route of infection varies based upon the purpose of the experiment, but in general, peripheral infections (including subcutaneous [s.c.], i.p., foodpad [f.p.] and intraveinus) of vertebrate hosts mimics mosquito infection.

AVIANS

Birds are an integral part of the WNV transmission cycle in nature. Infected birds produce viremias with high titers, and therefore are thought to be required for the maintenance of WNV. Despite the critical role of numerous avian species in WNV transmission, relatively few studies prior to the 1990s have focused on the natural history of WNV infection in birds. Recently, due to the increased virulence WNV in avians during the 1990s, many reports have detailed WNV pathogenesis in birds. One of the hallmarks of the New York 1999 outbreak was the abundance of dead birds (Eidson et al., 2001a). Prior to 1997, WNV infections were not associated with mortality in avian species. In 1998, a flock of white storks landed in Israel, and shortly thereafter, WNV was isolated from the brains of 13 dead or dying storks. The mortality of WNV goose flocks in Israel was so devastating that researchers investigated ways to vaccinate flocks using inactivated WNV and/or a commercially available vaccine against turkey meningoencephalitis virus (another flavivirus) in hopes of offering cross protection against WNV infection (Malkinson et al., 2001).

The New York 1999 outbreak was pivotal in spawning research that lead to our understanding on WNV infection in birds. Several species were infected with a NY isolate of WNV via mosquito bite to evaluate the kinetics and distribution of infection. Most, but not all, of the avian families tested developed a detectable viremia that was readily identified on day 1 pi and lasted for 5-7 days (Komar et al., 2003). Interestingly, the onset of detectable viremia was dependent upon the mode of infection; mosquito-infected crows had high viremia titers on day 1, but virus could not be detected in orally infected or contact-exposed crows until days 2 pi and day 6 pi, respectively (Komar et al., 2003). The highest viremia titers were produced in passerine and charadriiform birds (Komar et al., 2003). Passerine species (of which the American crow is a member) produced titers as high as 10 $\log_{10}$ pfu/ml of serum on day 3 pi (Komar et al., 2003). Those birds that became ill showed signs including ruffled feathers, lethargy and unnatural postures, and death followed less than a day later (Komar et al., 2003). Virus was detected in the brain, eye, heart, kidney, spleen, liver, lung, intestines, gonads,

esophagus and skin of birds necropsied after they succumb to infection (Komar et al., 2003). All American crows, common grackles, ring-billed gulls and house finches infected during this study died of infection (Komar et al., 2003). WNV is so virulent in American crows that these birds have been used as sentinels to detect circulating WNV (Eidson et al., 2001a; Eidson et al., 2001b).

American crows are not equally susceptible to all strains of WNV. Crows infected with Kenyan WNV (lineage Ia) or KUNV (lineage Ib) showed a low level viremia (less than 4 $\log_{10}$ pfu/ml serum at highest titer) whereas NY99 WNV-infected crows had a viremia of approximately 9 $\log_{10}$ pfu/ml serum (Brault et al., 2004). Only one crow died of Kenyan WNV infection and no KUNV-infected crows died from infection, but all NY99 WNV-infected crows died by day 6 pi, indicating that the lack of avian deaths noted in outbreaks prior to 1996 was not due to failure to detect dead bird populations or an innate susceptibility of the American crow to WNV (Brault et al., 2004). Interestingly, the enhanced virulence of the NY99 WNV strain in crows may be attributed to a point mutation (T249P) in NS3 (Brault et al., 2007).

RODENTS

Most of the current knowledge of WNV pathogenesis has originated from experimental infections of rodents. Most of these studies have focused on acute disease caused by lineage Ia viruses, especially the NY99 strain, with the goals of understanding the natural history of infection in man and developing models needed to evaluate vaccine candidates and therapeutics. The natural course of WNV infection is dependent upon several factors including the age of the rodent, the viral dose and the route of inoculation. For most experiments, virus is delivered via needle inoculation, which may not accurately reproduce the course of infection in nature (Schneider et al., 2006).

Mice

Mice are the most commonly used animal model to assess WNV virulence and pathogenesis and to identity the factors of the immune system that are responsible for

limiting the infection. WNV inoculated into the periphery either via mosquito infection (natural infection) or by needle (experimental infection) replicated and caused a viremia similar to that described for birds. Within 24 hours post infection (hpi), virus was detectable in the blood and this viremia typically peaked on days 3-4 pi (Chambers and Diamond, 2003; Kramer and Bernard, 2001). Beginning at 48 hpi, virus was be found in the heart, spleen, kidney and lymph nodes (Chambers and Diamond, 2003). Anti-WNV IgM coincided with a waning viremia and viral load in the organs (Diamond et al., 2003a). WNV-infected mice were usually healthy during the first 5 dpi. Around day 6, signs of illness (ruffled fur and lethargy) were observed and these signs rapidly progressed to neurological disease (ataxia and paralysis) and death. Severe illness correlated with large numbers of infected neurons (Shrestha, Gottlieb, and Diamond, 2003) and a high viral load (Diamond et al., 2003a; Kramer and Bernard, 2001) in the brain. These infected neurons died of apoptosis (Diniz et al., 2006; Samuel, Morrey, and Diamond, 2007; Shrestha, Gottlieb, and Diamond, 2003) and depleted this non-renewable cell type was believed to result in neurological disease.

Genetically altered mice have provided insight into the factors that help control lethal WNV (Samuel and Diamond, 2006). Both T (Shrestha and Diamond, 2004; Shrestha, Samuel, and Diamond, 2006; Sitati and Diamond, 2006; Wang et al., 2003) and B (Diamond et al., 2003a) cells help control infection. Antibodies, especially early IgM, limit virus dissemination into the CNS and reduce levels of viremia (Diamond et al., 2003b). Molecules involved in the innate immune response are also important to controlling the spread to WNV infection, including type I IFN (IFN α and β) (Samuel and Diamond, 2005) and type II IFN (IFN γ) (Shrestha, Samuel, and Diamond, 2006). TLR3, a molecule that detects and responds to dsRNA (see above), may contribute to WNV neuroinvasiveness (Wang et al., 2004).

In many experimental infections, the virus is delivered by needle, but this mode of infection may not produce a disease that accurately mimics that seen in nature. Mice infected with WNV in the presence of mosquito salivary gland extract (SGE, used to mimic saliva) or by a WNV-infected mosquito died sooner than mice infected with WNV

alone (Schneider et al., 2006). There was a higher WNV viremia (day 2 pi) and viral load in the brain (days 4 and 7 pi) in mice infected in the presence of a feeding mosquito than with WNV alone, indicating that the presence of mosquito saliva enhances WNV infection in the mice (Schneider et al., 2006). Sensitizing mice with mosquito saliva (by feeding mosquitoes) prior to WNV infection can enhance early viremia levels and significantly impact the virulence of the virus in mice, presumably via the recruitment of WNV-susceptible immune cells to the site of saliva and virus deposition (Schneider et al., 2007).

Hamsters

The course of infection in hamsters is similar to that described for mice. Golden Syrian hamsters infected i.p. with $1x10^4$ $TCID_{50}$ units of virus display no signs of illness during the first 3 dpi (Morrey et al., 2004) or 5 dpi (Xiao et al., 2001). Viremia is detected 24 hpi and peaks by day 2-3 pi (approximately 10^5 $TCID_{50}$/ml serum), followed by a reduction in titer that is undetectable by day 7 pi (Xiao et al., 2001). Young hamsters (4-5 weeks) had early (2-5 dpi) and high titer ($10^{4.3-5.9}$ $TCID_{50}$/ml serum) viremia, which is consistent with the results described by Xiao and colleagues. In older hamsters (7-11 weeks), viremia was found later (3-5 dpi) and reached lower titers ($10^{3.6-4.9}$ $TCID_{50}$/ml serum) (Morrey et al., 2004). Anti-WNV antibody titers are first detectable on day 5 pi (Xiao et al., 2001). On days 6-9 p.i., WNV antigen and severe pathology accompanied by apoptotic cells in the CNS were noted (Xiao et al., 2001). Some hamsters display signs of illness starting on day 6 (lethargy) and progresses to neurologic symptoms by day 7-10, which is characterized by tremors and difficulty walking and maintaining balance (Xiao et al., 2001). A high viral load ($10^{3-6.5}$ $TCID^{50}$) is detected in the brains of hamsters that died following neuralogic illness (Xiao et al., 2001).

NON-HUMAN PRIMATES

WNV infections in nonhuman primates generally do not produce signs of illness. Rhesus monkeys experimentally infected with $1x10^5$ pfu of NY99 WNV intradermally

produced a viremia detectable by RTPCR that lasted for the first 5 dpi (Ratterree et al., 2004). The waning viremia was coincident with the detection of anti-WNV antibodies in the serum. Neutralizing antibodies were first detected on day 9 pi and interestingly, one of the five infected monkeys still had high IgM titers on day 45 pi (Ratterree et al., 2004). All five experimentally infected monkeys produced no detectable signs of illness (Ratterree et al., 2004). In support of the data obtained during experimental infections, captive primates naturally exposed to WNV (lineage Ia) in southern Louisiana in the summer of 2002 also developed antibodies against WNV in the absence of any reported illness (Ratterree et al., 2003). However, some monkeys developed encephalitis when WNV was injected directly into the brain (Pogodina et al., 1983; Smithburn et al., 1940). This is consistent with the observation that many viruses that are attenuated when injected in the periphery of a mouse are still neurovirulent following i.c. inoculation.

HUMANS

The infrequent nature of symptomatic human WNV infections made it difficult to understand the full range of pathology and symptoms. Some strains of WNV, like lineage Ib and II strains, are naturally less virulent in humans, as determined from the symptoms of patients during outbreaks. However, recent infections in North America with the highly virulent WNV strains have provided a wealth of knowledge about the transmission and symptomology of lineage Ia WNV infections. Relatively little is known about the timecourse of events during a human infection since experimental studies cannot be ethically conducted. Serum gathered from individual volunteers (naturally infected) during the Israeli outbreak in the 1950s revealed that virus was detectable in the blood of patients prior to (as well as during) the presentation of symptoms (Goldblum, Sterk, and Jasinskaklingberg, 1957), which is consistent with the viremia and onset of illness data obtained from experimental infections in mice. There is also a correlation between the length of viremia and disease severity (Goldblum, Sterk, and Jasinskaklingberg, 1957). The majority of human WNV infections are asymptomatic. If symptoms occur, they are estimated to do so 7-14 dpi. Fewer than 20% of infections result in West Nile fever

(WNF), which is characterized by fever, malaise, anorexia, headache, nausea and sometimes rash (Petersen and Marfin, 2002). This febrile illness typically lasts 3-6 days. Severe symptoms, including encephalitis, meningitis, and paralysis, are less common and occur in approximately 1 out of every 150 infections (Petersen and Marfin, 2002). Risk factors for developing severe illness include age and a compromised immune system (Anonymous, 1999; Petersen and Marfin, 2002). Patients over the age of 70 were at a much higher risk of dying from the infection than younger patients (Petersen and Marfin, 2002).

West Nile Virus Persistence

Persistent infections have been demonstrated following infections from viruses in all three genera of the family *Flaviviridae*. HCV readily establishes persistent infections in more than 80% of infected patients (Major, Rehermann, and Feinstone, 2001). JEV (Mathur et al., 1986; Ravi et al., 1993; Sharma et al., 1991), St. Louis encephalitis virus (Siirin et al., 2007), MODV (Johnson, 1970), TBEV (Gritsun et al., 2003; Pogodina et al., 1981) and Rio Bravo virus (Constantine and Woodall, 1964) have all been documented to cause persistent infections in mammals, although some of these flaviviruses are more generally associated with self-limiting acute infections.

WNV persistence has been reported following experimental infections of birds, hamsters and monkeys. Chronic infections have been experimentally demonstrated in several bird species. Birds were injected with s.c. with $1x10^3$ pfu of NY99 WNV and survivors were housed for over 6 weeks, after which select organs (sera, lung, spleen and kidney) were removed and tested for the presence of WNV infection by RTPCR (Reisen et al., 2006). Thirty-four percent of all birds tested contained at least one organ that was positive for WNV RNA, including one house sparrow with RNA present in its serum (Reisen et al., 2006). Over half of the infected house finches were persistently infected as detected by RTPCR and infectious virus was recovered from extracted tissues cultivated in C6/36 cells (Reisen et al., 2006). With few exceptions, viral RNA was not present in

the serum, indicating that persistent infections are found in the organs and not circulating within the blood (Reisen et al., 2006). The authors speculated that chronically infected birds may 'relapse' and shed infectious virus in the serum upon reactivation, so these persistent infections in birds may be capable of reintroducing the virus into a feeding mosquito and initiating transmission (Reisen et al., 2006).

WNV persistence has been reported in Syrian hamsters; NY99 WNV was recovered from the brains (Xiao et al., 2001) and urine (Tonry et al., 2005b) of experimentally infected hamsters at 52 dpi. Hamster-passaged NY99 WNV passaged was capable of producing high-titer viruria, chronic kidney infection, reduced neurovirulence and increased renal tropism compared to its parental virus in infected hamsters (Tesh et al., 2005). Several mutations in the E, NS1, NS2B and NS5 proteins were observed in viruses isolated from a persistently infected hamsters, but the contribution of these individual mutations on the propensity of the virus to persist in the kidney and be shed in the urine is unknown (Ding et al., 2005). Evidence from primary cultures of murine astrocytes, a type of brain cell, suggests that this cell type can harbor a productive persistent WNV infection and may contribute to persistent WNV infections in the CNS (Diniz et al., 2006).

In the case of rhesus monkeys, Pogodina and colleagues analyzed the survivors of intrathalmic or s.c. infections with several different WNV strains (Pogodina et al., 1983). Virus isolation from tissue homogenates or by antigen detection in tissues harvested at the time of necropsy identified several persistently infected (defined by isolation at and after 20 dpi) animals (Pogodina et al., 1983). No correlations between the ability to establish persistence and the severity of illness could be drawn from these experiments (Pogodina et al., 1983). Persistently infected monkeys had anti-WNV neutralizing antibodies, indicating that the inability of the animals to clear the infection was not due to an ineffective humoral immune response and that persistent infections could exist in the presence of a functional antibody response (Pogodina et al., 1983). Interestingly, viruses isolated 5 months pi from persistently infected monkeys were less virulent in white mice than the parental inoculated virus (Pogodina et al., 1983).

There have only been two reports of persistent infections in humans and both demonstrate long-term WNV antigen or genome detection in immunosuppressed individuals. The first case involved a 50-year-old woman with a viremia detectable by RTPCR for longer than 60 days (Brenner et al., 2005). Viral RNA was also detected in the cerebrospinal fluid (CSF) (Brenner et al., 2005). At the time of her admittance to the hospital, she was febrile and weak, but her symptoms worsened to encephalitis, seizures and paralysis (Brenner et al., 2005). At the time of her death from pneumonia, serum and CSF were RTPCR negative for WNV RNA (Brenner et al., 2005). The second case involved a 57-year-old man on chemotherapy whom also had prolonged viral RNA in his serum and CSF and was admitted to the hospital with fever and weakness (Penn et al., 2006). Viral RNA was detected by RTPCR in his serum (up to day 30) and CSF (up to day 77) as well as viral antigen in his nervous tissue, but no anti-WNV antibodies were generated during the infection (Penn et al., 2006). The autopsy report revealed severe damage to the neuronal tissue (Penn et al., 2006), which is consistent with the reports of apoptotic death in the neurons of experimentally infected mice and hamsters (see above).

Although there are only two documented cases of persistent WNV infection in humans, there is indirect evidence of long-term WNV infection. Many patients display long-lasting WNV-specific IgM antibody (Kapoor et al., 2004; Prince et al., 2005; Roehrig et al., 2003), which is typically considered indicative of acute viral infections, suggesting ongoing low levels of antigen production. Isotype switching to IgG antibodies is expected later in infection. Antibody production to WNV infection could be affected by the immunocompromised nature of many symptomatic patients. Persistence in asymptomatic individuals has not been reported, but these have been no reported failures to detect this type of infection in patients either. Data from infected hamsters suggest testing urine to identify persistently infected patients rather than by the presence of anti-WNV antibodies, and WNV could only be detected in a patient's urine during the acute phase of illness (Tonry et al., 2005a).

Impetus for this Research

Most WNV infections in vertebrates and vertebrate cell lines are acute. At the beginning of this dissertation, little was known about the ability of WNV to cause a persistent infection, or the host/viral factors that influenced persistence. Most likely, a persistent WNV infection results from the combination of a number of viral and cellular events and the interaction between them. Therefore, changes to these factors or the way these factors interact with each other could have a dramatic effect on the duration of infection. The goal of this research was to define the viral factors that influenced the ability of the viral genome to persist in cell culture. To achieve this goal, a subgenomic replicon genome forced to replicate within mammalian cells in culture was used to identify changes within the genome that resulted a noncytopathic, presistent infection. These cell-adapted, noncytopathic genomes produced less viral antigen than wt genomes in cell culture. These initial results led to the generation of this overall hypothesis for this dissertation, *mutations selected during the establishment of WNV replicon-bearing cells will reduce the levels of replicon and viral genome replication, thereby avoiding the cell's antiviral responses and enabling persistent infection of the host cell*. The specific aims that were outlined in the dissertation proposal were: **(1)** demonstrate that cell-adapted mutations selected during establishment of persistent WNV subgenomic replicon infection confer an adapted phenotype in cell culture, **(2)** determine the effect of these cell-adapted mutations on viral replication *in vitro* and virulence *in vivo* and **(3)** demonstrate reduced apoptotic and type I interferon responses in cells infected with WNV or subgenomic replicons encoding cell-adapted mutations.

The research summarized in this dissertation expands upon the knowledge of WNV replication and the affects of replication on the duration of infection. With this knowledge, we can better understand how the interaction between the virus and host cell are altered (compared to a wt cytopathic infection) to favor a persistent infection. Data gathered within the last 5 years from human serology suggest and natural human infections as well as experimental infections in laboratory animals indicate that infections

can become persistent within a proportion of infected individuals. Recently, there have been numerous studies that identified, characterized and altered the interactions between the host cell and WNV genome. This field is rapidly changing as new proteins are being described and/or new functions for previously described molecules are being determined. The effect of the virus on the cell's innate immune response has also widely studied in the recently years, but there are still many unanswered questions.

CHAPTER 2: GENERATION AND CHARACTERIZATION OF REPLICON-BEARING CELLS[2]

Abstract

WNV subgenomic replicons (WNR) are an effective tool for studying the interactions between the viral genome and the host cell in the absence of virion production. To identify factors that influenced the ability of a WNR genome to persist in cell culture, several cell types were electroporated with the WNR RNA that encoded the antibiotic resistance gene neomycin phosphotransferase (NPT) and cells that contained an actively replicating WNR were selected using the antibiotic G418. Individual G418-resistant cells could grow into colonies, which were amplified into replicon-bearing clonally-derived cell cultures. The percentage of G418-resistant cell colonies depended greatly upon the cell type used: BHK and Vero cells readily produced G418-resistant colonies whereas relatively few antibiotic-resistant Huh7 colonies were obtained. During the process of generating the WNR-bearing clones, multiple cell-adapted mutations were selected relative to the parental (unadapted) WNR that reproduced noncytopathically and produced sufficient levels of NPT. Interestingly, one mutation in the NS4B protein (E249G) was found in nearly all clonally derived G418-resistent cultures and more than half of the cell-adapted genomes contained a mutation within the NS2A protein. Many mutations observed in the WNR harvested from WNR-bearing clonally derived cultures were engineered into the WNR by reverse genetics. These mutant WNR genomes were

[2] A significant portion of this chapter has been previously published in two manuscripts in Virology in 2005 and 2007. Virology does not require copyright permission as long as proper citation is provided. The citations for those articles are:

S.L. Rossi, R.Z. Fayzulin, N. Dewsbury, N. Bourne and P.M. Mason (2007) Mutations in West Nile Virus Nonstructural Proteins that Facilitate Replication Persistence in Vitro Attenuate Virus Replication in Vitro and in Vivo. Virology 364(1): 184-195.

S.L. Rossi, Q. Zhao, V. O'Donnel and P.W. Mason (2005) Adaptaton of West Nile Virus Replicons to Cells in Culture and Use of Replicon-Bearing Cells to Probe Antiviral Action. Virology, 331(2): 457-470.

retested for their ability to generate WNR-bearing cells. Three cell-adapted mutations, one within the NS3 protein (117Kinsertion) and two within the NS2A protein (D73H and M108K), were able to increase the percentage of WNR-transfected cells that were capable to forming G418-resistant colonies compared to the wt WNR. These data indicate that the wt WNR must change to efficiently produce an antibiotic-resistant, noncytopathic replicon infection in Huh7 cells, but this pressure was not as strong in BHK or Vero cells.

Introduction

REPLICON CDNA CLONES

Infectious cDNA clones are extremely useful and important tools to study the molecular biology of RNA viruses. These clones are generated by inserting a cDNA version of the genome into a plasmid but between a DNA-dependent RNA polymerase promoter, a polymerase termination sequence and a unique restriction endonuclease (RE) site downstream of the terminator. Oftentimes, a ribozyme is added at the end of the 3' UTR to ensure that the genome has an authentic end (rather than one created by RE cut site), which results in an efficient viral genome replication. The RNA polymerase promoter allows for the genome inserted directly after to be transcribed into genomic (infectious viral) RNA. An RNA genome can be generated by an *in vitro* transcription reaction using the cDNA-containing plasmid as a template. These plasmids can be introduced into bacteria, which maintain the plasmid during their growth and amplification. Placing the flavivirus RNA genome into DNA form has offered many advantages (described in detail in Chapter 3), but one of the most important consequences has been the ability to manipulate the genome. Reverse genetic molecular techniques allow for the manipulation of the cDNA genome to create insertions, deletions, or mutations. The altered cDNA plasmid is used as a template to create the altered RNA genome. These deliberate alterations of genomes have allowed for the detailed description of the requirements of genome replication, packaging and processing and

expanded the knowledge base of flaviviriology. Such characterizations would have been exceedingly difficult if infectious cDNA clones and reverse genetic technologies did not exist.

Deletion studies of the flavivirus genome indicated that the majority of the structural gene-encoding nucleotide sequence is dispensable with regard to flaviviral RNA genome replication. Subgenomic RNA capable of self-replication (replicon) has been described by deletion studies. These replicons lack the structural genes, and as a result, no virions can be produced from this infection. This marooned infection enables the analysis of aspects of the viral genome replication. Replicons have been reported for KUNV (Khromykh and Westaway, 1997), WNV (Shi, Tilgner, and Lo, 2002), YFV (Corver et al., 2003; Molenkamp et al., 2003), DENV (Pang, Zhang, and Dayton, 2001), and TBEV (Gehrke et al., 2003; Hayasaka et al., 2004). Flavivirus replicon genomes are often engineered to contain foreign genes, including markers [like green fluorescent protein (GFP), firefly or renilla luciferase or chloramphenicol acetyltransferase (CAT)] or antibiotic resistance genes [like NPT or puromycin N-acetyl transferase (pac)], to easily identify or select cells that contain the replicating replicon RNA. In some cases, an IRES is added (usually inserted within the 3' UTR) to help drive the translation of these reporter/selection genes. In other replicons, the foreign gene is inserted in the ORF in lieu of the structural genes. The level of reporter gene correlates with the level of RNA replication and levels of viral protein expression, making these markers useful tools to measure genome replication.

WNV REPLICON-BEARING CELL LINES

Cells that harbor a replicon can be selected using antibiotics if the replicon genome contains an antibiotic-resistance gene. The most common combination is a flavivirus replicon containing the NPT gene and selecting for replicon-bearing cells using G418. This compound is toxic for cells that do not contain the NPT gene, and therefore allows for the selection of cells that contain an NPT gene. Many replicon-bearing cell lines have been created and used for a variety of purposes. Interactions between the WNR

or KUNV replicon (KUNR) and host cell with regard to the innate immune response have been extensively studied in replicon-bearing cells (Fredericksen and Gale, 2006; Gilfoy and Mason, 2007; Guo, Hayashi, and Seeger, 2005; Khromykh and Westaway, 1997; Liu et al., 2004; Liu et al., 2005; Scholle and Mason, 2005; Yamshchikov et al., 2001). The interactions between flavivirus replicon-bearing cells and the innate immune response are further discussed in Chapter 5. Replicon-bearing cell lines have also been used as a efficient screening tool to identify antiviral compounds (Chang and George, 2007; Gu et al., 2006; Lo, Tilgner, and Shi, 2003; Puig-Basagoiti et al., 2005; Shi, 2002a). Potential drugs can be tested for both their toxicity and their effectiveness in reducing WNR infection. Cells bearing WNR (Shi, Tilgner, and Lo, 2002) or Kunjin virus replicons (Khromykh and Westaway, 1997; Liu et al., 2004) have been created to address certain aspects of flavivirus replication in the cell. An advantage of these cells is that the viral components that are responsible for replication can be studied without interference from virion packaging and virus shedding. Therefore, these cells can used under biosafety level (BSL) 2 conditions rather than the BSL3 conditions needed to work with WNV. Once the replicon has been adapted to the cell, the genome replicates without causing cytopathic effect [CPE] (Khromykh and Westaway, 1997; Shi, Tilgner, and Lo, 2002). Furthermore, these replicon-bearing cells are stable and can be maintained for long periods of time without losing the WNR genome.

GENOME ADAPTATION TO CELLS IN CULTURE

In order to generate a cell that will persistently harbor a flavivirus replicon, there must be an equilibrium between the antiviral response of the cell and the cytopathogenicity of the replicon. There are many ways in which this is achieved. In some cases (WNR, KUNR, and Sindbis replicons), the replication of the introduced replicon must be reduced, and in some cases (HCV) the replicon needs to be replicated to higher levels.

KUNR (containing the pac and β-galactosidase genes) were adapted to BHK cells, and the β-galactosidase expression from several KUNR-bearing clones showed a

wide range of expression (Liu et al., 2004). Some KUNR-bearing BHK clones had no difference in the level of KUNR replication, other clones contained KUNR that replicated more poorly (Liu et al., 2004). A reduction in WNR antigen accumulation may have also been observed in WNR-bearing BHK-21 cells described by Shi and colleagues as measured by immunofluorescence staining (Shi, Tilgner, and Lo, 2002). Sindbis virus replicons (SINR) that harbored the pac gene under the 26s subgenomic promoter were also transfected and selected to persistently replicate in BHK cells (Frolov et al., 1999). Two SINR-bearing clones contained mutations in the SINR nsP2 gene (position 726 and 779) (Frolov et al., 1999). When these mutations were introduced into the parental SINR and re-transfected into BHK cells, all transfected SINR cells could form pac-resistant cultures (Frolov et al., 1999). A detailed analysis of a panel of amino acid substitutions at the 726 nsP2 locus revealed that most introduced mutations reduced SINR genome replication (Frolov et al., 1999).

Plasmids carrying HCV replicon cDNA encoding the NPT resistance gene were constructed (Lohmann et al., 1999). Antibiotic-resistant colonies were harvested and sequenced cell-adapted HCV genomes revealed several mutations in NS5A upstream of the interferon sensitivity determining region that increased colony formation and genome replication, but had no effect on IFN sensitivity (Blight, Kolykhalov, and Rice, 2000). HCV replicons "long-term" adaptation to cell culture acquired mutations that had the ability to increase replication, increase colony formation efficiency, were resistant to IFNα and had reduced expression of antiviral products (Sumpter et al., 2004). Additional mutations were observed by other group in every region of the replicon except for NS4A and the 5' or 3' UTRs; most of the individually expressed mutations were able to increase the percentage of antibiotic-resistant colonies, but were not always synergistic when expressed in pairs or groups (Krieger, Lohmann, and Bartenschlager, 2001; Lohmann et al., 2001). Two sets of mutations, one at NS5B R2884G and the other pair of NS3 E1202G/S2197P, were able to increase colony formation efficiency by ~500 and ~10,000 fold over the parental replicon, respectively (Krieger, Lohmann, and Bartenschlager, 2001; Lohmann et al., 2001). It is hypothesized that although the replication of HCV

replicons during transient transfection is high, cell-adaptive mutations are necessary to retain a high level of replication and therefore antibiotic-resistance (Krieger, Lohmann, and Bartenschlager, 2001).

RATIONALE

Based upon previous studies of replicon-bearing cells, it was expected that the generation of WNR-bearing cell clones would be accompanied by changes to the WNR genome (compared to the wt WNR genome) and a reduction in WNR genome replication. This observation was the foundation for the generation of the first specific aim of this dissertation, to demonstrate that cell-adapted mutations selected during establishment of persistent WNV subgenomic replicon infection confer an adapted phenotype in cell culture. It was, therefore, hypothesized that replicons present in antibiotic-selected, replicon-bearing cell clones harbored mutations that conferred the adapted phenotype.

Materials and Methods

CONSTRUCTION OF THE WEST NILE VIRUS REPLICON GENOME

A WNR infectious cDNA clone was generated based on an isolate taken from an immunocompromised patient in Texas in 2002. A series of overlapping RTPCR products that ran the length of the genome were ligated together into a low-copy plasmid using unique RE sites found in the RTPCR products (Figure 8A). The WNR cDNA sequence was inserted downstream of a T7 RNA polymerase promoter and before the T7 termination and hepatitis delta virus ribozyme sequences. The ribozyme was included to generate a clean cut at the end of the 3' UTR. WNR NS1-5 RNA (produced from an *in vitro* transcription reaction that used the WNR clone as a template) was infectious, since antigen-positive cells could be visualized using immunohistochemical staining. Detection of viral antigen was limited to those cells initially electroporated and their daughter cells, indicating that this replicon genome was unable to package and cause a spreading infection within the culture.

Figure 8: Replicon and Full Length Infectious cDNA Construction

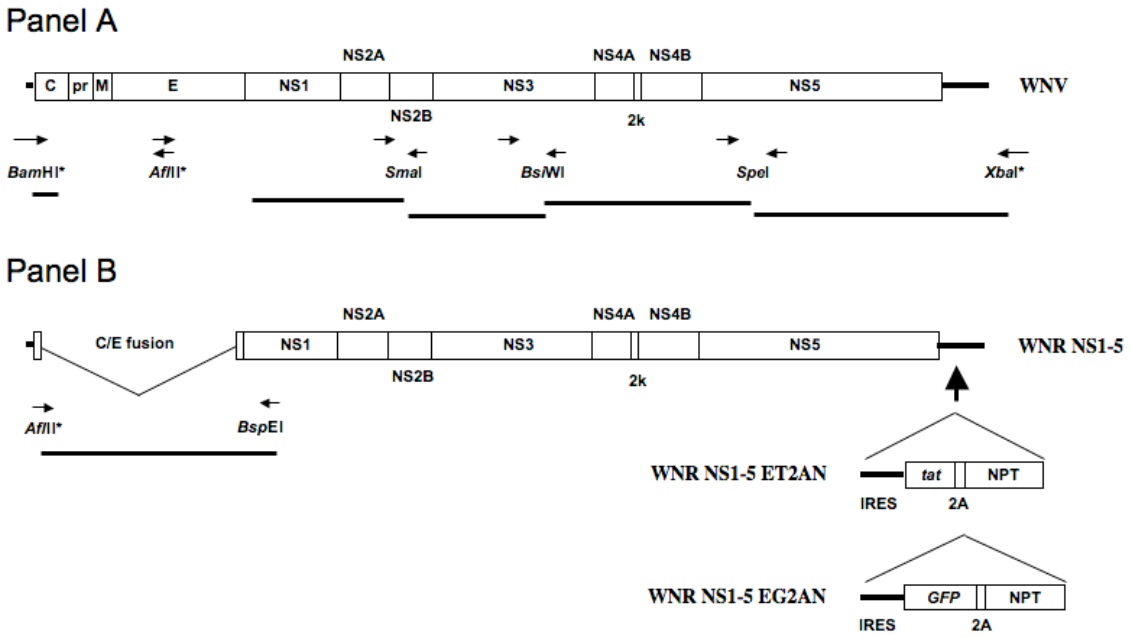

Figure 8: Schematic diagrams of the WNV and WNR. **(Panel A)** A diagram of the WNV genome. Thick horizontal bars show the RTPCR products and the unique restriction enzyme cites flanking the product ends. *Bsp*EI, *Sma*I, *Spe*I and *Nsi*I were found within the genome and *Bam*HI, *Afl*II and *Xba*I sites were created using oligo-directed site mutagenesis. **(Panel B)** The WNR NS1-5 replicon was used as the basic construction to generate the full-length infectious clone (WNV) and the minipolyprotein-encoding replicons. The minipolyprotein, which was inserted into the 3' UTR at the *Nsi*I sites, contained NPT and a reporter gene (tat in WNR NS1-5 ET2AN or GFP in WNR NS1-5 EG2AN) under the control of an EMCV IRES.

CELL LINES USED AND THEIR MAINTENANCE

Vero 76 (green monkey kidney) cells were obtained from R.B. Tesh. I. Frolov kindly provided the BHK (baby hamster kidney) as well as mouse embryo fibroblast (MEF) and RNaseL$^{-/-}$ MEF cells. J. Durbin (Ohio State University) provided the STAT1$^{-/-}$ MEF cells. Huh7 (human hepatocarcinoma) and HeLa (human cervical cancer) cells were obtained from S. Lemon. Huh7.5 cells were a gift from C. Rice. L293 cells were kindly provided by R. Davey. Multiple mammalian cell lines were used during these studies. K.

Narayanan provided the A459 and Hec1B cells. MRC5 cells were purchased from ATCC.

Vero cells were grown in Modified Eagle's Media (MEM) supplemented with 6% Fetal Bovine Serum (FBS, Hyclone), 1x antibiotic/antimycotic solution (abx, Invitrogen) and 20 μg/ml gentamycin. BHK cells were maintained in MEM with 10% FBS (Gemini), 1x abx and 20 μg/ml gentamycin. Huh7 and HeLa cells were maintained in Dubecco's MEM (DMEM) with 10% FBS (Hyclone), 1x abx and 20 μg/ml gentamycin. Hec1B cells were grown in DMEM with 10% FBS (Hyclone) with 1x abx, 1% nonessential amino acids (NEAA), 1% sodium pyruvate (NaPyr) and 20 μg/ml gentamycin. A549 and MRC5 cells were maintained in DMEM with 10% FBS (Gemini) with 1x abx, 1% NEAA, 1% NaPyr and 20 μg/ml gentamycin. MEF cells (wt, $STAT1^{-/-}$ and $RNaseL^{-/-}$) were maintained in DMEM with 5% FBS (Gemini), 1x abx, 1% NEAA, 1% NaPyr and 20 μg/ml gentamycin. All cells were maintained at 37°C with 5% carbon dioxide.

Cells bearing replicons encoding NPT were selected and maintained by the addition of G418 to their growth media. The concentration of G418 varied depending on the cell line, although most cells were maintained in 400 μg/ml G418. Higher concentrations of G418 were necessary to kill untransfected L293 and Vero cells. In these cases, 600 μg/ml and 800 μg/ml of G418 in the growth media were required for L293 and Vero cells, respectively.

IDENTIFYING CELL-ADAPTED MUTATIONS

Total RNA was extracted from G418-resistant clones of cells bearing replicons in tissue culture flasks (typically a confluent monolayer in a T75 or T150 flask) by using either the RNaqueous kit (Ambion) or Trizol LS Reagent (Life Technologies). Manufacturer's recommendations and products were followed to extract RNA using the RNaqueous kit. For the Trizol LS Reagent-based extraction, the samples were lysed in a mixture of media (25% of final volume) and Trizol LS (75% of final volume) and allowed to sit for 10 minutes. One millileter of Trizol LS/media was sufficient to lyse a T75 flask. A cell scrapper was used to dislodge and collect the lysed monolayers, which

were then pipetted several times to reduce the viscosity and transferred to an eppendorf tube. At this point, the lysates were either frozen at -80°C or processed directly by adding chloroform and extracting the aqueous phase containing the RNA, which was precipitated by adding isopropanol. RNA was resuspended in nuclease-free water supplemented with an RNase inhibitor and was quantified by spectrophotometry at 260 nm. Approximately 1 μg of extracted RNA was used as a template for reverse transcription (RT) reactions (using the ImProm II kit, Promega) using either 1.25 μl of 2 μg/μl random hexamers and/or 10 μM specific anti-sense primers that anneal at the end of the 3′ UTR of WNV (U8n: 5′ AGATCCTGTGTTCTCGCACC 3′). The RT reaction was treated with an equal volume mixture of RNases H and T_1 at 37°C for 15 minutes to degrade the extracted RNA. The generated cDNA was then used for the template in subsequent PCR reactions.

PCR reactions were performed using a high-fidelity polymerase (Herculase [Strategene] or AccuTaq [Sigma]) WNV-specific primer pairs are shown in Table 7 (in appendix). All PCR reactions used to amplify the NS2A genes were done using U129 and U28 (Table 7). These products were purified by agarose gel electrophoresis and extracted from the gel using the Qiagen gel extraction kit. Final elutions were made in water and the products were sequenced at the Protein Chemistry Core Facility at UTMB using a variety of sequencing primers that annealed within the PCR product (see Table 7). Sequences were compared to the previously sequenced parental WNR plasmid using the Sequencher software program (Gene Codes).

ENGINEERING SELECTED CELL-ADAPTED MUTATIONS INTO THE PARENTAL WNR

PCR-amplified cDNA fragments collected from replicon-bearing cells were cloned into replicon-encoding low-copy plasmids (pACNR) using standard molecular DNA techniques. In some cases, PCR products were introduced into intermediate plasmids to be sequenced and screened prior to being cloned into the WNR NS1-5 ET2AN plasmid. The NS2A D73H and M108K mutations were generated by PCR amplification from the WNR RNA harvested from the Huh7 1.1 and 11.6 clones, respectively.

In other cases, oligo-mediated mutagenesis was also used to generate some fragments for cloning. The primers indicated below contained the introduced mutations in lowercase font. Some mutations altered the nucleotide sequence that introduced or destroyed a naturally occurring ER site. The NS2A D73H mutation destroyed a naturally existing *Bsm*BI site, so genomes harboring this mutation were distinguished from non-mutated genomes by digestion with this enzyme. If a restriction site was added to create a marked genome that did not alter the encoded protein, it is denoted in blue text. The NS2A A30P, NS3 117Kins, NS4B E249G and NS5 P528H mutants were created in this way. The NS2A A30P was introduced using a primer encoding the NS2A A30P mutation and a naturally occurring *Sph*I site (U170: 5' AGCTGGCATGCTGATCTTGG GTGTCC). Some mutants interest were recreated by overlap PCR mutagenesis (Higuchi, Krummel, and Saiki, 1988). The NS3 117Kinsertion mutation was introduced (shown as bold-faced type in the oligo sequence) using oligo-directed mutagenesis using the following two primers in an overlapping nested PCR reaction using the following primer set: (U294) 5' CCTTCCGGAGTTTT**ctt**GAACACCCCTGGTTTCGT and (U295) 5' C**aag**AAAACTCCGGAAGGAGAAATCGGG. These primers introduced a *Bsp*EI site without changing the amino acid coding sequence. The NS4B E249G mutation was created similarly to the NS3 117Kins mutation using the primers (U137) 5' CATAAAGAACATGGgAAAACCAGGCCTAAAAAGAGGTGGGGCA and (U138n) 5' GCCCCACCTCTTTTTAGGCCTGGTTTTcCCATGTTCTTTATGAG. Within these primers is a silent mutation that encodes a *Stu*I restriction site for easy identification of the mutation. The NS5 P528H mutation was also introduced by overlapping PCR mutagenesis. These oligos were (U199) 5' GAAGTTGGCATCCGCCaTGG CGGCAAGATCTATGCTG and (U200) 5' CAGCATAGATCTTGCCGCCAtGG CGGATGCCAACTTC. An *Nco*I RE site was added to mark the genome with the NS5 P528H.

To introduce the mutated PCR fragment into the WNR NS1-5 ET2AN clone, the PCR amplicon was cut with the same restriction enzymes that were used to cut the wt WNR product. Digestion products were purified using agarose gel electrophoresis. These

fragments were ligated together using T4 DNA ligase (NEB) and transformed into TOP10 competent *E. coli* cells and plated on Terrific or LB broth plates supplemented with 50 μg/ml of ampicilin. Plates were incubated at 30°C or 37°C overnight. Colonies that contained the desired plasmid clone were grown in Terrific or LB broth supplemented with ampicilin shaking in a heated incubator overnight. A permanent stock of the culture was created by adding an equal volume of the turbid culture into a 50% glycerol in water solution, which was then stored at -80°C. When the cultures became turbid, the bacteria were pelleted by centrifugation. Plasmid DNA was extracted from the bacteria, most often by cesium chloride gradient. All mutant cDNA plasmid clones were sequenced through the PCR-amplified region to ensure only the desired missense mutations were present. In some cases, identification of the desired clones was facilitated by the deliberate introduction or natural occurring RE sites within or directly next to the introduced mutation.

LARGE-SCALE PLASMID PREPARATIONS BY CESIUM CHLORIDE GRADIENTS

In most cases, when the final cDNA cloned candidate was identified, a stock of the plasmid DNA was generated. When the inoculated bacterial cultures containing the clone of interest shaking overnight in antibiotic-containing Terrific broth became turbid (bacteria were in stationary phase of growth), the bacteria were pelleted out of solution by centrifugation (10 minutes at 7000 rpm). The pellet was resuspended using a reconstitution buffer (25 mM TrisHCl, 100 mM NaCl, 10 mM EDTA pH 7.5 in water) and lysed using 0.2M NaOH in 1% SDS. The lysate was neutralized by a solution containing 3 M potassium acetate and allowed to sit on ice for 10 minutes prior to centrifuging the debris containing most of the protein and the majority of the bacterial chromosomal DNA at 7000 rpm for 10 minutes. The lysate supernatant was precipitated by storing the solution at -20°C for at least 15 minutes in isopropanol, and after the nucleic acids were pelleted by centrifugation at 4000 rpm for 10 minutes at 4°C. RNA was selectively precipitated from the DNA using 5 M LiCl on ice for 10 minutes. The supernatant containing low molecular weight DNA was separated from the RNA by

centrifugation 4000 rpm, followed by a precipitation in ethanol at -20°C for at least 30 minutes. DNA was pelleted by centrifugation (4000 rpm for 10 minutes at 4C), the resuspended into 3 ml of TE, 50 μl of 10 mg/ml ethidium bromide and 4.8 g of cesium chloride were added to the resuspended DNA, sealed in an ultracentrifuge tube and spun at 60,000 rpm for approximately 16 hours. Purified supercoiled DNA was aspirated from the sealed tube using a needle. This DNA was further purified by ethanol precipitation, followed by a phenol:chloroform extraction. After sodium chloride addition to the DNA, an equal volume of phenol was added and the sample was vortexed and centrifuged to separate the aqueous from the organic phase. A second phenol extraction followed by a chloroform extraction was performed on the aqueous phase. The purified DNA was then concentrated by ethanol precipitation, and resuspended in TE and quantitated by spectrophotometry.

IN VITRO TRANSCRIPTION OF WNR RNA

WNR RNA was generated using the cDNA clones as a template. A unique *Swa*I site downstream of the ribozyme was used to linearize the cDNA plasmid. This plasmid was purified by phenol:cholorform extraction and ethanol precipitation, similarly to that described above. A MEGAscript T7 *in vitro* transcription kit supplemented with a cap analog (at 4 μM final concentration; New England Biolabs) was used to generate WNR RNA, in accordance with manufacturer's instructions. The WNR RNA was run on an agarose gel containing ethidium bromide and visualized under ultraviolet light (UV) to ensure its integrity and estimate the reaction's concentration.

ELECTROPORATION OF CELLS

Cells were grown in tissue culture flasks until the monolayers were 60-80% confluent. Often times, multiple flasks were trypsinized and pooled together to obtain a sufficient cell number. After the cells were released from the monolayers by trypsinization, the cells were pelleted by centrifugation (3-5 minutes at 1000 rpm), and washed twice by resuspending the pellets in ice-cold phosphate buffered saline (PBS) and

centrifuging again. After the washes, cells were resuspended at a final concentration of $1x10^7$ cell/ml in ice-cold, self-made PBS. Each electroporation consisted of *in vitro* transcribed RNA mixed with 400 µl of the washed cells ($4x10^6$ cells total) and electroporated in a 2 mm-gap cuvette. BHK, Huh7 and MEF cells were electroporated using an electroporator (BioRad, model Gene Pulser Xcell) with the following conditions: 2 pulses/cuvette at 750 volts, 25 microfarad and infinite resistance. Vero cells were electroporated with the same conditions except that the voltage was doubled to 1500 volts. Electroporated samples were allowed to rest for 5-10 minutes at room temperature prior to their removal from the cuvette and seeding into flasks or plates containing growth media.

TESTING COLONY FORMATION EFFICIENCY (CFE)

CFE was determined by electroporating replicon RNA harboring the NPT gene (WNR NS1-5 ET2AN or WNR NS1-5 EG2AN) into cells and determined the effective establishment of persistence by antibiotic resistance. A schematic diagram of the method is shown in Figure 9.

Figure 9: Diagram of how CFE was determined

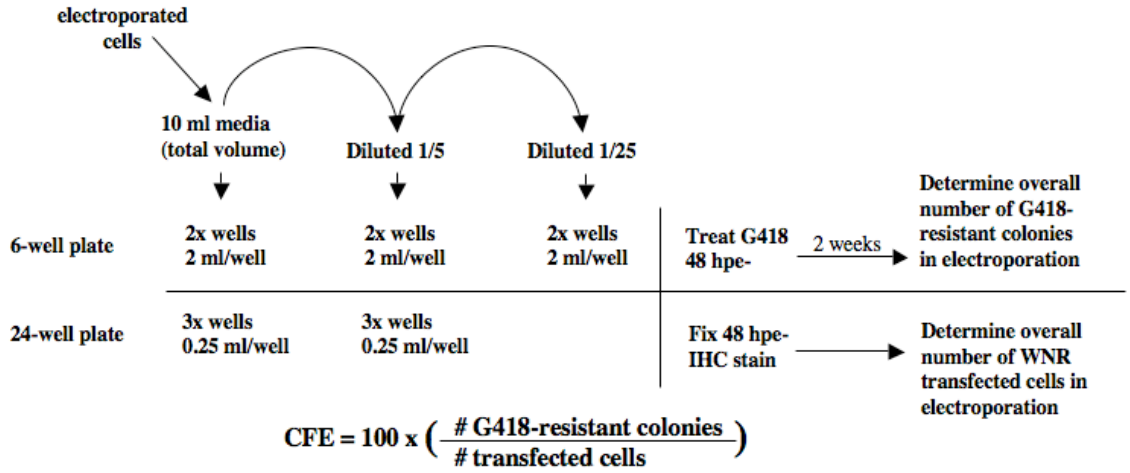

Figure 9: Cells electroporated with the WNR NS1-5 ET2AN or WNR NS1-5 EG2AN cultures were used to determine the CFE of the cell or replicon.

Cells were electroporated with the WNR RNA and diluted/aliquoted as shown in Figure 10 in growth media. The cells were seeded in a 24-well plates and were fixed and immunostained (IHC) at 48 hours post electroporation (hpe-) to determine the number of productively transfected cells in the original electroporation. At 48 hpe-, the transfected cells prepared in 6-well plates were re-fed new growth media supplemented with 33% conditioned media (filtered media removed from a parallel culture of healthy growing cells) and 400 μg/ml G418. Vero and L293 cells required higher concentrations of G418 to ensure untransfected cells died, so 800 μg/ml and 600 μg/ml were used. The selective media were changed every 3 days for 2 weeks. This time frame was sufficient to allow for G418-resistant colonies to grow from a single cell (clonal population). Two weeks after electroporation, the colonies were stained with crystal violet and counted. No colonies were detected in cell cultures that were electroporated with no RNA and maintained under the same conditions. CFE was calculated as the ratio of G418-resistant colonies to the number of positively transfected cells (see formula in Figure 9).

GENERATING REPLICON-BERING CELLS

Clonally derived populations of replicon-bearing cells were generated in a means similar to that previously described under CFE heading. However, after 2 weeks under G418-selection, colonies were counted by eye rather than being fixed and stained with crystal violet. Colonies that were spatially separated from other colonies were removed from the 6-well plate using autoclaved paper (Whatman chromatography paper) discs soaked in trypsin. The discs were removed once the cells were sufficiently trypsinized and placed into 48-well plates containing growth media and G418. Conditioned media was not used after the initial 2-week selection. Cultures were allowed to grow until the well reached near confluency (usually 3-7 days, depending on the cell line and the number of recovered cells). From here on, the population was considered a clonal isolate of the original electroporation.

IMMUNOHISTOCHEMISTRY

To detect antigen-positive cells by immunohistochemistry (IHC), monolayers fixed with a 1:1 (v/v) mixture of methanol and acetone (MeOH:acetone) for at least 30 minutes at -20°C. After fixation, monolayers were completely air-dried, then rehydrated in blocking buffer [PBS supplemented with 1% normal horse serum (NHS)]. After blocking, monolayers were incubated with the primary antibody in blocking buffer (usually 30 minutes). After washing thrice in PBS, monolayers were incubated for 30 minutes with a peroxidase-conjugated (HRP) secondary antibody generated against the species of the primary antibody diluted in blocking buffer. Antigen-positive (HRP-coated) cells were detected by using a peroxidase detection assay (Vector VIP, Vector Laboratories), which was turned a red precipitate by cell-bound HRP. In some cases, the signal from the IHC procedure listed above was too weak to accurately identify antigen-positive cells, so the signal was amplified by biotin-straptavidin (Vectastain, Vector Laboratories) prior to detection. To detect WNV antigen, WNV-specific murine hyperimmune ascitic fluid (MHIAF) was diluted 1/500 or 1/1000 and used as the primary antibody. The corresponding secondary antibody was goat anti-mouse, HRP (KPL laboratories).

Results

This infectious minimal WNR (WNR NS1-5, Figure 8B) served as the basic construction from which other replicon genomes were generated. One modification included the addition of a minipolyprotein into the 3' UTR of the replicon. The minipolyprotein consisted of an IRES from encephalomyocarditis virus (EMCV) that drove the expression of a cassette containing a reporter gene (the tat protein from HIV is shown in Figure 1B) and NPT (Yi, Bodola, and Lemon, 2002). Since the cassette is expressed as a single protein, the autocatalytic FMDV 2A peptide is necessary to cleave these two protein products from each other. Cells expressing this replicon produce the

reporter and NPT genes and can be readily distinguished from untransfected cells by detection of the reporter gene or viral antigen or treating cultures with G418. Furthermore, there is a relationship between WNR genome replication and the accumulation of proteins expressed under the IRES, so genome level replication will determine reporter gene production levels.

SOME CELL TYPES ARE PERMISSIVE TO PERSISTENT WNR GENOME REPLICATION

During the process of creating multiple replicon-bearing cell lines, there was a readily detectable difference in the percentage of transiently transfected cells that could form G418-resistant colonies obtained between different cell lines. The ease with which replicons were adapted to cell culture was measured by determining the percentage of cells transiently transfected with the WNR that could form a colony during G418 selection. This measurement, coined CFE, was determined as described in the Methods section. All cell types tested were able to support WNR replication since individual antigen-positive cells (as determined by IHC staining) were observed 48 hpe-. No CPE was noted in cells transfected with the WNR at this time, consistent with the observations made by other laboratories that adapted WNR and KUNR to cell culture (Khromykh and Westaway, 1997; Shi, Tilgner, and Lo, 2002). However, CPE might have been observed after 48 hpe-, but G418 selection occurred during this time so it was not possible to distinguish between cell death caused by WNR CPE or from G418-mediated death of untransfected cells. Approximately 10% of BHK cells and 35% of Vero cells that were transfected with the WNR were able to form G148 colonies (Table 1). In contrast, less than 1% of WNR-transfected Huh7 that could form a G418-resistant colony. The differences in CFE between cell types are likely to result from the differences in the properties of these cell lines towards the establishment of persistent, noncytopathic 'infections'. These WNR infections were stable since WNR antigen-positive, replicon-bearing cells could be maintained without G418 for several passages, indicating that an equilibrium had been achieved between WNR genome and host cell antiviral responses in these cultures.

Table 1: Colony formation efficiency of wt WNR in multiple cell types

Cell Line	CFE[a]
BHK	~ 10%
Vero	~ 35%
Huh7	< 1%

[a] CFE = colony formation efficiency = 100 x (# transfected cells/# G418-resistant colonies)

WNR PHENOTYPE IN REPLICON-BEARING CELLS

To begin to characterize the phenotype of the WNR selected in WNR NS1-5 EG2AN-bearing BHK cells, a replicon encoding the GFP reporter gene (WNR NS1-5 EG2AN) was introduced into BHK cells. WNR genome copy numbers were quantitated using dot-blot hybridization (Figure 10B) and levels of WNR genome replication were determined by flow cytometry that measured GFP fluorescence intensity (Figure 10A). Uncapped RNA was used as a control for background fluorescence levels since these genomes cannot be translated by the host cell, and therefore cannot produce GFP. Additionally, uncapped RNA cannot replicate since the viral genes required for replication are not translated from the RNA, thus serving as an effective control to measure genome copy numbers. GFP expression and genome copy number were highest from transiently expressed (48 hours post electroporation [hpe-], not G418 selected) WNR NS1-5 EG2AN. In two replicon-bearing clonally derived BHK cell populations (clones, cl 7.4 and cl 9.4), GFP fluorescence and genome copy number were both at lower levels compared to transiently expressed replicons. The level of GFP fluorescence detected in the WNR NS1-5 EG2AN-bearing BHK clones was so low that it was difficult to readily distinguish the GFP fluorescence from the background levels of fluorescence from untransfected cell cultures or cells electroporated with uncapped replicon RNA despite the fact that 100% of these cells were positive for WNV antigen by IHC staining (Figure 10A). The intensity of GFP fluorescence paralleled the reduced number of genome copies/infected cell (Figure 10B). In summary, genomes that were transiently expressed in BHK cells produced a brighter GFP fluorescence and had higher genome

copy numbers per infected cell than WNR NS1-5 EG2AN genomes that were selected to persistently replicate within the replicon-bearing BHK cell.

Figure 10: Phenotype of the WNR within WNR-bearing BHK cells

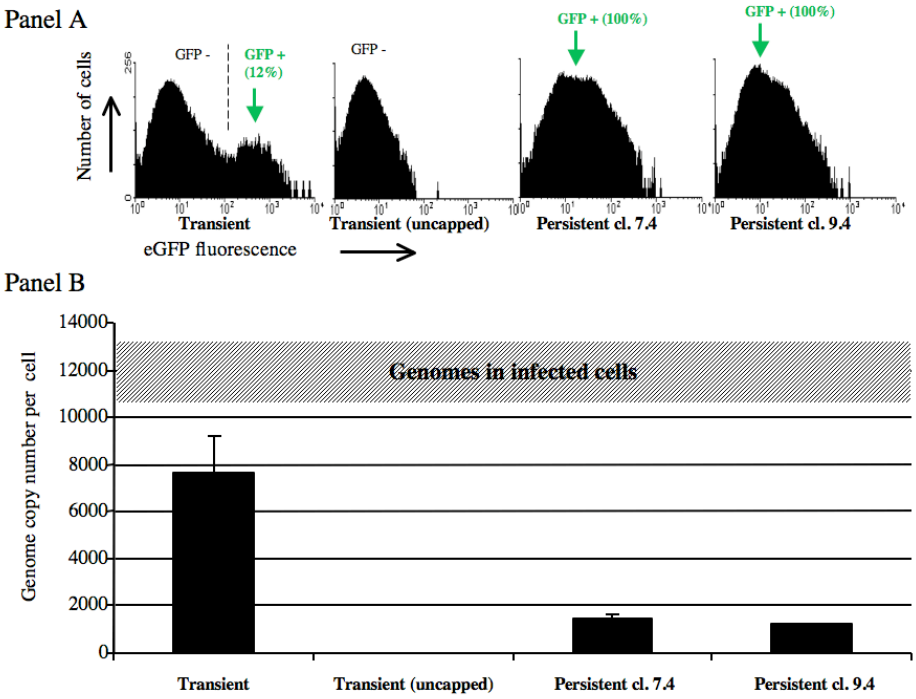

Figure 10: GFP fluorescence and genome copy number in BHK cells transiently or persistently harboring WNR NS1-5 EG2AN. (**Panel A**) FACS profiles from BHK cells analyzed 48 h post electroporation, or cultures prepared from two cloned BHK cell populations (cl. 7.4 and 9.4) 31 passages after isolation of G418-resistant WNV-replicon carrying colonies. The green arrow indicates the fluorescence intensity that corresponds to the highest population of GFP-expressing cells. (**Panel B**) Genome copy number (error bars indicate standard deviation) measured for the same cultures by dot-blot hybridization (O'Donnell et al., 2001) and standardized to the numbers of antigen-positive cells (12.4% for transient, 100% for persistent colonies 7.4 and 9.4). A culture transfected with a uncapped replicon RNA was included in both analyses to show specificity of RNA hybridization and GFP fluorescence; no antigen-positive cells or viral RNAs were detected on this culture. Genome copy number values and standard deviations were determined using hybridization data obtained from duplicate dot-blots from the same sample. The horizontal bar in panel B indicates genome copy number (12,300 +/- 900) detected in culture infected at an MOI of 1 with WNV and harvested 24 hpi (at this time point, 100% of the cells were antigen positive by IHC staining).

THE WNR GENOME SELECTED DURING GENERATION OF WNR-BEARING CELL LINES

The low CFE of wt WNR NS1-5 ET2AN genomes in Huh7 indicated that there was a barrier to the establishment of replicon-bearing Huh7 cells. To begin to characterize that barrier, a clonally derived, G418-resistant Huh7 clone (designated clone [cl] 1.1) was cured of the replicon using IFNα in the cell culture media. Curing the cell of its replicon created a naïve cell that was previously able to harbor a persistent WNR infection. Three treatments at 100 units (U)/ml IFNα were able to clear all detectable antigen-positive cells from replicon-bearing Huh7 cell cultures without any reductions in cell viability, thereby 'curing' the cells. Reducing the concentration of IFNα also reduced the percentage of cured cells in the culture, but it is possible that complete curing would have been achieved in additional IFNα treatments. If the barrier was due to a stable change in the cell, or the selection of a rare type of cell from the electroporated culture, then re-introducing the wt WNR1-5 ET2AN genome should result in a high CFE value. This was not observed; the CFE of wt Huh7 and cured Huh7 cells were identical. To further identify if an altered cellular phenotype could influence the CFE produced from the WNR NS1-5 ET2AN transfection, Huh7.5 cells were used. These cells were initially described for their ability to harbor HCV replicons (Blight, McKeating, and Rice, 2002) and were subsequently shown to be defective in RIG-I signaling (Sumpter et al., 2005). The CFE of the WNR NS1-5 ET2AN genome in Huh7.5 cells was 2-fold higher than the CFE in Huh7 cells. This indicated that there may be a slight contribution of the cellular phenotype on the ability to generate WNR-bearing cells, but unlike for HCV replicons, this is not the major contributing factor for the generation of WNR-bearing cells.

The WNR cell-adapted genomes, however, are the other portion of the factors contributing to CFE. When the WNR was harvested from a clonally derived, G418-resistant Huh7 culture (cl 1.1) and reintroduced in a naïve Huh7 culture, the CFE was 100%. This indicated that the WNR genome, and not the host cell, influenced the ease with which replicon-bearing cells could be generated. This also indicated that these cell-

adapted WNR genomes could be harvested from the cell and sequenced to identify mutations selected within genome that resulted in a high CFE value.

REPLICON GENOMES FROM ANTIBIOTIC-RESISTANT REPLICON-BEARING CELL CLONES ENCODE A VARIETY MUTATIONS

To identify mutations within the WNR genomes selected during the generation of WNR-bearing cells, total RNA was harvested from five independently derived WNR-bearing, G418-resistant Huh7, Vero or BHK clones and the WNR genomes contained within were sequenced. These sequence analyses revealed a small number of mutations present in the cell-propagated WNR genomes relative to the parental WNR NS1-5 ET2AN genomes (Figure 11).

Figure 11: Position of mutations identified in WNR-bearing cells

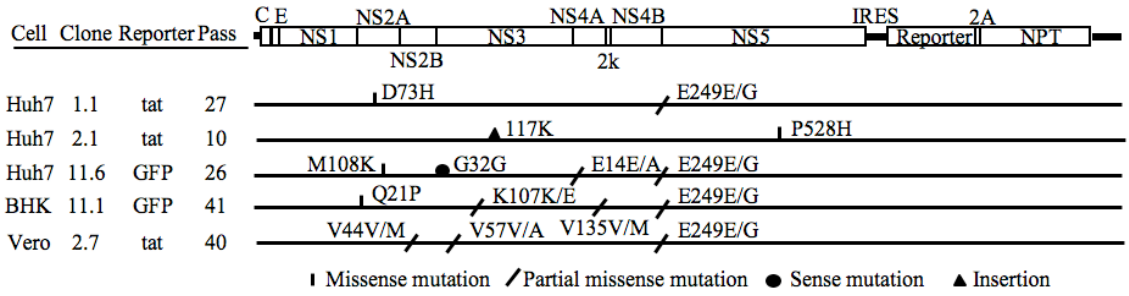

Figure 11: Position of mutations detected in WNR NS1-5 ET2AN or WNR NS1-5 EG2AN genomes present in replicon-bearing cell lines. The left side of each panel shows cell line, clone name, reporter gene and passage number (passages in G418 after initial antibiotic selection) at sequencing. Horizontal lines denote regions where PCR products of harvested replicons were sequenced. Five genomes were sequenced in their entirety. Missense mutations are denoted by small vertical lines, a mixture of mutations at a particular locus is identified by a slashed line, sense mutations are shown as a circle and an insertion is denoted by a triangle.

No mutations, insertions or deletions in the 5' or 3' UTR were detected in any of the genomes that were sequenced in their entirety (Figure 11). Within the coding region, no mutations were identified within the structural (small portion of C and E genes) or

NS1 genes. Several loci showed mixtures of wt and mutant nucleotides, resulting in mixtures of wt and mutant residues in the encoded proteins (partial missense mutations) including NS2B V44V/M, NS3 V57V/A, NS3 K107K/E, NS4A E14E/A, NS4A V135V/M and NS4B E249E/G. Only one sense (synonymous) mutation from all five fully sequenced genomes was observed (NS3 G32G). The mutations of the greatest interest were ones that completely changed (instead of partial changes) the translated protein. These changes included an insertion and several missense (nonsynonymous) mutations. An insertion of three additional nucleotides encoded an in-frame lysine residue insertion at position 117 (NS3 117Kins) in the WNR genomes. Several missense mutations were also observed that resulted in changes to the NS2A and NS5 proteins. These included mutations NS2A D73H, NS2A M108K, NS2A Q21P and NS5 P528H.

The NS4B mutation E249E/G is interesting and puzzling, since it was found in 4 out of the 5 fully sequenced genomes, but always as a mixture of nucleotides (partial missense mutation) at this site. As expected, this mutation was not detected in any bacterially propagated cDNA clone used to generate the RNA electroporated into these cells, so the mutation was selected for in 4 out of 5 independently derived clonal isolates (colonies). Interestingly, this mixed population appeared to be stable since it was observed after up to 41 passages in G418.

The frequency with which mutations were detected within the NS2A gene was striking. KUNR adapted to BHK cell cultures also showed NS2A mutations (A30P and N101D), suggesting that this was a potential ‘hotspot' for accumulation of cell-adapted mutations (Liu et al., 2004). When replicons contained within additional G418-resistant cell lines from multiple cell types were harvested and sequenced in their entirety or across the NS2A gene, more than half of the genomes sequenced had a mutation within the NS2A gene (Figure 12). The NS2A G71E mutation was observed in a population of cells that was transfected and selected after the transfection the WNR NS1-5 ET2AN genome containing a NS4B E249G mutation. The remainder of the clones listed in Figure 12 was accumulated in cells transfected with wt WNR NS1-5 ET2AN or wt WNR NS1-5 EG2AN genomes. Multiple Missense NS2A mutations were observed, including G17E,

L13F, V112F, L60F and E189K. With the exception of a partial missense mutation in a WNR harvested from a BHK cell line (F83F/S), all mutations were 'complete' mutations observed in the sequenced population.

Figure 12: Cell-adapted NS2A mutations are present in the WNR genomes in replicon-bearing cells

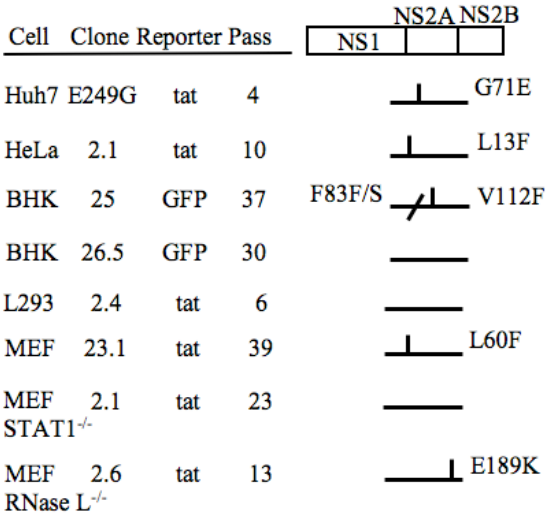

Figure 12: Several additional WNR harbored within WN replicon-bearing cell lines were sequenced in addition to those shown in Figure 11. The cell line used, the clonally derived population sequenced, the reporter gene contained within the replicon and the pass number (passages in G418 after initial antibiotic selection) at which the genomes were harvested are shown for each genome. The portion of the WNR genome sequenced for each clone is shown as the thick black horizontal lines. Each mutation is shown as a slash through the horizontal line. Vertical slashes denote missense mutations and slanted slashes show partial missense mutations at the indicated locus. The corresponding mutation is also noted next to the line.

SPECIFIC NS2A AND NS3 MUTATIONS INCREASE THE ABILITY OF REPLICONS TO PERSISTENTLY INFECT HUH7 CELLS

To evaluate the influence of chosen individual mutations on *in vitro* persistence, several mutations were selected for further analysis (Table 2). These mutations, which were from the three replicon-bearing Huh7 cell lines that were sequenced in their entirety

were genetically engineered into the WNR NS1-5 ET2AN cDNA clone by standard reverse-genetic techniques. The mutant replicons were then tested for their CFE in Huh7 cells. WNR NS1-5 ET2AN harboring NS2A D73H, NS2A M108K or NS3 117Kins displayed CFEs of 100% whereas side-by-side analyses revealed that the wt replicon had a CFE of less than 1%. Another NS2A mutation found within a replicon selected in BHK cells, NS2A Q21P, had a partial cell-adapted phenotype since the CFE (~20%) was 27 times higher than the CFE associated with wt replicons. Interestingly, a NS2A A30P mutation [reported to increase antibiotic-resistant colony formation in KUNR (Liu et al., 2004)] displayed a CFE of 3.5% in our WNR (Table 1). The NS4B E249G and NS5 P528H mutations produced very low CFE values, very similar to wt WNR NS1-5 ET2AN (Table 2). It is important to note that these mutations (NS4B E249G and NS5 P528H) were observed in genomes that also contained mutations (NS2A D73H, NS2A M108K and NS3 117Kins) that produced a high CFE (see Figure 11). This coupling of low-CFE and high-CFE mutations in the same genomes suggests that the low-CFE mutation was 'carried along' by the high-CFE mutation and contributed little (if any) towards the establishment of G418-resistant cells in culture.

Table 2: Colony formation efficiency of mutant WNR genomes in Huh7 cells

Mutation	CFE (%)[a]	Increase in CPE over wt
NS2A Q21P	~20	~27x
NS2A A30P	3.5	4.7x
NS2A D73H	100	133x
NS2A M108K	100	133x
NS3 117Kins	100	133x
NS4B E249G	1.5	2x
NS5 P528H	1.3	1.7x
NONE (wt)	0.75	n/a[b]

[a] CFE = colony-formation efficiency
[b] not applicable

NS2A MUTANT WNR PRODUCE LOW LEVELS OF WNV ANTIGEN

There was a notable difference in the intensity of antigen staining in cells transfected with some mutant WNR NS1-5 ET2AN genomes. There was no detectable difference in staining intensity among cells containing the wt, NS2A A30P, NS4B E249G or NS5 P528H mutant replicons, which all stained strongly with the anti-WNV MHIAF by IHC. However, cells transfected with WNR containing NS2A mutations D73H and M108K or NS3 117Kins stained less intensely than cells expressing wt WNR, suggesting that these mutations reduced WNR replication. Among these mutants, replicons harboring the NS3 117Kins stained most poorly and cells transfected with this WNR required amplification of the antibody signal by biotin–streptavidin for consistent detection. Figure 13 shows the IHC staining intensity for some of the previously mentioned replicons after 48 hpe- in Huh7 cells. This reduction in staining intensity suggests that those genomes cannot replicate as efficiently as the genomes that produce strong IHC staining in Huh7 cells. These results parallel the low intensity of GFP staining produced from WNR NS1-5 EG2AN genomes in G418-resistant BHK clones (cl 7.4 and 9.4) compared to the intensity from transiently expressed WNR NS1-5 EG2AN genomes in BHK cells (Figure 10A).

Figure 13: IHC staining of WNR-transfected Huh7 cells

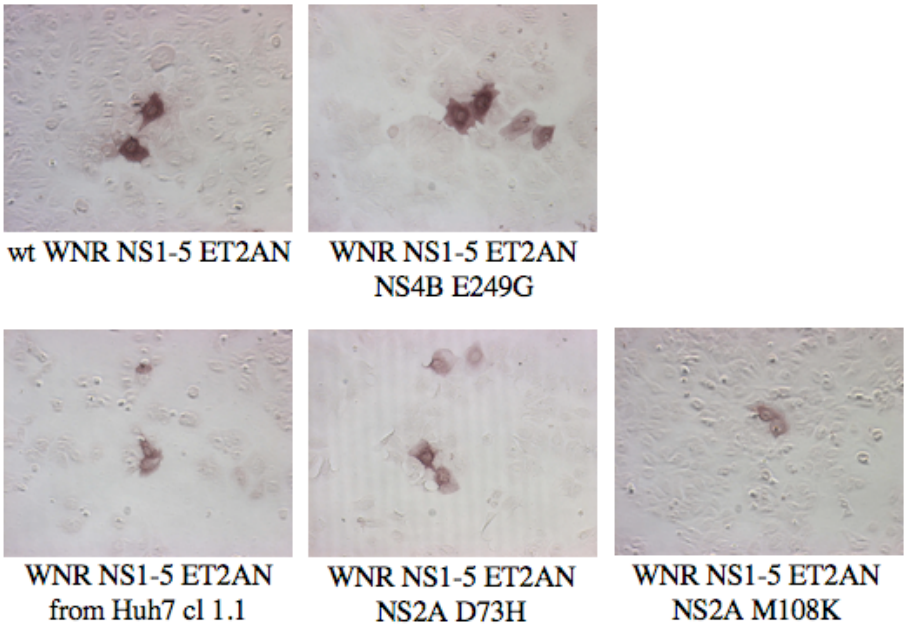

Figure 13: Huh7 cells transfected with wt or mutant WNR NS1-5 ET2AN genomes were fixed 48 hpe- (transient expression). Antigen was detected by IHC using the anti-WNV MHIAF.

Discussion

Eukaryotic cells employ several mechanisms to detect and eliminate viral infection whereas viruses have evolved ways to avoid, alter, delay or redirect the cell's innate immune responses. Studying the interactions between WNRs and cells can reveal information related to this complex interaction and will be described in detail in Chapters 3-5. In this chapter, mutations selected during the generation of WNR-bearing cells were identified.

A difference was observed between cell types with regard to the percentage of WNR NS1-5 ET2AN transfected cells that could form G418-resistant colonies. Fewer replicon-transfected Huh7 cells formed G418 colonies compared to transfected Vero or BHK cells. This difference could be explained in the intrinsic properties of the cell lines.

For example, Huh7 cells differ from both Vero and BHK cells in their ability to produce and respond to IFN. Vero cells can respond to, but not produce IFN. Conversely, BHK cells can produce, but not respond to exogenous IFN. Huh7, Vero and BHK cells all come from different mammalian species and may have differences in their ability to harbor a WNR infection. Mutations that greatly enhanced CFE were observed predominately in WNR genomes that were adapted to Huh7 cells. As expected from the lack of proofreading ability in the viral or T7 polymerases, point mutations could have arisen during the early stages of flavivirus genome replication within the cell or during the transcription of viral genomic RNA from the cDNA clone. The small number of sense mutations relative to missense mutations within the five fully sequenced WNR harvested from replicon-bearing cultures indicates that there is a positive selective pressure for specific coding changes within the replicons that successfully adapted to cell culture, especially to Huh7 cells.

On the other hand, Vero cells readily harbored WNR persistent infections as evident by the high CFE generated from the wt WNR (35%) and the decreased need to generate cell-adapted mutations. As a result, the WNR harvested from the Vero cl 2.7 had no fixed missense mutations in the consensus population. Wt WNR NS1-5 ET2AN genomes had an intermediate CFE in BHK cells, and a genome fully sequenced from WNR-bearing BHK clonally derived cells revealed only one missense mutation and two partial missense mutations (Figure 11). The mutation found in this genome, NS2A Q21P, had a CFE of only 20% in Huh7 cells, suggesting that the CFE value of this mutation may be higher in BHK cells.

The barriers to establishment of antibiotic-resistant replicon-expressing colonies of mammalian cells are likely to be multifold and include replicon-mediated cell destruction and the anti-viral response of the cells. The antiviral responses can be further subdivided into responses that eliminate the replicon (rendering the cells sensitive to antibiotic) and responses that eliminate the infected cell (killing the replicon-bearing cells). In several viral systems, induction of antiviral responses, including production of IFN in association with dsRNA, can induce apoptosis (Roulston, Marcellus, and Branton,

1999). Apoptosis has been associated with many flaviviral infections in a variety of cell types in culture (Despres et al., 1996; Jan et al., 2000; Liao et al., 1997; Marianneau et al., 1997; Marianneau et al., 1998; Parquet et al., 2002; Parquet et al., 2001). Specific flaviviral proteins, notably C, prM, E, NS3 and/or the NS2B/NS3 complex, can also initiate apoptosis when individually expressed (Catteau et al., 2003; Prikhod'ko et al., 2001; Prikhod'ko et al., 2002; Ramanathan et al., 2006; Shafee and AbuBakar, 2003; Yang et al., 2002). The mechanisms by which flaviviruses and their proteins initiate apoptosis are discussed in detail in Chapter 5. Due to the timing of G418-selection in the generation of replicon-bearing cell lines, the cell death observed after 48 hpe- could not be directly attributed to CPE (resulting in apoptosis) from the WNR since G418-induced cell death was occurring in untransfected cells. Following isolation of replicon-bearing cell lines, these cells stably maintained the cell-adapted WNR for dozens of passages, even in the absence of G418. This indicates that the equilibrium between WNR and cell is not dependent upon the presence of an antibiotic after the selection process had occurred. This implies that if a viral genome encoded one of the identified cell-adapted mutations, that a persistent infection was be easily generated. This is further explored in Chapter 3.

In our derivation of these cells, it was discovered that during the establishment of persistence, replicon genome levels were reduced WNR NS1-5 EG2AN-bearing BHK cells (Figure 10B). The average fluorescence was decreased in WNR NS1-5 EG2AN-bearing BHK cells compared to transiently expressed WNR NS1-5 EG2AN in BHK cells (Figure 10A). Decreased levels of viral antigen found upon immunohistochemically staining Huh7 cells transiently expressing the cell-adapted WNR compared to the wt WNR (Figure 13). There was a direct correlation between the high CFE found from WNR expressing NS2A D73H, NS2A M108K or NS3 117Kins mutations (Table 2) and the reduction in IHC staining intensity at 48 hpe- (Figure 13) indicating low levels of antigen accumulation. Similarly, genomes that had a low CFE, including wt WNR and WNR containing NS2A A30P, NS4B E249G or NS5 P528H mutations, also had a dark

intense stain after IHC detection, indicating that the level of WNV antigen was not altered in these transfections.

The partial missense mutation detected in many WNR cell-adapted genomes in NS4B is puzzling. The reason why a missense mutation would be selected for in several different independent clones, but only as a mixture of wt and mutant nucleotides, is unknown. The nature of this mixture was not analyzed; it is possible that one cell would contain a mixture of genomes with the wt and NS4B E249G genomes or that each cell contains one type of genome, but the cell population contains a mixture of cells that contain the wt genome and cells that contain the NS4B E249G genome. Alternatively, it is also possible that this mutation is continuously being lost and regenerated in the population (highly unlikely), or is slowly being selected for within the population. The only fully sequenced genome that did not contain this partial mutation was the Huh7 cl2.1 genome, which was sequenced at passage 10. All other genomes listed in Figure 11 were sequenced at passage 26 and above. Perhaps this observation is merely coincidental, but it would suggest that the genomes within the WNR-bearing G418-resistant cell lines slowly acquire this mutation through passaging. The method used to harvest and sequence these cell-adapted genomes from the G418-resistant cell populations cannot differentiate between these possibilities. This NS4B E249G mutation has also been identified by two other investigators, one within a naturally occurring WNV isolate (Davis et al., 2004; Lanciotti et al., 2002) and the other in a C3H/He cell-adapted WNR genome (Puig-Basagoiti et al., 2007). In accordance with the results presented above (Table 2), this NY00 WNR acquired the same NS4B E249G mutation during adaptation to C3H/He cells, and genetically engineered WNR with this mutation were shown to be twice as likely as the parental replicon to produce antibiotic-resistant colonies in C3H/He and BHK21 cells (Puig-Basagoiti et al., 2007).

It is unclear why the NS2A gene appears to be a ‘hotspot’ for the accumulation of cell-adapted mutations. NS2A mutations were observed in multiple cell lines representing both rodent and human cell lines, so this observation was not an artifact of the cell line used. Although the possibility that NS2A could coordinate virion assembly (Kummerer

and Rice, 2002) is of great interest, this activity is unlikely to be relevant to the adaptation of WNR to persist in the cell since these genomes are not packaged into virions in these cell lines. Rather, it is likely that the interactions between the NS2A protein and other proteins in the replication complex are disrupted. This is supported by the decreased intensity of antigen staining seen in NS2A mutant WNR-transfected cells. A detailed description of the phenotypes associated with the NS2A mutations is found in Chapters 3 and 4. Point mutations detected within NS2A reported here and observed by others [in the laboratory propagated genomes (Liu et al., 2004) and natural WNV isolates (Beasley et al., 2005; Lanciotti et al., 2002)] cluster in linear amino acid sequences within hydrophilic domains interspersed between long hydrophobic domains which are likely buried in the ER membrane. A proposed model of the NS2A protein within the ER membrane, along with the locations of the WNR and KUNR cell-adapted mutations previously described, is shown in Figure 14. These mutations could induce subtle changes in RNA replication activity that might be harder to induce by point mutations in soluble globular proteins such as helicases, proteases and polymerases, which may help to explain why NS2A appears to be a 'hotspot' for adaptive mutations. Furthermore, mutations that increased CFE and decreased antigen accumulation in WNR ET2AN genomes occurred in multiple places in the NS2A protein, suggesting that these disruptions are achieved in many ways and not through one specific locus in NS2A.

Figure 14: Model of the NS2A protein within the ER membrane

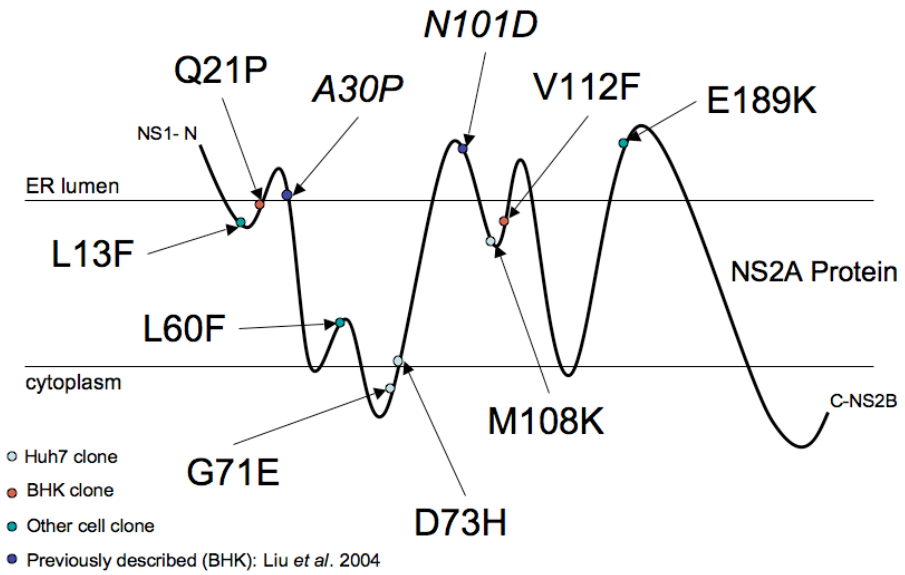

Figure 14: A model for the association of the NS2A protein within the ER membrane. Kyte/Doolittle hydrophobicity values for each residue within the NS2A protein were determined using MacVector. At least one transmembrane domain must be present in the NS2A protein since the NS1 protein is found in the ER lumen and NS2B is located in the cytoplasm. Any stretch of greater than 20 consecutive hydrophobic amino acids was considered a transmembrane domain. Any consecutive stretch of fewer than 20 hydrophobic residues was placed inside, but not spanning, the membrane. Mutations found in replicons adapted to cell culture are shown by colored circles. Mutations in italic font were described in BHK cell-adapted KUNR (Liu et al., 2004).

It was also curious that the WNR-bearing Huh7 (clone 1.1 at passage 22 in G418) cells were "easily" cured by passaging the cells three times in growth media containing IFNα. These results contrast to these published in the literature, and there are several explanations why these Huh7 cells were cured. *First*, the process of isolating the Huh7 replicon-bearing cells could have selected a subpopulation of Huh7 cells that is not sensitive to replicon-mediated interference of IFN activation. Second, during isolation of our replicon-bearing cells, replicons with altered properties, which are impaired in their ability to block the action of IFN, could have been selected. The anti-IFN activity of the replicon is dependent on level of expression, and our replicon-bearing cells express

genomes and proteins at levels that only have a partial effect on IFN-induced antiviral activities. Third, the different cell lines utilized in these studies have different abilities to interact with flavivirus genomes and their nonstructural proteins than cell lines used in previous studies.

The selection of a special cell type in the derivation of our WNV replicon-bearing cells would consistent with studies with an HCV virus replicon, showing that Huh7 cells with enhanced ability to replicate HCV replicons were obtained from cells that had been selected for their ability to carry HCV replicons and were then cured of the replicons (Blight, McKeating, and Rice, 2002). However, this is unlikely to have happened in our system since curing the replicon-bearing cell and retransfecting this population with the wt WNV replicon did not enhance CFE in the cured population. HCV replicons have been selected that have acquired mutations that enhance their ability to establish replication in Huh7 cells (Blight, Kolykhalov, and Rice, 2000; Lohmann et al., 2001), and it has been shown that WNV replicons adapted to Huh7 cells have an enhanced ability to form colonies when reintroduced into naive Huh7 cells. Thus, the changes in these replicons produce this altered colony formation phenotype could also result from a change in their ability to suppress the IFN response, which is consistent with our second explanation for the differences observed between these aforementioned WNV observations and the flavivirus studies reported by others.

The second explanation is most likely, especially if the production of viral proteins is limited with regard to the proteins in the IFN signaling pathway. WNV has the ability to block IFN signaling in cell culture (Guo, Hayashi, and Seeger, 2005; Liu et al., 2005; Scholle and Mason, 2005). WNR NS1-5 ET2AN replicates more poorly than WNV genomes as shown by the decreased number of genome copies in the infected cells (Figure 10). WNR NS1-5 ET2AN genomes that were selected to replicate in cells selected with G418 showed approximately 4-fold fewer genomes per infected cell than the wt WNR NS1-5 ET2AN genomes (Figure 10). Recently, a lineage II WNV (Mad78) that replicated more poorly and more sensitive to exogenous IFN added after infection than a lineage Ia WNV (TX02) in A549 (immunocompetent) cells in culture (Keller et

al., 2006). Interestingly, the NS2A A30P mutation in KUNR ablated NS2A's ability to block the production of IFN in BHK cells, leading to an increase of IFN production in NS2A A30P KUNR-bearing cells compared to wt KUNR-bearing cells (Liu et al., 2004). Additionally, when this mutant protein was expressed in the absence of the genome (in reporter constructs), this phenotype was still seen, indicating that the A30P mutation destroyed the ability of NS2A protein to interfere with IFN production (Liu et al., 2004). The work presented here suggests that the ability of the genome to replicate influences the infected cell's responsiveness to IFN.

CHAPTER 3: GENOMES ENCODING CELL-ADAPTED MUTATIONS ARE ATTENUATED *IN VITRO*[3]

Abstract

Several mutations selected during WNR adaptation to cell culture that were shown to confer the ability to persist within Huh7 cells (demonstrated by their high CFE) appeared to reduce the ability of the WNR NS1-5 ET2AN genome to produce viral antigen. The reduction in antigen levels was likely due to low levels of replicon replication. To confirm that these mutations reduced genome replication, the NS2A A30P, NS2A D73H, NS2A M108K, NS3 117Kins, NS4B E249G and NS5 P28H mutations were introduced into WNR C-eGFP-NS1-5 and WNV genomes to determine their effects on the growth phenotypes of replicon and viral genomes in cell culture. NS2A mutant D73H and M108K WNR C-eGFP-NS1-5 genomes produced less eGFP per cell, indicating that these genomes replicated more poorly than wt WNR *in vitro*. Viruses encoding these NS2A mutations produced small antigen-positive foci and grew to lower titers in cell culture. WNV with a large deletion in the 3' UTR produced an attenuated phenotype similar to the NS2A mutant genomes in both the WNR and WNV. However, WNR C-eGFP-NS1-5 or WNV genomes encoding NS2A A30P, NS4B E249G and NS5 P528H mutations had phenotypes most similar to wt genomes. In summary, mutations that confirmed a high CFE in WNR NS1-5 ET2AN genomes in Huh7 cells also caused a reduction in eGFP expression in WNR C-eGFP-NS1-5 genomes in Vero cells and a

[3] A significant portion of this chapter has been previously published in two manuscripts in Virology in 2005 and 2007. Virology does not require copyright permission as long as proper citation is provided. The citations for those articles are:

S.L. Rossi, R.Z. Fayzulin, N. Dewsbury, N. Bourne and P.M. Mason (2007) Mutations in West Nile Virus Nonstructural Proteins that Facilitate Replication Persistence in Vitro Attenuate Virus Replication in Vitro and in Vivo. Virology 364(1): 184-195.

S.L. Rossi, Q. Zhao, V. O'Donnel and P.W. Mason (2005) Adaptaton of West Nile Virus Replicons to Cells in Culture and Use of Replicon-Bearing Cells to Probe Antiviral Action. Virology, 331(2): 457-470.

reduction in viral titers in WNV in Huh7 and Vero cells. These results show the correlation between the low levels of genome replication and the ability of these genomes to persist within the cell.

Introduction

FULL-LENGTH INFECTIOUS CDNA CLONES

Many viral genomes have been incorporated into DNA plasmids for the purpose of manipulating their genomes through molecular biology techniques, as described in Chapter 2. Full-length infectious cDNA (FLIC) clones encoding the genomes of many flaviviruses. These include the FLICs TBEV (Mandl et al., 1997), YFV (Bredenbeek et al., 2003; Rice et al., 1989), DENV (Kapoor et al., 1995; Kinney et al., 1997; Lai et al., 1991), JEV (Sumiyoshi, Hoke, and Trent, 1992), KUNV (Khromykh and Westaway, 1994) and WNV (Shi et al., 2002).

There are many advantages to using the genomic RNA *in vitro* transcribed from these FLIC rather than viruses that have been propagated in culture. An additional advantage to generating FLICs is the genetic consistency of the plasmids during amplification in the bacteria. Virus stocks of a known genetic background can be created with minimal amplification of the virus *in vitro* by electroporating *in vitro* transcribed RNA into cells and recovering the generated WNV within days of the transfection. Amplifying virus stocks by infecting naïve cells in culture or animals in some circumstances leads to the selection of mutations that allow the virus to grow better in that infected tissue. If there is a mutation that adversely affects an aspect of the virus' life cycle (i.e. decreased ability to infect, replicate, package, etc.), then the viruses will be quickly out competed (eliminated) from the population if a wt-like virus is produced. Under these conditions, it would be impossible to generate a mutant virus stock to analyze. Similarly, repeatedly amplifying a wt virus in one type of tissue (cell line or animal organ) can cause that virus to accumulate mutations that allow that virus to replicate well in that tissue and may result in an altered phenotype in other tissues. This

principle has been successfully employed to generate vaccines like YFV 17D and to study the constraints of using multiple hosts on virus evolution in nature. By incorporating the viral genome into a plasmid, the viral RNA genome can be generated from this cDNA template and the viruses recovered from cells transfected with this RNA would be genetically more homogeneous than populations that were amplified by passage in cell culture or animal tissue.

Perhaps the most enticing feature of the FLIC is the ability to deliberately engineer point mutations into the genome and recover viruses with the introduced mutation. This facilitates the investigation into a single mutation's influence of the phenotype of the virus. This type of virus would be exceedingly difficult to design in the absence of the FLIC and reverse genetic technology. Additionally, viruses with deleterious mutations can be generated from the FLIC with minimal concern that a wt-like virus will be generated early during the production of virus in cell culture.

VIRUS-LIKE PARTICLES

As described in Chapter 2, flavivirus replicon genomes lacking the structural genes are capable of self-replication. Without the structural proteins, the replicon genome cannot form virions. The structural proteins, however, do not have to be provided by the WNR genome. Instead they can be produced within the cell by means of alternative expression systems, like another replicon or by expression plasmids. If the basic requirements of the structural genes are met (such as E and prM co-expression and folding into the ER membrane), they are capable of facilitating of self-assembling into SVPs and packaging replicons into VLPs (virus-like particles). By providing the structural proteins C, prM and E *in trans* using an alphavirus replicon, the replicon genomes can be encapsidated into VLPs and used as a surrogate for virus infection.

VLPs are functionally indistinguishable from the virus particle (Khromykh, Varnavski, and Westaway, 1998). Instead of harboring the viral RNA within nucleocapsid, VLPs contain replicon RNA. Therefore, the VLP can infect a cell as would a virus particle, but the infection cannot spread between normal cells (except during cell

division) since VLPs cannot be produced in the absence of the structural proteins. VLPs have been generated by several labs for many flaviviruses, using replicons generated for KUNV (Harvey et al., 2004; Khromykh, Varnavski, and Westaway, 1998), YFV (Jones, Patkar, and Kuhn, 2005), TBEV (Gehrke et al., 2003), and WNV (Hanna et al., 2005; Puig-Basagoiti et al., 2005).

Using VLPs as a method for introducing WNR RNAs into cells has several advantages. First, VLPs are indistinguishable from virus particles with respect to their ability to infect a cell. Therefore, the WNR genome can be delivered into the cell by an infection, rather than by transfection methods that use electroporation or liposomes. Secondly, these transfection methods have varied rates of success in cell lines and primary cell cultures. VLP infections help to circumvent this problem. Third, VLPs can be quantitated and delivered via infection in controlled doses (multiplicity of infection or MOI), which makes it possible to control the percentage of cells to be infected in the culture. Fourth, VLPs can deliver the replicon genome to cells in vivo. This has been done to identify the first infected cells in the host (Bourne et al., 2007; Scholle et al., 2004), or to measure the host's response to infection (Mason, Shustov, and Frolov, 2006; Scholle and Mason, 2005).

VLPs have been generated in our lab by transfecting a WNR (Scholle and Mason, 2005) into BHK packaging cell line, which provides the structural proteins *in trans* to package the replicon genome (Fayzulin et al., 2006). The packaging cell line was generated using a noncytopathic Venezuelan equine encephalitis virus (VEEV) replicon (VEER) (Petrakova et al., 2005) that expresses the WNV structural genes and the pac gene under one or more 26s subgenomic promoter(s) (Fayzulin et al., 2006). BHK cells that persistently harbor the VEER were selected using 10 μg/ml puromycin in the growth media, and these packaging cells were used to stably produce large amounts of the WNV structural proteins at high concentrations permitting the production of high titer VLP preparations.

VLP PACKAGING CELL LINES

In principle, VLPs can be created from any cell that expresses both the WNR genome and the structural proteins. Our lab has used two approaches to generate VLPs: sequential transfection and transfection of stable packaging cell lines. VLPs were obtained to a high titer (up to 10^9 focus forming units (ffu)/ml) by electroporating the WNR genomes into BHK cells, then 24 hours later, electroporating the same cultures with a Sindbis virus replicon expressing C, prM and E genes under the subgenomic promoter (Scholle et al., 2004). Generating VLPs by this method, albeit effective, was laborious. To facilitate packaging with only one transfection setup, alphavirus replicon that encoded the WNV structural proteins as well as an antibiotic-resistance gene that permitted the generation of a stable packaging cell line. The noncytopathic VEER previously described by Petrakova and colleagues (Petrakova et al., 2005) was engineered to contain the structural genes of WNV and the pac gene under one or two subgenomic promoter(s) (Fayzulin et al., 2006). BHK cells that harbored this VEER RNA were selected using puromycin in the cell culture media (Fayzulin et al., 2006). These cells were then stably propagated and were electroporated with the WNR of interest and VLPs were harvested from the cell culture supernatant. The replication of the VEER genome within these cells did not interfere with the replication of the WNR (Fayzulin et al., 2006). The titers obtained from packaging cells were slightly lower than those harvested from sequentially electroporated cells (~10^8 i.u./ml), but were still suitable for most studies (Fayzulin et al., 2006). In these studies, the packaging cell lines produced high levels of structural proteins (as measured by E) and the limiting factor in the production of VLPs using the packaging cell lines was the replication of the input WNR RNA genome. Thus, VLPs harboring the wt WNR NS1-5 ET2AN genome produced larger antigen-positive foci on packaging cell monolayers than did VLPs encoding the cell-adapted WNR NS1-5 ET2AN cl 1.1 genome, indicating that more VLPs were produced from the wt WNR infection than the cell-adapted WNR infection (Fayzulin et al., 2006).

RATIONALE

In this chapter, the phenotypes of the NS2A A30P, NS2A D73H, NS2A M108K, NS3 117Kins, NS4B E249G and NS5 P28H mutations in the WNR and are discussed. It was *expected* that genomes harboring cell-adapted mutations would produce less cytopathic effect, smaller infectious foci, slower viral replication and prolonged infection *in vitro* when compared to the wt genome. It was *hypothesized* that cell-adapted mutations would reduce replicon and virus genome replication, resulting in a noncytopathic infection.

Materials and Methods

GENERATING MUTANT WNR AND WNV CDNA CLONES

The generation of plasmid-propagated cDNA clones of WNR containing individual mutations is described in Chapter 2. To create various WNR and WNV genomes, unique restriction sites that surrounded the mutation were chosen to swap the fragment from the mutant WNR NS1-5 ET2AN genomes into the desired WNR or WNV cDNA clone. The newly constructed clones were verified to contain the mutation either by direct sequencing of the region or by using of a naturally occurring or genetically engineered RE sites in or directly near the mutation (NS2A A30P created *Sph*I, NS2A D73H ablated *Bsm*BI, NS3 117Kins created *Bsp*EI, NS4B E249G created *Stu*I and NS5 P528H created *Nco*I) to confirm successful plasmid creation. A WNR and FLIC with a large deletion in the 3′ UTR of the virus was also generated using similar methods. A primer that annealed to the 3’ UTR (U215: 5’GCCATGCATGTTAACCAGGGCGAA AGG) and contained an *Nsi*I site (in blue) produced a PCR fragment that was ligated into a naturally occurring *Nsi*I site within the cDNA encoded in the WNV 3’ UTR, thereby creating a cDNA clone with a deletion between nucleotides 43 and 388 of the 3′ UTR.

GENERATING VIRUS-LIKE PARTICLES (VLPS)

VLPs were created by electroporating *in vitro* transcribed WNR RNA into BHK packaging cells (Fayzulin et al., 2006). A portion (0.1 ml from a 10 ml final resuspension) was used for a focus formation assay (FFA) and the remainder was seeded into a tissue culture flask. After the cells adhered to the flask, the media was removed and replaced with MEM supplemented with 1% abx, 1% FBS and 1% HEPES (MEM+++) to help limit cell growth and buffer any pH changes (done approximately 6-18 hpe-). Supernatant was harvested from the electroporated cultures after 48 hpe- and monolayers were re-fed with MEM+++. Tissue culture media containing the VLPs were centrifuged to remove cellular debris (5 minutes at 1000 rpm), then the supernatants were aliquoted and frozen at -20°C. Supernatant harvests were collected every day until the cell monolayer was destroyed due to CPE or over confluence. In most cases, only the 48-70 hpe- harvests were used.

FOCUS-FORMATION ASSAY

FFAs were performed from the cells that were electroporated with either the replicon or viral genome. These cells were either serially diluted (10-fold) in growth media and added to a unelectroporated cell monolayer, or were serially diluted in a suspension of unelectroporated cells. In the case of replicons, electroporated cells need to be seeded into packaging cells. For WNV, electroporated cells were seeded into either BHK or Vero cells. Once the cells adhered to the cell culture plate (~4-6 hpe-), the media was gently removed and replaced with an overlay consisting of 0.6% tragacanth, MEM without phenol red, 1% FBS and 1% abx. After 2-3 days, the overlay was removed, and monolayers were washed with PBS and fixed with MeOH:acetone at -20°C for at least 30 minutes. Antigen-positive cells were visualized by IHC, as described in Chapter 2.

FLOW CYTOMETRY TO DETECT EGFP FLUORESCENCE IN VLP-INFECTED CELLS

Vero cells were infected with VLPs bearing eGFP (WNR C-eGFP-NS1-5) at a MOI of 1, incubated for 1 hr to allow for VLP adsorption, washed, re-fed with growth

media and incubated for the indicated times. At harvest, cells were trypsinized, resuspended in PBS supplemented with 1% fetal calf serum and analyzed by flow cytometry (Flow Cytometry and Cell Sorting Core Laboratory, UTMB). Cells were gated first based on the population of live cells (by fitting size criteria), thereby eliminating the cellular debris and cell clumps. To determine the cell population that expressed eGFP, mock cells (known to be eGFP-negative) were used to determine the cut-off point for the eGFP-negative population. Live cells that were not gated in the eGFP-negative field were considered eGFP-positive. FloJo software (version 8.1) was used to calculate geometric mean (GM) eGFP fluorescence for the eGFP-positive cells in each sample.

CONSTRUCTION OF THE WEST NILE VIRUS FULL-LENTGH INFECTIOUS CLONE GENOME

The FLIC of TX02 WNV was created by adding the structural genes into the WNR cDNA clone. This was achieved by a single RTPCR generated fragment that cloned into the WNR NS1-5 genome, as shown in Figure 8. This genome was cloned into the low-copy plasmid pACNR (ampicilin resistance). Like the previously described WNR NS1-5 ET2AN, the FLIC had a ribozyme at the end of the 3' UTR to ensure a precise end on the 3' UTR. The FLIC (viral genomic) RNA was generated by an *in vitro* transcription reaction with T7 polymerase. The plasmid DNA clone encoding the FLIC was sequenced to identify changes that arose during PCR amplification. Only two changes were noted between the FLIC and the sequence reported for the TX02 viral RNA (Granwehr et al., 2004a): one silent (sense) mutation in C that was used to genetically introduce the *Afl*II cloning site (see Figure 8B) and a silent mutation in NS1. However, there were multiple sequence differences between the TX02 cDNA and WNV isolates from 1999 (NY). To facilitate analyses of the differences, the FLIC was compared to a NY99 sequence harvested from a flamingo (GenBank accession AF196835) that shows the greatest similarity with the consensus sequence for the NY99 strains. There were no differences in the 5' UTR, and 3 changes in the 3' UTR. Twenty-five silent mutations were identified within the ORF. Missense mutations included E T76A, NS1 E94G, NS2A

V138I, NS4B V161I and NS5 T526I. The *in vitro* transcribed FLIC RNA was very effective in generating infectious virus particles in BHK cells. Forty-eight to seventy-two hpe-, high titers were readily achieved. The FLIC cDNA contained within the pACNR low-copy plasmid was slightly unstable when grown in large cultures (~250 ml) and so the FLIC cDNA was transferred into a bacterial artificial chromosome (BAC). This clone was similar to the first clone except the BAC was chloromphenacol resistant.

GENERATING VIRUS STOCKS

All *in vitro* studies using WNV were performed in the BSL3 located on the 5th floor of Mary Moody Northen. Live virus recovered from cells transfected with RNA *in vitro* transcribed from linearized infectious cDNA clones (see Chapter 2). BHK cells were harvested from flasks when the monolayers were approximately 70% confluent and electroporated (as described in Chapter 2) with *in vitro* transcribed viral RNA. Typically, an aliquot of electroporated cells were used for the FFA to determine the specific infectivity of the mutant FLICs. The remaining electroporated cells were placed in T75 flasks with growth media until the cells adhered to the flask, usually about 3-5 hours. After the cells adhered, the media was replaced with MEM+++. Cultures were monitored for CPE and harvests were taken at various times after electroporation (24, 48, 72 and sometimes 96 hpe-). Harvests were performed by removing the culture media from the flask and replenishing them with new MEM+++. Supernatant was centrifuged (5 minutes at 1000 rpm) to remove cellular debris, then aliquoted and frozen at -80°C.

Viruses were genotypically and phenotypically characterized prior to use in experiments. Viruses engineered to contain a known mutation were sequenced through the region containing the mutation and FFAs were performed to ensure that homogeneous antigen-positive foci were produced. Due to the risks of attenuated viruses reverting to a wt phenotype, the earliest possible harvest with a sufficient titer to perform the indicated experiment was used. This titer was typically achieved 48 hpe-, but in some cases harvests made at 72 hpe- were used.

SEQUENCING VIRUS POOLS

Vero cell monolayers in 6-well plates were infected with the indicated WNV in the BSL3. Monolayers were rocked for 1 hr at 37C, then the infection inoculum was removed, replaced with Vero growth media and incubated overnight. Twenty-four hours later, the media was aspirated and a mixture of Trizol LS (Invitrogen) and media (750 µl Trizol LS + 250 µl Vero media or PBS) were used to lyse the cells directly in each well. Lysates were allowed to sit for 10 minutes, then pipetted several times to reduce the lysate's viscosity, transferred to a 2 ml screw-cap tube and transferred to the BSL2. RNA was recovered from the lysate in accordance with Invitrogen instructions. Once the RNA was extracted, it was resuspended and sequenced as described in Chapter 2.

VLP AND VIRUS TITRATIONS

The basic method for titrating VLP and WNV is identical. There are only a few differences that distinguish between these methods, including the use of different size tissue culture plates and changing the media to an overlay after infection. For both VLP and WNV titrations, antigen-positive cells or foci were observed after IHC staining using the MHIAF anti-WNV sera.

VLPs were titrated in the 96-well format. VLPs were serially diluted (10-fold) in MEM+++. A typical dilution series usually diluted 20 µl VLP into 180 µl MEM+++ and dilutions ranged from $10^{-1} \rightarrow 10^{-8}$. Duplicate wells were infected with the 50 µl/well for each dilution. The VLPs were not removed from the cell monolayer after infection. Monolayers were rinsed with PBS and fixed at 24-36 hpi with MeOH:acetone at -20C for at least 30 minutes.

WNV were titrated in the BSL3 in either 24-well or 96-well plates, depending on the experiment. 96-well plates were used to titrate the viruses used for the growth curves. 24-well plates were used to titrate the viruses that would be used for the animal experiments, as described in Chapter 4. In either case, viruses were serially diluted in MEM+++ (10-fold). Monolayers in 24-well or 96-well plates were infected in duplicate wells with 150 µl or 30 µl of the diluent, respectively, and rocked for 1 hour. The

inoculum in 24-well plates was removed and monolayers were overlaid with a tragacanth solution (0.6% tragacanth in MEM without phenol red, supplemented with 1% FBS and 1% abx). The inoculum in 96-well plates was not removed, but instead 170 μl of tragacanth overlay was added directly to the well. In either case, plates were left undisturbed. Monolayers in 96-well plates were fixed 30 hpi for wt and non-attenuated (NS2A A30P, NS4B E249G, NS5 P528H) WNV and 48 hpi for attenuated WNV (NS2A D73H, NS2A M108K or 3' UTR Δ). The difference in time was to ensure that the attenuated viruses had ample time to form foci that were large enough to easily visualize after IHC staining. Monolayers in 24-well plates were fixed at different times as indicated by the particular experiment. Fixation was achieved by removing the overlay, washing once with PBS, then fixing with MeOH:acetone at -20C for at least 30 minutes. After fixation, the plates were transported to the BSL2 for processing.

Results

CELL-ADAPTED MUTATIONS REDUCE GENOME REPLICATION

To quantitate the replication of WNRs bearing cell-adapted mutations, a replicon was generated that contained the reporter gene eGFP in place of prM and E genes, between the C gene and NS1 (WNR C-eGFP-NS1-5). For a diagram of this replicon, see Figure 32 in Appendix. The NS2A A30P, NS2A D73H, NS2A M108K, NS3 117Kins, NS4B E249G and NS5 P528H mutations were introduced into this replicon and subsequently packaged into VLPs. The full C gene was included in this replicon because the presence of a full C gene was able to increase the ability of the genomes to replicate and/or be packaged into VLPs (Fayzulin et al., 2006). Since some of the aforementioned mutations negatively affected genome replication, it was critical to get a good VLP titer from the packaging cells since propagating them in the packaging cells could lead to phenotypic revertants.

These VLPs were then used to infect Vero cells and at the indicated times post infection, cells were harvested and eGFP fluorescence intensity was measured by flow

cytometry. Figure 15A shows histograms depicting eGFP fluorescence intensity at 24 h post infection (hpi) of VLP-infected cells. Two populations of cells are depicted on these histograms: the population peak on the left corresponds to uninfected eGFP-negative cells (superimposable on the MOCK-infected population) and the population peak on the right corresponds to the eGFP-positive cells. The measure of fluorescence intensity, GM, was determined from the population of eGFP-positive cells. The arrows indicate the a peak in the infected cell population that corresponds to the average GM for eGFP fluorescence intensity.

Cells infected with genomes encoding NS5 P528H (GM=8561) or NS2A A30P (GM=8408) exhibited eGFP fluorescence intensity comparable to wt-infected cells (GM=8489). EGFP intensity of cells infected with genomes containing the NS4B E249G mutation (GM=7705) was slightly less than wt. NS2A M108K WNR (GM=2801) and NS2A D73H (GM=3317) infected cells showed the weakest expression of eGFP, consistent with the weak antigen staining observed in NS1-5 ET2AN WNR-transfected Huh7 cells. Results from NS3 117Kins WNR were not reported since VLPs encoding this mutation produced a fluorescence intensity similar to wt levels. This unexpected level of fluorescence intensity suggests that a phenotypic reversion had occurred and that this mutation was unstable under these conditions, consistent with the reversion seen in the NS3 117Kins WNV mutant (see NS3 117Kins WNV characterization below). A reduced level of genome-encoded GFP fluorescence was previously noted in two NS1-5 EG2AN WNR-bearing BHK cell clones that were passaged 31 times in G418-containing media compared to a cell population that was transiently infected with the same replicon (Figure 10A). These GFP data from the WNR-bearing BHK clones data correlated with the reduction in overall genome copy levels in the cell (Figure 10B). EGFP VLP infections were also analyzed for changes in eGFP fluorescence over time to observe the rates of C-eGFP- NS1-5 WNR replication. Figure 15B shows the GM eGFP fluorescence intensity over the course of infection. EGFP fluorescence intensity increased over time in all infected samples but more slowly for cultures infected with eGFP-NS1-5 NS2A D73H or NS2A M108K WNR. Genomes expressing the NS2A A30P mutation showed a lag in the

establishment of efficient genome replication but at 24 hpi, eGFP expression was similar to wt levels.

Figure 15: eGFP fluorescence from transient VLP-infected Vero cells

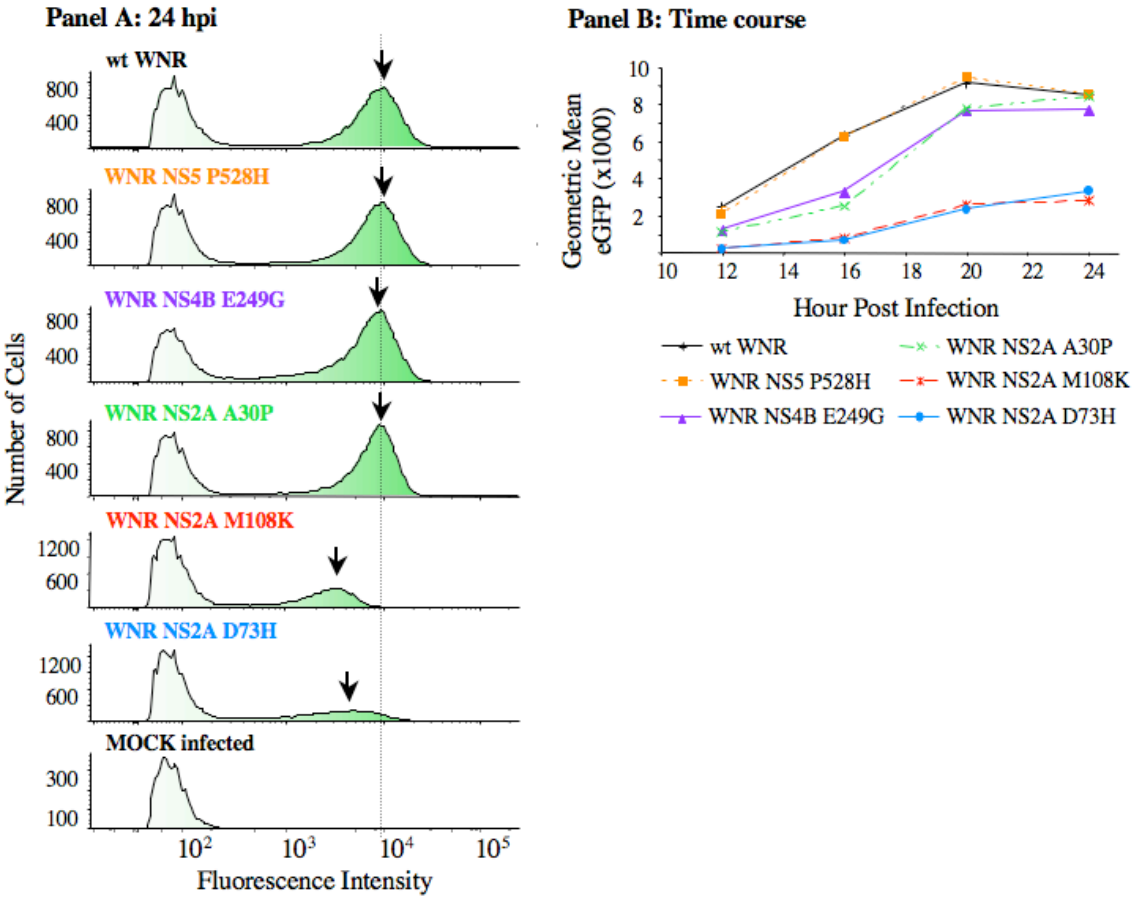

Figure 15: Levels of eGFP fluorescence in cultures infected with VLPs containing WNR C-eGFP-NS1-5 with selected cell-adapted mutations. (**Panel A**) Histograms showing eGFP fluorescence in cell populations at 24 hpi with WNR C-eGFPNS1-5 VLPs containing the indicated mutations. In this experiment, uninfected cells showed a peak fluorescence intensity of approximately 66. The arrow above each peak of eGFP-expressing cells indicates the GM intensity of eGFP expression at the peak of the infected cell population. (**Panel B**) Time course of eGFP fluorescence intensity at different times post infection. Both panels show data from one of three experiments that showed similar trends.

VIRUSES ENCODING CELL-ADAPTED MUTATIONS REPLICATE POORLY *IN VITRO*

To evaluate the affect of cell-adapted mutations on the viral genome, full-length genomes were engineered to contain the aforementioned mutations using standard molecular biology techniques. A virus with a large deletion in the 3' UTR (3' UTRΔ) was included in these studies as a control for a virus that reduced genome replication but did so without specific introduced mutations to the NS proteins. Little CPE was noted in BHK cultures electroporated with *in vitro* transcribed viral RNA encoding NS2A D73H, NS2A M108K or 3′ UTRΔ mutations at any time (up to 72 hpe-). In contrast, CPE was readily evident in cultures electroporated with NS2A A30P WNV, NS4B E249G WNV, NS5 P528H WNV and wt WNV. CPE was first noted in these cultures at 48 hpe- and by 72 hpe-, the cell monolayer was nearly destroyed. WNV titers varied, but on average, 10^7 ffu/ml (on Vero) were obtained for NS2A D73H, NS2A M108K and 3' UTRΔ WNV and 10^8 ffu/ml (on Vero) were obtained for NS2A A30P, NS4B E249G, NS5 P528H and wt WNV.

The sizes of infectious foci produced from these viruses were dramatically different between the wt virus and viruses harboring cell-adapted mutations or a 3′ UTR deletion (Figure 16). Specifically, viruses harboring cell-adapted mutations NS2A D73H, NS2A M108K, 3′ UTRΔ produced much smaller antigen-positive foci than the wt virus in Vero cells at 48 hpi, whereas the NS2A A30P and NS4B E249G produced foci in Vero cells that were slightly smaller than the foci produced by wt virus, and the NS5 P528H virus displayed foci indistinguishable from those produced by the wt virus (Figure 16). Interesting, when a subset of these viruses were used to infect MEF cells, NS4B E249G and NS5 P528H viruses formed foci identical in size to wt virus, whereas NS2A D73H, NS2A M108K, and 3′ UTRΔ formed substantially smaller foci (data not shown).

The NS3 117Kins WNV produced large foci on cell monolayers, which was inconsistent with the correlation between high CFE (in WNR NS1-5 ET2AN genomes in Huh7 cells) and a deficiency in genome replication. However, the Vero cells infected with VLPs harboring the WNR C-eGFP-NS1-5 genome showed a level of eGFP expression indistinguishable from the eGFP fluorescence seen from the wt WNR C-

eGFP-NS1-5 genomes. This indicated that in both the WNR C-eGFP-NS1-5 and WNV genomes, the NS3 117Kins mutation was highly unstable and these genomes quickly reverted to a wt phenotype. Vero cells infected with the virus recovered from BHK cells electroporated with *in vitro* transcribed NS3 117Kins WNV RNA were lysed and the viral RNA was harvested and sequenced through the NS3 gene. Interestingly, the phenotypically reverted virus still had an insertion at position 117, but the inserted lysine residue was changed to a methionine. This indicated that the lysine reside, and not the act of inserting an amino acid at this locus, resulted in the phenotype previously observed in the WNR NS1-5 ET2AN genomes.

Figure 16: WNV antigen-positive foci

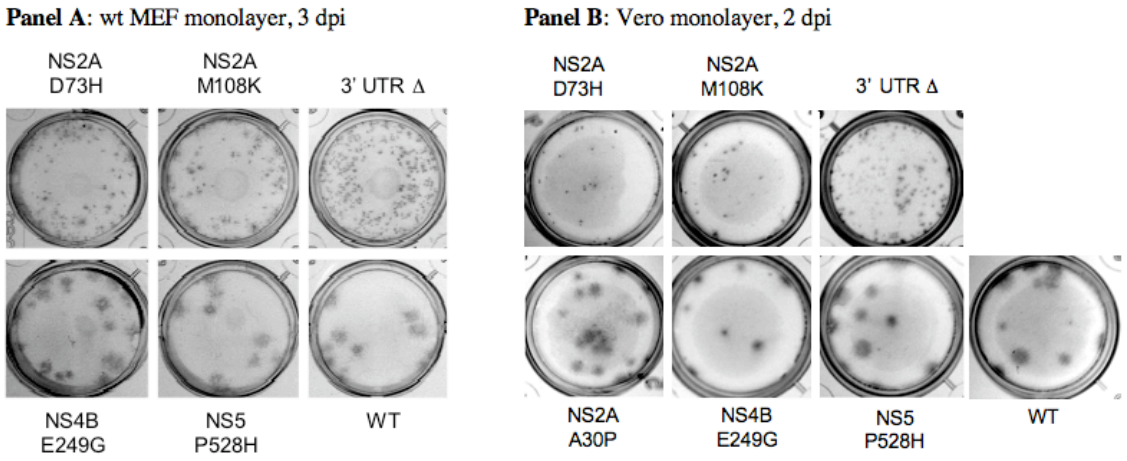

Figure 16: Antigen-positive foci produced from wt and mutant WNV on (**Panel A**) wt MEF cell monolayers and (**Panel B**) Vero cell monolayers. Wt MEF monoayers were fixed on day 3 pi, Vero at 2 dpi. WNV antigen was detected by IHC using the anti-WNV MHIAF.

Vero and Huh7 cells were used to produce growth curves for chosen viruses. Cell monolayers were infected with an MOI of 0.1 for 1 hr, then washed and re-fed with minimal growth media (DMEM+++). Samples of the supernatant were taken at indicated time points and titrated on Vero or Huh7 cell monolayers (Figure 17). At 48 hpi, peak

titers were reached for wt WNV and WNV NS2A A30P at which point WNV NS2A A30P produced a log fewer infectious particles than wt WNV. At 48 hpi, titers of WNV NS2A M108K and WNV NS2A D73H were 2–3 logs lower than wt in both cell types. By 72 hpi, peak titers had not been attained for WNV harboring either NS2A D73H or M108K mutations in Vero cells or for NS2A M108K infection of Huh7 cells. These findings suggest that viral replication level is the most important aspect determining *in vitro* persistence since the growth trends of these NS2A D73H and M108K viruses were similar between two cell lines, even thought differences in *in vitro* persistence are only observed in the Huh7 cells (see above). As mentioned above, at 72 hpi, CPE was only evident in Huh7 cells infected with wt WNV or WNV NS2A A30P and was not present in MOCK infected cultures or cultures infected with WNV NS2A D73H and WNV NS2A M108K. Little CPE was noted in infected Vero cells with any virus at 72 hpi. However, a small proportion of the foci produced the 72 hpi titration samples taken from NS2A D73H and NS2A M108K WNV-infected cells were larger than those observed at earlier time points, indicating that a reversion to a wt-like phenotype was occurring. No such reversions were noted in any titration samples taken before 72 hpi.

Figure 17: Wt and NS2A mutant WNV growth curves

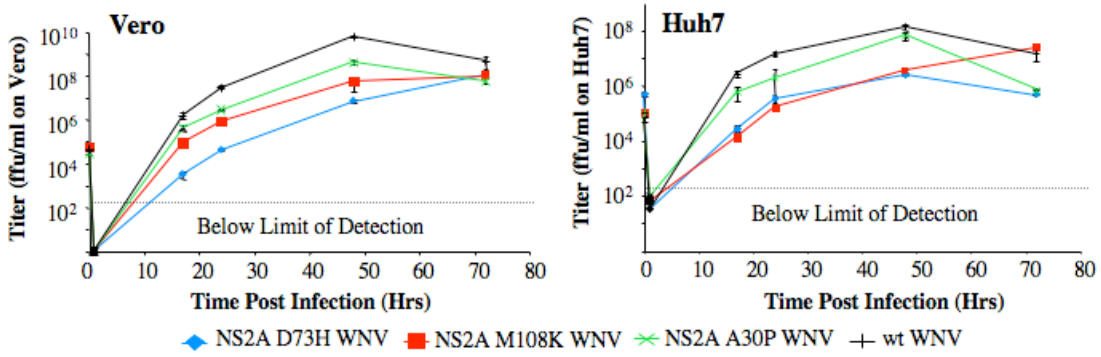

Figure 17: Vero or Huh7 cells were infected with wt or NS2A mutant WNV at an MOI of 0.1 and lysates were harvested at the various times post infection. Samples were titrated on either Vero or Huh7 monolayers (as indicated in figure). Error bars denote the standard deviation of the titration. The limit of detection for the titration (shown by the dashed line) was 3.3×10^2 ffu/ml.

Discussion

The data presented in this chapter support the hypothesis that reduced replication is associated with a lack of replicon cytopathogenicity. Mutations that led to a reduction in antigen accumulation in the WNR NS1-5 ET2AN genomes also showed a reduction in reporter gene levels in the WNR C-eGFP-NS1-5 genomes. The decreased levels of eGFP expression from NS2A D73H and NS2A M108K WNR C-eGFP-NS1-5 genomes (compared to other mutant and wt replicons) paralleled the expression of GFP from BHK cells transiently transfected with the wt WNR NS1-5 EG2AN genome (Figure 10). Vero cells expressing the wt WNR C-eGFP-NS1-5 genome show two peaks that correspond to cells that do and do not express eGFP, just as BHK cells transiently transfected with the wt WNR NS1-5 EG2AN genome, but the peaks are better defined from each other and the fluorescence intensity is higher than seen on the transiently transfected BHK cells. These differences could be explained by the differences in the ability of the WNR C-eGFP-NS1-5 and WNR NS1-5 EG2AN genomes to replicate. The presence of the full C gene has a positive influence on genome replication (Fayzulin et al., 2006). The GFP expression in the WNR NS1-5 EG2AN is driven by an IRES rather than by the replicon itself. Lastly, the cell type used may also have an effect on the levels of GFP expression. However, the trend still remains: wt genomes produce higher levels of WNV antigen and reporter genes than genomes with cell-adapted mutations.

There was an approximate 4-fold reduction in eGFP expression in Vero cells infected with the C-eGFP-NS1-5 genomes expressing the NS2A D73H or M108K mutations compared to the wt C-eGFP-NS1-5 genomes (Figure 15). In the virus growth curves, however, the differences seen between the wt WNV and the NS2A D73H and NS2A M108K WNVs were several logs different (about 100-500-fold reduction, Figure 17). The apparent discrepancy between these results can be explained by the production and spread of virions from the WNV infection. The C-eGFP-NS1-5 replicon can only replicate within the cell and cannot spread. If the NS2A D73H and M108K WNVs replicate to 25% of the ability of the wt WNV to replicate, this effect is amplified by

subsequent rounds of infection and virus spread. In this way, a 4-fold difference in replication can result in a several hundred-fold different in virion production within the same 24-hour timeframe.

The phenotype of the NS3 Kins mutant could not be fully characterized due to its instability. Based on the extremely weak immunohistochemical staining of NS3 117Kins WNR NS1-5 ET2AN genomes (discussed in Chapter 2), this mutation appeared to have a greater effect on the ability of the replicon genome to replicate than did the NS2A D73H or M108K mutations. However, this expected phenotype was not seen when the NS3 117Kins was incorporated into WNR C-eGFP-NS1-5 or WNV genomes. Instead, the VLPs and viruses harvested from packaging cells or BHK cells electroporated with the NS3 117Kins WNR C-eGFP-NS1-5 or NS3 117Kins WNV *in vitro* transcribed RNA had a phenotype that was indistinguishable from the wt replicon or virus.

Mutations in NS2A have been linked to reductions in replication in several systems. Two mutations in NS2A were found within KUNR that were selected during the generation of KUNR-bearing BHK cells; A30P and N101D (Liu et al., 2004). The NS2A A30P mutation did not affect the ability to KUNR to replicate (Liu et al., 2004), which is consistent with the wt-like phenotype seen in NS2A A30P WNR and NS2A A30P WNV infections that are described above. The NS2A N101D mutation did have a modest affect on replication in KUNR (Liu et al., 2004), but it is uncertain whether a similar affect would be observed in WNR genomes. An NS2A mutation (V61A) was associated with a small-plaque virus detected within an isolate from a crow in New York in 2000 (Jia et al., 2007). The original infectious KUNV cDNA clone described by Khromykh and Westaway had a smaller plaque phenotype compared to the parental strain, which was potentially attributed to a single missense mutation in NS2A (R175K) (Khromykh and Westaway, 1994).

Naturally occurring viruses harboring several mutations including the NS4B E249G mutation produced small foci that were temperature sensitive (Davis et al., 2004). However, a NY99 WNV genetically engineered to only contain the NS4B E249G mutation produced large antigen-positive foci (Davis et al., 2007). Growth kinetics of the

NS4B E249G WNV in Vero cells demonstrated no differences in replication profiles compared to wt NY99 WNV (Davis et al., 2007). Additionally, Puig-Basagoiti and colleagues reported that NS4B E249G WNR replicated more poorly compared to wt replicons in C3H/He and BHK21 but not Vero cells (Puig-Basagoiti et al., 2007). The phenotypes of the NS4B E249G mutation described by other investigators are consistent with the phenotype of NS4B E249G TX02 WNV described here.

Phenotypic reversion of highly attenuated genomes is expected under different selective pressures. The NS3 117Kins mutation was stable in the WNR NS1-5 ET2AN genome since, in this system using G418 selection to generate replicon-bearing cells, genomes that replicate poorly are highly favored. This scenario operates under purifying selection. If a genome that replicated well was produced, it would likely lead to the death of the cell and be taken out of the population. The WNR NS1-5 ET2AN genomes cannot spread from cell to cell and so a phenotypic reversion in one cell would be unlikely to out compete other cells in the population. In this way, genomes that replicate well are selected against. However, without the selective pressure to be maintained within the cell, genomes that replicate well will be favored. By Darwinian selection, the 'fit' genomes that efficiently replicate will produce more VLP or virion progeny (as seen by higher titers). These fit VLPs or viruses will out compete the 'unfit' or replication deficient VLPs or viruses in the same population. These genomes are not constrained by one host cell and the death of the cell is irrelevant. These types of selections explain why the NS3 117Kins mutation was highly stable in the WNR NS1-5 ET2AN genome, but not the WNR C-eGFP-NS1-5 or WNV genomes.

The phenotype of the NS2A D73H and NS2A M108K mutations could be assessed in the WNR C-eGFP-NS1-5 and WNV genomes since these mutations did not reduce genome replication as severely as the NS3 117Kins mutation. WNV antigen staining by IHC was barely detectable from Huh7 cells transiently transfected with the NS3 117Kins WNR NS1-5 ET2AN genome, whereas low, but readily detectable levels of WNV antigen were produced from NS2A D73H and NS2A M108K WNR NS1-5 ET2AN genomes (Chapter 2). This suggests that the NS3 117Kins mutation had a greater

effect on genome replication than either NS2A mutations, and this is the reason why the NS3 117Kins-containing genomes reverted to quickly. The NS2A D73H and NS2A M108K mutations are also unstable (compared to the non-attenuating mutations), but longer periods of time were needed to see evidence of phenotypic reversion.

CHAPTER 4: WNV ENCODING CELL-ADAPTED MUTATIONS ARE ATTENUATED IN MICE[4]

Abstract

WNV encoding cell-adapted mutations NS2A D73H and NS2A M108K, as well as the 3' UTRΔ, produced small antigen-positive foci on cell monolayers and cause little CPE in cell culture. Adult mice infected with a range of doses of these aforementioned viruses do not die from infection. Only one death was produced following the inoculation of NS2A D73H WNV into mice, and the virus recovered from this animal had reverted to the wt genotype at this locus. In addition to replicating poorly in cell culture, the NS2A D73H WNV produced a lower and more transient viremia in adult mice than wt WNV. The phenotypes of the remaining mutant viruses (encoding mutations NS2A A30P, NS4B E249G and NS5 P528H) were phenotypically indistinguishable from the wt WNV phenotype. However, the NS2A D73H WNV was not attenuated in all systems; the virus still retained its virulence in the ultrasensitive newborn mice. Taken together, WNV with cell-adapted mutations are attenuated in adult mice compared to wt WNV.

Introduction

Rodents have been used to study the pathogenesis of WNV infection. Mice were used to isolate and characterize the first WNV isolate (Smithburn et al., 1940). More recently, infections of mice were used to a particular protein, physiological condition or pathway during the course of a flavivirus infection. Other studies have used mice as models to demonstrate the effectiveness and safety of vaccine or antiviral candidates

[4] Significant portions of this chapter have been previously published in Virology, which does not require copyright permission so long as proper citation is provided. The citation for this work is: **S.L. Rossi**, R.Z. Fayzulin, N. Dewsbury, N. Bourne and P.M. Mason (2007) Mutations in West Nile Virus Nonstructural Proteins that Facilitate Replication Persistence in Vitro Attenuate Virus Replication in Vitro and in Vivo. Virology 364(1): 184-195.

since the mice are sensitive to WNV infection. Mice have widely been used to determine the virulence of different WNV strains or the change in virulence associated with mutations within WNVs. Attenuation is typically measured as the number of mice that survive infection at a given dose compared to another strain of known virulence. If multiple doses are used, and some doses yield greater than 50% mortality within a group, then the number of ffu needed to cause death to 50% of the mice (LD_{50} value) can be measured. This value is very useful because it allows a direct, objective comparison between viruses. The lower the LD_{50} value, the fewer infectious units (i.u.) are required to kill half of the infected mice. Sometimes, two viruses can have the same LD_{50} value, but differ in the time it takes to kill the mice, and so attenuation can also be measured in average survival time.

WNVs that show an attenuated phenotype when injected in the periphery of a mouse often are still virulent and cause death when injected directly into the brain (Beasley et al., 2002). In other words, viruses that are attenuated by the i.p. route may not cause death because the virus cannot enter the brain (not neuroinvasive). However, if these viruses did infect the brain, signs of disease would be seen that would likely result in death (neurovirulent). As a result, virus attenuation is generally measured by the i.p. route. Inoculations directly into the brain are more often done to demonstrate the safety of a virus by observing the lack of death. For example, high doses (approximately $2x10^6$ i.u.) of pseudoinfectious particles based upon the WNV and YFV genomes can be injected directly into the brains of suckling mice and not cause death, whereas low doses of the full-length virus (~ 1 ffu) kill all the infected mice (Mason, Shustov, and Frolov, 2006).

WNV mortality in mice is age-dependent (Umrigar and Pavri, 1977; Weiner, Cole, and Nathanson, 1970). Suckling (newborn) mice are extremely susceptible to WNV infection, most likely due to their underdeveloped immune response system. Newborns are commonly used as a sensitive assay to measure the virulence of a WNV infection. The dose of a virulent lineage I WNV (TX02) that is needed to cause death in 50% of the infected animals (LD_{50} value) when injected into the brain of a 3-to-4-day-old suckling

Swiss-Webster mouse is approximately 1 pfu (Mason, Shustov, and Frolov, 2006). Adult mice with developed immune systems are more resistant to WNV-induced death. By 12-weeks of age, no outbred albino Swiss mice infected with $1x10^6$ newborn mouse i.c. LD_{50} units of Eg101 WNV died of infection whereas all similarly infected newborn or 4-week-old mice died (Weiner, Cole, and Nathanson, 1970). As a result of the age-dependent mortality, most experimental infections are performed in mice that are 3-to-5 weeks old. The LD_{50} value of wt WNV injected i.p. into adult mice (3-5 weeks of age) is less than 10 pfu. The LD_{50} was less than 1 pfu of the TX02 WNV strain in 4- to 5-week-old outbred Swiss Webster mice (Mason, Shustov, and Frolov, 2006). In 3- to 4-week-old Swiss Webster mice infected with the NY99 WNV strain, the LD_{50} has been reported in the range of 0.5-1.7 pfu (Beasley et al., 2002; Borisevich et al., 2006; Davis et al., 2004; Wicker et al., 2006). Similar LD_{50} values were observed in older Swiss-Webster mice (7-to-8 and 15-to-16-week-old mice) infected i.p. with NY99 WNV (Beasley et al., 2002).

Differences in virulence between strains or mutants of WNV are detectable using the mouse models. The most common method for detecting differences in WNV virulence is to inject adult mice i.p. with several dilutions of the desired virus and recording death. Survival curves show the kinetics of WNV-induced death over a 2-3 week period for each virus dose. It was determined that lineage I WNVs are generally more virulent than lineage II WNVs (Beasley et al., 2002). KUNV isolates have LD_{50} values greater than 10,000 ffu (Beasley et al., 2002). Levels of attenuation from WNV harboring mutations have also been measured by using this model (Davis et al., 2004; Davis et al., 2007; Puig-Basagoiti et al., 2007; Wicker et al., 2006). Oftentimes, this attenuation is in accordance with an attenuated phenotype *in vitro*.

RATIONALE

Due to the differences in phenotypes *in vitro* between the NS2A D73H, NS2A M108K and 3' UTRΔ WNV and the NS2A A30P, NS4B E249G, NS5 P528H and wt WNV, it was expected that the viruses that showed an attenuated phenotype *in vitro* would also be attenuated *in vivo*. Therefore, the second-half of aim 2 was to determine

the effect of these cell-adapted mutations on viral replication and virulence in vivo. It is hypothesized that the viruses that replicate poorly *in vitro* (NS2A D73H, NS2A M108K and 3' UTRΔ WNV) will also replicate poorly *in vivo* and not result in the death when injected into the periphery of a mouse. The levels and kinetics of viremia were assessed to determine the effects of the cell-adapted mutation on the ability of the virus to replicate *in vivo*. Virulence was measured by comparing LD_{50} values among the panel of wt and mutant viruses.

Materials and Methods

DETERMINING OF 50% LETHAL DOSE IN ADULT MICE

Groups of 5 4-week-old female Swiss-Webster mice (Harlan) were inoculated i.p. with viruses diluted in PBS supplemented with 10% FBS. Mutant and wt WNV were all recovered from BHK cells electroporated with the RNA transcribed from the FLIC-BAC clone template were transfected 48-72 hours previously. Viruses was titrated on Vero cell monolayers and diluted in diluent (PBS with 10% FBS, filtered) so that 100 μl would deliver a dose of 0.1, 1, 10, 100 or 1000 ffu to each mouse. Mice were observed daily for 15 days after inoculation for signs of illness or death. A mouse classified as moribund if the signs of illness were so severe that the mouse was not expected to survive until the next day. These severe signs included ruffled fur, hunched posture and ataxia upon examination. Moribund mice were humanely euthanized to reduce their suffering, in accordance with UTMB Animal Care and Use requirements. The moribund mouse's death was recorded as the next day. LD_{50} values were calculated for each virus using the methods described by Reed and Meunch (Reed and Meunch, 1938).

Mice that survived this challenge were housed for an additional 2 weeks (4 weeks p.i.). No mice died during this time. At one month p.i., mice were euthanized by CO_2 asphyxiation then bled by cardiac punch. Death was confirmed by cervical dislocation.

Blood was centrifuged in serum separator tubes (5 minutes at 5000 rpm) to isolate sera. Sera were heat inactivated at 56°C for 30 min then transported to the BSL2.

NEUTRALIZATION (PRNT80) ASSAY

Serum was collected from all surviving mice 1 month after challenge and tested for the presence of neutralizing WNV antibodies, as described above. Heat-inactivated sera were diluted two-fold in DMEM+++ media (starting at 1/20 and ending at 1/2560), then incubated at 37°C for 2 h with approximately 100 i.u. of WNV VLPs containing WNR C-NS1-5. At the end of the antibody-VLP incubation, this mixture was used to infect duplicate wells of Vero cells seeded in 96-well plates. Twenty-four hours later, cells were fixed and immunostained as previously described using the anti-WNV MHIAF. For each serum sample, antigen-positive cells were counted and compared against the no-serum control. Wells that contained no mouse serum produced approximately 90 antigen-positive cells. The serum dilution that produced an 80% reduction in antigen-positive cells was read as the antibody titer for the sample (PRNT80). In this assay, NMS collected from age-matched outbred mice displayed an 80% reduction in antigen-positive cells at a dilution of 1/80. Therefore, any titer above 1/160 was considered positive for the presence of anti-WNV antibodies in this assay.

QUANTIFYING VIREMIA IN WNV-INFECTED ADULT MICE

Four-week-old female Swiss-Webster mice were inoculated i.p. with $1x10^5$ ffu of NS2A D73H WNV or wt WNV diluted in 10% FBS in PBS. Viruses were titrated previously on Vero cell monolayers. Three mice/virus were sacrificed on days 1–6 pi and blood was collected from each mouse by cardiac punch. Blood was centrifuged in serum separator tubes (5 minutes at 5000 rpm) to isolate the sera, which were transferred to new eppendorf tubes and then frozen at -80°C until needed. Viremia was determined by titrating the serum samples in duplicate on Vero cells in 24-well plates, as described in Chapter 3. To determine statistical significance in the viremia experiments, a repeated-measures ANOVA test was performed for all sera samples on all days. Then, a Tukey-

Kramer post-hoc test was used to measure the difference between the two viral groups on each day.

DETERMINING NEUROVIRULENCE IN SUCKLING MICE

Suckling mice were used to determine the level of neurovirulence associated with the NS2A D73H WNV and wt WNV. All newborns of the same litter (10 or 11 newborns) were infected with the same virus and same dose. Newborns were housed with the uninfected mother for the duration of the experiment.

For this experiment, the wt and NS2A D73H FLIC contained within the pACNR backbone were used. Viruses were harvested from cells electroporated with RNA recovered from the FLIC-pACNR clone at 48 hpe- and stored frozen until needed. Viruses were titrated on Huh7 cells prior to animal inoculation. Wt and NS2A D73H WNV stocks were diluted in PBS containing 10% FBS (filter sterilized) at the time of inoculation. Twenty μl of the diluted virus stocks were used for the i.c. inoculation of each litter of suckling mice. NS2A D73H WNV was tested at 500, 50 and 5 ffu/mouse. Wt WNV was used at doses of only 5 and 0.5 ffu/mouse.

Mice were observed daily for signs of illness and death. The day of death was recorded in the same way as it was for the adult mice. Moribund pups infected with 500 ffu of NS2A D73H WNV were euthanized and their brains were harvested and the viral RNA contained within was sequenced to confirm and characterize the lethal viral infection.

SEQUENCING VIRUSES FROM MORIBUND/DEAD ADULT MICE

Sequencing brain homogenates from adult mice

Individual brains from moribund (or in some cases, dead) mice from each virus group were cut in half and one half was frozen in 2-ml eppendorf tubes with a 5 mm steel ball (GlenMills, Inc.) at -80C. Brain hemispheres were thawed on ice, resuspended in 1 ml of L15 and disrupted using a bead mill (set for 4 minutes at 30 cycles/second). The

homogenate was clarified by centrifugation and approximately 10% (volume) of the supernatant was used to infect a monolayer of Vero cells in a 6-well plate. The infection was allowed to rock for 1 hour at 37°C, then the inoculum was removed and the cells were maintained for 24 hours in Vero growth media. The next day, the media was removed and the monolayers were washed 1x in PBS. Trizol LS was used to lyse the monolayer (750 μl Trizol LS and 250 μl media) at room temperature for 10 minutes prior to transferring to an eppendorf tube and transporting to the BSL2 for processing. Total RNA was extracted from the infected cell lysate by adding chloroform to facilitate phase separation and alcohol to precipitate the RNA as described in Chapter 2. cDNA was generated from 1μg extracted RNA using the Improm II RT kit (Promega) as per manufacturer's instructions with either the individual or a mixture of the following primers: random hexamer and a specific anti-sense primer (U8n: 5' AGATCCTGTGTTCTCGCACC) that anneals to the WNV 3' UTR. The RNA template was then degraded prior to running the PCR reaction using a mixture of RNases H and T_1 at 37°C for 15 minutes. Table x shows the primer pairs used to generate a PCR-derived DNA fragment that spanned the introduced mutation for each mutant virus. Gel-purified PCR products were sent to the UTMB protein chemistry core facility for sequencing using primers that annealed within the PCR products.

Table 3: RTPCR primers used to amplify WNV harvested from moribund mouse brain

Mouse #	Mutation (WNV)	Forward primer (Name) 5' sequence	Reverse primer (Name) 5' sequence
37	NS4B E249G	(U139)- 5' AGAACGCTGTAGTGGATGG	(U6)- 5' GGGTGTCACAACACTCAG
38 *	NS5 P528H	Rxn 1: (U46)- 5' TCCATCCATTCATTCTCC Rxn 2: (U48)- 5' ACTGACAGCCATGCGGCT	Rxn 1: (U31)- 5' GGGACTGGTCAGAAACCC Rxn 2: (U130)- 5' TGGTCAATGGAGTGGTCAGG
39	NS2A A30P	(U25)- 5' GGTCATCGATCAGTTTCC	(U4)- 5' CCCTGATCAAGCTGCCTA
40	NS2A A30P	(U129)- 5' TTACTGCCCAGGAACTACG	(U4)- 5' CCCTGATCAAGCTGCCTA
41	NS2A D73H	(U129)- 5' TTACTGCCCAGGAACTACG	(U4)- 5' CCCTGATCAAGCTGCCTA

* Nested PCR reaction was performed. The reaction using U46 and U31 was performed first.

Sequencing brain homogenates from suckling mice

The brains from moribund newborn mice infected with NS2A D73H WNV were harvested and pooled on day 6 pi. The pooled brains were homogenized using a ball bearing (as described above). A cell monolayer was infected with the suckling mouse brain homogenate and lysed 24 hpi using an RNA extraction kit (RNaqueous, Ambion). RNA was extracted as per the manufacturer's recommendations. The homogenate was sequenced spanning the NS1 and NS2A genes to ensure the presence of the introduced mutation. RTPCR (Improm II kit, Promega) was performed using 1µg the extracted viral RNA using a random hexamer to create the cDNA template. PCR was performed on the cDNA using AccuTaq polymerase and specific oligos that annealed to the NS1 (U129: 5' TTACTGCCCAGGAACTACG) and NS3 (U 28: 5' TGTCTGGTACCGGATGGG). The PCR product was purified by agarose gel electrophoresis and then sequenced at the UTMB protein chemistry core facility. To completely span the NS2A gene region, sense (U5: 5' GGATGATACTGAGAGCCA) and anti-sense (U4: 5' CCCTGATCAAGCT GCCTA) sequencing primers that annealed on the NS2A gene were used.

Results

VIRUSES ENCODING CELL-ADAPTED MUTATIONS ARE ATTENUATED *IN VIVO*

Based upon the small size of the foci produced on wt MEF and Vero cells (Figure 16), it was anticipated that WNV with cell-adapted mutations (NS2A mutations D73H and M108K) would be attenuated in mice compared to the wt WNV or the WNV that encoded non-cell-adapted mutations (NS2A A30P, NS4B E249G and NS5 P528H). A WNV that contained a large deletion in the 3' UTR, which included no introduced point mutations, was included as a control for attenuation. The degree of viral attenuation for each virus was measured by the percentage of death caused to groups of 5 outbred Swiss-Webster mice inoculated with each virus at a variety of doses ranging from 0.1 – 1000 ffu. Data from these experiments were used to generate the survival curves (Figures 18-21) and calculate LD_{50} values (Table 4). The dose of each virus needed to cause death in half the infected mice (LD_{50}) providing an objective measure of the virulence of these viruses.

No mice died that were infected with any virus at the 0.1 ffu dose, so no survival curve is shown for those data. Figure 18 shows the survival curve for mice infected with all viruses at the 1 ffu dose. All mice infected with the NS2A D73H, NS2A M108K or the 3' UTR Δ WNV survived infection with 1 ffu. On day 9 pi, one mouse from the group infected with either the NS4B E429G or wt WNV died. On days 10 and 11 pi, one mouse died from the NS5 P5228H and NS2A A30P WNV infection, respectively. The percent mouse survival for all WNV with non-cell-adapted mutations, 80%, was the same as wt WNV.

Figure 18: Survival curve of adult Swiss-Webster mice infected with 1 ffu of mutant and wt WNV

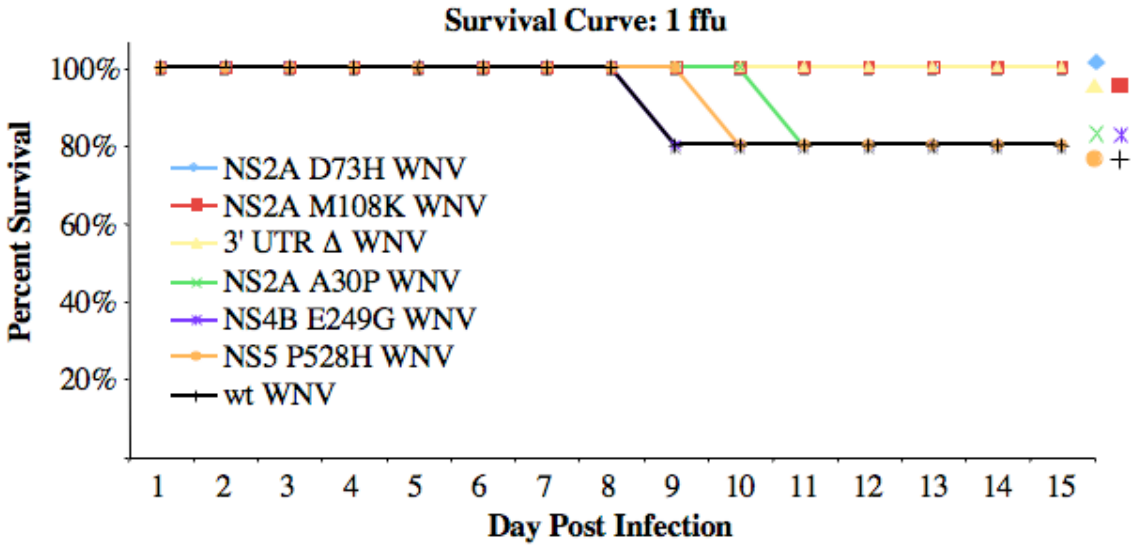

Figure 18: Swiss-Webster mice infected with 1 ffu of mutant or wt WNV were monitored daily for signs of illness or death. The number of mice that survived each day was recorded as the percent of all infected animals that survived. The symbol that corresponds to each virus is shown at the end of day 15 pi to indicate the percent survival for each virus. Light blue diamonds indicate the NS2A D73H WNV, red squares indicate NS2A M108K WNV, yellow triangles indicate 3' UTR Δ WNV, green "x"s indicate NS2A A30P WNV, purple asterixes indicate NS4B E249G WNV, orange circles indicate NS5 P528H WNV and black crosses indicate wt WNV.

More mice within each group died from a 10 ffu dose of the non-attenuated and wt WNV, as shown in Figure 19. At this dose, no mouse died from the NS2A D73H, NS2A M108K or the 3' UTR Δ WNV infection. The first death seen at this dose occurred at day 7 pi with the wt virus. By day 8 dpi, mice infected with the NS2A A30P, NS4B E249G and NS5 P528H WNV were dying. The final percentage of mice surviving the NS4B E249G WNV infection was 40%. All other non-cell-adapted mutant viruses and the wt WNV had only 20% of infected mice survive infection with 10 ffu.

Figure 19: Survival curve of adult Swiss-Webster mice infected with 10 ffu of mutant and wt WNV

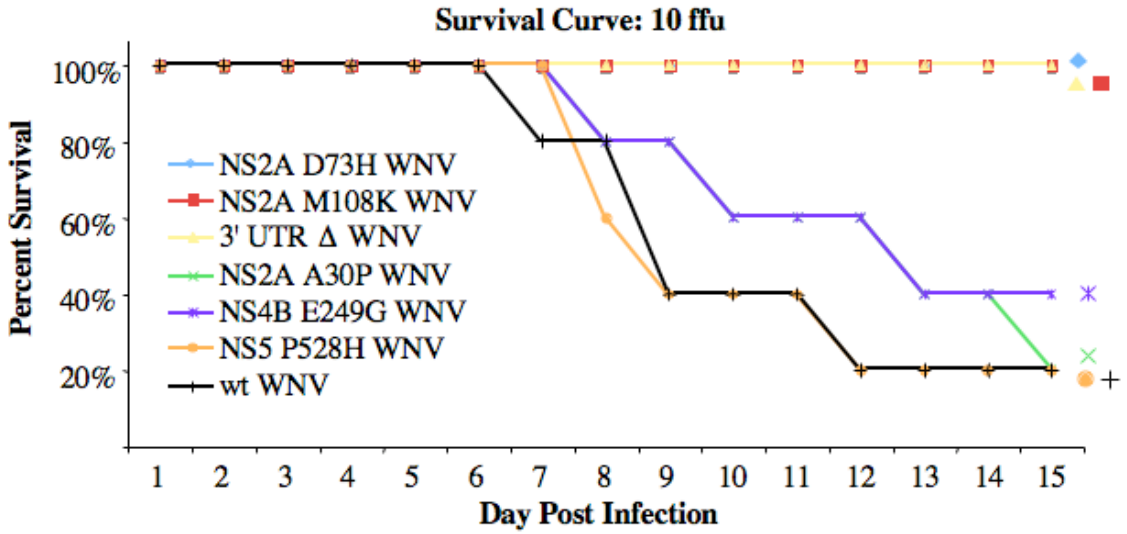

Figure 19: Swiss-Webster mice infected with 10 ffu of mutant or wt WNV were monitored daily for signs of illness or death. The number of mice that survived each day was recorded as the percent of all infected animals that survived. The key for this curve is the same as Figure 18.

The highest mortality was observed in mice infected with 100 ffu of mutant and wt WNV (Figure 20). All mice infected with the NS2A M108K or the 3' UTR Δ WNV survived infection. There was one death observed in the group infected with NS2A D73H WNV. This mouse had died on day 13 dpi, which was later than the average day of death observed for all other non-attenuated viruses (range of 8.8-10.3 days). The genotype of the virus that killed this mouse is discussed in detail in the next section. The wt WNV had killed all mice by day 10 pi. Although the kinetics of death were slightly different for the NS2A A30P, NS4B E249G and NS5 P528H WNV, all viruses had killed 80% of the mice by day 15 pi.

Figure 20: Survival curve of adult Swiss-Webster mice infected with 100 ffu of mutant and wt WNV

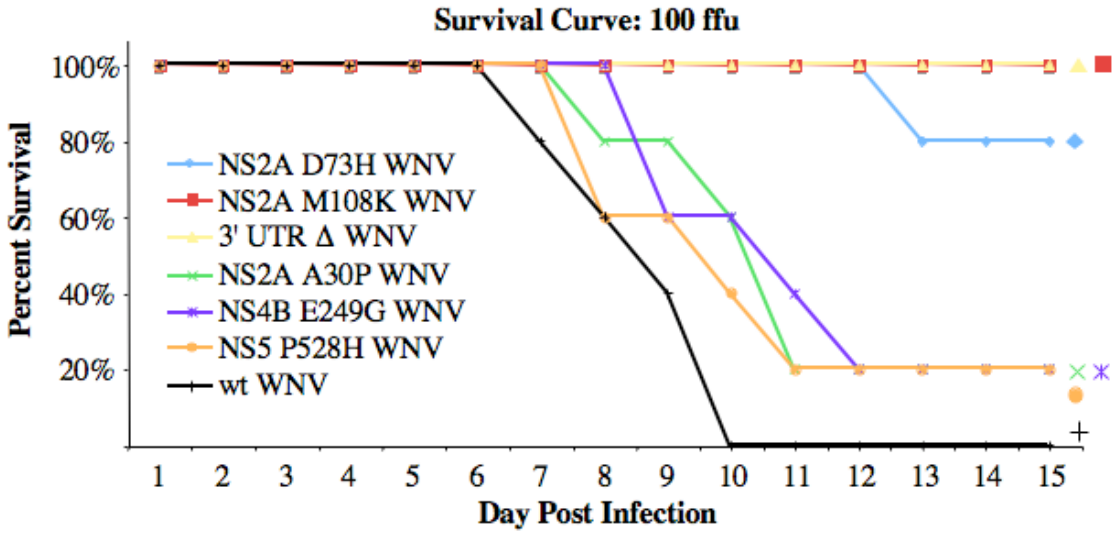

Figure 20: Swiss-Webster mice infected with 100 ffu of mutant or wt WNV were monitored daily for signs of illness or death. The number of mice that survived each day was recorded as the percent of all infected animals that survived. The key for this curve is the same as Figure 18.

The highest virus dose tested in the mice was 1000 ffu (Figure 21). No mice died from infection with the NS2A D73H, NS2A M108K or the 3' UTR Δ WNV. On the other hand, all mice infected with NS5 P528H died. Twenty percent of mice infected with NS4B E249G died. In some groups, there was less death observed with the 1000 ffu dose than the 100 ffu dose. Eighty percent of mice infected with 1000 ffu of NS2A A30P survived. Only 60% of wt WNV-infected mice died with 1000 ffu whereas all mice infected with 100 ffu of wt WNV died. The potential reason for the high percentage of surviving mice at the higher viral doses is explored in the discussion for this chapter.

Figure 21: Survival curve of adult Swiss-Webster mice infected with 1000 ffu of mutant and wt WNV

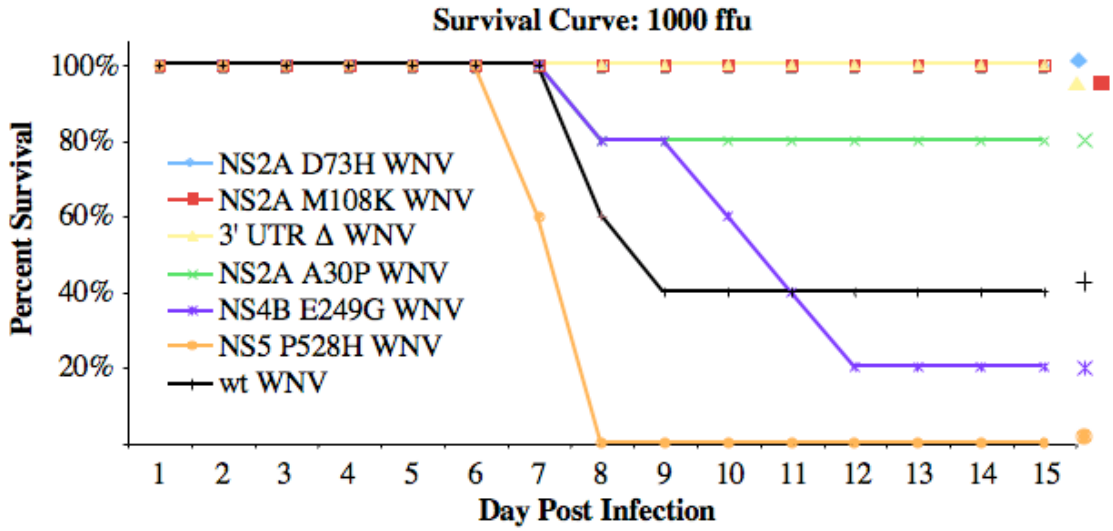

Figure 21: Swiss-Webster mice infected with 100 ffu of mutant or wt WNV were monitored daily for signs of illness or death. The number of mice that survived each day was recorded as the percent of all infected animals that survived. The key for this curve is the same as Figure 18.

LD_{50} values determined for each virus are summarized in Table 4. To accurately determine LD_{50} values, the 1000 ffu group for all viruses was omitted from the calculation. Viruses that showed no or very little reduction in replication and CPE *in vitro* compared to wt WNV were virulent *in vivo* and had similar LD_{50} values. These non-attenuated viruses included NS2A A30P, NS4B E249G and NS5 P528H WNVs. On the other hand, viruses that replicated poorly and caused little CPE *in vitro* compared to wt WNV were avirulent in mice. These viruses included NS2A D73H, NS2A M108K and 3' UTR Δ WNVs. No LD_{50} value could be accurately calculated for these attenuated viruses since less than 50% of the mice died at all doses, therefore the LD_{50} value is recorded as being above 1000 ffu (Table 4).

Table 4: LD_{50} values for mutant and wt WNVs in Swiss-Webster adult mice

Virus	LD_{50} (ffu)
NS2A A30P WNV	4.2
NS2A D73H WNV	$>1x10^{3}$ [a]
NS2A M108K WNV	$>1x10^{3}$ [a]
NS4B E249G WNV	6.9
NS5 P528H WNV	4.2
3' UTRΔ WNV	$>1x10^{3}$ [a]
wt WNV	3.2

[a] LD_{50} values for these viruses are greater than the highest dose given in this experiment (1000 ffu), so the LD_{50} is recorded as greater than 1000 ffu.

To ensure that the survival curves accurately represented mice that were infection, the mice that survived past 15 dpi were housed for an additional two weeks. At one-month pi, the mice were euthanized and bleed. Their sera from groups infected with 100 or 1000 ffu of virus were tested for the presence of antibodies against WNV. The neutralization assay was performed using VLPs containing the wt WNR C-NS1-5 genomes. The anti-WNV antibody titers for individual mice are listed in Table 5. Uninfected (MOCK) mice from the same experiment were also used as controls. These mice gave a PRNT80 titer of 1/40 to 1/80 (mice # 167-170 in Table 5) using this assay. Therefore any titer of 1/160 or greater was considered to be indicative of the ability of the WNV to replicate within the mouse. The highest PRNT80 titer that could be accurately measured in this assay was 1/1280, but many sera efficiently neutralized the VLPs at a higher dilution and where therefore recorded with a PRNT80 titer of >1/2560.

Table 5: Anti-WNV PRNT80 titers from mice that survived infection with mutant and wt WNV at 100 and 1000 ffu doses

Mouse #[a]	Mutation[b]	Dose	PRNT80 Titer	Mouse #	Mutation	Dose	PRNT80 Titer
57	NS2A D73H	100	1/1280	106	3' UTR Δ	100	1/1280
58	NS2A D73H	100	1/1280	107	3' UTR Δ	100	1/320
59	NS2A D73H	100	>1/2560	108	3' UTR Δ	100	>1/2560
60	NS2A D73H	100	>1/2560	109	3' UTR Δ	100	1/320
61	NS2A D73H	1000	>1/2560	110	3' UTR Δ	100	>1/2560
62	NS2A D73H	1000	>1/2560	111	3' UTR Δ	1000	1/80
63	NS2A D73H	1000	>1/2560	112	3' UTR Δ	1000	>1/2560
64	NS2A D73H	1000	>1/2560	113	3' UTR Δ	1000	>1/2560
65	NS2A D73H	1000	>1/2560	114	3' UTR Δ	1000	>1/2560
81	NS2A M108K	100	>1/2560	115	3' UTR Δ	1000	>1/2560
82	NS2A M108K	100	>1/2560	126	NS2A A30P	100	>1/2560
83	NS2A M108K	100	>1/2560	127	NS2A A30P	1000	>1/2560
84	NS2A M108K	100	>1/2560	128	NS2A A30P	1000	>1/2560
85	NS2A M108K	100	>1/2560	129	NS2A A30P	1000	>1/2560
86	NS2A M108K	1000	>1/2560	130	NS2A A30P	1000	>1/2560
87	NS2A M108K	1000	>1/2560	141	NS4B E249G	100	>1/2560
88	NS2A M108K	1000	1/320	142	NS4B E249G	1000	>1/2560
89	NS2A M108K	1000	>1/2560	154	NS5 P528H	100	>1/2560
90	NS2A M108K	1000	>1/2560	165	NONE (wt)	1000	>1/2560
				166	NONE (wt)	1000	>1/2560
167	MOCK	n/a	1/40	169	MOCK	n/a	1/80
168	MOCK	n/a	1/80	170	MOCK	n/a	1/80

[a] the designation number given to each individual mouse
[b] the mutation contained within the WNV genome. No mutations (listed as NONE) indicates the wt WNV. MOCK denotes uninfected mice.

All animals infected with 100 or 1000 ffu of the mutant or wt WNV produced antibodies in response to infection except for one animal infected with 1000 ffu of the 3' UTR Δ WNV (mouse # 111). This animal had a neutralizing antibody titer of 1/80, which was determined to be the background level of neutralization within this assay. High neutralizing antibody titers were measured in sera collected from mice infected with non-attenuated or wt WNVs (mice #126-130, 141-142, 154, 165-166).

Most mice infected with 1000 ffu of NS2A D73H, NS2A M108K or 3' UTR Δ WNVs produced anti-WNV neutralizing antibody titers of >1/2560. The lowest PRNT80 titers were obtained from the mice infected with 3' UTR Δ WNV. This difference is readily seen in the group infected with 100 ffu; two mice in this group (#107 and #109) had PRNT titers of only 1/320. PRNT80 values from mice infected with 100 ffu of NS2A D73H WNV were higher, but some mice within these groups also had measurable titers of 1/1280 (#57, #58). For comparison, the PRNT80 titers from the mice that survived 100 ffu of NS2A A30P (#126), NS4B E249G (#141), and NS5 P528H (#154) were all greater than 1/2560. The PRNT80 titer obtained from these mice also correlated with the ability of the inoculated virus to replicate *in vitro*, suggesting that these viruses replicated poorly *in vivo* and therefore, were not as efficiently recognized by the mouse's immune system.

NS2A D73H WNV REVERSION TO THE WT GENOTYPE RESULTED IN MOUSE MORTALITY

Brains from moribund or dead mice infected with 100 ffu of each virus were used to examine the genotype of the virus responsible that were capable of killing the mouse. The brain from mouse #37 (infected with NS4B E249G WNV) was moribund and sacrificed on day 8 pi. On day 9 pi, the brain from moribund mouse #38 (infected with NS5 P528H WNV) was harvested. Two mice (#40 and #41) infected with NS2A A30P were moribund and both were harvested on day 10 pi. On day 13 pi, one mouse infected with NS2A D73H WNV died (#41). This mouse was dead upon inspection, but the body was still warm and *rigor mortis* had not set in, so the brain was harvested.

It was especially important to identify the virus responsible for the one death following NS2A D73H WNV infection, since this virus was expected to be avirulent. As discussed in Chapter 3, the Darwinian evolution favors viruses that replicate efficiently in this system, and so the NS2A D73H WNV is at a disadvantage in the mouse compared to the wt WNV. Therefore, this attenuated virus may revert to a virus that can kill the mouse (wt phenotype). To identify the genotype of these lethal viruses, the virus contained within the brain of each mouse was sequenced as described in Materials and Methods.

The results of these studies are outlined in Table 6. Brains were selectively extracted from moribund animals to ensure a high viral load, as viral titer drops after death. The only exception was the brain from the mouse that had died (not moribund) from the NS2A D73H WNV infection. Two mice were obtained from the NS2A A30P WNV-infected group, and one mouse from each NS2A D73H, NS4B E249G and NS5 P528H WNV-infected groups.

Table 6: Summary of the genotype of viruses extracted from moribund/dead mouse brains infected with 100 ffu of virus

Inoculated Virus[a]	Genotype[b]
NS2A A30P WNV	P, P
NS2A D73H WNV	D[c]
NS4B E249G WNV	G
NS5 P528H WNV	H

[a] The genotype of the virus that as inoculated into the mice
[b] The residue present in the virus harvested from the brain homogenate of dead or moribund mice at the mutated locus
[c] Indicates genotypic reversion to the wt residue

Most viruses sequenced from the mouse brain homogenate showed the genotype of the mutant virus. These viruses represented the group that had low LD_{50} values and produced large antigen-positive foci on cell monolayers *in vitro*. The lack of genotypic reversion in these mice indicated that the mutant viruses were virulent. However, the brain harvested from mouse that died from the NS2A D73H WNV infection showed a genotypic reversion at the 73rd residue in NS2A. The mutant histidine (H) residue had reverted to the wt aspartic acid (D) residue at that locus. This direct reversion to the wt genotype indicated that NS2A D73H WNV had an attenuated phenotype in mice and that a reversion to the wt residue at this position was responsible for the lethal phenotype observed in the one mouse that succumb to infection.

NS2A D73H IS NEUROVIRULENT IN SUCKLING MICE

The previously described experiments indicated that NS2A D73H WNV is attenuated in mice when injected into the peritoneum. We were interested in determining if the NS2A D73H WNV was neurovirulent in newborn mice. The suckling mouse is sensitive to WNV infection since these mice have not developed a functional immune response. In this model, ~1 ffu of wt WNV can kill a newborn (suckling) mouse. To test the attenuated virus' neurovirulence, newborn litters of outbred Swiss-Webster mice were infected with 0.5 or 5 ffu of wt WNV or 5, 50 or 500 ffu of NS2A D73H WNV. Mice were then observed for signs of illness (severe illness was classified as moribund) and death. Death was first observed in the wt WNV-infected newborns on day 6 pi. This death was noted in the group infected with 0.5 ffu of wt WNV. The remaining littermates were all dead the next day (7dpi). Unfortunately, the newborns inoculated with 5 ffu of wt WNV were eaten by their mother within the first 4 days pi, so no conclusions can be drawn from that dose. The litter infected with 500 ffu of NS2A D73H WNV began to show signs of illness on days 4 and 5 pi and all newborns in this group were moribund on day 6 pi. These pups were sacrificed and their brains were pooled and homogenized to determine the characteristics of the NS2 D73H WNV that caused their death. In litters infected with 50 and 5 ffu of NS2A D73H WNV, illness was not noted until day 5 pi. Two dead and 8 moribund newborns infected with 50 ffu were observed on day 7 pi. All newborns infected with 5 ffu were moribund on day 7 pi. The survival curve for these studies is shown as Figure 22.

Figure 22: Survival Curve for Suckling Mice: NS2A D73H WNV vs. wt WNV

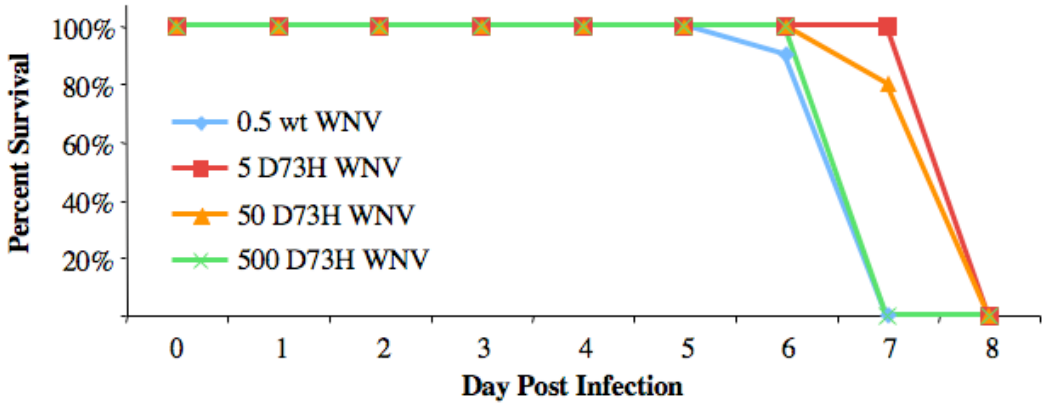

Figure 22: Litters of mice were infected i.c. with the indicated doses of either NS2A D73H or wt WNV. Newborns were monitored daily for signs of illness and death. All moribund mice were humanely euthanized and recorded as dead for the next day.

There was a slight dose-dependent effect of the amount of input NS2A D73H WNV and the onset of death; as expected, the higher the input dose of virus, the quicker the mice succumb to infection. The mice infected with 5 or 50 ffu of NS2A D73H WNV survived, on average, a day longer than mice inoculated with 0.5 ffu of wt WNV or 500 ffu of NS2A D73H WNV. This suggests that the NS2A D73H WNV may be less neurovirulent than wt WNV, but this would be a small difference if it were real. Nevertheless, all mice infected with NS2A D73H WNV died at all doses, indicating that this virus is neurovirulent for newborn mice.

To ensure that the virus that was responsible for killing the newborn mice had not reverted to a wt genotype at the mutated locus, moribund mice infected with 500 ffu of NS2A D73H WNV were euthanized on day 6 pi, and the virus contained within the pool of several newborn brains was sequenced. The original inoculum was similarly processed to serve as a reference point for the accumulation of mutations within the mice. The NS2A D73H mutation was observed in the virus present in the mouse brain homogenate (MBH). Additionally, both the original inoculum and the MBH produced small antigen-positive foci on Huh7 cell monolayers (data not shown). These data indicate that the virus

with the original NS2A D73H mutation was responsible for killing the newborn mice, and that reversion at this locus was not required for neurovirulence in this model.

NS2A D73H WNV PRODUCES A LOW LEVEL VIREMIA IN MICE

As described in Chapter 3, NS2A D73H WNV replicates more poorly than wt WNV in cell culture. To assess the relative levels of viremia of mice infected with either NS2A D73H WNV or wt WNV. Mice were infected i.p. with $1x10^5$ ffu of virus and sera were harvested from three animals on each day for 6 days. Mice infected with NS2A D73H WNV produced a lower viremia than wt WNV-infected mice on all days tested (Figure 23).

Figure 23: Viremia detected in NS2A D73H- and wt WNV-infected mice

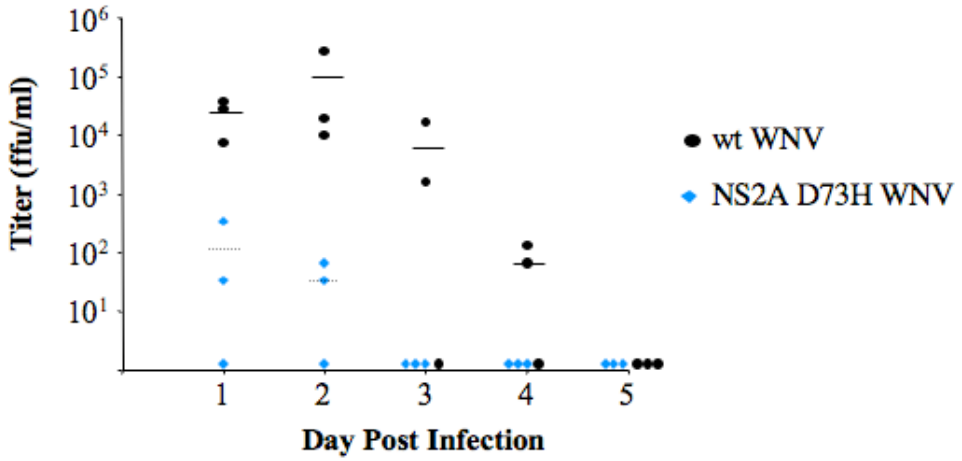

Figure 23: Viremia in mice infected with either wt or NS2A D73H WNV. Each plot point represents the data collected from one mouse on the indicated day. The limit of detection for this assay is 33 ffu/ml. Solid and dotted horizontal lines show the average titer for samples at that time point for wt WNV and WNV NS2A D73H viruses, respectively. A repeated-measured ANOVA (df= 7, $P < 0.05$) revealed no statistical effect of either virus or dpi on detected viremia levels.

On day 1 pi, mice infected with NS2A D73H WNV had 100x less virus than wt WNV-infected mice. After day 3 pi, no virus was detectable in NS2A D73H WNV-

infected mice. The wt WNV-infected mice had a peak viremia on day 2 pi with an average of $1x10^5$ ffu/ml and the viremia lasted for 4 days. Virus was undetectable in mice on days 5 and 6 pi. Although there is a trend towards significance, no statistical differences between the levels of viremia produced from either NS2A D73H or wt WNV infection on day examined using the repeated-measures ANOVA (fd = 7, $P < 0.05$ for all comparisons).

Discussion

The results discussed in this chapter fit the hypothesis put forth in aim 2. Specifically, genomes that were attenuated *in vitro* will be attenuated *in vivo* (as measured by death in a mouse after i.p. infection). This observation suggests that the attenuated mutant lineage Ia WNV are more like lineage II WNV with regard to their virulence in mice. Mice infected with NS2A D73H WNV produced a lower titer and more transient viremia compared to wt WNV-infected mice, which correlated well with the replication and spread of these viruses *in vitro* (Chapter 3). No mortality was associated with the NS2A M108K or 3' UTRΔ WNV infections. The one death in the group inoculated with 100 ffu of NS2A D73H WNV was due to a reversion of this virus back to the wt phenotype and genotype (NS2A D73D). The mortality associated with infections from the wt or and other viruses that showed little or no attenuation *in vitro* (NS2A A30P, NS4B E249G and NS5 P528H) were identical with regard to LD_{50} values. These values were also similar to those reported in the literature for a wt NY99 WNV infection in 3-4 week-old Swiss-Webster mice (Beasley et al., 2005).

The LD_{50} determined for the wt WNV derived from the FLIC cDNA had a similar LD_{50} when injected i.p. into outbred Swiss-Webster mice (3.2 ffu) to NY99 WNV in 3-4 week-old Swiss-Webster mice (approximately 1 pfu) (Beasley et al., 2005). Interestingly, fewer mice died when infected with 1000 ffu of virulent wt WNV than died from a 10-fold lower dose (Figures 20 and 21). This counter-intuitive result may reflect the rapid and efficient engagement of the innate immune response, which is essential for

controlling WNV infection *in vivo*. If the first infected cells can produce high levels of secreted IFN, this IFN would have an early protective effect on (nearby) uninfected cells (discussed in detail in Chapter 5). IFN α/β are critical to controlling WNV infection *in vivo* (Samuel and Diamond, 2005). Furthermore, genome replication is required for IFN induction in mice (Bourne et al., 2007). Therefore, genomes that replicate efficiently are recognized by the cell and IFN is secreted into the bloodstream (within 8 hours post inoculation) (Bourne et al., 2007). This rapid induction of the IFN response may not be quickly or fully engaged at lower wt WNV doses, which may indicate why more mice die of WNV infection at a lower dose (100 ffu).

Viruses harboring the NS2A mutations D73H or M108K were attenuated in mice whereas the NS2A A30P WNV was not. These data contrast to the results described in NS2A A30P KUNV i.p. infections of 3-week-old Swiss Webster mice (Liu et al., 2006). NS2A A30P KUNV was highly attenuated in mice; as much as 10^4 i.u. of NS2A A30P KUNV (titrated on BHK cells) injected i.p. failed to cause any death in these mice and only one death of ten mice infected with 10^5 i.u. of this virus died (Liu et al., 2006). For comparison, 60% of mice infected with 1 i.u. of wt KUNV i.p. died, indicating that the parental virus was lethal for mice by this route (Liu et al., 2006). The LD_{50} value for NS2A A30P WNV in our experiments was 4.2 ffu (Table 4). This mutation rendered the NS2A A30P KUNV unable to block IFN production, and as a result, replicated poorly in immunocompetent cells that could respond to IFN (A549) but not immunocompromised cells that were insensitive to IFN (BHK) (Liu et al., 2006). In Swiss-Webster mice with an intact IFN response, the NS2A A30P KUNV infection was successfully controlled and no mice die from infection (Liu et al., 2006). The NS2A A30P KUNV was lethal in mice that are unable to recognize IFN (IFN α/β/γ receptor knockout mice, AG129) (Liu et al., 2006). AG129 mice infected intravenously with 10^3 i.u. of wt or NS2A A30P KUNV all died of infection, although the wt KUNV killed the mice slightly quicker (Liu et al., 2006). These data suggest that IFN is critical in controlling KUNV infection. The role of type I IFN on the phenotype of cell-adapted genomes will be discussed in Chapter 5.

Our results indicate that the phenotype of the NS2A A30P within a North American lineage Ia WNV was virulent and had an LD_{50} value nearly identical to the wt WNV (Table 4). This disparity between the virulence of NS2A A30P KUNV and NS2A A30P WNV is likely due to the presence of other attenuating mutations in the KUNV genome. Although KUNV is classified as a lineage Ib WNV, the phenotype of KUNV is different from lineage Ia WNV with respect to the disease it produces in humans (Hall et al., 2002). Most importantly, the LD_{50} of two KUNV (AUS60 and AUS91) route were greater than 10^4 pfu (titrated on Vero cells) in 3-4 week-old Swiss outbred mice when inoculated i.p. (Beasley et al., 2002). Additionally, no signs of illness were reported in mice infected with the KUNV strains (Beasley et al., 2002). Based on these results, it is unclear why the wt KUNV was so lethal in the experiments described by Liu and coworkers. The effect of the A30P mutation may be greater in KUNV since this virus is attenuated in mice compared to lineage Ia WNV strains. The A30P mutation does not have a strong effect on the phenotype in the TX02 WNV background. However, a delay in genome replication was noted in Vero cells infected with NS2A A30P VLPs harboring the WNR C-eGFP-NS1-5 genome (Figure 15) as well as in Vero (and to a lesser extent in Huh7) cells infected with the NS2A A30P WNV in vitro (Figure 17).

Puig-Basagoiti and colleagues showed that NY00 NS4B E249G WNV was slightly less virulent than NY00 wt WNV by f.p. inoculation of 1000 pfu in 6-week-old C3H/HeN mice (Puig-Basagoiti et al., 2007). However, the *in vivo* attenuated phenotype of the NS4B E249G WNV reported by Shi and coworkers, differ from our data with a TX02 WNV NS4B E249G mutant and the work of Davis and colleagues with a NY99 WNV NS4B E249G mutant (C.T. Davis and A.D.T. Barrett, personal communication), which failed to detect an affect of this NS4B E249G mutation on LD_{50} values in i.p.-inoculated outbred mice. The discrepancy among these *in vivo* results likely reflects the differences in WNV strains, mouse strains, and/or inoculation routes employed in these studies.

The virulence of wt WNV in sucking mice was similar to the virulence described previously that showed 0.2 ffu of wt WNV was sufficient to kill newborn mice (Mason, Shustov, and Frolov, 2006). Newborn mice infected with 0.5 ffu all succumb to infection by day 7 pi. All newborn mice infected with 5 or 50 ffu of NS2A D73H WNV also died, but their death occurred one day later. Although there was a slight increase in average survival time, it is doubtful that this change is significant since no mice survived infection. Although the NS2A D73H WNV is attenuated in adult mice by the i.p. route, this virus is still neurovirulent in newborn mice by the i.c. route.

Viruses that are attenuated *in vivo* may revert back to the wt phenotype during the process of infection. As discussed in Chapter 3, Darwinian selection will favor viruses that replicate efficiently in the host. The reversion of the NS2A D73H *in vivo* was clearly demonstrated in the adult mouse that died following infection. Moreover, this mouse died on day 13 pi, which was 3-5 days later than the mice infected with nonattenuated mutant and wt WNVs. This suggests that the reversion occurred in the periphery (body) mouse within the first few days of infection and that the revertant out competed the inoculated attenuated virus. Not surprisingly, the death associated with the NS2A D73H WNV infections of newborn mice was not due to a genotypic reversion, as it was with adult mice. Many flaviviruses that are attenuated by the i.p. route are virulent by the i.c. route, indicating that the selective pressures facing virus replication in the periphery are not the same as in the brain. Therefore, an attenuated virus would not be selected against in the brain to the same degree as this virus would be in the body, and so phenotypic reversion of the attenuated virus is not necessary to cause death in the mouse.

A direct reversion of the mutant NS2A D73H virus into the wt NS2A D73D WNV only requires changing one nucleotide. Due to the error-prone NS5 viral polymerase, this can be readily achieved. Reversion of the 3' UTRΔ to a wt phenotype would be more difficult since a direct reversion (an insertion of the missing nucleotides) is highly unlikely to occur in the individually infected cell. Mutations of this nature may be more stable. However, compensatory mutations in other regions of the genome may

restore the virus' ability to replicate and its virulence. Evidence of 3' UTR Δ phenotypic revertants was not seen in any of our *in vitro* or *in vivo* studies.

CHAPTER 5: CELLS EXPRESSING ATTENUATED REPLICONS PRODUCE LOW LEVELS OF IFN AND AVOID APOPTOSIS[5]

Abstract

There are many antiviral and homeostasis-restoring mechanisms engaged in virus infected cells. IFN is produced in WNV-infected mice and VLP-infected cells. Mice infected with wt WNV produce high levels of IFN during the first 4 days of inoculation, whereas few mice infected with NS2A D73H WNV produce IFN during this time. In cell culture, high levels of IFN production were detected from wt heparan-binding VLP^{HS}-infected cells and lower levels of IFN were produced from NS2A D73H or 3' UTR Δ VLP^{HS}-infected cells. The wt VLP infection is also cytopathic in cell culture. The majority of the cells infected with wt VLP^{HS} died of apoptosis, coincident with high levels of the ER stress-induced pro-apoptotic protein CHOP at 24 hpi. On the other hand, cells infected with either NS2A D73H or 3' UTR Δ VLP^{HS} did not die of infection and had low levels of CHOP expression. Collectively, these data indicate that innate immune and ER stress responses are engaged in wt VLP^{HS}-infected cells. These responses are greatly reduced in NS2A D73H and 3' UTR Δ VLP^{HS}-infected cells, likely due to the low quantity of PAMPs present or low level of stress placed on these cells, which is directly correlated with the lower levels of genome replication compared to wt genomes.

---

[5] Some experiments and ideas in chapter have been previously published in Virology in 2007 and Future Virology in 2008. Both of these journals do not require copyright permission, as long as proper citation is provided. The citations for those articles are:

S.L. Rossi, R.Z. Fayzulin, N. Dewsbury, N. Bourne and P.M. Mason (2007) Mutations in West Nile Virus Nonstructural Proteins that Facilitate Replication Persistence in Vitro Attenuate Virus Replication in Vitro and in Vivo. Virology 364(1): 184-195.

S.L. Rossi and P.W. Mason. (2008) Persistent Infections of Mammals and Mammalian Cell Cultures with West Nile Virus. Future Virology, 3(1): 25-34.

Introduction

Cells infected with viruses face several outcomes of infection. First, if the cell can recognize the invading virus and mount an appropriate anti-viral response, the cell can theoretically clear the infection. Second, if the infected cell cannot combat infection, it may die (usually seen as cytopathic effect). The third outcome is a balance between these two situations, and results in a persistently infected cell. The interaction between the virus and host cell dictates their fates. Two important intracellular responses to infection include the innate immune and ER stress responses, and the interaction between these responses and the virus can influence the outcome of infection.

FLAVIVIRUSES AND THE INNATE IMMUNE RESPONSE

Interfering with the cellular immune response is beneficial for viral infection, and so many members of the *Flaviviridae* family have evolved mechanisms to block IFN production and/or IFN signaling. The components and pathways in the cellular innate immune response were described in detail in Chapter 1. Briefly, the products of flaviviral replication are detected by the cell via the recognition of PAMPs by TLR3, PKR, RIG-I and mda5.

Controlling the host cell's ability to produce IFN is critical for HCV infections, which may be critical to the establishment of persistent HCV infections. HCV has recently been shown to modulate the cell's ability to produce IFN impeding the ability of IRF3 to induce IFN synthesis (Sumpter et al., 2005). The HCV NS3/4A protease disrupts RIG-I and TRIF functions, the molecules upstream of IRF3 activation. TLR3 signaling is blocked in HCV-infected cells by cleaving TRIF, the adaptor protein linking TLR3 and IRF 3 (Li et al., 2005). RIG-I signaling is disrupted in HCV and GB virus (human and primate virus with close homology to HCV) viruses by cleaving the RIG-I adaptor protein MAVS (also called IPS-1/Cardif/VISA) (Chen et al., 2007b; Cheng, Zhong, and Chisari, 2006; Foy et al., 2005; Johnson, Owen, and Gale, 2007; Kaukinen et al., 2006).

Cells infected with WNV produce IFN in response to infection. PRRs and their downstream signaling molecules are able to detect and respond to PAMPs created during WNV infection *in vitro*. WNV blocks TLR3-mediated IRF3 signaling early in infection (12 hpi) (Scholle and Mason, 2005), but this effect is lost at later times during infection (36 hpi) (Fredericksen et al., 2004). IRF3 is critical for the antiviral response to WNV since WNV produces larger antigen-positive foci and sustained virus production on IRF3-null MEF cells than wt MEF cells (Fredericksen et al., 2004). RIG-I has also been shown to be involved in the WNV (Fredericksen and Gale, 2006), JEV (Chang, Liao, and Lin, 2006) and DENV (Kato et al., 2006) infections.

On the other hand, viruses in the genus *Flaviviridae* have also evolved mechanisms to inhibit the ability of the infected cell to detect exogenous IFN. Recently, HCV NS5A protein has been shown to block STAT1 phosphorylation, a necessary step in the IFN signaling pathway (Lan et al., 2007). STAT1 phosphorylation is also blocked by the genomes or individual viral proteins of TBEV, DENV, JEV, WNV and KUNV (Best et al., 2005; Guo, Hayashi, and Seeger, 2005; Ho et al., 2005; Lin et al., 2006; Lin et al., 2004; Liu et al., 2005; Mackenzie, Khromykh, and Parton, 2007; Munoz-Jordan et al., 2005; Munoz-Jordan et al., 2003; Scholle and Mason, 2005). The ability of WNV to block the IFN response may be a contributing factor to the differences in virulence detected between lineage Ia and II WNVs. A low-virulence lineage II WNV was more sensitive to the effects of IFNα, most likely due to the reduced ability of this virus to block STAT phosphorylation and nuclear translocation following IFN treatment in infected cells (Keller et al., 2006). IFN is extremely effective in priming uninfected cells since cell cultures treated with IFN are resistant to WNV infection (Anderson and Rahal, 2002; Crance et al., 2003; Samuel and Diamond, 2005). IFN α/β production is also critical to controlling WNV infection *in vivo* (Samuel and Diamond, 2005).

ER STRESS

For some organelles, such as the ER, recognizing and responding to events that threaten homeostasis is critical for the health of the cell. The intracellular membranes (ER

and Golgi apparatus) form a pathway by which cellular proteins are shuttled to the cell surface or transported to other vesicles. It is along this pathway that the flavivirus virion is exocytosed from the cell (see Chapter 1). The ER is also the venue for lipid and protein biosynthesis and signal-transduction pathways (Kaufman, 1999). As a result of the myriad of events that transpire within the ER, this organelle must be able to respond and correct events that can be deleterious for the cell. For example, when the normal function of the ER is disrupted by an increased concentration of (misfolded) protein, incorrect calcium ion gradient, inhibition of N-linked glycosylation, and/or nutrient starvation, the cell initiates an "ER stress" response. There are two pathways that are part of the ER stress: the unfolded protein response (UPR) and the ER overload response (EOR). Both pathways have overlapping functions and are generally characterized by a halt in protein translation, an increase in chaperone protein synthesis and ion-stablalizing proteins and the activation of apoptotic proteins (Faitova et al., 2006). Activating the pathways involved in ER stress results in either the restoration of homeostasis (recovery) or the initiation of apoptosis (death).

The lumen of the ER is where approximately one-third of the cell's proteins are folded and/or modified (Kaufman, 1999). To facilitate this process, two classes of proteins are abundant in the ER and promote proper protein folding: (i) isomerases (i.e. protein disulfide isomerase [PDI] and cis-trans prolyl isomerase), which catalyze the refolding of misfolded proteins (Kaufman, 1999), and (ii) chaperone proteins (i.e. BiP/GRP78), which have no enzymatic activity but serve as scaffolds during protein folding and prevent protein aggregates from forming. Under conditions of homeostasis (unstressed), BiP is expressed and associates with folding proteins and ER-localized signaling molecules, such as IRE1 (inositol-requiring gene 1), AFT6 (activating transcription factor 6) and PERK (PRK-like ER kinase). When protein or misfolded protein concentrations become elevated, BiP dissociates from the signaling molecules and binds to the overabundant proteins. After BiP dissociation, IRE1 becomes activated and cleaves XBP (X-Box protein) mRNA. Cleaved (activated) XBP1 is a transcription factor for ER chaperone genes. AFT6 traffics to the Golgi apparatus, where it is cleaved

and the cytosolic domain serves as a transcription factor that results in the transcription of XBP1, chaperone genes and Gadd153/CHOP (referred to herein as CHOP). The function of CHOP (C/EBP homologous protein) is discussed in detail below. PERK phosphorylates eukaryotic initiation factor 2α (eIF-2α) to shut-off host cell translation and is necessary for NFκB (nuclear factor κB) activation, which promotes the transcription of anti-apoptotic genes like Bcl-2. This signaling cascade results in the reduction new protein translation, the increased capacity to promote folding of existing proteins and the promotion of cell survival.

Regulation of the ER stress response is critical to its function. During ER stress, many molecules are activated or produced that have opposing functions. For example, overexpression of BiP blocks CHOP protein function (Wang and Ron, 1996) and perhaps PERK-mediated eIF2α phosphorylation (Morris et al., 1997). AFT4, a protein induced by PERK that is able to be translated in the presence of eIF2α phosporylation, can bind to C/EBPβ and transactivate CHOP transcription (Ma et al., 2002). Gadd34 upregulates both BiP and CHOP and promotes the dephosphorylation of eIF2α (Kojima et al., 2003; Novoa et al., 2001). Halting protein translation promotes cell survival by limiting the synthesis of new proteins, but in some cases, it can promote the production of proteins that can be translated even when eIF2α is inactivated by phosphorylation. It is the concentration or 'strength' of the total of these functions that dictates the outcome of the stress response. If the stimuli for stress are weak or transient, then the cell will recover and homeostasis will be restored. However, if the stimulus is chronic or strong, the mechanisms favoring cell death will overpower the survival response and result in apoptosis.

APOPTOSIS

Programmed cell death, or apoptosis, is an irreversible, energy-requiring, well coordinated set of reactions that result in chromatin condensation, fragmentation and cell shrinkage. Unlike necrosis, which requires no energy and is a passive, 'messy' cell death, apoptosis contains the contents of the dying cell within condensed blebs, minimizing

damage to neighboring cells. Apoptosis is usually initiated by the signaling cascade of caspase cleavage, but calpains, cathepsins and apoptosis inducing factor (AIF) can produce caspase-independent apoptosis (Hail et al., 2006; Kroemer and Martin, 2005). Mammalian caspases are a family of at least 14 distinct cysteine-dependent aspartate-specific acid proteases, which exist in the cell as inactive procaspases and are activated upon cleavage (Shi, 2002b). An activated caspase can promote the cleavage of procaspases, leading to a rapid amplification of the death signal within the cell. Some caspases initiate the signal (caspases-1, 2, 4, 5, 8, 9, 10, 11, 12, 13, 14), while others (caspases-3,6,7) are activated downstream and execute the induction of apoptosis (Fan et al., 2005). Initiatior caspases establish the signaling cascade, which amplifies the death signal by activating caspases downstream in the pathway.

There are two main pathways by which apoptosis is initiated: from external stimuli (extrinsic pathway or receptor-mediated apoptosis) or from internal stimuli (mitochondria-mediated apoptosis). The extrinsic pathway is activated by external stimuli that are recognized by the cell upon ligand binding to cell-surface receptors. Ligand binding to Fas and TRAIL (TNF-related apoptosis-inducing ligand) receptors leads to the activation of procaspase-8 and 10. Caspase-10 activation is independent of caspase-8 cleavage and may only play an important role in immune (lymphoid) cells (Wang et al., 2001). Activated caspase-8 cleaves Bid to form the functionally active tBid, which translocates to the mitochondria and results in cytochrome *c* release. Intrinsic stimulation is often associated with mitochondrial damage. The apoptosome, the classic workhorse of the intrinsic apoptotic pathway, is comprised of caspase-9, apaf-1 and cytochrome *c* (Salvesen and Renatus, 2002; Shi, 2002b). Procaspases-3 and 7 are the effector caspases that are typically regarded as the last step in caspase activation by either pathway.

In addition to the caspase-cleavage cascade, apoptosis is regulated by members of the Bcl-2 protein family. This family is comprised of both pro- and anti-apoptotic proteins (Fan et al., 2005). Anti-apoptotic proteins include Bcl-2 and Bcl-xL. Pro-apoptotic proteins include Bad, Bax, Bak, Bid and Bim. Pro-apoptotic Bcl-2 proteins interact with the mitochondria to release intramitochondrial stores of cytochrome *c*, a

component required for the assembly and function of the apoptosome. Conversely, the release of cytochrome *c* is blocked by Bcl-2.

THE RELATIONSHIP BETWEEN ER STRESS AND APOPTOSIS

CHOP has been linked to the induction of apoptosis after engaging the ER stress response in many systems (Kaufman, 1999). CHOP is a transcription factor that forms heterodimers with other members of the C/EBP (CCAAT/enhancer-binding proteins) family (Lekstrom-Himes and Xanthopoulos, 1998; Ubeda et al., 1996). The level of CHOP induction directly correlates to the severity of the ER stress stimuli. All three ER-stress signal transduction pathways are required for maximal expression of CHOP. CHOP can be phosphorylated by MAP (mitogen-activated protein) kinase, which has been demonstrated to enhance the protein's ability to induce apoptosis (Wang and Ron, 1996). MEF cells derived from $CHOP^{-/-}$ transgenic mice were significantly less susceptible to tunicamyin-induced cell death than the wt MEF cells (Zinszner et al., 1998).

The precise mechanism for CHOP-induced death is poorly characterized. CHOP down-regulates the anti-apoptotic protein Bcl-2 and depletes the redox-stabalizing compound glutathione (McCullough et al., 2001). Pro-apoptotic proteins are also engaged; BH3-only protein, Bim is activated by CHOP/C/EBPα heterodimers (Puthalakath et al., 2007). CHOP overexpression induces the translocation of the pro-apoptotic protein Bax from the cytoplasm to the mitochondria (Gotoh et al., 2004), where Bax can interact with Bak to oligomerize to form pores in the outer membrane of the mitochondria, thereby releasing cytochrome *c* (Breckenridge et al., 2003). $Bax^{-/-}/Bak^{-/-}$ MEF are resistant to apoptosis from the ER-stress inducing compounds thapsigargin, tunicamycin and brefildin A (Wei et al., 2001), further implicating their role in ER stress-induced apoptosis.

Interestingly, CHOP expression induces its own negative feedback by the expression TRB3 (tribbles-related protein 3), which binds to CHOP and inhibits its activity (Ohoka et al., 2005). At 'high' levels of CHOP induction, excessive amounts of TRB3 are produced, which may actually help contribute to apoptosis (Ohoka et al., 2005)

by interacting with and preventing the phosphorylation of Akt (Du et al., 2003). Phosphorylated Akt promotes cell survival by phosphorylating the pro-apoptotic protein Bad and preventing Bad-induced cell death (Datta et al., 1997; del Peso et al., 1997).

ER stress may influence the extrinsic apoptosis pathway. A recent report suggested that thapsigargin or tunicamycin-treated cells have increased levels of TRAIL-R2 (that appear to be initially dependent upon IRE1 and ATF6), suggesting that ER stress can prime the cell to become more responsive to the extrinsic apoptotic pathway (Chen et al., 2007a; Jiang et al., 2007). However, the extrinsic pathway signals via the activation of procaspase 8, which has not been shown to be activated during ER stress (Masud et al., 2007). Instead, caspases-2, 3, 7 and 9 have been shown to be important during ER stress (Dahmer, 2005; Masud et al., 2007).

There is also a link between the ER stress response and caspase cleavage, although the supporting evidence has been somewhat controversial. Recently, it has been proposed that CHOP may be important in the activation of procaspase-11, which is required for procaspase-1 cleavage and IL-1β secretion (Endo et al., 2005). Caspase-12 is an ER-resident caspase that is cleaved only during ER stress (Nakagawa et al., 2000). Procaspase-12 is located on the cytoplasmic side of the ER and becomes activated by m-calpain, a calcium-responsive serine protease (Shi, 2002b). Recently, it has also been shown that IRE1 signaling leads to the dissociation of procaspase-12/TRAF2 heterodimers, resulting in the dimerization and theorized subsequent activation of procaspase-12 (Yoneda et al., 2001). Moreover, renal epithelial cells in caspase-$12^{-/-}$ mice were resistant to tunicamycin-induced death (Nakagawa et al., 2000). Active caspase-12 leads to the activation of procaspases-9, 3, 6 and 7. The role of caspase-12 in ER stress induced apoptosis has been complicated by the observation that most humans have a stop codon in the procaspase-12 gene, so it is assumed by many that most humans produce a nonfunctional procaspase-12 protein (Fischer et al., 2002). Surprisingly, this mutant truncated caspase-12 may play a physiologic role in the cell's response to bacterial infection (Saleh et al., 2004), and evolutionary is thought to be positively selected for the human population (Xue et al., 2006). However, procaspase-4 is homologous to the

murine procaspase-12 and may serve as an ER-resident procaspase in human cells (Hitomi et al., 2004).

FLAVIVIRUS INFECTION INDUCES ER STRESS AND APOPTOSIS

Like some other members in the flavivirus genus, WNV causes cytopathic effect (CPE) and cell death *in vitro*. The mechanism of cell death is dependent upon the multiplicity of infection (MOI); Vero cells infected with high doses (MOI 10-100) of WNV die of necrosis, whereas cells infected with low doses of WNV (MOI 0.1-1) tend to die of apoptosis (Chu and Ng, 2003). Apoptosis was observed in murine neurons (Samuel, Morrey, and Diamond, 2007; Shrestha, Gottlieb, and Diamond, 2003), as well as in the neurons of hamsters experimentally infected with WNV (Xiao et al., 2001). Individually expressed flaviviral proteins, particularly C, prM, E, NS3 and/or the NS2B/NS3 complex, have also been demonstrated to trigger apoptosis in cell culture (Catteau et al., 2003; Prikhod'ko et al., 2001; Prikhod'ko et al., 2002; Ramanathan et al., 2006; Shafee and AbuBakar, 2003; Yang et al., 2002). Additionally, expression of the HCV C protein has also been shown to induce apoptosis (Zhu, Ware, and Lai, 2001).

Several members of the *Flaviviridae* family have been shown to induce the ER stress response in cells. Expression of the HCV E2 protein (but significantly not from E1) has been correlated to an increase in BiP (Liberman et al., 1999) and CHOP protein (Chan and Egan, 2005). Increased CHOP and GRP78/BIP expression has been observed in JEV-infected (Su, Liao, and Lin, 2002) and WNV-infected cells (Medigeshi et al., 2007). WNV infection also results in XBP RNA cleavage and eIF2α phosphorylation (Medigeshi et al., 2007). Cells infected with JEV and DENV have elevated levels of cleaved XBP1 RNA compared to uninfected cells (Yu et al., 2006). Neuro 2a cells infected with DENV 1 showed increased levels of GRP78/BIP compared to uninfected cells (Despres et al., 1996).

RATIONALE

Based on what is known about the interactions of the viral infection and the host cell, reduced apoptotic and type I interferon responses in cells infected with WNV or subgenomic replicons encoding cell-adapted mutations were expected. It was hypothesized that replicons with noncytopathic, cell-adapted mutations will not be efficiently recognized by the cell due to their low levels of replication, resulting in low levels of IFNβ production and low levels of apoptosis. It is expected that cells infected with virus or replicons containing cell-adapted mutations will not trigger strong intracellular responses to induce either an apoptotic or interferon response, thereby allowing both cell and viral genome to coexist without cell death or viral clearance.

Materials and Methods

IMMUNOFLUORESCENCE ASSAY (IFA)

Specific antigens were detected by immunofluorescence as an alternative to IHC. PBS-washed cell monolayers were fixed in 4% paraformaldehyde for at least 30 minutes (no longer than 1 hour) at room temperature. Paraformaldehyde-fixed cells were washed 3 times with PBS, incubated with 10 mM glycine in PBS and permeabilized with 0.1% Triton X-100 in PBS. In some cases, the assay was stored in 10mM glycine in PBS at 4°C prior to permeabilization. If the TUNEL assay preceded IFA staining, a different permeabilization buffer was used. Monolayers were blocked with an IFA blocking buffer (filter sterilized solution of 2% BSA, 5% NHS and 10 mM glycine in PBS). Primary antibodies were diluted in blocking buffer. Secondary antibodies were directly conjugated to a fluorescent die. DAPI (20 μg/ml) was used to counterstain nuclei. If cells were fixed on a glass slide (rather than a tissue culture plate), monolayers were treated with Vectamount shield (Vector) prior to sealing the slide with a coverslip. Plates and slides processed by IFA were stored in the dark at 4°C until images were taken by fluorescence or confocal microscopy.

Anti-WNV MHIAF (previously described) was used to identify VLPHS-infected cells. GADD153 antibody (Santa Cruz Biotechnology) was used to detect CHOP protein. Goat anti-mouse and Goat anti-rabbit secondary antibodies conjugated to AlexaFluor 488 or AlexaFluor 568 were used after MHIAF and GADD153 antibodies, respectively.

ACQUIRING IMAGES

Fluorescent images were acquired in two ways: fluorescent and confocal microscopy. Fluorescent or bright field images were taken on the Zeiss fluorescent microscope. In some cases, images were taken using confocal microscopy through the UTMB Infectious Disease and Toxicology Optical Imaging Core Facility at 63x magnification. All confocal images were taken at the same exposure. To allow for better visualization in this document, the contract and brightness of the images was enhanced using Photoshop and was done equally for all images of similar treatments.

IFN BIOASSAY

Supernatants harvested from VLP-infected cells were serially diluted in MEM+++ and 50 μl/well was used to pre-treat cells overnight. Dilutions were performed in duplicate for each sample. Murine or human IFNβ (NIH standard) were similarly diluted in MEM+++ to generate a standard curve. The NIH standard murine IFNβ and human IFNα were obtained from the NIAID Reference Reagent Repository, which is operated by KamTek, Inc. Media was aspirated from the wells the next morning (approximately 16-18 hpt) and infected with VLP^{HS} containing the WNR genome that expressed firefly luciferase (WNR C-luc-NS1-5). The amount of luc-VLP^{HS} (VLP^{HS} harboring the C-luc-NS1-5 genome) used to infect these cultures was sufficient to produce luciferase values of several hundred photons/second within each well. At 24 hpi, the plates were lysed using the luciferase assay lysis buffer [75% lysis buffer (40 mM Tricine, 8 mM magnesium acetate, 33 mM DTT, 0.13 mM EDTA, 0.1% Trixon X-100) mixed with 25% SteadyGlo Luciferase Assay System (Promega)]. After a 10-min incubation period with occasional shaking, the monolayers were lysed and the plates were read on a luminometer

(TR 717 Microplate Luminometer manufactured by Applied Biosystems). The photon/second values obtained from each well treated with the IFNβ standard were used to establish the μl of IFN that reduced luciferase activity by 50% (compared to IFN-untreated wells). This value (U/50% activity) was then used to establish the U/ml in each sample based on a similarly derived standard curve relating each dilution to photon/second values.

DETECTION OF IFN ACTIVITY IN WNV-INFECTED ADULT MICE

Sera collected from mice to determine viremia (in Chapter 4) were also used to determine the levels of IFNα/β production, which were measured using a bioassay conducted in the BSL3. Serum samples were diluted with three volumes of MEM without serum or phenol red and treated with UV light (254 nm, 4 watts, 10 cm) for 10 min to inactivate infectious virus. Then the UV-inactivated samples were further diluted four-fold and used to inoculate MEF monolayers in 96-well, black-wall plates. Samples were then run in duplicate by bioassay. For this experiment, the exact concentration of IFN within the serum sample was not calculated so the standard curve was not performed. Instead, the percent reduction of the luciferase value from the well (percent inhibition) was determined by normalizing photon/second of each sample to a sample that contained the same concentration of uninfected normal mouse serum (NMS) alone. NMS containing a known amount of murine IFNβ (NIH standard; 0, 50 or 250 U/ml final concentration) were analyzed in parallel to show the percent inhibition of infection produced in mouse sera containing known IFNβ concentrations.

An antibody to type I IFN was obtained from the NIAID Reference Reagent Repository, which is operated by KamTek, Inc. or Braton Biotech, Inc., respectively. Anti-type I IFN was used to determine the specificity of our inhibition by pre-incubating serum with this antibody prior to analysis. Adding the anti-type I IFN antibody to the serum samples lead to no inhibition of the luc-VLPs, indicating that the reduction in luciferase value was due to the presence of IFN and not another antiviral compound.

GENERATION OF VLP^{HS}

VLP^{HS} are VLPs that are able to use heparan sulfate as a co-receptor for infection were generated to increase the ability of VLPs to infect certain types of cells. For example, the ability to infect wt MEF cells increased 1,000-fold when VLP^{HS}s were used as compared to VLPs (Gilfoy and Mason, 2007). For other cell lines, such as Vero cells, there was no difference in the infection produced from VLP^{HS}s and VLPs.

This was done by engineering a point mutation into the E gene (E138K) VEER-packaging replicon (described in Chapter 3). This E138K mutation was shown to increase the ability of flaviviruses to bind to heparan sulfate (Lee and Lobigs, 2000). Stable BHK cell lines harboring the E138K VEEV genome were selected and maintained in growth media supplemented with 10 μg/ml puromycin (similar to the generation of the VEEV-packaging cell line previously described in Chapter 3). To generate stocks of VLP^{HS}, mutant and wt WNR C-NS1-5 genomes were electroporated into these packaging cells. VLP^{HS} were harvested as previously described in Chapter 3.

DETERMINING IFN PRODUCED FROM VLP^{HS}-INFECTED CELLS

Cell lines were seeded in 48-well plates and infected with VLP^{HS}s at an MOI of 0.15-5 diluted in MEM+++, depending on the cell line. The MOI was determined based on the VLP^{HS} titration on the same cell line to be infected. Cells were infected with VLP^{HS} in a minimal volume (100 μl) and rocked for 1 hr at 37°C. The infection media was replaced with 200 μl/well of MEM+++ and incubated for 24 hours. At 24 hpi, supernatant was removed and cell debris was pelleted by centrifugation and used for the bioassay. The cells used for the bioassay depended upon the cells that produced IFN in response to VLP^{HS} infection. Huh7 cells were used to detect IFN produced from the A549, MRC5 and Hec1B human cell lines. Wt MEFs were used to detect IFN produced from wt MEFs and STAT$^{-/-}$ MEF cells. Huh7 or wt MEF cells were seeded in black-walled 96-well plates so that they were approximately 60-80% confluent at the time of the assay. The infected monolayer was fixed with 4% paraformaldehyde for 0.5-1 hr at room temperature, then washed three times with PBS and stored in 10mM glycine in PBS

at 4°C until the IFA was performed. Multiple images (at least 5) for each infected well were taken using the fluorescent microscope. The percentage of infected cells (number of VLP^{HS}-positive cells over the number of cells as measured using DAPI fluorescence) per image was counted and the average for all images was used to normalize the data obtained from the bioassay. The data after normalization to percent infection were the U of IFN produced from every $1x10^5$ VLP^{HS} infected cells. The statistical significance of the IFN levels within a cell line was determined by a one-way analysis of variance (ANOVA) using Tukey's multiple comparison test.

VLP SENSITIVITY TO IFN PRETREATMENT

Wt MEF cells were seeded in 96-well plates to be confluent at the time of the assay. An murine IFNα standard (Sigma) was diluted in MEM+++ starting at a concentration of 50 U/ml. Two-fold dilutions were made in MEM+++ until the concentration of IFN reached 0.78 U/ml. Cells were incubated in duplicate with 50 μl/well of the serially diluted IFNα solutions overnight (~16 hours). The next morning, all wells were infected with a known titer of VLP^{HS} containing the wt, NS2A D73H or 3' UTRΔ C-NS1-5 genome (~50 infectious units/well). At 24 hpi (~40 hrs post IFN treatment), monolayers were fixed with MeOH:acetone and antigen-positive cells were visualized by IHC using anti-WNV MHIAF. The number of antigen-positive cells was counted in each well and expressed as the percentage of antigen-positive cells in the untreated (no IFNα) well.

MEASURING CELL VIABILITY (MTT ASSAY)

Huh7 cells were seeded at a sub-confluent density in 96-well plates. After the cells adhered, they were infected at an MOI of 4 (based on Huh7 titrations) with VLPs containing the WNR NS1-5 genomes that contained no, NS2A D73H or 3' UTR Δ mutations. Cells were kept in MEM with 1% FBS, 1% abx and 2% HEPES and maintained at 37°C with 5% CO_2 for 5 days. On day 5, monolayers were incubated with 1 mg/ml MTT for 3 h at 37°C. The MTT is compound that is converted to a colored

precipitate in respiring cells, providing an indication of the number of live cells within a culture. Following removal of the MTT-containing media, isopropanol was used to solubilize the colored crystals formed within live cells, which were quantified by measuring the OD at 560 nm. All data presented were normalized to a well of cells treated with media only (MOCK normalized).

A similarly infected plate was fixed 6 dpi with MeOH:acetone as previously described in Chapter 2. Monolayers were dried and VLP antigen was visualized using the anti-WNV MHIAF by IHC. Images of the cells were taken using the Zeiss microscope.

DETECTING APOPTOTIC CELLS BY TUNEL ASSAY

Wt MEF cells were seeded in glass chamber slides at a density of $2x10^4$ cells/well. The next day, the cells were infected with VLP^{HS} containing the wt, NS2A D73H or 3' UTR Δ WNR C-NS1-5 genomes diluted in MEM+++ in a minimal volume. The slides were rocked for 1 hr at 37°C with 5% CO_2 to allow for the VLP^{HS}s to infect the cells. After this hour, the infection media was removed and replaced with MEM+++. These cultures were maintained for 5 days in the incubator at 37°C in 5% CO_2.

In some cases, chemicals were used to induce apoptosis. Camptothecin, a well-established inducer of apoptosis, was used as a positive control. Some wells were treated with 10 μM camptothecin (dissolved in DMSO) for 4-6 hrs prior to replacing the media with wt MEF growth media. Negative controls included wt MEF media-only and the solvent control consisting of DMSO at the same concentration present in the camptothecin-treated sample.

After the 5 days incubation, the media were carefully removed from the wells and monolayers were washed once in PBS prior to fixation. Cells were fixed using 4% paraformaldehyde and stored overnight at 4°C in PBS containing 10 mM glycine. Slides were assayed using TUNEL and IFA within 2 days of fixation. Apoptotic cells were analyzed using the TUNEL assay and viral antigen was detected by IFA. Cells were permeabilized on ice for 2 minutes with a solution containing 0.1% Trixon-100 and 0.1% sodium citrate in water, then washed twice with PBS. Apoptotic cells were visualized

using the In Situ Cell Death Detection Kit, TMR red (Roche) as per manufacturer's instructions. Briefly, TUNEL staining detects nicks in the chromatin that are indicative of late-stage apoptotic death. Following TUNEL staining, viral antigen was detected using IFA. Viral antigens were detected using the polyclonal WNV anti-sera (anti-WNV MHIAF) followed by the secondary goat anti-mouse, AlexaFluor 488 antibody (Invitrogen). Slides were kept in the dark at 4°C until images were taken by fluorescence and confocal microscopy.

At least 5 images were taken using the fluorescent microscope for each infected or treated well. The number of VLP^{HS} antigen-positive cells (VLP^{HS}+), and VLP^{HS} antigen-positive and TUNEL-positive cells (VLP^{HS}+TUN+) were counted for each image. The percentage of infected apoptotic cells was determined by the ratio of VLP^{HS}+TUN+ over VLP^{HS} cells. Cells that were VLP^{HS}-negative (VLP^{HS}-) were also counted in the well and divided by the total number of cells in the well to give the background level of apoptosis (percent of uninfected wells undergoing apoptosis) in each well.

WESTERN BLOTS

Wt MEF cells were seeded in 24-well plates to form a subconfluent monolayer and infected at an MOI of 10 (based on titrations on wt MEF monolayers) with wt, NS2A D73H or 3' UTRΔ VLP^{HS} diluted in MEM+++. The MOI was determined based on a titer of the VLP^{HS} determined by infecting wt MEF monolayers. Thapsigargin was used at a concentration of 2μM as a positive control for the induction of CHOP proteins and DMSO (0.1%) was used as a solvent control. VLP^{HS} infection or drug treatment occurred in a minimal volume and was rocked for 1 hr at 37°C. The media was removed and replaced with MEF growth media and incubated for the indicated time. At the time of harvest, the supernatants (containing any floating cells) were spun to pellet any floating cells. Both the cell pellet and monolayer were washed once in PBS, then combined together and lysed in lysis buffer (0.1% Triton X-100, 300mM NaCl, 50 mM Tris, pH 7.8) on ice for 15 minutes. Lysates were transferred to eppendorf tubes and spun at 13000

rpm for 10 minutes at 4°C to pellet debris. The lysate supernatant was transferred to a new tube and stored at -20°C until ready for use.

The protein concentration within the lysate was determined using the DC Protein Assay (BioRad) as per manufacturer's instructions. A known concentration of BSA was used to generate the standard curve. The same amount of protein (1.5 μg/well) for all samples were diluted in LDS buffer (Invitrogen), heated and loaded into a 4-12% Bis-Tris LDS PAGE gel (Invitrogen). After resolution on the gel, proteins were transferred into PVDF membranes (0.45 μm, Millipore). Membranes were blocked in 5% nonfat powered milk in PBS with 0.1% Tween-20. Membranes were cut into three sections based upon the expected migration of WNV NS3, β-actin and CHOP, and incubated with the appropriate antibody. The top section was incubated using antibodies specific against WNV NS3 (BD), the middle section was incubated with β-actin (Sigma-Aldrich) antibodies and the bottom section was incubated with antibodies against CHOP (Santa Cruz). Secondary antibodies conjugated to horseradish peroxidase (KPL) against goat (for NS3), mouse (for β-actin), and rabbit (for CHOP) were used to detect the primary antibody. Signal was detected by chemiluminescence (ECL Plus; Amersham) and exposed on BioMax XAR Film (Kodak). β-actin was used as a loading control in all blots.

STATISTICAL ANALYSES

A repeated-measures ANOVA was used to determine the level of significance between mice infected with either the NS2A D73H WNV or wt WNV on days 2-4 pi. To determine statistical significance from IFN values measured from VLP-infected cell cultures, a one-way analysis of variance (ANOVA) using Tukey's multiple comparison test. A Fischer's exact test was used to determine the significance in the number of animals that produced IFN in response to NS2A D73H or wt WNV.

Results

MICE INFECTED WITH NS2A D73H WNV PRODUCED LESS IFN THAN MICE INFECTED WITH WT WNV

IFN activity was measured in serum samples from mice infected with $1x10^5$ ffu of either NS2A D73H or wt WNV within the first 4 days of infection. Previous work has shown low levels of IFN in WNV-infected mice (Bourne et al., 2007; Samuel et al., 2006). Murine serum interferes with the bioassay that is typically used to detect IFN based upon serial dilutions. Therefore, a bioassay based upon a single dilution of serum was used and the results were recorded as percent inhibition of VLP infection rather than by IFN concentration. To calibrate the assay, a side-by-side test of normal mouse serum (NMS) with known amounts of murine IFNβ (at a final concentration of 0, 50 or 250 U/ml) was also added. The results of these bioassays are shown in Figure 24.

The number of mice that produced detectable levels of IFN in response to WNV NS2A D73H infection (3 out of 12) was statistically different from the number of mice (12 out of 12) that produced IFN in response to wt WNV infection (Fisher's exact test; $p<0.0005$, Figure 24). There was also a statistically significant difference between the level of VLP neutralization detected in sera of mice sacrificed 2 dpi with WNV NS2A D73H compared to wt WNV (repeated-measures ANOVA, $P < 0.05$). Pretreatment of selected samples showing a high inhibition of VLP infection with anti-IFN blocked their activity, indicating that the inhibition detected in this assay was due to IFN (results not shown). Collectively, these data indicate that WNV with a reduced ability to replicate elicits a lower level of IFN production than a replication-competent (wt) WNV *in vivo*.

Figure 24: IFN levels in NS2A D73H and wt WNV-infected mice

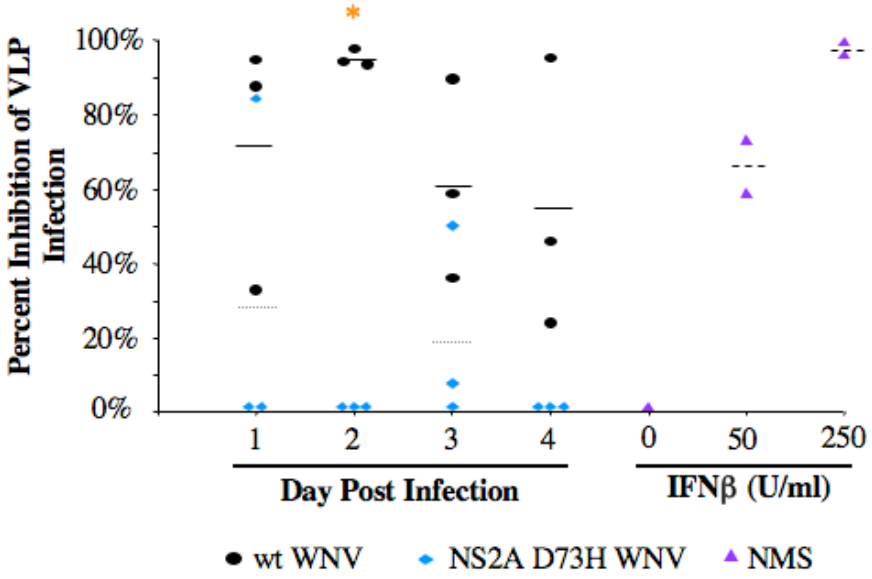

Figure 24: IFN activity detected in serum of mice infected with $1x10^5$ ffu of either wt or NS2A D73H WNV. Values are expressed as percent inhibition of luciferase-VLP infection relative to wells infected with these VLPs in the presence of the same concentration of NMS. Each plot point represents the data collected from one mouse at the indicated day or treatment. Solid and dotted horizontal lines show the mean titer for samples at that time point for wt and WNV NS2A D73H viruses, respectively. The right side of this figure shows the effect of murine IFNβ added to the same concentration of NMS used in the infected samples at a final concentration of 50 U/ml or 250 U/ml within sera. The average of these two points is shown as a dashed horizontal line. Significance for difference between titers, as shown by the asterisk, was determined by ANOVA.

WT VLP^{HS} INDUCE MORE IFN THAN MUTANT VLP^{HS}

To determine if the amounts of IFN produced from a wt (WNR C-NS1-5) or attenuated (WNR C-NS2A D73H and WNR C-3' UTR Δ) VLP^{HS} infection, STAT$^{-/-}$ MEF, wt MEF, Hec1B, A549 and MRC5 cells were infected with VLP^{HS} and measured the amount of IFN produced 24 hpi by bioassay. VLP^{HS} were used rather than virus because VLP^{HS} infection is limited only to the first infected cell. Supernatants assayed from uninfected cells (MEM alone) showed undetectable levels of IFN (below the limit

of detection for each assay). All cell lines infected with VLP^{HS} produced IFN, but the highest levels of IFN were detected in cell lines infected with the wt VLP^{HS} (Figure 25). Lower levels of IFN were produced from NS2A D73H or 3' UTR Δ VLP^{HS} infections compared to wt VLP^{HS} infections in several cell lines (Figure 25). Overall, the lowest and highest amounts of IFN were produced from cell lines infected with 3' UTR Δ VLP^{HS} and wt VLP^{HS}, respectively. In some cell lines, there was a clear correlation between the amount of IFN produced from the VLP^{HS} infection and the ability of the infecting genome to replicate. Genomes harboring the 3' UTR deletion replicated more poorly than genomes with the NS2A D73H mutation, and both mutant genomes replicated more poorly than the wt genomes in infected cells (see Chapter 3). Since wt MEF cells showed a clear correlation between IFN production and genome replication, these cells were used in all experiments to analyze the engagement of anti-WNV responses in the cell.

Figure 25: IFN produced from VLP^{HS}-infected cell lines

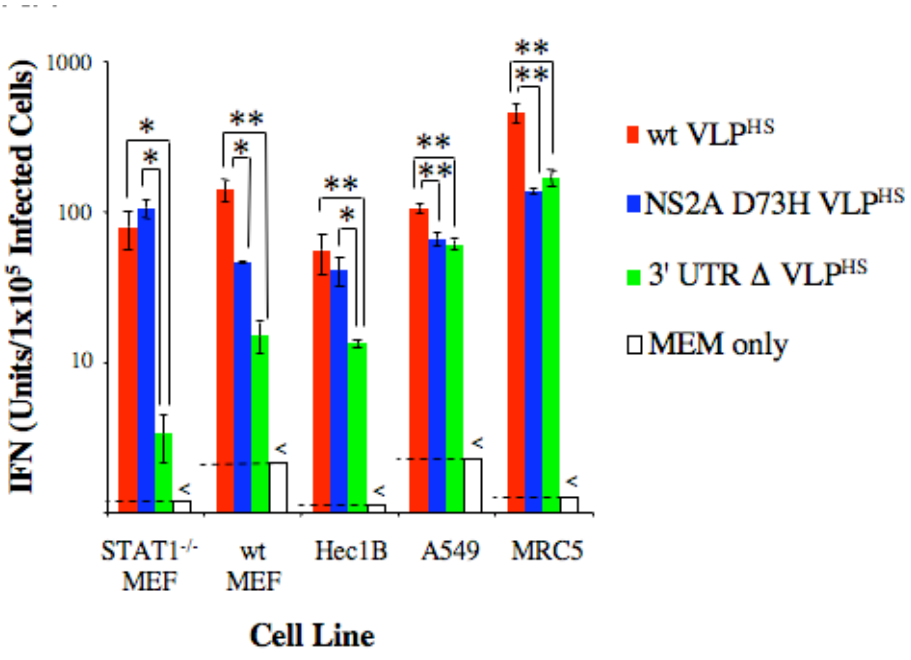

Figure 25: Cells infected with VLP^{HS} produce IFN. Various cell lines were infected with the indicated VLP^{HS} and at 24 hpi, the supernatant was removed and the monolayers were

fixed. IFN within the supernatant was detected by bioassay on either wt MEF cells (for murine IFN) or Huh7 cells (for human IFN) and compared to a known murine or human IFN-β NIH standard. Infected cells were identified in the same monolayers by IFA using a MHIAF specific for WNV antigen. IFN levels are expressed as Units per every $1x10^5$ antigen-positive cells. Cultures incubated with media only produced no detectable levels of IFN in any cell line (empty black box, as determined by $1x10^5$ total cells). The < sign above bars denotes the limit of detection, which is shown as a dotted back line. Statistical values based on one-way ANOVA (Tukey's Multiple Comparison) tests; * $p<0.05$, ** $p<0.01$. Error bars show standard deviation between biological replicates within the same experiment. Data shown for each cell line is representative of at least two experiments.

MUTANT AND WT VLP^{HS} ARE EQUALLY SENSITIVE TO IFN

In order to ensure that the NS2A D73H and 3' UTRΔ mutations had no effect on the genome sensitivity to the actions of IFN, wt MEF cell monolayers were pretreated with murine IFNβ overnight to prime the cells to an antiviral state. The next day, the monolayers were infected with wt and mutant VLP^{HS} and the number of VLP^{HS}-infected cells were visualized by IHC and counted. Figure 26 shows the percentage of antigen-positive cells detected in IFNβ-pretreated monolayers compared to untreated cells. All three VLP^{HS} were unable to efficiently infect wt MEF cells that were in an antiviral state. There may have been a slight decreased sensitivity of the 3' UTR Δ VLP^{HS}, but this effect was minor and may not be biologically significant.

Figure 26: VLP^{HS} sensitivity to IFNβ pretreatment

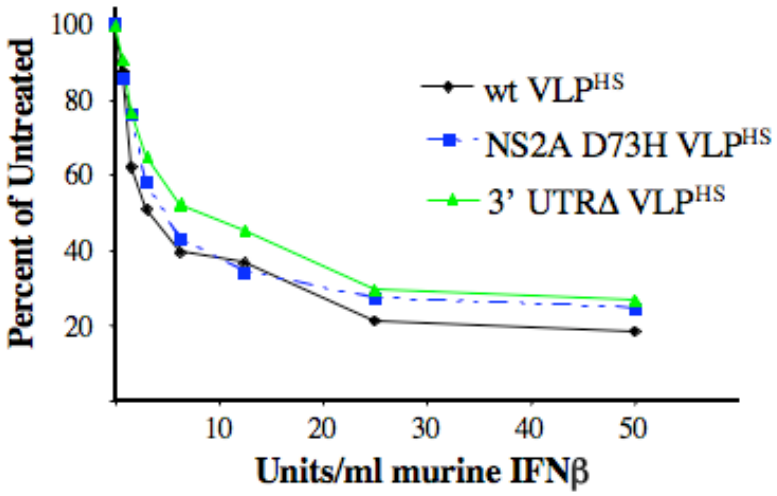

Figure 26: Reduction in the number of antigen-positive cells following IFN-pretreated wt MEF monolayers. The antigen-positive foci were visualized by IHC using the anti-WNV MHIAF. Wt VLP^{HS} is shown in black diamonds, NS2A D73H VLP^{HS} is shown in blue squares and 3' UTRΔ VLP^{HS} is shown in green triangles.

REPLICONS WITH CELL-ADAPTED MUTATIONS CAUSE LITTLE CPE

During the generation of WNV harboring cell-adapted mutations, a significant difference in the CPE associated with differences in several WNV genome replication was noted (discussed in Chapter 3). Specifically, NS2A D73H, NS2A M108K, and 3' UTRΔ WNV failed to produce robust CPE within 72 hpi, whereas the wt WNV completely obliterated the monolayer at this time (Figure 17). To quantify the cytopathology produced by the WNR NS1-5 encapsidated into VLPs, Huh7 monolayers were infected with VLPs harboring selected NS2A mutations at an MOI of 5 and monitored for cell number using an MTT assay (Figure 27A). VLPs were used to ensure that all of the cells in the culture were infected simultaneously and that the infection did not spread to naïve cells. The number of cells was measured at each day for 5 days and normalized to an uninfected control. Although no differences in cell number were observed between the different VLP-infected cultures for the first 4 days (results not

shown), cultures containing the wt and NS2A A30P mutant showed a precipitous drop in cell number at day 5 (Figure 27A). Moreover, cells infected with the VLPs encoding either NS2A D73H or NS2A M108K mutation appeared similar in morphology to mock-infected cells at this time point. When parallel cultures were immunostained at day 6, nearly all of the cells were antigen-positive (Figure 27B), independent of the VLP they were infected with, confirming that most of the cells were infected. This is an important control since uninfected cells could confound the results obtained within this experiment. Most uninfected and NS2A D73H-infected cells had cellular morphology consistent with healthy and dividing cells whereas wt or NS2A A30P infected cells were in the process of dying (condensed and rounded; Figure 27B).

Figure 27: Cells infected with cell-adapted VLPs cause little CPE

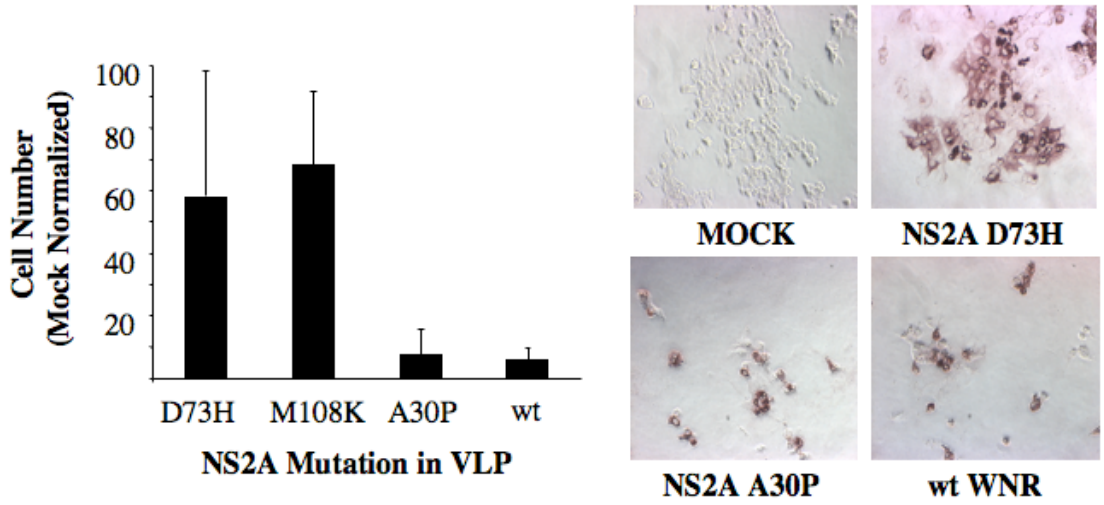

Figure 27: Survival of Huh7 cells infected with VLPs encoding selected NS2A cell-adapted mutations. Huh7 cells were infected with VLPs (harboring WNR NS1-5) at an MOI of 5. The bar graph shows cell number determined by MTT staining at 5 dpi; values are shown normalized to MTT data from mock-infected cells. Error bars denote standard deviation. Micrographs of cell monolayers from parallel cultures that were fixed 6 dpi and immunostained for WNV proteins are shown on the right. Cultures infected with WNR NS1-5 NS2A M108K were not fixed and stained for analysis. Arrows denote viable cells positive for WNR antigen.

CELLS INFECTED WITH WT VLP^{HS} UNDERGO APOPTOSIS

Several investigators have shown that WNV induces apoptosis in multiple cell types (Chu and Ng, 2003; Medigeshi et al., 2007; Parquet et al., 2001; Shrestha, Gottlieb, and Diamond, 2003), so it was likely that the death shown in Figure 27 was due to apoptosis. To test this hypothesis, MEF cells were infected with wt and mutant VLP^{HS}, and apoptotic and WNV-infected cells were quantitated by TUNEL assay and IFA respectively. The percentage of cells undergoing apoptosis (TUNEL-positive) that were both infected (WNV antigen-positive) and uninfected (WNV antigen-negative) is recorded in Figure 28. Cells infected with wt VLP^{HS} induce apoptosis in wt MEF cells. On 5 dpi, 58% of WNV antigen-positive cells were undergoing apoptosis whereas fewer than 10% of cells infected with either NS2A D73H or 3' UTR Δ VLP^{HS} were apoptotic (light bars, Figure 28). Furthermore, most of wt VLP^{HS}-infected cells on day 5 pi had lost their morphology and were condensed or had died and antigen-filled blebs were found around the apoptotic nucleus (Figure 28). MEF cells infected with either the NS2A D73H or 3' UTR Δ VLP^{HS} had morphologies similar to uninfected healthy MEF cells (Figure 28). There was a significant decrease in the average number of WNV antigen-positive, TUNEL-positive cells infected with either 3' UTR Δ or NS2A D73H VLP^{HS} compared to wt VLP^{HS} infection (Figure 28, ANOVA $p < 0.01$). The induction of apoptosis was not due to the presence of IFN in these cultures since the differences in levels of IFN expected previously shown to be present (Figure 25) did not effect the percentage of uninfected cells undergoing apoptosis (Figure 3, dark bars). Furthermore, incubating wt MEF cells with 200 U/ml of murine IFN β did not increase the percentage of apoptotic cells when compared to MOCK-treated cells (data not shown).

Figure 28: Wt VLP^{HS} infection induces apoptosis

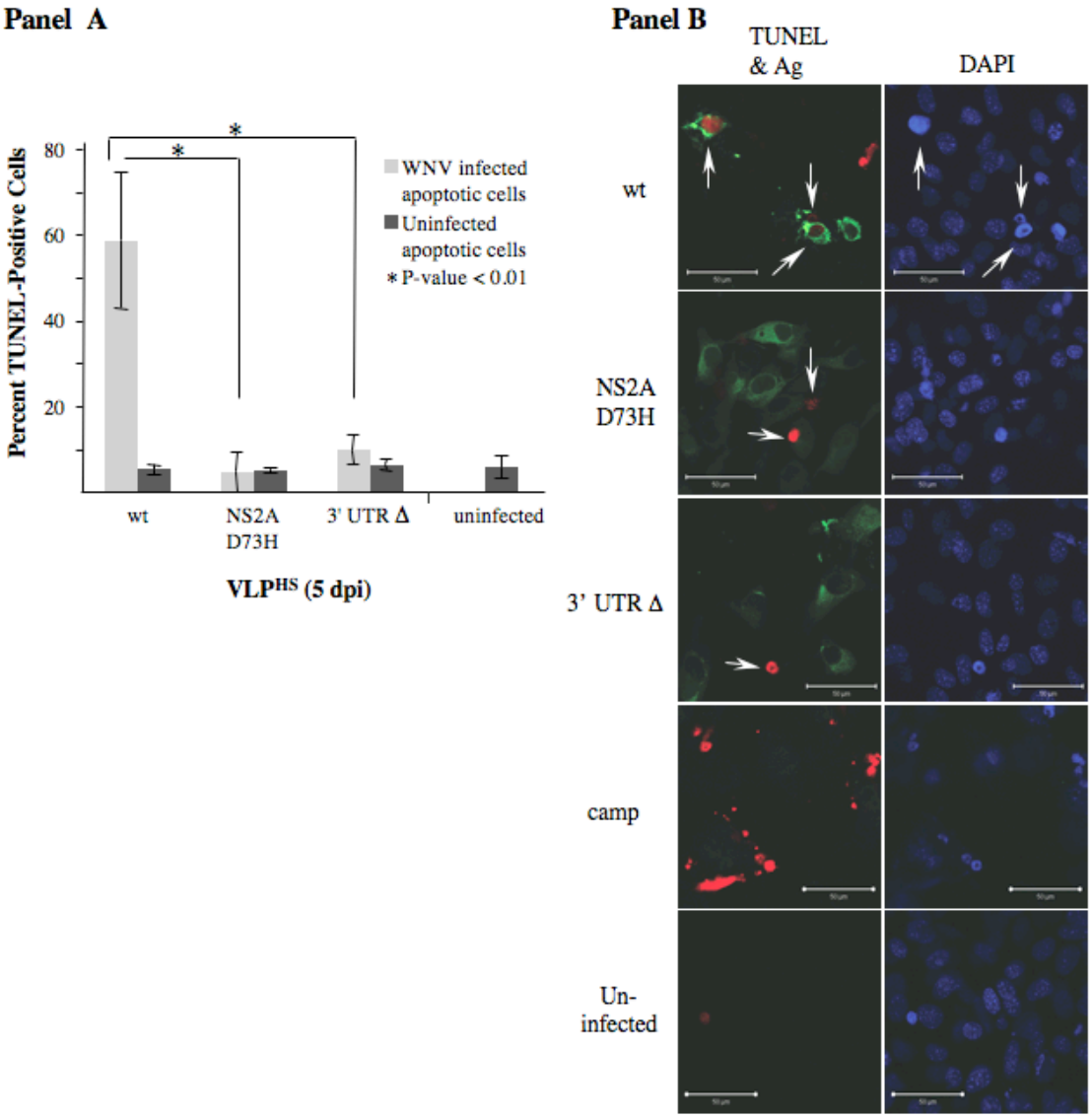

Figure 28: Cells infected with VLP^{HS}s encoding cytopathic WNR genomes die of apoptosis. (**Panel A**) Wt MEF cells were infected with wt, NS2A D73H or 3' UTR Δ VLP^{HS}. MOCK cells were maintained in media only. Some monolayers were treated with 10 μM camptothecin or DMSO. Cells were infected with VLP^{HS} at an MOI of 0.5 and fixed at 5 dpi. Apoptotic cells were detected by TUNEL assay and infected cells were identified by IFA using a hyperimmune ascites fluid against WNV. The percentage of VLP^{HS}-infected apoptotic cells is shown in light grey and the percentage of uninfected apoptotic cells is shown in dark grey. Error bars represent the standard deviation of the percentages of apoptotic cells counted in at least 5 fields within a well. Statistical values

based on one-way ANOVA (Tukey's Multiple Comparison) tests; * $p<0.001$. (**Panel B**) The images correspond to a representative field taken by confocal microscopy, 63x magnification. Cells that are undergoing apoptosis (TUNEL-positive) have red fluorescent nuclei. VLP^{HS}-infected cells are shown in green and the nuclei of all cells are stained with DAPI (blue). The white line on the images shows 50 μm.

CHOP IS INDUCED IN WT VLP^{HS}-INFECTED CELLS

Both intrinsic and extrinsic stimuli can result in apoptosis. ER stress is an established trigger of apoptosis in WNV-infected cells (Medigeshi et al., 2007). To monitor the levels of ER stress, the induction of CHOP was examined. CHOP is produced at very low levels in healthy, non-stressed cells (Ron and Habener, 1992), and the intensity of the stimulus results in a weak or strong ER stress response (Oyadomari and Mori, 2004).

Figure 29: Western blot detecting CHOP induction

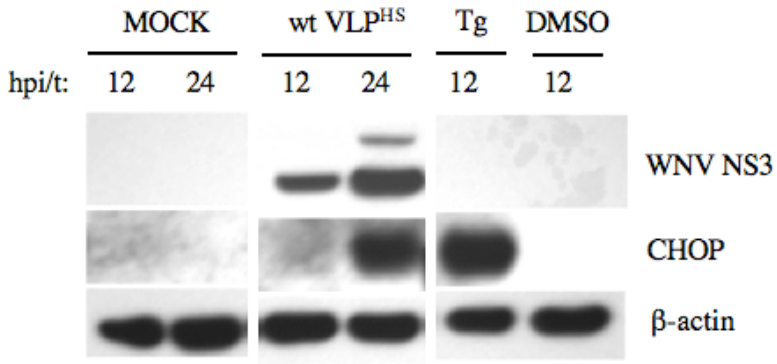

Figure 29: Western blot showing CHOP induction in wt MEF cells. MEF cells infected at an MOI of 10 with VLP^{HS} WNR C-NS1-5, thapsigargin (Tg, 2 μM) or DMSO were lysed at the indicated hour post infection. 1.5 μg of total protein was analyzed by Western blot as described in Materials and Methods. The membrane was cut horizontally to expose regions of the same blot to different antibodies for visualization of WNV NS3, CHOP and β-actin proteins. The exposed film was photographed and the sections of the gel corresponding to the locations of the detected proteins are shown.

To determine whether CHOP was induced upon WNV VLP infection, wt MEF cells were infected with VLPs and lysates at various times post infection were analyzed by Western blot to detect levels of CHOP protein (Figure 29). Cells were infected with

VLP^{HS} containing the wt WNR C-NS1-5 genome at an MOI of 10. Thapsigargin is a well-characterized inducer of ER stress and was used as a positive control for CHOP induction. Some monolayers were treated with 2 μM of thapsigargin, or DMSO for use as a solvent control. Cells maintained in growth media only were used to determine the baseline levels of CHOP expression in these cells (MOCK wells).

High levels of CHOP expression have been shown in multiple cell types lead to apoptosis. Due to the low percentage of mutant VLP^{HS}-infected cells undergoing apoptosis compared to wt VLP^{HS}-infected cells, it was hypothesized that cells expressing the NS2A D73H or 3' UTR Δ genomes induce less CHOP expression than wt genomes. Wt MEF cells that were infected with the indicated VLP^{HS} were fixed 24 hpi. WNV antigen (red) and CHOP (green) proteins were visualized by immunofluorescence (see Materials and Methods). This method allowed the identification the CHOP expression in individually infected cells. CHOP expression was detected cells that were uninfected (MOCK) or treated with DMSO as a solvent control for thapsigargin (Figure 29). Thapsigargin-treated cells showed much higher levels of CHOP, and nearly all CHOP detected in the cell was located in the nucleus. As indicated above, CHOP is a transcription factor known to induce the expression of pro-apoptotic proteins. Cells infected with wt and mutant VLP^{HS} displayed different levels of CHOP induction and nuclear translocation (Figure 30). Low levels of cytoplasmic CHOP were detected in wt VLP^{HS}-infected cells and the intensity of nuclear CHOP staining was weaker than observed in thapsigargin-treated cells. However, wt VLP^{HS} infection induced more CHOP expression in infected cells than NS2A D73H or 3' UTR Δ VLP^{HS} infections. More cells infected with NS2A D73H VLP^{HS} than 3' UT Δ VLP^{HS} showed CHOP nuclear translocation (shown by arrows), but cells infected with the NS2A D73H or 3' UTR Δ VLP^{HS} showed a CHOP cytoplasmic staining equal in intensity to that observed in MOCK or DMSO-treated cells (Figure 30). WNV antigen staining was strongest in intensity in wt VLP^{HS}-infected cells. The weakest WNV antigen staining intensity was seen in 3' UTRΔ VLP^{HS}-infected cells, which is consistent with the previous observations that this genome replicates poorly. Cells infected with NS2A D73H VLP^{HS} showed a

staining an intermediate staining intensity compared to wt and 3' UTR Δ VLP^{HS}-infected cells.

Figure 30: Wt VLP^{HS} induces CHOP expression

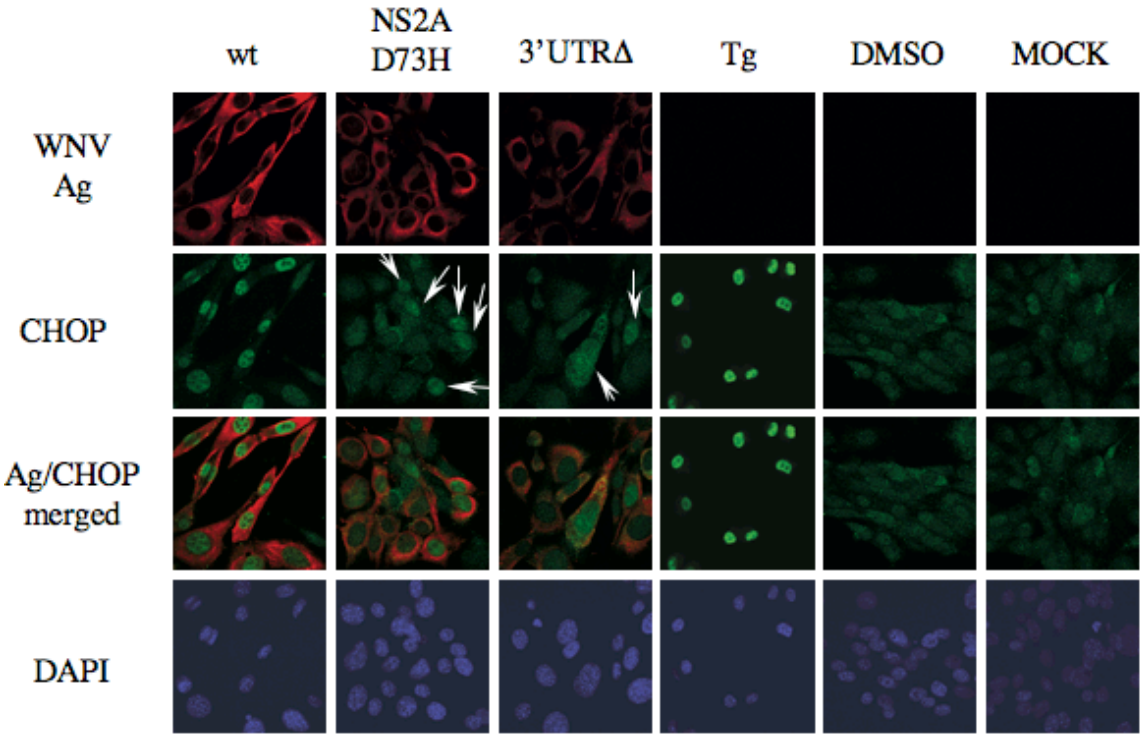

Figure 30: GADD153/CHOP is induced in VLP^{HS}-infected cells. Wt MEF cells were infected with wt, NS2A D73H or 3' UTR Δ VLP^{HS}, or treated with 2 μM thapsigargin (Tg), DMSO or media only (MOCK). Twenty-four hours later, monolayers were fixed and IFA was performed to visualize VLP^{HS}-infected cells (red) or CHOP induction/nuclear translocation (green). DAPI was used to counterstain nuclei. Images were taken by confocal microscopy, 63x magnification. Images show a representative field of the monolayer.

Discussion

The data presented in this chapter support the hypothesis that cells harboring replicons that encode noncytopathic, cell-adapted mutations are not efficiently recognized by the cell due to their low levels of replication, resulting in low levels of type I IFN production and low levels of apoptosis. Less IFN was produced in mice infected with

NS2A D73H WNV when compared to wt WNV-infected mice (Figure 24). The same trend was observed *in vitro*; in general, cells infected with VLP^{HS} encoding NS2A D73H WNR C-NS1-5 or 3' UTRΔ WNR C-NS1-5 genomes produced less IFN than wt VLP^{HS} (Figure 25). The differences in the overall level of IFN produced from the five different cell lines is most likely due to the intrinsic properties of the individual cell lines. It is possible for some cell types to have a higher threshold for the induction of IFN. In this case, more PAMPs would be required for the cell to recognize infection and produce IFN, and the amount of IFN produced from the NS2A D73H and 3' UTR Δ VLP^{HS}-infected cells would be much lower than from a wt VLP^{HS} infection. However, if the threshold is low, then fewer PAMPs would be necessary and genomes that replicate poorly would be detected. The levels of IFN production from the 3' UTRΔ VLP^{HS} infected cultures were always lower than the other VLP^{HS} infections in all cell lines examined, consistent with the observation that the 3' UTRΔ WNV C-N1-5 genome replicates more poorly than either NS2A D73H or wt WNR C-NS1-5. This reduced replication was readily apparent in the low level accumulation of viral proteins (as seen by the low intensity IFA) produced during infection (Figure 30).

Our studies revealed less IFN is produced in mice infected with $1x10^5$ ffu of NS2A D73H than wt WNV (Figure 24). The difference in IFN levels was significant on day 2 pi. There is a correlation between the viremia produced during infection and the amount of IFN detected in the same sera samples. Studies using VLPs in mice indicate that genome replication is required for the production of IFN in infected mice (Bourne et al., 2007). This correlation was also seen for cells in culture infected with mutant or wt VLP^{HS}: the NS2A D73H and 3' UTRΔ VLP^{HS}-infected cells produced less IFN than wt VLP^{HS}-infected cells (Figure 25). These data support the hypothesis that reduced genome replication (NS2A D73H and 3' UTR Δ) results in poor induction of the IFN response *in vitro* and *in vivo* when compared to genomes that can replicate efficiently (wt).

The phenotype of our NS2A D73H WNV differs significantly from the phenotype described for another NS2A mutant, NS2A A30P, in KUNV. This mutant virus induced more IFN α/β than wt KUNV at 24 hpi in A549 cells and within 5-week-old Swiss

outbred mice (Liu et al., 2006). Furthermore, the NS2A A30P KUNV mutant virus could only produce a spreading infection in immunocompromised (BHK) and not immunocompetent (A549) cells (Liu et al., 2006), suggesting that NS2A A30P KUNV efficient induction of IFN limited this mutant virus' ability to establish an infection in naïve (neighboring) cells.

Persistent viral infections are the result of a balance between the antiviral response in the host cell and the cytopathogenicity of the virus. Therefore, there are, many ways to influence this balance, such as creating a state within the cell that is more tolerant or resistant to cytopathic infections or attenuating the virus. By forcing the expression of the anti-apoptotic protein Bcl2, the percentage of JEV persistently infected BHK-21 and CHO cells increased with no detectable CPE (Liao et al., 1998). *In vivo*, blocking apoptosis has been shown to increase survival after WNV (Samuel, Morrey, and Diamond, 2007) and Sindbis virus infections (Levine et al., 1996). In our model system, the balance appears to be facilitated by the replicon and not the host cell. Genomes that do not replicate efficiently do not place excessive stress upon the cell, and minimal amounts of CHOP protein are expressed. The cells infected with attenuated VLP^{HS} have increased expression of CHOP, which is associated with apoptotic death.

Cells infected with NS2A D73H NS1-5, NS2A M108K NS1-5, NS2A D73H C-NS1-5 or 3' UTRΔ C-NS1-5 genomes did not die from infection within the first 5 days pi, whereas cells infected with wt WNR NS1-5, wt WNR C-NS1-5 and NS2A A30P WNR NS1-5 genomes succumb to infection. This death was consistent with the ability to induce apoptosis, as measured by TUNEL assay (Figures 27 and 28). Moreover, CHOP was induced in cells infected with the wt (cytopathic) VLP^{HS} (Figure 30). Excessive levels of CHOP have been associated with apoptosis, suggesting that the high concentration of CHOP observed 24 hpi in our VLP^{HS}-infected cultures is contributing to the induction of apoptosis seen by day 5 pi. These data agree with recent evidence describing CHOP induction upon WNV infection in neuroblastoma cells (Medigeshi et al., 2007).

One would imagine that initiating the ER stress response would be detrimental to infection. However, a weak induction of the ER stress may be beneficial for the attenuated VLP^{HS}-infected cells. During ER stress, many other proteins are expressed and activated that promote cell survival, including BiP (Medigeshi et al., 2007). *XBP1* is an RNA that is expressed upon AFT6 cleavage and promotes cell survival. Flaviviral infections, including WNV infection, lead to the cleavage of *XBP1* mRNA (Medigeshi et al., 2007; Yu et al., 2006), and XBP1 cleavage has been linked to the membrane expansion in DENV-infected N18 cells (Yu et al., 2006). XBP1 cleavage leads to the production of lipid biosynthesis by a poorly understood mechanism (Sriburi et al., 2007). Inducing low levels of ER stress to increase lipid production could be advantageous to the replicating virus because these membranes may provide more places for viral replication and translation (see Introduction). WNV infection has recently been shown to increase cholesterol levels in infected cells, which is a necessary component of intracellular membrane synthesis (Mackenzie, Khromykh, and Parton, 2007). Therefore, during an attenuated WNV infection, the lack of strong CHOP induction does not result in apoptosis and the weak ER stress response may upregulate factors that help facilitate genome replication.

CHAPTER 6: CONCLUSIONS AND FUTURE DIRECTIONS[6]

There are many complex and constantly changing interactions that exist between the host cell and the virus during the course of infection within a single cell. The intensity and balance between these interactions dictates the ultimate outcome of the infection: destruction of the virus, the cell, neither or both. There are many ways to tip the scales to favor one outcome over another. In the case for WNV, the cell can be primed early (such as treating the cells with IFN prior to infection) to mount an effective antiviral response. The cell can be made resistant to virus-induced apoptosis by expressing anti-apoptotic proteins or blocking the effects of pro-apoptotic molecules. Alternatively, mutant viruses with noncytopathic phenotypes may be capable of evading the host cell's innate immune response. To study some of these interactions, we forced a WNV replicon expressing the NPT gene to persistently replicate in cells in culture by adding G418 to the growth media. Mutations that were selected during this process were found to reduce the ability of the WNR genome to replicate. This observation lead to the overall hypothesis of this dissertation: *Mutations selected during the establishment of WNV replicon-bearing cells will reduce the levels of replicon and viral genome replication, thereby avoiding the cell's antiviral responses and enabling persistent infection of the host cell.*

SUMMARY

WNR NS1-5 ET2AN genomes harboring cell-adapted mutations that conferred a high CFE in cell culture (NS2A D73H, NS2A M108K and NS3 117K ins) produced less viral antigen than wt WNR NS1-5 ET2AN genomes in cell culture. Likewise, low levels of eGFP fluorescence were detected from cells infected with either the NS2A D73H or M108K WNR C-eGFP-NS1-5 genomes compared to the wt C-eGFP-NS1-5 genomes. These NS2A mutant WNVs, as well as a genetically engineered WNV genomes with a

[6] A portion of the ideas presented here are included in a review article submitted to Future Virology. This journal grants permission with the requirement of proper citation. **Rossi, S.L.** and Mason, P.M. Persistent Infections of Mammals and Mammalian Cell Cultures with West Nile Virus. Future Virology, 3(1): 25-34.

large deletion in the 3' UTR (3' UTR Δ), replicated more poorly than wt genomes *in vitro*.

The *in vivo* results obtained from these viruses correlated well with the results *in vitro*; NS2A D73H, NS2A M108K and 3' UTR Δ WNV were avirulent in adult mice. The precise LD_{50} values could not be accurately determined for these viruses but were $>1x10^3$ ffu. Interestingly, virus recovered from the single mouse that died following inoculation with the NS2A D73H WNV contained a direct reversion of the D73H mutation to the wt codon. All other mutants (NS2A A30P, NS4B E249G and NS5 P528H) WNV had LD_{50} values similar to the wt WNV in adult mice (less than 10 ffu). Furthermore, the NS2A D73H WNV produced a transient, lower titer viremia in mice than the wt WNV, which produced a longer, higher titer viremia in mice.

There was also a large difference in the antiviral response in cells infected with wt and mutant (NS2A D73H, NS2A M108K and 3' UTR Δ) genomes. The wt WNR C-NS1-5 produced IFN after 24 hours of infection than either the NS2A D73H or 3' UTR Δ mutants on any cell line tested. Mice infected with wt WNV produced a higher and longer-lasting IFN response within the first 4 days following infection than NS2A D73H WNV-infected mice. These results suggest that the innate immune response is not efficiently engaged in cells or mice infected with the attenuated genomes compared to the wt genomes.

Some genomes (NS2A A30P and wt WNR NS1-5) induced death in the host cell while others (NS2A D73H and NS2A M108K WNR NS1-5) appeared to replicate without causing overt CPE and death in the host cell. This cell death was determined to be primarily due to apoptosis; the percentage of cells infected with the NS2A D73H or 3' UTR Δ WNR C-NS1-5 undergoing apoptosis at 5 dpi was statistically lower than the percentage of apoptotic wt WNR C-NS1-5-infected cells. The high percentage of apoptotic wt WNR NS1-5-infected cells correlated with the induction and nuclear translocation of the pro-apoptotic protein CHOP at 24 hpi. The cultures infected with the NS2A D73H and 3' UTR Δ WNR C-NS1-5 genomes showed low levels of CHOP induction and few cells showed CHOP nuclear translocation.

A MODEL OF WNV PERSISTENCE

The data presented in the previous chapters can be combined into a model that helps to explain how genomes harboring cell-adapted, attenuating mutations (NS2A D73H, NS2A M108K and 3' UTR Δ) are able to cause a noncytopathic, persistent infection in the host cell. This model was generated from a combination of our current understanding of flavivirus and host cell interactions within the infected cell and the data contained within this dissertation. It is important to note that this diagram is certainly an oversimplification of the actual events occurring within the cell, and there are other pathways and proteins involved in the response of the cell to a flavivirus infection. Nevertheless, our current working model of how both wt and mutant genomes interact with the host cell during infection is shown in Figure 31.

During a wt WNV (or WNR) infection, high levels of PAMPs (products of genome replication, including dsRNA) are likely produced as a product of the virus' (or replicon's) efficient replication. These PAMPs are recognized by the cell and lead to the production of IFN (Figure 4). This IFN can signal to the infected cell and neighboring cells via recognition by the IFN receptor. The infected cell cannot is less responsive to IFN since WNV blocks the STAT signaling pathway. However, this response makes neighboring uninfected cells more resistant to WNV infection. Products of replication (including the production of viral proteins) put stress on the cell, leading to CHOP induction by 24 hpi (Figures 29-30). ER stress (measured by the increase in pro-apoptotic CHOP induction) is likely to contribute to the apoptotic death seen in wt VLP^{HS}-infected MEF cells 5 days pi.

Genomes with stable attenuating mutations (NS2A D73H, NS2A M108K and 3' UTR Δ) replicate poorly and likely produce low quantities of PAMPs compared to the wt genome infection that are not readily recognized by the cell. This lack of recognition fails to fully engage the IFN response, resulting in low levels of IFN production (Figures 24 and 25). Low levels of replication also produce low levels of viral-encoded proteins (Figures 10, 13, 15, 28, 30), which place little stress on the ER. The ER stress response is still engaged during the infection with these attenuated genomes, as seen by low levels of

CHOP protein accumulation in the cytoplasm and nucleus of infected MEF cells. However, the intensity of the ER stress response is weak (when compared to the wt infection), which permits cell survival (Figure 27) and not the induction of apoptosis (Figure 28).

Figure 31: Overview of the mechanism of persistence in replication-deficient WNV infection

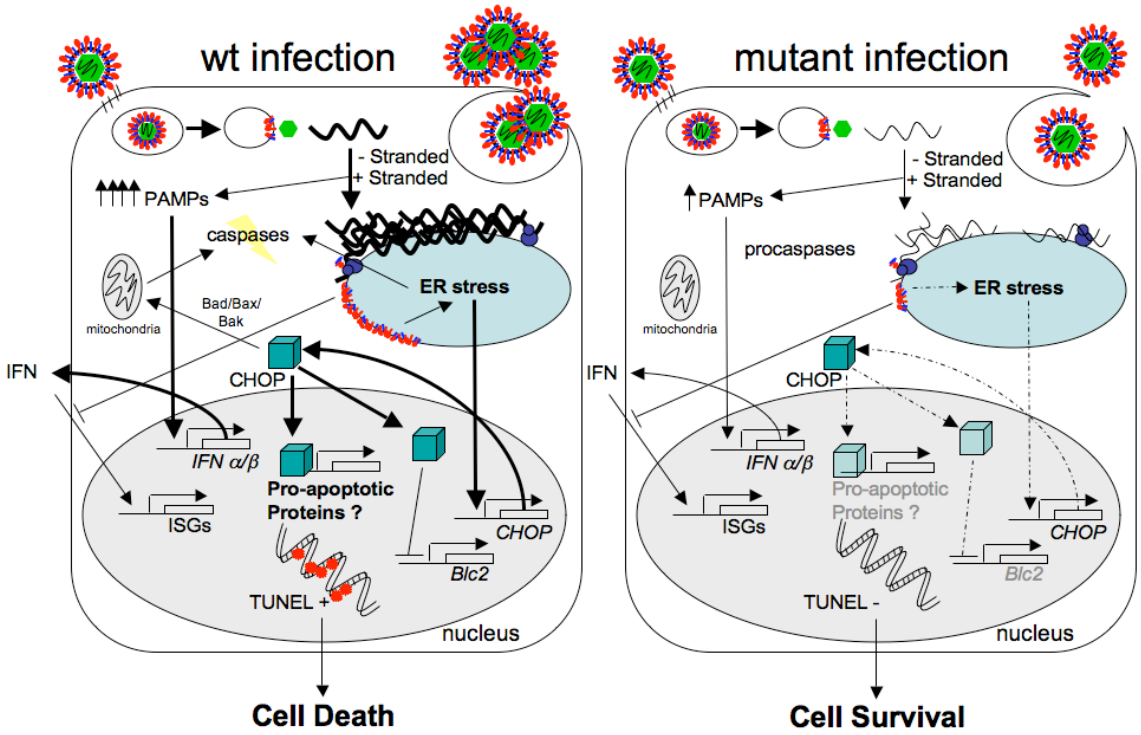

Figure 31: A model for how genomes with attenuating cell-adapted mutations are able to cause persistent noncytopathic infections within the host cell.

IMPLICATIONS AND DISCUSSION

The initial interactions between the virus and the host cell are critical for shaping the course of infection. When our research began, there was a growing interest in understanding how the infected cell recognizes viral infection. It was not clear from the

literature if and how these virus-host cell interactions would change with respect to genome replication within the cell. It was known that some WNV strains caused overt disease in the host and caused CPE within the cell while other strains did not. We have shown that the innate immune response is not as efficiently engaged in cells or mice infected with replicon and viral genomes that replicate more poorly than wt replicon and viral genomes. This is also the first description, to our knowledge, of the differences in the ER stress response with respect to differences in virus replication.

The function of the NS2A protein in persistence remains unclear. A disproportionate number of mutations were identified in the NS2A gene (compared to other viral genes) in WNR genomes that were selected during the generation of G418-resistant colonies in mammalian cells (Figures 11 and 12). Mutations in the NS2A gene were also observed in high frequency in KUNR recovered from antibiotic-resistant BHK clones (Liu et al., 2004). The flavivirus NS2A protein has been linked to virion production (Kummerer and Rice, 2002; Liu, Chen, and Khromykh, 2003), genome replication (Mackenzie et al., 1998), and altering the cellular IFN response (Liu et al., 2004; Liu et al., 2006; Munoz-Jordan et al., 2003). We have shown that point mutations in NS2A have a dramatic effect on viral replication and virulence in mice. In accordance with our overall hypothesis, it is likely the reduction in genome replication mediated by these NS2A mutations results in the poor engagement of the ER stress response and loss of CPE. The alternative explanation is that the wt NS2A protein itself is causing, or contributing to, the cytopathic effect observed in cells infected with wt genomes and these NS2A D73H and M108K mutations selectively destroy this property of the NS2A protein. Although this alternative hypothesis cannot be disproven based on our experiments, it is noteworthy that genomes harboring the 3' UTR Δ (which contains a wt NS2A protein) have a similar phenotype to genomes with the NS2A D73H mutation. Both the NS2A D73H and 3' UTR Δ WNR C-NS1-5 genomes induce lower IFN production and CHOP expression/nuclear translocation than wt WNR C-NS1-5. Future experiments to look closely at the effects of the NS2A D73H and wt NS2A proteins

themselves may provide additional information detailing the function of this poorly characterized viral protein.

Although WNR NS1-5 ET2AN genomes harboring cell-adapted mutations (NS2A D73H, NS2A M108K and NS3 117K ins) can be stably maintained in cells for dozens of passages, these mutations are quickly lost from genetically engineered WNV, as evident from the reversion to the wt phenotype when these viruses are passed in cell culture or amplified *in vivo* (Chapters 3 and 4). The difference in the behavior of genomes harboring these mutations under these two different conditions is readily explained by the differences in selective pressure. In the case of the engineered cell-adapted WNR that are trapped within all cells in a culture, the WNR must be maintained at low levels to allow cells to replicate normally, and spontaneous WNR revertants that replicate better are likely to make the cell they are trapped in less fit, so they are lost from the population. Furthermore, reducing genome replication was shown to reduce cytopathogenicity, allowing the persistently infected WNR-bearing cells able to maintain the WNR genome even in the absence of selective media. Long-term infection correlated with a reduction in genome copy number in each infected cell (Figure 10). On the other hand, better-replicating (wt-like) phenotypic revertants that arise from the WNV genomes engineered to encode cell-adapted sequences would have a significant selective advantage in cell culture where the viral genes that replicate more efficiently to naïve cells would be rapidly selected. The outcome of these differences in selective pressure observed in these two different *in vitro* systems suggests that selective pressure, rather than ability to tolerate mutations, may be the most important factor in establishment of persistence *in vivo*.

The overall objective of this research was to identify the factors and interactions between the WNV genome and the host cell that contributed to a persistent WNV infection at the cellular level. The application of these *in vitro* results to the long-term *in vivo* infections previously described for both hamsters and monkeys is not straightforward. There are several possibilities for how the virus can produce long-term infections these hosts. In one case, certain cells in the host may be persistently infected

and slowly shed infectious virus. However, the virus may cause a chronic infection rather than a persistent one; in this case, the infected cell need not survive, but only live long enough to produce progeny virions capable of infecting naïve neighboring cells. The virus does not persistently infect any individual cell, but rather the infection slowly spreads, resulting in a small number of infected cells that results in the stable long-term infection in the host. The unknown factor in these cenarios is the host's adaptive immune response. It is possible that these persistent or chronicially infected cells are not recognized and destroyed the cells of the immune response, but it is unclear how. It is known from the seroconversion data that mice mount antibody responses even against viruses that replicate poorly in cell culture and produce low levels of viremia in the host (Table 5). Additionally, hamsters with a long-term WNV infection (and may also be actively shedding virus in their urine) have antibodies that recognize WNV (Tesh et al., 2005; Xiao et al., 2001). Perhaps the infected cells are 'sequested' from the immune response, or maybe the infected cells downregulate the signals of infection so they are not recognized by cells of the immune response.

The phenotype of these mutant WNRs and WNVs in mice and mammalian cells has been described in the previous chapters. Mammals, however, are not believed to have a significant role in the transmission of WNV in nature (Figure 7). Therefore, the phenotypes of these mutant WNVs need to be assessed in both the avian and mosquito hosts. Until the phenotypes of attenuated, persistent WNVs are assessed in these hosts, it will be difficult to speculate the fitness of a replication-deficient WNV in nature. Based on the evidence from infected mice, it is expected that the NS2A D73H, NS2A M108K and 3' UTR Δ WNV will be attenuated (not cause disease or death) in birds. Many species of mosquito can transmit the wt WNV, but it is unknown if these mosquitoes will be able to become productively infected and transmit the mutant WNV also. For this to occur, these viruses would have to infect the mosquito's midgut cells, disseminate into the hemolymph, infect the salivary glands and be secreted into the saliva. Even if those events occur, the virus must be in a sufficient quantity to infect the host she feeds upon for transmission to occur. Certainly, viruses with a small plaque (attenuated) phenotype

are isolated from natural isolates (Davis et al., 2004; Jia et al., 2007), indicating that these types of viruses can be successfully transmitted in nature. However, these viruses would likely be less fit than viruses that replicate efficiently and would eventually be lost from natural populations. Viruses harboring the NS2A D73H and NS3 117Kins mutations have been shown to be unstable both *in vitro* and *in vivo*.

One of the reasons why WNV (as well as many other arboviruses) is studied is because of its impact on human health. Therefore, the ultimate application of flavivirus research is going to be towards developing vaccines and antiviral countermeasures to combat against infection and to help alleviate the symptoms and progression of disease of those already infected. Although WNV may not evolve into a virus that is capable of establishing a persistent phenotype that is successfully maintained for long periods of time in nature, persistence may have an impact on specific immunocompromised hosts. Within the last two years, clinicians have described persistent WNV infections in human patients. The persistent infections were only confirmed post-mortem, so there is no good estimate for the number of living patients with a persistent WNV infection. Better diagnostic tools are needed to be able to identify these individuals, and this may impact how clinicians care for those individuals persistently infected with WNV. However, other than supportive care, no treatment for the diseases caused by WNV infections in humans currently exists. The best way to prevent potential long-term infections with WNV in patients would be to eliminate the infection during the acute phase of illness. The development of vaccines and therapeutics to control the diseases caused by WNV is still a priority for many flavivirologists.

The next few years will bring many new developments to our understanding of virus-host cell interactions. The field has been focused on exploring the innate immune response with a specific interest in how flaviviruses interact with this response. In the future, the field is likely to expand to characterize more molecules and proteins involved in this response. At the same time, the interaction between those new proteins and multiple flaviviruses will be evaluated. The focus has been to utilize the most virulent forms of many flaviviruses to analyze these responses and interactions. However, little

attention has been given to the attenuated forms of these virulent strains, such as vaccine candidates or viruses genetically engineered to contain attenuating mutations. Studying these less virulent viral forms, in addition to the virulent strains, will be critical to fully appreciating how the host responds to infection and how to make potential vaccines more efficacious and safer for human use.

REFERENCES

Adelman, Z. N., Blair, C. D., Carlson, J. O., Beaty, B. J., and Olson, K. E. (2001). Sindbis virus-induced silencing of dengue viruses in mosquitoes. *Insect Mol Biol* **10**(3)**,** 265-273.

Alcon, S., Talarmin, A., Debruyne, M., Falconar, A., Deubel, V., and Flamand, M. (2002). Enzyme-linked immunosorbent assay specific to Dengue virus type 1 nonstructural protein NS1 reveals circulation of the antigen in the blood during the acute phase of disease in patients experiencing primary or secondary infections. *J Clin Microbiol* **40**(2)**,** 376-381.

Alcon-LePoder, S., Drouet, M. T., Roux, P., Frenkiel, M. P., Arborio, M., Durand-Schneider, A. M., Maurice, M., Le Blanc, I., Gruenberg, J., and Flamand, M. (2005). The secreted form of dengue virus nonstructural protein NS1 is endocytosed by hepatocytes and accumulates in late endosomes: implications for viral infectivity. *J Virol* **79**(17)**,** 11403-11411.

Alexopoulou, L., Holt, A. C., Medzhitov, R., and Flavell, R. A. (2001). Recognition of double-stranded RNA and activation of NF-kappaB by Toll-like receptor 3. *Nature* **413**(6857)**,** 732-738.

Amberg, S. M., Nestorowicz, A., McCourt, D. W., and Rice, C. M. (1994). NS2B-3 proteinase-mediated processing in the yellow fever virus structural region: in vitro and in vivo studies. *J Virol* **68**(6)**,** 3794-3802.

Amberg, S. M., and Rice, C. M. (1999). Mutagenesis of the NS2B-NS3-mediated cleavage site in the flavivirus capsid protein demonstrates a requirement for coordinated processing. *J Virol* **73**(10)**,** 8083-8094.

Anderson, J. F., and Rahal, J. J. (2002). Efficacy of interferon alpha-2b and ribavirin against West Nile virus in vitro. *Emerg Infect Dis* **8**(1)**,** 107-108.

Andrejeva, J., Childs, K. S., Young, D. F., Carlos, T. S., Stock, N., Goodbourn, S., and Randall, R. E. (2004). The V proteins of paramyxoviruses bind the IFN-inducible RNA helicase, mda-5, and inhibit its activation of the IFN-beta promoter. *Proc Natl Acad Sci U S A* **101**(49)**,** 17264-17269.

Anonymous (1999). Outbreak of West Nile-like viral encephalitis--New York, 1999. *MMWR Morb Mortal Wkly Rep* **48**(38)**,** 845-849.

Anonymous (2002). West Nile virus activity--United States, September 26-October 2, 2002, and investigations of West Nile virus infections in recipients of blood transfusion and organ transplantation. *MMWR Morb Mortal Wkly Rep* **51**(39)**,** 884, 895.

Anonymous (2004). Global burden of disease (GBD) for hepatitis C. *J Clin Pharmacol* **44**(1)**,** 20-29.

Anonymous (2007). West Nile virus transmission through blood transfusion--South Dakota, 2006. *MMWR Morb Mortal Wkly Rep* **56**(4)**,** 76-79.

Arya, R., Mallik, M., and Lakhotia, S. C. (2007). Heat shock genes - integrating cell survival and death. *J Biosci* **32**(3)**,** 595-610.

Bakonyi, T., Hubalek, Z., Rudolf, I., and Nowotny, N. (2005). Novel flavivirus or new lineage of West Nile virus, central Europe. *Emerg Infect Dis* **11**(2)**,** 225-231.

Banet-Noach, C., Simanov, L., and Malkinson, M. (2003). Direct (non-vector) transmission of West Nile virus in geese. *Avian Pathol* **32**(5)**,** 489-494.

Baqar, S., Hayes, C. G., Murphy, J. R., and Watts, D. M. (1993). Vertical transmission of West Nile virus by Culex and Aedes species mosquitoes. *Am J Trop Med Hyg* **48**(6)**,** 757-762.

Beasley, D. W., Li, L., Suderman, M. T., and Barrett, A. D. (2002). Mouse neuroinvasive phenotype of West Nile virus strains varies depending upon virus genotype. *Virology* **296**(1)**,** 17-23.

Beasley, D. W., Whiteman, M. C., Zhang, S., Huang, C. Y., Schneider, B. S., Smith, D. R., Gromowski, G. D., Higgs, S., Kinney, R. M., and Barrett, A. D. (2005). Envelope protein glycosylation status influences mouse neuroinvasion phenotype of genetic lineage 1 West Nile virus strains. *J Virol* **79**(13)**,** 8339-8347.

Beerntsen, B. T., James, A. A., and Christensen, B. M. (2000). Genetics of mosquito vector competence. *Microbiol Mol Biol Rev* **64**(1)**,** 115-137.

Bernard, K. A., Maffei, J. G., Jones, S. A., Kauffman, E. B., Ebel, G., Dupuis, A. P., 2nd, Ngo, K. A., Nicholas, D. C., Young, D. M., Shi, P. Y., Kulasekera, V. L., Eidson, M., White, D. J., Stone, W. B., and Kramer, L. D. (2001). West Nile virus infection in birds and mosquitoes, New York State, 2000. *Emerg Infect Dis* **7**(4)**,** 679-685.

Berthet, F. X., Zeller, H. G., Drouet, M. T., Rauzier, J., Digoutte, J. P., and Deubel, V. (1997). Extensive nucleotide changes and deletions within the envelope glycoprotein gene of Euro-African West Nile viruses. *J Gen Virol* **78 (Pt 9),** 2293-2297.

Best, S. M., Morris, K. L., Shannon, J. G., Robertson, S. J., Mitzel, D. N., Park, G. S., Boer, E., Wolfinbarger, J. B., and Bloom, M. E. (2005). Inhibition of interferon-stimulated JAK-STAT signaling by a tick-borne flavivirus and identification of NS5 as an interferon antagonist. *J Virol* **79**(20)**,** 12828-12839.

Bian, G., Shin, S. W., Cheon, H. M., Kokoza, V., and Raikhel, A. S. (2005). Transgenic alteration of Toll immune pathway in the female mosquito Aedes aegypti. *Proc Natl Acad Sci U S A* **102**(38)**,** 13568-13573.

Biggerstaff, B. J., and Petersen, L. R. (2003). Estimated risk of transmission of the West Nile virus through blood transfusion in the US, 2002. *Transfusion* **43**(8)**,** 1007-1017.

Bin, H., Grossman, Z., Pokamunski, S., Malkinson, M., Weiss, L., Duvdevani, P., Banet, C., Weisman, Y., Annis, E., Gandaku, D., Yahalom, V., Hindyieh, M., Shulman, L., and Mendelson, E. (2001). West Nile fever in Israel 1999-2000: from geese to humans. *Ann N Y Acad Sci* **951,** 127-142.

Blackwell, J. L., and Brinton, M. A. (1995). BHK cell proteins that bind to the 3' stem-loop structure of the West Nile virus genome RNA. *J Virol* **69**(9)**,** 5650-5658.

Blackwell, J. L., and Brinton, M. A. (1997). Translation elongation factor-1 alpha interacts with the 3' stem-loop region of West Nile virus genomic RNA. *J Virol* **71**(9)**,** 6433-44.

Blair, C. D., Adelman, Z. N., and Olson, K. E. (2000). Molecular strategies for interrupting arthropod-borne virus transmission by mosquitoes. *Clin Microbiol Rev* **13**(4)**,** 651-61.

Blight, K. J., Kolykhalov, A. A., and Rice, C. M. (2000). Efficient initiation of HCV RNA replication in cell culture. *Science* **290**(5498)**,** 1972-4.

Blight, K. J., McKeating, J. A., and Rice, C. M. (2002). Highly permissive cell lines for subgenomic and genomic hepatitis C virus RNA replication. *J Virol* **76**(24)**,** 13001-13014.

Blitvich, B. J., Scanlon, D., Shiell, B. J., Mackenzie, J. S., and Hall, R. A. (1999). Identification and analysis of truncated and elongated species of the flavivirus NS1 protein. *Virus Res* **60**(1)**,** 67-79.

Bondre, V. P., Jadi, R. S., Mishra, A. C., Yergolkar, P. N., and Arankalle, V. A. (2007). West Nile virus isolates from India: evidence for a distinct genetic lineage. *J Gen Virol* **88**(Pt 3)**,** 875-884.

Borisevich, V., Seregin, A., Nistler, R., Mutabazi, D., and Yamshchikov, V. (2006). Biological properties of chimeric West Nile viruses. *Virology* **349**(2)**,** 371-381.

Bourne, N., Scholle, F., Silva, M. C., Rossi, S. L., Dewsbury, N., Judy, B., De Aguiar, J. B., Leon, M. A., Estes, D. M., Fayzulin, R., and Mason, P. W. (2007). Early production of type I interferon during West Nile virus infection: role for lymphoid tissues in IRF3-independent interferon production. *J Virol* **81**(17)**,** 9100-9108.

Brault, A. C., Huang, C. Y., Langevin, S. A., Kinney, R. M., Bowen, R. A., Ramey, W. N., Panella, N. A., Holmes, E. C., Powers, A. M., and Miller, B. R. (2007). A single positively selected West Nile viral mutation confers increased virogenesis in American crows. *Nat Genet* **39**(9)**,** 1162-1166.

Brault, A. C., Langevin, S. A., Bowen, R. A., Panella, N. A., Biggerstaff, B. J., Miller, B. R., and Komar, N. (2004). Differential virulence of West Nile strains for American crows. *Emerg Infect Dis* **10**(12)**,** 2161-2168.

Breckenridge, D. G., Germain, M., Mathai, J. P., Nguyen, M., and Shore, G. C. (2003). Regulation of apoptosis by endoplasmic reticulum pathways. *Oncogene* **22**(53)**,** 8608-8618.

Bredenbeek, P. J., Kooi, E. A., Lindenbach, B., Huijkman, N., Rice, C. M., and Spaan, W. J. (2003). A stable full-length yellow fever virus cDNA clone and the role of conserved RNA elements in flavivirus replication. *J Gen Virol* **84**(Pt 5)**,** 1261-1268.

Brenner, W., Storch, G., Buller, R., Vij, R., Devine, S., and DiPersio, J. (2005). West Nile Virus encephalopathy in an allogeneic stem cell transplant recipient: use of quantitative PCR for diagnosis and assessment of viral clearance. *Bone Marrow Transplant* **36**(4)**,** 369-370.

Brinton, M. A., and Dispoto, J. H. (1988). Sequence and secondary structure analysis of the 5'-terminal region of flavivirus genome RNA. *Virology* **162**(2)**,** 290-299.

Burke, D. S., and Monath, T. P. (2001). Flaviviruses. 4 ed. *In* "Fields Virology" (D. M. Knipe, P. M. Howley, D. E. Griffin, M. A. Hartin, R. A. Lamb, B. Roizman, and S. E. Straus, Eds.), Vol. 1, pp. 1043-1125. 2 vols. Lippincott Williams & Wilkins, Philadelphia.

Cahour, A., Pletnev, A., Vazielle-Falcoz, M., Rosen, L., and Lai, C. J. (1995). Growth-restricted dengue virus mutants containing deletions in the 5' noncoding region of the RNA genome. *Virology* **207**(1)**,** 68-76.

Caplen, N. J., Zheng, Z., Falgout, B., and Morgan, R. A. (2002). Inhibition of viral gene expression and replication in mosquito cells by dsRNA-triggered RNA interference. *Mol Ther* **6**(2)**,** 243-251.

Catteau, A., Kalinina, O., Wagner, M. C., Deubel, V., Courageot, M. P., and Despres, P. (2003). Dengue virus M protein contains a proapoptotic sequence referred to as ApoptoM. *J Gen Virol* **84**(Pt 10)**,** 2781-2793.

Chambers, T. J., and Diamond, M. S. (2003). Pathogenesis of flavivirus encephalitis. *Adv Virus Res* **60,** 273-342.

Chambers, T. J., Hahn, C. S., Galler, R., and Rice, C. M. (1990). Flavivirus genome organization, expression, and replication. *Annu Rev Microbiol* **44,** 649-688.

Chambers, T. J., Nestorowicz, A., Amberg, S. M., and Rice, C. M. (1993). Mutagenesis of the yellow fever virus NS2B protein: effects on proteolytic processing, NS2B-NS3 complex formation, and viral replication. *J Virol* **67**(11)**,** 6797-6807.

Chan, S. W., and Egan, P. A. (2005). Hepatitis C virus envelope proteins regulate CHOP via induction of the unfolded protein response. *Faseb J* **19**(11)**,** 1510-1512.

Chang, K. O., and George, D. W. (2007). Interferons and Ribavirin Effectively Inhibit Norwalk Virus Replication in Replicon-Bearing Cells. *J Virol* **81**(22)**,** 12111-12118.

Chang, T. H., Liao, C. L., and Lin, Y. L. (2006). Flavivirus induces interferon-beta gene expression through a pathway involving RIG-I-dependent IRF-3 and PI3K-dependent NF-kappaB activation. *Microbes Infect* **8**(1)**,** 157-171.

Chen, C. J., Kuo, M. D., Chien, L. J., Hsu, S. L., Wang, Y. M., and Lin, J. H. (1997). RNA-protein interactions: involvement of NS3, NS5, and 3' noncoding regions of Japanese encephalitis virus genomic RNA. *J Virol* **71**(5)**,** 3466-3473.

Chen, L. H., Jiang, C. C., Kiejda, K. A., Wang, Y. F., Thorne, R. F., Zhang, X. D., and Hersey, P. (2007a). Thapsigargin sensitizes human melanoma cells to TRAIL-induced apoptosis by up-regulation of TRAIL-R2 through the unfolded protein response. *Carcinogenesis* **28**(11)**,** 2328-2336.

Chen, Z., Benureau, Y., Rijnbrand, R., Yi, J., Wang, T., Warter, L., Lanford, R. E., Weinman, S. A., Lemon, S. M., Martin, A., and Li, K. (2007b). GB virus B disrupts RIG-I signaling by NS3/4A-mediated cleavage of the adaptor protein MAVS. *J Virol* **81**(2)**,** 964-976.

Cheng, G., Zhong, J., and Chisari, F. V. (2006). Inhibition of dsRNA-induced signaling in hepatitis C virus-infected cells by NS3 protease-dependent and -independent mechanisms. *Proc Natl Acad Sci U S A* **103**(22)**,** 8499-8504.

Christensen, B. M., Li, J., Chen, C. C., and Nappi, A. J. (2005). Melanization immune responses in mosquito vectors. *Trends Parasitol* **21**(4)**,** 192-199.

Chu, J. J., and Ng, M. L. (2003). The mechanism of cell death during West Nile virus infection is dependent on initial infectious dose. *J Gen Virol* **84**(Pt 12)**,** 3305-3314.

Chung, K. M., Liszewski, M. K., Nybakken, G., Davis, A. E., Townsend, R. R., Fremont, D. H., Atkinson, J. P., and Diamond, M. S. (2006). West Nile virus nonstructural protein NS1 inhibits complement activation by binding the regulatory protein factor H. *Proc Natl Acad Sci U S A* **103**(50)**,** 19111-19116.

Chung, K. M., Thompson, B. S., Fremont, D. H., and Diamond, M. S. (2007). Antibody recognition of cell surface-associated NS1 triggers Fc-gamma receptor-mediated phagocytosis and clearance of West Nile Virus-infected cells. *J Virol* **81**(17)**,** 9551-9555.

Cleaves, G. R., Ryan, T. E., and Schlesinger, R. W. (1981). Identification and characterization of type 2 dengue virus replicative intermediate and replicative form RNAs. *Virology* **111**(1)**,** 73-83.

Clemens, M. J. (1997). PKR--a protein kinase regulated by double-stranded RNA. *Int J Biochem Cell Biol* **29**(7)**,** 945-949.

Constantine, D. G., and Woodall, D. F. (1964). Latent Infection of Rio Bravo Virus in Salivary Glands of Bats. *Public Health Rep* **79,** 1033-1039.

Cornberg, M., and Manna, M. P. (2006). Future trends in hepatitis C therapy. *Future Virology* **1**(1)**,** 99-107.

Corver, J., Lenches, E., Smith, K., Robison, R. A., Sando, T., Strauss, E. G., and Strauss, J. H. (2003). Fine mapping of a cis-acting sequence element in yellow fever virus RNA that is required for RNA replication and cyclization. *J Virol* **77**(3)**,** 2265-2270.

Costa, S. M., Azevedo, A. S., Paes, M. V., Sarges, F. S., Freire, M. S., and Alves, A. M. (2007). DNA vaccines against dengue virus based on the ns1 gene: the influence of different signal sequences on the protein expression and its correlation to the immune response elicited in mice. *Virology* **358**(2)**,** 413-423.

Crance, J. M., Scaramozzino, N., Jouan, A., and Garin, D. (2003). Interferon, ribavirin, 6-azauridine and glycyrrhizin: antiviral compounds active against pathogenic flaviviruses. *Antiviral Res* **58**(1)**,** 73-79.

Dahmer, M. K. (2005). Caspases-2, -3, and -7 are involved in thapsigargin-induced apoptosis of SH-SY5Y neuroblastoma cells. *J Neurosci Res* **80**(4)**,** 576-583.

Datta, S. R., Dudek, H., Tao, X., Masters, S., Fu, H., Gotoh, Y., and Greenberg, M. E. (1997). Akt phosphorylation of BAD couples survival signals to the cell-intrinsic death machinery. *Cell* **91**(2)**,** 231-241.

Daugaard, M., Rohde, M., and Jaattela, M. (2007). The heat shock protein 70 family: Highly homologous proteins with overlapping and distinct functions. *FEBS Lett* **581**(19)**,** 3702-3710.

Davis, C. T., Beasley, D. W., Guzman, H., Siirin, M., Parsons, R. E., Tesh, R. B., and Barrett, A. D. (2004). Emergence of attenuated West Nile virus variants in Texas, 2003. *Virology* **330**(1)**,** 342-350.

Davis, C. T., Ebel, G. D., Lanciotti, R. S., Brault, A. C., Guzman, H., Siirin, M., Lambert, A., Parsons, R. E., Beasley, D. W., Novak, R. J., Elizondo-Quiroga, D., Green, E. N., Young, D. S., Stark, L. M., Drebot, M. A., Artsob, H., Tesh, R. B., Kramer, L. D., and Barrett, A. D. (2005). Phylogenetic analysis of North American West Nile virus isolates, 2001-2004: evidence for the emergence of a dominant genotype. *Virology* **342**(2)**,** 252-265.

Davis, C. T., Galbraith, S. E., Zhang, S., Whiteman, M. C., Li, L., Kinney, R. M., and Barrett, A. D. (2007). A combination of naturally occurring mutations in north american west nile virus nonstructural protein genes and in the 3' untranslated region alters virus phenotype. *J Virol* **81**(11)**,** 6111-6116.

Davis, J. W., and Hardy, J. L. (1974). Characterization of persistent Modoc viral infections in Syrian hamsters. *Infect Immun* **10**(2)**,** 328-334.

Davis, J. W., Hardy, J. L., and Reeves, W. C. (1974). Modoc viral infections in the deer mouse Peromyscus maniculatus. *Infect Immun* **10**(6)**,** 1362-1369.

De Nova-Ocampo, M., Villegas-Sepulveda, N., and del Angel, R. M. (2002). Translation elongation factor-1alpha, La, and PTB interact with the 3' untranslated region of dengue 4 virus RNA. *Virology* **295**(2)**,** 337-347.

del Peso, L., Gonzalez-Garcia, M., Page, C., Herrera, R., and Nunez, G. (1997). Interleukin-3-induced phosphorylation of BAD through the protein kinase Akt. *Science* **278**(5338)**,** 687-689.

Despres, P., Flamand, M., Ceccaldi, P. E., and Deubel, V. (1996). Human isolates of dengue type 1 virus induce apoptosis in mouse neuroblastoma cells. *J Virol* **70**(6)**,** 4090-4096.

Diamond, M. S., Shrestha, B., Marri, A., Mahan, D., and Engle, M. (2003a). B cells and antibody play critical roles in the immediate defense of disseminated infection by West Nile encephalitis virus. *J Virol* **77**(4)**,** 2578-2586.

Diamond, M. S., Sitati, E. M., Friend, L. D., Higgs, S., Shrestha, B., and Engle, M. (2003b). A critical role for induced IgM in the protection against West Nile virus infection. *J Exp Med* **198**(12)**,** 1853-1862.

Diebold, S. S., Kaisho, T., Hemmi, H., Akira, S., and Reis e Sousa, C. (2004). Innate antiviral responses by means of TLR7-mediated recognition of single-stranded RNA. *Science* **303**(5663)**,** 1529-1531.

Ding, X., Wu, X., Duan, T., Siirin, M., Guzman, H., Yang, Z., Tesh, R. B., and Xiao, S. Y. (2005). Nucleotide and amino acid changes in West Nile virus strains exhibiting renal tropism in hamsters. *Am J Trop Med Hyg* **73**(4)**,** 803-807.

Diniz, J. A., Da Rosa, A. P., Guzman, H., Xu, F., Xiao, S. Y., Popov, V. L., Vasconcelos, P. F., and Tesh, R. B. (2006). West Nile virus infection of primary mouse

neuronal and neuroglial cells: the role of astrocytes in chronic infection. *Am J Trop Med Hyg* **75**(4)**,** 691-696.

Droll, D. A., Krishna Murthy, H. M., and Chambers, T. J. (2000). Yellow fever virus NS2B-NS3 protease: charged-to-alanine mutagenesis and deletion analysis define regions important for protease complex formation and function. *Virology* **275**(2)**,** 335-347.

Du, K., Herzig, S., Kulkarni, R. N., and Montminy, M. (2003). TRB3: a tribbles homolog that inhibits Akt/PKB activation by insulin in liver. *Science* **300**(5625)**,** 1574-1577.

Ebel, G. D., Carricaburu, J., Young, D., Bernard, K. A., and Kramer, L. D. (2004). Genetic and phenotypic variation of West Nile virus in New York, 2000-2003. *Am J Trop Med Hyg* **71**(4)**,** 493-500.

Edgil, D., Polacek, C., and Harris, E. (2006). Dengue virus utilizes a novel strategy for translation initiation when cap-dependent translation is inhibited. *J Virol* **80**(6)**,** 2976-2986.

Eidson, M., Komar, N., Sorhage, F., Nelson, R., Talbot, T., Mostashari, F., and McLean, R. (2001a). Crow deaths as a sentinel surveillance system for West Nile virus in the northeastern United States, 1999. *Emerg Infect Dis* **7**(4)**,** 615-620.

Eidson, M., Miller, J., Kramer, L., Cherry, B., and Hagiwara, Y. (2001b). Dead crow densities and human cases of West Nile virus, New York State, 2000. *Emerg Infect Dis* **7**(4)**,** 662-664.

Elshuber, S., Allison, S. L., Heinz, F. X., and Mandl, C. W. (2003). Cleavage of protein prM is necessary for infection of BHK-21 cells by tick-borne encephalitis virus. *J Gen Virol* **84**(Pt 1)**,** 183-191.

Endo, M., Oyadomari, S., Suga, M., Mori, M., and Gotoh, T. (2005). The ER stress pathway involving CHOP is activated in the lungs of LPS-treated mice. *J Biochem (Tokyo)* **138**(4)**,** 501-507.

Evans, J. D., and Seeger, C. (2007). Differential effects of mutations in NS4B on West Nile virus replication and inhibition of interferon signaling. *J Virol* **81**(21)**,** 11809-11816.

Faitova, J., Krekac, D., Hrstka, R., and Vojtesek, B. (2006). Endoplasmic reticulum stress and apoptosis. *Cell Mol Biol Lett* **11**(4)**,** 488-505.

Falconar, A. K. (1997). The dengue virus nonstructural-1 protein (NS1) generates antibodies to common epitopes on human blood clotting, integrin/adhesin proteins and binds to human endothelial cells: potential implications in haemorrhagic fever pathogenesis. *Arch Virol* **142**(5)**,** 897-916.

Falgout, B., and Markoff, L. (1995). Evidence that flavivirus NS1-NS2A cleavage is mediated by a membrane-bound host protease in the endoplasmic reticulum. *J Virol* **69**(11)**,** 7232-7243.

Fan, T. J., Han, L. H., Cong, R. S., and Liang, J. (2005). Caspase family proteases and apoptosis. *Acta Biochim Biophys Sin (Shanghai)* **37**(11)**,** 719-727.

Fayzulin, R., Scholle, F., Petrakova, O., Frolov, I., and Mason, P. W. (2006). Evaluation of replicative capacity and genetic stability of West Nile virus replicons using highly efficient packaging cell lines. *Virology* **351**(1)**,** 196-209.

Ferrandon, D., Imler, J. L., Hetru, C., and Hoffmann, J. A. (2007). The Drosophila systemic immune response: sensing and signalling during bacterial and fungal infections. *Nat Rev Immunol* **7**(11)**,** 862-874.

Fire, A., Xu, S., Montgomery, M. K., Kostas, S. A., Driver, S. E., and Mello, C. C. (1998). Potent and specific genetic interference by double-stranded RNA in Caenorhabditis elegans. *Nature* **391**(6669)**,** 806-811.

Fischer, H., Koenig, U., Eckhart, L., and Tschachler, E. (2002). Human caspase 12 has acquired deleterious mutations. *Biochem Biophys Res Commun* **293**(2)**,** 722-726.

Fitzgerald, K. A., McWhirter, S. M., Faia, K. L., Rowe, D. C., Latz, E., Golenbock, D. T., Coyle, A. J., Liao, S. M., and Maniatis, T. (2003). IKKepsilon and TBK1 are essential components of the IRF3 signaling pathway. *Nat Immunol* **4**(5)**,** 491-496.

Fleeton, M. N., Sheahan, B. J., Gould, E. A., Atkins, G. J., and Liljestrom, P. (1999). Recombinant Semliki Forest virus particles encoding the prME or NS1 proteins of louping ill virus protect mice from lethal challenge. *J Gen Virol* **80 (Pt 5),** 1189-98.

Foy, E., Li, K., Sumpter, R., Jr., Loo, Y. M., Johnson, C. L., Wang, C., Fish, P. M., Yoneyama, M., Fujita, T., Lemon, S. M., and Gale, M., Jr. (2005). Control of antiviral defenses through hepatitis C virus disruption of retinoic acid-inducible gene-I signaling. *Proc Natl Acad Sci U S A* **102**(8)**,** 2986-91.

Fredericksen, B. L., and Gale, M., Jr. (2006). West Nile virus evades activation of interferon regulatory factor 3 through RIG-I-dependent and -independent pathways without antagonizing host defense signaling. *J Virol* **80**(6)**,** 2913-2923.

Fredericksen, B. L., Smith, M., Katze, M. G., Shi, P. Y., and Gale, M., Jr. (2004). The host response to West Nile Virus infection limits viral spread through the activation of the interferon regulatory factor 3 pathway. *J Virol* **78**(14)**,** 7737-7747.

Frolov, I., Agapov, E., Hoffman, T. A., Jr., Pragai, B. M., Lippa, M., Schlesinger, S., and Rice, C. M. (1999). Selection of RNA replicons capable of persistent noncytopathic replication in mammalian cells. *J Virol* **73**(5)**,** 3854-3865.

Fyodorova, M. V., Savage, H. M., Lopatina, J. V., Bulgakova, T. A., Ivanitsky, A. V., Platonova, O. V., and Platonov, A. E. (2006). Evaluation of potential West Nile virus vectors in Volgograd region, Russia, 2003 (Diptera: Culicidae): species composition, bloodmeal host utilization, and virus infection rates of mosquitoes. *J Med Entomol* **43**(3)**,** 552-563.

Garcia-Montalvo, B. M., Medina, F., and del Angel, R. M. (2004). La protein binds to NS5 and NS3 and to the 5' and 3' ends of Dengue 4 virus RNA. *Virus Res* **102**(2)**,** 141-150.

Garmendia, A. E., Van Kruiningen, H. J., French, R. A., Anderson, J. F., Andreadis, T. G., Kumar, A., and West, A. B. (2000). Recovery and identification of West Nile virus from a hawk in winter. *J Clin Microbiol* **38**(8)**,** 3110-3111.

Gehrke, R., Ecker, M., Aberle, S. W., Allison, S. L., Heinz, F. X., and Mandl, C. W. (2003). Incorporation of tick-borne encephalitis virus replicons into virus-like particles by a packaging cell line. *J Virol* **77**(16)**,** 8924-8933.

Gilfoy, F. D., and Mason, P. W. (2007). West Nile Virus-Induced Interferon Production Is Mediated by the Double-Stranded RNA-Dependent Protein Kinase PKR. *J Virol* **81**(20)**,** 11148-11158.

Girard, Y. A., Klingler, K. A., and Higgs, S. (2004). West Nile virus dissemination and tissue tropisms in orally infected Culex pipiens quinquefasciatus. *Vector Borne Zoonotic Dis* **4**(2)**,** 109-122.

Girard, Y. A., Schneider, B. S., McGee, C. E., Wen, J., Han, V. C., Popov, V., Mason, P. W., and Higgs, S. (2007). Salivary gland morphology and virus transmission during long-term cytopathologic West Nile virus infection in Culex mosquitoes. *Am J Trop Med Hyg* **76**(1)**,** 118-128.

Goldblum, N., Sterk, V. V., and Jasinskaklingberg, W. (1957). The natural history of West Nile fever. II. Virological findings and the development of homologous and heterologous antibodies in West Nile infection in man. *Am J Hyg* **66**(3)**,** 363-380.

Gollins, S. W., and Porterfield, J. S. (1985). Flavivirus infection enhancement in macrophages: an electron microscopic study of viral cellular entry. *J Gen Virol* **66 (Pt 9),** 1969-1982.

Gollins, S. W., and Porterfield, J. S. (1986). The uncoating and infectivity of the flavivirus West Nile on interaction with cells: effects of pH and ammonium chloride. *J Gen Virol* **67 (Pt 9),** 1941-1950.

Gotoh, T., Terada, K., Oyadomari, S., and Mori, M. (2004). hsp70-DnaJ chaperone pair prevents nitric oxide- and CHOP-induced apoptosis by inhibiting translocation of Bax to mitochondria. *Cell Death Differ* **11**(4)**,** 390-402.

Granwehr, B. P., Li, L., Davis, C. T., Beasley, D. W., and Barrett, A. D. (2004a). Characterization of a West Nile virus isolate from a human on the Gulf Coast of Texas. *J Clin Microbiol* **42**(11)**,** 5375-5377.

Granwehr, B. P., Lillibridge, K. M., Higgs, S., Mason, P. W., Aronson, J. F., Campbell, G. A., and Barrett, A. D. (2004b). West Nile virus: where are we now? *Lancet Infect Dis* **4**(9)**,** 547-556.

Gritsun, T. S., Frolova, T. V., Zhankov, A. I., Armesto, M., Turner, S. L., Frolova, M. P., Pogodina, V. V., Lashkevich, V. A., and Gould, E. A. (2003). Characterization of a siberian virus isolated from a patient with progressive chronic tick-borne encephalitis. *J Virol* **77**(1)**,** 25-36.

Gu, B., Ouzunov, S., Wang, L., Mason, P., Bourne, N., Cuconati, A., and Block, T. M. (2006). Discovery of small molecule inhibitors of West Nile virus using a high-throughput sub-genomic replicon screen. *Antiviral Res* **70**(2)**,** 39-50.

Gubler, D. J. (2007). The continuing spread of West Nile virus in the western hemisphere. *Clin Infect Dis* **45**(8)**,** 1039-1046.

Guirakhoo, F., Heinz, F. X., Mandl, C. W., Holzmann, H., and Kunz, C. (1991). Fusion activity of flaviviruses: comparison of mature and immature (prM-containing) tick-borne encephalitis virions. *J Gen Virol* **72 (Pt 6),** 1323-1329.

Guo, J. T., Hayashi, J., and Seeger, C. (2005). West Nile virus inhibits the signal transduction pathway of alpha interferon. *J Virol* **79**(3)**,** 1343-1350.

Hahn, C. S., Hahn, Y. S., Rice, C. M., Lee, E., Dalgarno, L., Strauss, E. G., and Strauss, J. H. (1987). Conserved elements in the 3' untranslated region of flavivirus RNAs and potential cyclization sequences. *J Mol Biol* **198**(1)**,** 33-41.

Hail, N., Jr., Carter, B. Z., Konopleva, M., and Andreeff, M. (2006). Apoptosis effector mechanisms: a requiem performed in different keys. *Apoptosis* **11**(6)**,** 889-904.

Hall, R. A., Broom, A. K., Smith, D. W., and Mackenzie, J. S. (2002). The ecology and epidemiology of Kunjin virus. *Curr Top Microbiol Immunol* **267,** 253-269.

Hall, R. A., Khromykh, A. A., Mackenzie, J. M., Scherret, J. H., Khromykh, T. I., and Mackenzie, J. S. (1999). Loss of dimerisation of the nonstructural protein NS1 of Kunjin virus delays viral replication and reduces virulence in mice, but still allows secretion of NS1. *Virology* **264**(1)**,** 66-75.

Hammam, H. M., and Price, W. H. (1966). Further observations on geographic variation in the antigenic character of West Nile and Japanese B viruses. *Am J Epidemiol* **83**(1)**,** 113-122.

Hanna, S. L., Pierson, T. C., Sanchez, M. D., Ahmed, A. A., Murtadha, M. M., and Doms, R. W. (2005). N-linked glycosylation of west nile virus envelope proteins influences particle assembly and infectivity. *J Virol* **79**(21)**,** 13262-13274.

Harvey, T. J., Liu, W. J., Wang, X. J., Linedale, R., Jacobs, M., Davidson, A., Le, T. T., Anraku, I., Suhrbier, A., Shi, P. Y., and Khromykh, A. A. (2004). Tetracycline-inducible packaging cell line for production of flavivirus replicon particles. *J Virol* **78**(1)**,** 531-538.

Hayasaka, D., Yoshii, K., Ueki, T., Iwasaki, T., and Takashima, I. (2004). Sub-genomic replicons of Tick-borne encephalitis virus. *Arch Virol* **149**(6)**,** 1245-1256.

Hayes, C. G. (2001). West Nile virus: Uganda, 1937, to New York City, 1999. *Ann N Y Acad Sci* **951,** 25-37.

Heinz, F. X., Stiasny, K., Puschner-Auer, G., Holzmann, H., Allison, S. L., Mandl, C. W., and Kunz, C. (1994). Structural changes and functional control of the tick-borne encephalitis virus glycoprotein E by the heterodimeric association with protein prM. *Virology* **198**(1)**,** 109-117.

Higgs, S., Rayner, J. O., Olson, K. E., Davis, B. S., Beaty, B. J., and Blair, C. D. (1998). Engineered resistance in Aedes aegypti to a West African and a South American strain of yellow fever virus. *Am J Trop Med Hyg* **58**(5)**,** 663-670.

Higgs, S., Schneider, B. S., Vanlandingham, D. L., Klingler, K. A., and Gould, E. A. (2005). Nonviremic transmission of West Nile virus. *Proc Natl Acad Sci U S A* **102**(25)**,** 8871-8874.

Higuchi, R., Krummel, B., and Saiki, R. K. (1988). A general method of in vitro preparation and specific mutagenesis of DNA fragments: study of protein and DNA interactions. *Nucleic Acids Res* **16**(15)**,** 7351-7367.

Hiscott, J., Nguyen, T. L., Arguello, M., Nakhaei, P., and Paz, S. (2006). Manipulation of the nuclear factor-kappaB pathway and the innate immune response by viruses. *Oncogene* **25**(51)**,** 6844-6867.

Hitomi, J., Katayama, T., Eguchi, Y., Kudo, T., Taniguchi, M., Koyama, Y., Manabe, T., Yamagishi, S., Bando, Y., Imaizumi, K., Tsujimoto, Y., and Tohyama, M. (2004). Involvement of caspase-4 in endoplasmic reticulum stress-induced apoptosis and Abeta-induced cell death. *J Cell Biol* **165**(3)**,** 347-356.

Ho, L. J., Hung, L. F., Weng, C. Y., Wu, W. L., Chou, P., Lin, Y. L., Chang, D. M., Tai, T. Y., and Lai, J. H. (2005). Dengue virus type 2 antagonizes IFN-alpha but not IFN-gamma antiviral effect via down-regulating Tyk2-STAT signaling in the human dendritic cell. *J Immunol* **174**(12)**,** 8163-8172.

Hornung, V., Ellegast, J., Kim, S., Brzozka, K., Jung, A., Kato, H., Poeck, H., Akira, S., Conzelmann, K. K., Schlee, M., Endres, S., and Hartmann, G. (2006). 5'-Triphosphate RNA is the ligand for RIG-I. *Science* **314**(5801)**,** 994-997.

Horvath, C. M., Stark, G. R., Kerr, I. M., and Darnell, J. E., Jr. (1996). Interactions between STAT and non-STAT proteins in the interferon-stimulated gene factor 3 transcription complex. *Mol Cell Biol* **16**(12)**,** 6957-6964.

Jan, J. T., Chen, B. H., Ma, S. H., Liu, C. I., Tsai, H. P., Wu, H. C., Jiang, S. Y., Yang, K. D., and Shaio, M. F. (2000). Potential dengue virus-triggered apoptotic pathway in human neuroblastoma cells: arachidonic acid, superoxide anion, and NF-kappaB are sequentially involved. *J Virol* **74**(18)**,** 8680-8691.

Jia, Y., Moudy, R. M., Dupuis, A. P., 2nd, Ngo, K. A., Maffei, J. G., Jerzak, G. V., Franke, M. A., Kauffman, E. B., and Kramer, L. D. (2007). Characterization of a small plaque variant of West Nile virus isolated in New York in 2000. *Virology* **367**(2)**,** 339-347.

Jiang, C. C., Chen, L. H., Gillespie, S., Kiejda, K. A., Mhaidat, N., Wang, Y. F., Thorne, R., Zhang, X. D., and Hersey, P. (2007). Tunicamycin sensitizes human melanoma cells to tumor necrosis factor-related apoptosis-inducing ligand-induced apoptosis by up-regulation of TRAIL-R2 via the unfolded protein response. *Cancer Res* **67**(12)**,** 5880-5888.

Johnson, C. L., Owen, D. M., and Gale, M., Jr. (2007). Functional and therapeutic analysis of hepatitis C virus NS3.4A protease control of antiviral immune defense. *J Biol Chem* **282**(14)**,** 10792-10803.

Johnson, H. N. (1967). Ecological implications of antigenically related mammalian viruses for which arthropod vectors are unknown and avian associated soft tick viruses. *Jpn J Med Sci Biol* **20 Suppl,** 160-166.

Johnson, H. N. (1970). Long-term persistence of Modoc virus in hamster-kidney cells. In vivo and in vitro demonstration. *Am J Trop Med Hyg* **19**(3)**,** 537-539.

Jones, C. T., Patkar, C. G., and Kuhn, R. J. (2005). Construction and applications of yellow fever virus replicons. *Virology* **331**(2)**,** 247-259.

Joubert, L., Oudar, J., Mouchet, J., and Hannoun, C. (1967). [Transmission of myxomatosis by mosquitoes in Camargue. Preeminent role of Aedes caspius and Anopheles of the maculipennis group]. *Bull Acad Vet Fr* **40**(7)**,** 315-322.

Kapoor, H., Signs, K., Somsel, P., Downes, F. P., Clark, P. A., and Massey, J. P. (2004). Persistence of West Nile Virus (WNV) IgM antibodies in cerebrospinal fluid from patients with CNS disease. *J Clin Virol* **31**(4)**,** 289-291.

Kapoor, M., Zhang, L., Mohan, P. M., and Padmanabhan, R. (1995). Synthesis and characterization of an infectious dengue virus type-2 RNA genome (New Guinea C strain). *Gene* **162**(2)**,** 175-180.

Karabatsos, N. (1985). "International Catalogue of Arboviruses Including Certain Other Viruses of Vertebrates." Third ed. American Society of Tropical Medicine and Hygiene, San Antonio.

Kato, H., Takeuchi, O., Sato, S., Yoneyama, M., Yamamoto, M., Matsui, K., Uematsu, S., Jung, A., Kawai, T., Ishii, K. J., Yamaguchi, O., Otsu, K., Tsujimura, T., Koh, C. S., Reis e Sousa, C., Matsuura, Y., Fujita, T., and Akira, S. (2006). Differential roles of MDA5 and RIG-I helicases in the recognition of RNA viruses. *Nature* **441**(7089)**,** 101-105.

Kaufman, R. J. (1999). Stress signaling from the lumen of the endoplasmic reticulum: coordination of gene transcriptional and translational controls. *Genes Dev* **13**(10)**,** 1211-1233.

Kaukinen, P., Sillanpaa, M., Kotenko, S., Lin, R., Hiscott, J., Melen, K., and Julkunen, I. (2006). Hepatitis C virus NS2 and NS3/4A proteins are potent inhibitors of host cell cytokine/chemokine gene expression. *Virol J* **3,** 66.

Kawai, T., Takahashi, K., Sato, S., Coban, C., Kumar, H., Kato, H., Ishii, K. J., Takeuchi, O., and Akira, S. (2005). IPS-1, an adaptor triggering RIG-I- and Mda5-mediated type I interferon induction. *Nat Immunol* **6**(10)**,** 981-988.

Keene, K. M., Foy, B. D., Sanchez-Vargas, I., Beaty, B. J., Blair, C. D., and Olson, K. E. (2004). RNA interference acts as a natural antiviral response to O'nyong-nyong virus (Alphavirus; Togaviridae) infection of Anopheles gambiae. *Proc Natl Acad Sci U S A* **101**(49)**,** 17240-17245.

Keller, B. C., Fredericksen, B. L., Samuel, M. A., Mock, R. E., Mason, P. W., Diamond, M. S., and Gale, M., Jr. (2006). Resistance to alpha/beta interferon is a determinant of West Nile virus replication fitness and virulence. *J Virol* **80**(19)**,** 9424-9434.

Khromykh, A. A., Varnavski, A. N., and Westaway, E. G. (1998). Encapsidation of the flavivirus kunjin replicon RNA by using a complementation system providing Kunjin virus structural proteins in trans. *J Virol* **72**(7)**,** 5967-5977.

Khromykh, A. A., and Westaway, E. G. (1994). Completion of Kunjin virus RNA sequence and recovery of an infectious RNA transcribed from stably cloned full-length cDNA. *J Virol* **68**(7)**,** 4580-4588.

Khromykh, A. A., and Westaway, E. G. (1997). Subgenomic replicons of the flavivirus Kunjin: construction and applications. *J Virol* **71**(2)**,** 1497-1505.

Kiberd, B. A., and Forward, K. (2004). Screening for West Nile virus in organ transplantation: a medical decision analysis. *Am J Transplant* **4**(8)**,** 1296-1301.

Kinney, R. M., Butrapet, S., Chang, G. J., Tsuchiya, K. R., Roehrig, J. T., Bhamarapravati, N., and Gubler, D. J. (1997). Construction of infectious cDNA clones for dengue 2 virus: strain 16681 and its attenuated vaccine derivative, strain PDK-53. *Virology* **230**(2)**,** 300-308.

Klenk, K., and Komar, N. (2003). Poor replication of West Nile virus (New York 1999 strain) in three reptilian and one amphibian species. *Am J Trop Med Hyg* **69**(3)**,** 260-262.

Kofler, R. M., Heinz, F. X., and Mandl, C. W. (2002). Capsid protein C of tick-borne encephalitis virus tolerates large internal deletions and is a favorable target for attenuation of virulence. *J Virol* **76**(7)**,** 3534-3543.

Kojima, E., Takeuchi, A., Haneda, M., Yagi, A., Hasegawa, T., Yamaki, K., Takeda, K., Akira, S., Shimokata, K., and Isobe, K. (2003). The function of GADD34 is a recovery from a shutoff of protein synthesis induced by ER stress: elucidation by GADD34-deficient mice. *Faseb J* **17**(11)**,** 1573-1575.

Komar, N., and Clark, G. G. (2006). West Nile virus activity in Latin America and the Caribbean. *Rev Panam Salud Publica* **19**(2)**,** 112-117.

Komar, N., Langevin, S., Hinten, S., Nemeth, N., Edwards, E., Hettler, D., Davis, B., Bowen, R., and Bunning, M. (2003). Experimental infection of North American birds with the New York 1999 strain of West Nile virus. *Emerg Infect Dis* **9**(3)**,** 311-232.

Komar, N., Panella, N. A., Burns, J. E., Dusza, S. W., Mascarenhas, T. M., and Talbot, T. O. (2001). Serologic evidence for West Nile virus infection in birds in the New York City vicinity during an outbreak in 1999. *Emerg Infect Dis* **7**(4)**,** 621-625.

Konishi, E., Fujii, A., and Mason, P. W. (2001). Generation and characterization of a mammalian cell line continuously expressing Japanese encephalitis virus subviral particles. *J Virol* **75**(5)**,** 2204-2212.

Konishi, E., and Mason, P. W. (1993). Proper maturation of the Japanese encephalitis virus envelope glycoprotein requires cosynthesis with the premembrane protein. *J Virol* **67**(3)**,** 1672-1675.

Konishi, E., Pincus, S., Fonseca, B. A., Shope, R. E., Paoletti, E., and Mason, P. W. (1991). Comparison of protective immunity elicited by recombinant vaccinia viruses that synthesize E or NS1 of Japanese encephalitis virus. *Virology* **185**(1)**,** 401-410.

Kramer, L. D., and Bernard, K. A. (2001). West Nile virus infection in birds and mammals. *Ann N Y Acad Sci* **951,** 84-93.

Krieger, N., Lohmann, V., and Bartenschlager, R. (2001). Enhancement of hepatitis C virus RNA replication by cell culture-adaptive mutations. *J Virol* **75**(10)**,** 4614-4624.

Kroemer, G., and Martin, S. J. (2005). Caspase-independent cell death. *Nat Med* **11**(7)**,** 725-730.

Kuhn, R. J., Zhang, W., Rossmann, M. G., Pletnev, S. V., Corver, J., Lenches, E., Jones, C. T., Mukhopadhyay, S., Chipman, P. R., Strauss, E. G., Baker, T. S., and Strauss, J. H. (2002). Structure of dengue virus: implications for flavivirus organization, maturation, and fusion. *Cell* **108**(5)**,** 717-725.

Kummerer, B. M., and Rice, C. M. (2002). Mutations in the yellow fever virus nonstructural protein NS2A selectively block production of infectious particles. *J Virol* **76**(10)**,** 4773-4784.

Kuno, G., Chang, G. J., Tsuchiya, K. R., Karabatsos, N., and Cropp, C. B. (1998). Phylogeny of the genus Flavivirus. *J Virol* **72**(1)**,** 73-83.

Lai, C. J., Zhao, B. T., Hori, H., and Bray, M. (1991). Infectious RNA transcribed from stably cloned full-length cDNA of dengue type 4 virus. *Proc Natl Acad Sci U S A* **88**(12)**,** 5139-5143.

Lai, M. M. C., and Holmes, K. (2001). Coronaviridae: The Viruses and Their Replication. 4 ed. *In* "Fields Virology" (D. M. Knipe, P. M. Howley, D. E. Griffin, M. A. Hartin, R. A. Lamb, B. Roizman, and S. E. Straus, Eds.), Vol. 1, pp. 1163-1185. 2 vols. Lippincott Willams & Wilkins, Philadelphia.

Lan, K. H., Lan, K. L., Lee, W. P., Sheu, M. L., Chen, M. Y., Lee, Y. L., Yen, S. H., Chang, F. Y., and Lee, S. D. (2007). HCV NS5A inhibits interferon-alpha signaling through suppression of STAT1 phosphorylation in hepatocyte-derived cell lines. *J Hepatol* **46**(5)**,** 759-767.

Lanciotti, R. S., Ebel, G. D., Deubel, V., Kerst, A. J., Murri, S., Meyer, R., Bowen, M., McKinney, N., Morrill, W. E., Crabtree, M. B., Kramer, L. D., and Roehrig, J. T. (2002). Complete genome sequences and phylogenetic analysis of West Nile virus strains isolated from the United States, Europe, and the Middle East. *Virology* **298**(1)**,** 96-105.

Lanciotti, R. S., Roehrig, J. T., Deubel, V., Smith, J., Parker, M., Steele, K., Crise, B., Volpe, K. E., Crabtree, M. B., Scherret, J. H., Hall, R. A., MacKenzie, J. S., Cropp, C. B., Panigrahy, B., Ostlund, E., Schmitt, B., Malkinson, M., Banet, C., Weissman, J., Komar, N., Savage, H. M., Stone, W., McNamara, T., and Gubler, D. J. (1999). Origin of the West Nile virus responsible for an outbreak of encephalitis in the northeastern United States. *Science* **286**(5448)**,** 2333-2337.

Lee, E., and Lobigs, M. (2000). Substitutions at the putative receptor-binding site of an encephalitic flavivirus alter virulence and host cell tropism and reveal a role for glycosaminoglycans in entry. *J Virol* **74**(19)**,** 8867-8875.

Lee, E., Stocks, C. E., Amberg, S. M., Rice, C. M., and Lobigs, M. (2000). Mutagenesis of the signal sequence of yellow fever virus prM protein: enhancement of signalase cleavage In vitro is lethal for virus production. *J Virol* **74**(1)**,** 24-32.

Lekstrom-Himes, J., and Xanthopoulos, K. G. (1998). Biological role of the CCAAT/enhancer-binding protein family of transcription factors. *J Biol Chem* **273**(44)**,** 28545-28548.

Levine, B., Goldman, J. E., Jiang, H. H., Griffin, D. E., and Hardwick, J. M. (1996). Bc1-2 protects mice against fatal alphavirus encephalitis. *Proc Natl Acad Sci U S A* **93**(10)**,** 4810-4815.

Li, K., Foy, E., Ferreon, J. C., Nakamura, M., Ferreon, A. C., Ikeda, M., Ray, S. C., Gale, M., Jr., and Lemon, S. M. (2005). Immune evasion by hepatitis C virus NS3/4A protease-mediated cleavage of the Toll-like receptor 3 adaptor protein TRIF. *Proc Natl Acad Sci U S A* **102**(8)**,** 2992-2997.

Liao, C. L., Lin, Y. L., Shen, S. C., Shen, J. Y., Su, H. L., Huang, Y. L., Ma, S. H., Sun, Y. C., Chen, K. P., and Chen, L. K. (1998). Antiapoptotic but not antiviral

function of human bcl-2 assists establishment of Japanese encephalitis virus persistence in cultured cells. *J Virol* **72**(12)**,** 9844-9854.

Liao, C. L., Lin, Y. L., Wang, J. J., Huang, Y. L., Yeh, C. T., Ma, S. H., and Chen, L. K. (1997). Effect of enforced expression of human bcl-2 on Japanese encephalitis virus-induced apoptosis in cultured cells. *J Virol* **71**(8)**,** 5963-5971.

Liberman, E., Fong, Y. L., Selby, M. J., Choo, Q. L., Cousens, L., Houghton, M., and Yen, T. S. (1999). Activation of the grp78 and grp94 promoters by hepatitis C virus E2 envelope protein. *J Virol* **73**(5)**,** 3718-3722.

Lin, C. F., Lei, H. Y., Shiau, A. L., Liu, H. S., Yeh, T. M., Chen, S. H., Liu, C. C., Chiu, S. C., and Lin, Y. S. (2002). Endothelial cell apoptosis induced by antibodies against dengue virus nonstructural protein 1 via production of nitric oxide. *J Immunol* **169**(2)**,** 657-664.

Lin, C. W., Huang, H. D., Shiu, S. Y., Chen, W. J., Tsai, M. H., Huang, S. H., Wan, L., and Lin, Y. J. (2007). Functional determinants of NS2B for activation of Japanese encephalitis virus NS3 protease. *Virus Res* **127**(1)**,** 88-94.

Lin, R. J., Chang, B. L., Yu, H. P., Liao, C. L., and Lin, Y. L. (2006). Blocking of interferon-induced Jak-Stat signaling by Japanese encephalitis virus NS5 through a protein tyrosine phosphatase-mediated mechanism. *J Virol* **80**(12)**,** 5908-5918.

Lin, R. J., Liao, C. L., Lin, E., and Lin, Y. L. (2004). Blocking of the alpha interferon-induced Jak-Stat signaling pathway by Japanese encephalitis virus infection. *J Virol* **78**(17)**,** 9285-9294.

Lin, Y. L., Chen, L. K., Liao, C. L., Yeh, C. T., Ma, S. H., Chen, J. L., Huang, Y. L., Chen, S. S., and Chiang, H. Y. (1998). DNA immunization with Japanese encephalitis virus nonstructural protein NS1 elicits protective immunity in mice. *J Virol* **72**(1)**,** 191-200.

Lindenbach, B. D., Evans, M. J., Syder, A. J., Wolk, B., Tellinghuisen, T. L., Liu, C. C., Maruyama, T., Hynes, R. O., Burton, D. R., McKeating, J. A., and Rice, C. M. (2005). Complete replication of hepatitis C virus in cell culture. *Science* **309**(5734)**,** 623-626.

Lindenbach, B. D., and Rice, C. M. (1997). trans-Complementation of yellow fever virus NS1 reveals a role in early RNA replication. *J Virol* **71**(12)**,** 9608-17.

Lindenbach, B. D., and Rice, C. M. (1999). Genetic interaction of flavivirus nonstructural proteins NS1 and NS4A as a determinant of replicase function. *J Virol* **73**(6)**,** 4611-4621.

Lindenbach, B. D., and Rice, C. M. (2001). Flaviviridae: The Viruses and Their Replication. 4 ed. *In* "Fields Virology" (D. M. Knipe, P. M. Howley, D. E. Griffin, M. A. Hartin, R. A. Lamb, B. Roizman, and S. E. Straus, Eds.), Vol. 1, pp. 991-1041. 2 vols. Lippincott Williams & Wilkins, Philadelphia.

Liu, W. J., Chen, H. B., and Khromykh, A. A. (2003). Molecular and functional analyses of Kunjin virus infectious cDNA clones demonstrate the essential roles for NS2A in virus assembly and for a nonconservative residue in NS3 in RNA replication. *J Virol* **77**(14)**,** 7804-7813.

Liu, W. J., Chen, H. B., Wang, X. J., Huang, H., and Khromykh, A. A. (2004). Analysis of adaptive mutations in Kunjin virus replicon RNA reveals a novel role for the flavivirus nonstructural protein NS2A in inhibition of beta interferon promoter-driven transcription. *J Virol* **78**(22)**,** 12225-12235.

Liu, W. J., Wang, X. J., Clark, D. C., Lobigs, M., Hall, R. A., and Khromykh, A. A. (2006). A single amino acid substitution in the West Nile virus nonstructural protein NS2A disables its ability to inhibit alpha/beta interferon induction and attenuates virus virulence in mice. *J Virol* **80**(5)**,** 2396-2404.

Liu, W. J., Wang, X. J., Mokhonov, V. V., Shi, P. Y., Randall, R., and Khromykh, A. A. (2005). Inhibition of interferon signaling by the New York 99 strain and Kunjin subtype of West Nile virus involves blockage of STAT1 and STAT2 activation by nonstructural proteins. *J Virol* **79**(3)**,** 1934-1942.

Lo, M. K., Tilgner, M., and Shi, P. Y. (2003). Potential high-throughput assay for screening inhibitors of West Nile virus replication. *J Virol* **77**(23)**,** 12901-12906.

Lobigs, M., and Lee, E. (2004). Inefficient signalase cleavage promotes efficient nucleocapsid incorporation into budding flavivirus membranes. *J Virol* **78**(1)**,** 178-186.

Lohmann, V., Korner, F., Dobierzewska, A., and Bartenschlager, R. (2001). Mutations in hepatitis C virus RNAs conferring cell culture adaptation. *J Virol* **75**(3)**,** 1437-1449.

Lohmann, V., Korner, F., Koch, J., Herian, U., Theilmann, L., and Bartenschlager, R. (1999). Replication of subgenomic hepatitis C virus RNAs in a hepatoma cell line. *Science* **285**(5424)**,** 110-113.

Lorenz, I. C., Allison, S. L., Heinz, F. X., and Helenius, A. (2002). Folding and dimerization of tick-borne encephalitis virus envelope proteins prM and E in the endoplasmic reticulum. *J Virol* **76**(11)**,** 5480-5491.

Lowenberger, C. (2001). Innate immune response of Aedes aegypti. *Insect Biochem Mol Biol* **31**(3)**,** 219-229.

Luna, C., Wang, X., Huang, Y., Zhang, J., and Zheng, L. (2002). Characterization of four Toll related genes during development and immune responses in Anopheles gambiae. *Insect Biochem Mol Biol* **32**(9)**,** 1171-1179.

Ma, Y., Brewer, J. W., Diehl, J. A., and Hendershot, L. M. (2002). Two distinct stress signaling pathways converge upon the CHOP promoter during the mammalian unfolded protein response. *J Mol Biol* **318**(5)**,** 1351-1365.

Macdonald, J., Tonry, J., Hall, R. A., Williams, B., Palacios, G., Ashok, M. S., Jabado, O., Clark, D., Tesh, R. B., Briese, T., and Lipkin, W. I. (2005). NS1 protein secretion during the acute phase of West Nile virus infection. *J Virol* **79**(22)**,** 13924-13933.

Mackenzie, J. (2005). Wrapping things up about virus RNA replication. *Traffic* **6**(11)**,** 967-977.

Mackenzie, J. M., Jones, M. K., and Young, P. R. (1996). Immunolocalization of the dengue virus nonstructural glycoprotein NS1 suggests a role in viral RNA replication. *Virology* **220**(1)**,** 232-240.

Mackenzie, J. M., Khromykh, A. A., Jones, M. K., and Westaway, E. G. (1998). Subcellular localization and some biochemical properties of the flavivirus Kunjin nonstructural proteins NS2A and NS4A. *Virology* **245**(2)**,** 203-215.

Mackenzie, J. M., Khromykh, A. A., and Parton, R. G. (2007). Cholesterol manipulation by West Nile virus perturbs the cellular immune response. *Cell Host Microbe* **2**(4)**,** 229-239.

Mackenzie, J. M., and Westaway, E. G. (2001). Assembly and maturation of the flavivirus Kunjin virus appear to occur in the rough endoplasmic reticulum and along the secretory pathway, respectively. *J Virol* **75**(22)**,** 10787-10799.

Major, M. E., Rehermann, B., and Feinstone, S. M. (2001). Hepatitis C Viruses. 4 ed. *In* "Fields Virology" (D. M. Knipe, P. M. Howley, D. E. Griffin, M. A. Hartin, R. A. Lamb, B. Roizman, and S. E. Straus, Eds.), Vol. 1. 2 vols. Lippincott Williams & Wilkins, Philadelphia.

Malkinson, M., Banet, C., Khinich, Y., Samina, I., Pokamunski, S., and Weisman, Y. (2001). Use of live and inactivated vaccines in the control of West Nile fever in domestic geese. *Ann N Y Acad Sci* **951,** 255-261.

Malkinson, M., Banet, C., Weisman, Y., Pokamunski, S., King, R., Drouet, M. T., and Deubel, V. (2002). Introduction of West Nile virus in the Middle East by migrating white storks. *Emerg Infect Dis* **8**(4)**,** 392-397.

Mandl, C. W., Ecker, M., Holzmann, H., Kunz, C., and Heinz, F. X. (1997). Infectious cDNA clones of tick-borne encephalitis virus European subtype prototypic strain Neudoerfl and high virulence strain Hypr. *J Gen Virol* **78 (Pt 5),** 1049-1057.

Marianneau, P., Cardona, A., Edelman, L., Deubel, V., and Despres, P. (1997). Dengue virus replication in human hepatoma cells activates NF-kappaB which in turn induces apoptotic cell death. *J Virol* **71**(4)**,** 3244-3249.

Marianneau, P., Steffan, A. M., Royer, C., Drouet, M. T., Kirn, A., and Deubel, V. (1998). Differing infection patterns of dengue and yellow fever viruses in a human hepatoma cell line. *J Infect Dis* **178**(5)**,** 1270-1278.

Markoff, L. (1989). In vitro processing of dengue virus structural proteins: cleavage of the pre-membrane protein. *J Virol* **63**(8)**,** 3345-3352.

Mason, P. W., Pincus, S., Fournier, M. J., Mason, T. L., Shope, R. E., and Paoletti, E. (1991). Japanese encephalitis virus-vaccinia recombinants produce particulate forms of the structural membrane proteins and induce high levels of protection against lethal JEV infection. *Virology* **180**(1)**,** 294-305.

Mason, P. W., Shustov, A. V., and Frolov, I. (2006). Production and characterization of vaccines based on flaviviruses defective in replication. *Virology* **351**(2)**,** 432-4343.

Masud, A., Mohapatra, A., Lakhani, S. A., Ferrandino, A., Hakem, R., and Flavell, R. A. (2007). Endoplasmic reticulum stress-induced death of mouse embryonic fibroblasts requires the intrinsic pathway of apoptosis. *J Biol Chem* **282**(19)**,** 14132-14139.

Mathur, A., Arora, K. L., Rawat, S., and Chaturvedi, U. C. (1986). Persistence, latency and reactivation of Japanese encephalitis virus infection in mice. *J Gen Virol* **67 (Pt 2),** 381-385.

McCullough, K. D., Martindale, J. L., Klotz, L. O., Aw, T. Y., and Holbrook, N. J. (2001). Gadd153 sensitizes cells to endoplasmic reticulum stress by down-regulating Bcl2 and perturbing the cellular redox state. *Mol Cell Biol* **21**(4)**,** 1249-1259.

McIntosh, B. M., Jupp, P. G., Santos, I. D., and G.M.Meenehan (1976). Epidemics of West Nile and Sindbis viruses in South Africa with Culex (Culex) univittatus Theobald as vector. *South African Journal of Science* **72,** 295-300.

McLean, R. G., Ubico, S. R., Docherty, D. E., Hansen, W. R., Sileo, L., and McNamara, T. S. (2001). West Nile virus transmission and ecology in birds. *Ann N Y Acad Sci* **951,** 54-57.

Medigeshi, G. R., Lancaster, A. M., Hirsch, A. J., Briese, T., Lipkin, W. I., Defilippis, V., Fruh, K., Mason, P. W., Nikolich-Zugich, J., and Nelson, J. A. (2007). West Nile Virus Infection Activates the Unfolded Protein Response, Leading to CHOP Induction and Apoptosis. *J Virol* **81**(20)**,** 10849-60.

Men, R., Bray, M., Clark, D., Chanock, R. M., and Lai, C. J. (1996). Dengue type 4 virus mutants containing deletions in the 3' noncoding region of the RNA genome: analysis of growth restriction in cell culture and altered viremia pattern and immunogenicity in rhesus monkeys. *J Virol* **70**(6)**,** 3930-7.

Meylan, E., Curran, J., Hofmann, K., Moradpour, D., Binder, M., Bartenschlager, R., and Tschopp, J. (2005). Cardif is an adaptor protein in the RIG-I antiviral pathway and is targeted by hepatitis C virus. *Nature* **437**(7062)**,** 1167-72.

Miller, B. R., Nasci, R. S., Godsey, M. S., Savage, H. M., Lutwama, J. J., Lanciotti, R. S., and Peters, C. J. (2000). First field evidence for natural vertical transmission of West Nile virus in Culex univittatus complex mosquitoes from Rift Valley province, Kenya. *Am J Trop Med Hyg* **62**(2)**,** 240-6.

Miller, D. L., Mauel, M. J., Baldwin, C., Burtle, G., Ingram, D., Hines, M. E., 2nd, and Frazier, K. S. (2003). West Nile virus in farmed alligators. *Emerg Infect Dis* **9**(7)**,** 794-799.

Molaei, G., Andreadis, T. G., Armstrong, P. M., Bueno, R., Jr., Dennett, J. A., Real, S. V., Sargent, C., Bala, A., Randle, Y., Guzman, H., Travassos da Rosa, A., Wuithiranyagool, T., and Tesh, R. B. (2007). Host feeding pattern of Culex quinquefasciatus (Diptera: Culicidae) and its role in transmission of West Nile virus in Harris County, Texas. *Am J Trop Med Hyg* **77**(1)**,** 73-81.

Molenkamp, R., Kooi, E. A., Lucassen, M. A., Greve, S., Thijssen, J. C., Spaan, W. J., and Bredenbeek, P. J. (2003). Yellow fever virus replicons as an expression system for hepatitis C virus structural proteins. *J Virol* **77**(2)**,** 1644-1648.

Monath, T. P. (1985). Glad tidings from yellow fever research. *Science* **229**(4715)**,** 734-5.

Morrey, J. D., Day, C. W., Julander, J. G., Olsen, A. L., Sidwell, R. W., Cheney, C. D., and Blatt, L. M. (2004). Modeling hamsters for evaluating West Nile virus therapies. *Antiviral Res* **63**(1)**,** 41-50.

Morris, J. A., Dorner, A. J., Edwards, C. A., Hendershot, L. M., and Kaufman, R. J. (1997). Immunoglobulin binding protein (BiP) function is required to protect cells from endoplasmic reticulum stress but is not required for the secretion of selective proteins. *J Biol Chem* **272**(7)**,** 4327-4334.

Moudy, R. M., Meola, M. A., Morin, L. L., Ebel, G. D., and Kramer, L. D. (2007). A newly emergent genotype of West Nile virus is transmitted earlier and more efficiently by Culex mosquitoes. *Am J Trop Med Hyg* **77**(2)**,** 365-370.

Mukhopadhyay, S., Kim, B. S., Chipman, P. R., Rossmann, M. G., and Kuhn, R. J. (2003). Structure of West Nile virus. *Science* **302**(5643)**,** 248.

Mukhopadhyay, S., Kuhn, R. J., and Rossmann, M. G. (2005). A structural perspective of the flavivirus life cycle. *Nat Rev Microbiol* **3**(1)**,** 13-22.

Munoz-Jordan, J. L., Laurent-Rolle, M., Ashour, J., Martinez-Sobrido, L., Ashok, M., Lipkin, W. I., and Garcia-Sastre, A. (2005). Inhibition of alpha/beta interferon signaling by the NS4B protein of flaviviruses. *J Virol* **79**(13)**,** 8004-8013.

Munoz-Jordan, J. L., Sanchez-Burgos, G. G., Laurent-Rolle, M., and Garcia-Sastre, A. (2003). Inhibition of interferon signaling by dengue virus. *Proc Natl Acad Sci U S A* **100**(24)**,** 14333-8.

Murgue, B., Murri, S., Triki, H., Deubel, V., and Zeller, H. G. (2001). West Nile in the Mediterranean basin: 1950-2000. *Ann N Y Acad Sci* **951,** 117-26.

Murphy, F. A., Gibbs, E. P. J., Horzinek, M. C., and Studdert, M. J. (1999). Veterinary Virology. 3 ed. *In* "Flaviviridae" (F. A. Murphy, E. P. J. Gibbs, M. C. Horzinek, and M. J. Studdert, Eds.), pp. 555-569. Academic Press, San Diego.

Murray, J. M., Aaskov, J. G., and Wright, P. J. (1993). Processing of the dengue virus type 2 proteins prM and C-prM. *J Gen Virol* **74 (Pt 2),** 175-82.

Muylaert, I. R., Galler, R., and Rice, C. M. (1997). Genetic analysis of the yellow fever virus NS1 protein: identification of a temperature-sensitive mutation which blocks RNA accumulation. *J Virol* **71**(1)**,** 291-298.

Nakagawa, T., Zhu, H., Morishima, N., Li, E., Xu, J., Yankner, B. A., and Yuan, J. (2000). Caspase-12 mediates endoplasmic-reticulum-specific apoptosis and cytotoxicity by amyloid-beta. *Nature* **403**(6765)**,** 98-103.

Nestorowicz, A., Chambers, T. J., and Rice, C. M. (1994). Mutagenesis of the yellow fever virus NS2A/2B cleavage site: effects on proteolytic processing, viral replication, and evidence for alternative processing of the NS2A protein. *Virology* **199**(1)**,** 114-123.

Niyomrattanakit, P., Winoyanuwattikun, P., Chanprapaph, S., Angsuthanasombat, C., Panyim, S., and Katzenmeier, G. (2004). Identification of residues in the dengue virus type 2 NS2B cofactor that are critical for NS3 protease activation. *J Virol* **78**(24)**,** 13708-13716.

Novoa, I., Zeng, H., Harding, H. P., and Ron, D. (2001). Feedback inhibition of the unfolded protein response by GADD34-mediated dephosphorylation of eIF2alpha. *J Cell Biol* **153**(5)**,** 1011-1022.

O'Donnell, V. K., Pacheco, J. M., Henry, T. M., and Mason, P. W. (2001). Subcellular distribution of the foot-and-mouth disease virus 3A protein in cells infected with

viruses encoding wild-type and bovine-attenuated forms of 3A. *Virology* **287**(1)**,** 151-162.

Odelola, H. A., and Oduye, O. O. (1977). West Nile virus infection of adult mice by oral route. *Arch Virol* **54**(3)**,** 251-253.

Ohoka, N., Yoshii, S., Hattori, T., Onozaki, K., and Hayashi, H. (2005). TRB3, a novel ER stress-inducible gene, is induced via ATF4-CHOP pathway and is involved in cell death. *Embo J* **24**(6)**,** 1243-1255.

Olson, K. E., Adelman, Z. N., Travanty, E. A., Sanchez-Vargas, I., Beaty, B. J., and Blair, C. D. (2002). Developing arbovirus resistance in mosquitoes. *Insect Biochem Mol Biol* **32**(10)**,** 1333-1343.

Olson, K. E., Higgs, S., Gaines, P. J., Powers, A. M., Davis, B. S., Kamrud, K. I., Carlson, J. O., Blair, C. D., and Beaty, B. J. (1996). Genetically engineered resistance to dengue-2 virus transmission in mosquitoes. *Science* **272**(5263)**,** 884-886.

Oshiumi, H., Matsumoto, M., Funami, K., Akazawa, T., and Seya, T. (2003). TICAM-1, an adaptor molecule that participates in Toll-like receptor 3-mediated interferon-beta induction. *Nat Immunol* **4**(2)**,** 161-7.

Oyadomari, S., and Mori, M. (2004). Roles of CHOP/GADD153 in endoplasmic reticulum stress. *Cell Death Differ* **11**(4)**,** 381-389.

Pang, X., Zhang, M., and Dayton, A. I. (2001). Development of Dengue virus type 2 replicons capable of prolonged expression in host cells. *BMC Microbiol* **1,** 18.

Park, G. S., Morris, K. L., Hallett, R. G., Bloom, M. E., and Best, S. M. (2007). Identification of residues critical for the interferon antagonist function of Langat virus NS5 reveals a role for the RNA-dependent RNA polymerase domain. *J Virol* **81**(13)**,** 6936-6946.

Parquet, M. C., Kumatori, A., Hasebe, F., Mathenge, E. G., and Morita, K. (2002). St. Louis encephalitis virus induced pathology in cultured cells. *Arch Virol* **147**(6)**,** 1105-1119.

Parquet, M. C., Kumatori, A., Hasebe, F., Morita, K., and Igarashi, A. (2001). West Nile virus-induced bax-dependent apoptosis. *FEBS Lett* **500**(1-2)**,** 17-24.

Patkar, C. G., Jones, C. T., Chang, Y. H., Warrier, R., and Kuhn, R. J. (2007). Functional requirements of the yellow fever virus capsid protein. *J Virol* **81**(12)**,** 6471-6481.

Penn, R. G., Guarner, J., Sejvar, J. J., Hartman, H., McComb, R. D., Nevins, D. L., Bhatnagar, J., and Zaki, S. R. (2006). Persistent neuroinvasive west nile virus infection in an immunocompromised patient. *Clin Infect Dis* **42**(5)**,** 680-683.

Petersen, L. R., and Marfin, A. A. (2002). West Nile virus: a primer for the clinician. *Ann Intern Med* **137**(3)**,** 173-179.

Petrakova, O., Volkova, E., Gorchakov, R., Paessler, S., Kinney, R. M., and Frolov, I. (2005). Noncytopathic replication of Venezuelan equine encephalitis virus and eastern equine encephalitis virus replicons in Mammalian cells. *J Virol* **79**(12)**,** 7597-7608.

Pichlmair, A., Schulz, O., Tan, C. P., Naslund, T. I., Liljestrom, P., Weber, F., and Reis e Sousa, C. (2006). RIG-I-mediated antiviral responses to single-stranded RNA bearing 5'-phosphates. *Science* **314**(5801)**,** 997-1001.

Platonov, A. E., Shipulin, G. A., Shipulina, O. Y., Tyutyunnik, E. N., Frolochkina, T. I., Lanciotti, R. S., Yazyshina, S., Platonova, O. V., Obukhov, I. L., Zhukov, A. N., Vengerov, Y. Y., and Pokrovskii, V. I. (2001). Outbreak of West Nile virus infection, Volgograd Region, Russia, 1999. *Emerg Infect Dis* **7**(1)**,** 128-132.

Platt, K. B., Tucker, B. J., Halbur, P. G., Tiawsirisup, S., Blitvich, B. J., Fabiosa, F. G., Bartholomay, L. C., and Rowley, W. A. (2007). West Nile virus viremia in eastern chipmunks (Tamias striatus) sufficient for infecting different mosquitoes. *Emerg Infect Dis* **13**(6)**,** 831-837.

Plumet, S., Herschke, F., Bourhis, J. M., Valentin, H., Longhi, S., and Gerlier, D. (2007). Cytosolic 5'-triphosphate ended viral leader transcript of measles virus as activator of the RIG I-mediated interferon response. *PLoS ONE* **2**(3)**,** e279.

Pogodina, V. V., Frolova, M. P., Malenko, G. V., Fokina, G. I., Koreshkova, G. V., Kiseleva, L. L., Bochkova, N. G., and Ralph, N. M. (1983). Study on West Nile virus persistence in monkeys. *Arch Virol* **75**(1-2)**,** 71-86.

Pogodina, V. V., Frolova, M. P., Malenko, G. V., Fokina, G. I., Levina, L. S., Mamonenko, L. L., Koreshkova, G. V., and Ralf, N. M. (1981). Persistence of tick-borne encephalitis virus in monkeys. I. Features of experimental infection. *Acta Virol* **25**(6)**,** 337-343.

Prikhod'ko, G. G., Prikhod'ko, E. A., Cohen, J. I., and Pletnev, A. G. (2001). Infection with Langat Flavivirus or expression of the envelope protein induces apoptotic cell death. *Virology* **286**(2)**,** 328-335.

Prikhod'ko, G. G., Prikhod'ko, E. A., Pletnev, A. G., and Cohen, J. I. (2002). Langat flavivirus protease NS3 binds caspase-8 and induces apoptosis. *J Virol* **76**(11)**,** 5701-5710.

Prince, H. E., Tobler, L. H., Lape-Nixon, M., Foster, G. A., Stramer, S. L., and Busch, M. P. (2005). Development and persistence of West Nile virus-specific immunoglobulin M (IgM), IgA, and IgG in viremic blood donors. *J Clin Microbiol* **43**(9)**,** 4316-4320.

Puig-Basagoiti, F., Deas, T. S., Ren, P., Tilgner, M., Ferguson, D. M., and Shi, P. Y. (2005). High-throughput assays using a luciferase-expressing replicon, virus-like particles, and full-length virus for West Nile virus drug discovery. *Antimicrob Agents Chemother* **49**(12)**,** 4980-4988.

Puig-Basagoiti, F., Tilgner, M., Bennett, C. J., Zhou, Y., Munoz-Jordan, J. L., Garcia-Sastre, A., Bernard, K. A., and Shi, P. Y. (2007). A mouse cell-adapted NS4B mutation attenuates West Nile virus RNA synthesis. *Virology* **361**(1)**,** 229-241.

Puthalakath, H., O'Reilly, L. A., Gunn, P., Lee, L., Kelly, P. N., Huntington, N. D., Hughes, P. D., Michalak, E. M., McKimm-Breschkin, J., Motoyama, N., Gotoh, T., Akira, S., Bouillet, P., and Strasser, A. (2007). ER stress triggers apoptosis by activating BH3-only protein Bim. *Cell* **129**(7)**,** 1337-1349.

Ramanathan, M. P., Chambers, J. A., Pankhong, P., Chattergoon, M., Attatippaholkun, W., Dang, K., Shah, N., and Weiner, D. B. (2006). Host cell killing by the West Nile Virus NS2B-NS3 proteolytic complex: NS3 alone is sufficient to recruit caspase-8-based apoptotic pathway. *Virology* **345**(1)**,** 56-72.

Ratterree, M. S., da Rosa, A. P., Bohm, R. P., Jr., Cogswell, F. B., Phillippi, K. M., Caillouet, K., Schwanberger, S., Shope, R. E., and Tesh, R. B. (2003). West Nile virus infection in nonhuman primate breeding colony, concurrent with human epidemic, southern Louisiana. *Emerg Infect Dis* **9**(11)**,** 1388-1394.

Ratterree, M. S., Gutierrez, R. A., Travassos da Rosa, A. P., Dille, B. J., Beasley, D. W., Bohm, R. P., Desai, S. M., Didier, P. J., Bikenmeyer, L. G., Dawson, G. J., Leary, T. P., Schochetman, G., Phillippi-Falkenstein, K., Arroyo, J., Barrett, A. D., and Tesh, R. B. (2004). Experimental infection of rhesus macaques with West Nile virus: level and duration of viremia and kinetics of the antibody response after infection. *J Infect Dis* **189**(4)**,** 669-676.

Ravi, V., Desai, A. S., Shenoy, P. K., Satishchandra, P., Chandramuki, A., and Gourie-Devi, M. (1993). Persistence of Japanese encephalitis virus in the human nervous system. *J Med Virol* **40**(4)**,** 326-329.

Reed, L. J., and Meunch, H. (1938). A Simple Method for Estimating Fifty Per Cent Endpoints. *The American Journal of Hygiene* **27,** 493-497.

Reisen, W. K., Fang, Y., Lothrop, H. D., Martinez, V. M., Wilson, J., Oconnor, P., Carney, R., Cahoon-Young, B., Shafii, M., and Brault, A. C. (2006). Overwintering of West Nile virus in Southern California. *J Med Entomol* **43**(2)**,** 344-355.

Rey, F. A., Heinz, F. X., Mandl, C., Kunz, C., and Harrison, S. C. (1995). The envelope glycoprotein from tick-borne encephalitis virus at 2 A resolution. *Nature* **375**(6529)**,** 291-298.

Rice, C. M., Grakoui, A., Galler, R., and Chambers, T. J. (1989). Transcription of infectious yellow fever RNA from full-length cDNA templates produced by in vitro ligation. *New Biol* **1**(3)**,** 285-296.

Rice, C. M., Lenches, E. M., Eddy, S. R., Shin, S. J., Sheets, R. L., and Strauss, J. H. (1985). Nucleotide sequence of yellow fever virus: implications for flavivirus gene expression and evolution. *Science* **229**(4715)**,** 726-733.

Roehrig, J. T., Nash, D., Maldin, B., Labowitz, A., Martin, D. A., Lanciotti, R. S., and Campbell, G. L. (2003). Persistence of virus-reactive serum immunoglobulin m antibody in confirmed west nile virus encephalitis cases. *Emerg Infect Dis* **9**(3)**,** 376-379.

Ron, D., and Habener, J. F. (1992). CHOP, a novel developmentally regulated nuclear protein that dimerizes with transcription factors C/EBP and LAP and functions as a dominant-negative inhibitor of gene transcription. *Genes Dev* **6**(3)**,** 439-453.

Roosendaal, J., Westaway, E. G., Khromykh, A., and Mackenzie, J. M. (2006). Regulated cleavages at the West Nile virus NS4A-2K-NS4B junctions play a major role in rearranging cytoplasmic membranes and Golgi trafficking of the NS4A protein. *J Virol* **80**(9)**,** 4623-4632.

Root, J. J., Oesterle, P. T., Nemeth, N. M., Klenk, K., Gould, D. H., McLean, R. G., Clark, L., and Hall, J. S. (2006). Experimental infection of fox squirrels (Sciurus niger) with West Nile virus. *Am J Trop Med Hyg* **75**(4)**,** 697-701.

Roulston, A., Marcellus, R. C., and Branton, P. E. (1999). Viruses and apoptosis. *Annu Rev Microbiol* **53,** 577-628.

Ruiz-Linares, A., Cahour, A., Despres, P., Girard, M., and Bouloy, M. (1989). Processing of yellow fever virus polyprotein: role of cellular proteases in maturation of the structural proteins. *J Virol* **63**(10)**,** 4199-4209.

Saleh, M., Vaillancourt, J. P., Graham, R. K., Huyck, M., Srinivasula, S. M., Alnemri, E. S., Steinberg, M. H., Nolan, V., Baldwin, C. T., Hotchkiss, R. S., Buchman, T. G., Zehnbauer, B. A., Hayden, M. R., Farrer, L. A., Roy, S., and Nicholson, D. W. (2004). Differential modulation of endotoxin responsiveness by human caspase-12 polymorphisms. *Nature* **429**(6987)**,** 75-79.

Salvesen, G. S., and Renatus, M. (2002). Apoptosome: the seven-spoked death machine. *Dev Cell* **2**(3)**,** 256-257.

Samuel, M. A., and Diamond, M. S. (2005). Alpha/beta interferon protects against lethal West Nile virus infection by restricting cellular tropism and enhancing neuronal survival. *J Virol* **79**(21)**,** 13350-13361.

Samuel, M. A., and Diamond, M. S. (2006). Pathogenesis of West Nile Virus infection: a balance between virulence, innate and adaptive immunity, and viral evasion. *J Virol* **80**(19)**,** 9349-60.

Samuel, M. A., Morrey, J. D., and Diamond, M. S. (2007). Caspase 3-dependent cell death of neurons contributes to the pathogenesis of West Nile virus encephalitis. *J Virol* **81**(6)**,** 2614-23.

Samuel, M. A., Whitby, K., Keller, B. C., Marri, A., Barchet, W., Williams, B. R., Silverman, R. H., Gale, M., Jr., and Diamond, M. S. (2006). PKR and RNase L contribute to protection against lethal West Nile Virus infection by controlling early viral spread in the periphery and replication in neurons. *J Virol* **80**(14)**,** 7009-7019.

Sanchez-Vargas, I., Travanty, E. A., Keene, K. M., Franz, A. W., Beaty, B. J., Blair, C. D., and Olson, K. E. (2004). RNA interference, arthropod-borne viruses, and mosquitoes. *Virus Res* **102**(1)**,** 65-74.

Savage, H. M., Ceianu, C., Nicolescu, G., Karabatsos, N., Lanciotti, R., Vladimirescu, A., Laiv, L., Ungureanu, A., Romanca, C., and Tsai, T. F. (1999). Entomologic and avian investigations of an epidemic of West Nile fever in Romania in 1996, with serologic and molecular characterization of a virus isolate from mosquitoes. *Am J Trop Med Hyg* **61**(4)**,** 600-611.

Schalich, J., Allison, S. L., Stiasny, K., Mandl, C. W., Kunz, C., and Heinz, F. X. (1996). Recombinant subviral particles from tick-borne encephalitis virus are fusogenic and provide a model system for studying flavivirus envelope glycoprotein functions. *J Virol* **70**(7)**,** 4549-4557.

Schlesinger, S., and Schlesinger, M. J. (2001). Togaviridae: The Viruses and Their Replication. 4 ed. *In* "Fields Virology" (D. M. Knipe, P. M. Howley, D. E.

Griffin, M. A. Hartin, R. A. Lamb, B. Roizman, and S. E. Straus, Eds.), Vol. 1, pp. 895-916. 2 vols. Lippincott WIlliams & Wilkins, Philadelphia.

Schneider, B. S., McGee, C. E., Jordan, J. M., Stevenson, H. L., Soong, L., and Higgs, S. (2007). Prior Exposure to Uninfected Mosquitoes Enhances Mortality in Naturally-Transmitted West Nile Virus Infection. *PLoS ONE* **2**(11)**,** e1171.

Schneider, B. S., Soong, L., Girard, Y. A., Campbell, G., Mason, P., and Higgs, S. (2006). Potentiation of West Nile encephalitis by mosquito feeding. *Viral Immunol* **19**(1)**,** 74-82.

Scholle, F., Girard, Y. A., Zhao, Q., Higgs, S., and Mason, P. W. (2004). trans-Packaged West Nile virus-like particles: infectious properties in vitro and in infected mosquito vectors. *J Virol* **78**(21)**,** 11605-11614.

Scholle, F., and Mason, P. W. (2005). West Nile virus replication interferes with both poly(I:C)-induced interferon gene transcription and response to interferon treatment. *Virology* **342**(1)**,** 77-87.

Seth, R. B., Sun, L., Ea, C. K., and Chen, Z. J. (2005). Identification and characterization of MAVS, a mitochondrial antiviral signaling protein that activates NF-kappaB and IRF 3. *Cell* **122**(5)**,** 669-682.

Shafee, N., and AbuBakar, S. (2003). Dengue virus type 2 NS3 protease and NS2B-NS3 protease precursor induce apoptosis. *J Gen Virol* **84**(Pt 8)**,** 2191-2195.

Shah, B. B., and Wong, J. B. (2006). The economics of hepatitis C virus. *Clin Liver Dis* **10**(4)**,** 717-734.

Sharma, S., Mathur, A., Prakash, V., Kulshreshtha, R., Kumar, R., and Chaturvedi, U. C. (1991). Japanese encephalitis virus latency in peripheral blood lymphocytes and recurrence of infection in children. *Clin Exp Immunol* **85**(1)**,** 85-89.

Shi, P. Y. (2002a). Strategies for the identification of inhibitors of West Nile virus and other flaviviruses. *Curr Opin Investig Drugs* **3**(11)**,** 1567-1573.

Shi, P. Y., Tilgner, M., and Lo, M. K. (2002). Construction and characterization of subgenomic replicons of New York strain of West Nile virus. *Virology* **296**(2)**,** 219-233.

Shi, P. Y., Tilgner, M., Lo, M. K., Kent, K. A., and Bernard, K. A. (2002). Infectious cDNA clone of the epidemic west nile virus from New York City. *J Virol* **76**(12)**,** 5847-5856.

Shi, Y. (2002b). Mechanisms of caspase activation and inhibition during apoptosis. *Mol Cell* **9**(3)**,** 459-470.

Shin, S. W., Bian, G., and Raikhel, A. S. (2006). A toll receptor and a cytokine, Toll5A and Spz1C, are involved in toll antifungal immune signaling in the mosquito Aedes aegypti. *J Biol Chem* **281**(51)**,** 39388-39295.

Shirato, K., Miyoshi, H., Goto, A., Ako, Y., Ueki, T., Kariwa, H., and Takashima, I. (2004). Viral envelope protein glycosylation is a molecular determinant of the neuroinvasiveness of the New York strain of West Nile virus. *J Gen Virol* **85**(Pt 12)**,** 3637-3645.

Shrestha, B., and Diamond, M. S. (2004). Role of CD8+ T cells in control of West Nile virus infection. *J Virol* **78**(15)**,** 8312-8321.

Shrestha, B., Gottlieb, D., and Diamond, M. S. (2003). Infection and injury of neurons by West Nile encephalitis virus. *J Virol* **77**(24)**,** 13203-13213.

Shrestha, B., Samuel, M. A., and Diamond, M. S. (2006). CD8+ T cells require perforin to clear West Nile virus from infected neurons. *J Virol* **80**(1)**,** 119-129.

Siirin, M. T., Duan, T., Lei, H., Guzman, H., da Rosa, A. P., Watts, D. M., Xiao, S. Y., and Tesh, R. B. (2007). Chronic St. Louis encephalitis virus infection in the golden hamster (Mesocricetus auratus). *Am J Trop Med Hyg* **76**(2)**,** 299-306.

Sim, C., Hong, Y. S., Vanlandingham, D. L., Harker, B. W., Christophides, G. K., Kafatos, F. C., Higgs, S., and Collins, F. H. (2005). Modulation of Anopheles gambiae gene expression in response to o'nyong-nyong virus infection. *Insect Mol Biol* **14**(5)**,** 475-481.

Sitati, E. M., and Diamond, M. S. (2006). CD4+ T-cell responses are required for clearance of West Nile virus from the central nervous system. *J Virol* **80**(24)**,** 12060-12069.

Smith, G. W., and Wright, P. J. (1985). Synthesis of proteins and glycoproteins in dengue type 2 virus-infected vero and Aedes albopictus cells. *J Gen Virol* **66 (Pt 3),** 559-571.

Smithburn, K. C., Hughes, T. P., Burke, A. W., and Paul, J. H. (1940). A Neurotropic Virus Isolated From The Blood Of a Native of Uganda. *American Journal of Tropical Medicine* **20,** 471-492.

Sriburi, R., Bommiasamy, H., Buldak, G. L., Robbins, G. R., Frank, M., Jackowski, S., and Brewer, J. W. (2007). Coordinate regulation of phospholipid biosynthesis and secretory pathway gene expression in XBP-1(S)-induced endoplasmic reticulum biogenesis. *J Biol Chem* **282**(10), 7024-7034.

Stadler, K., Allison, S. L., Schalich, J., and Heinz, F. X. (1997). Proteolytic activation of tick-borne encephalitis virus by furin. *J Virol* **71**(11)**,** 8475-8481.

Stark, G. R., Kerr, I. M., Williams, B. R., Silverman, R. H., and Schreiber, R. D. (1998). How cells respond to interferons. *Annu Rev Biochem* **67,** 227-264.

Steinman, A., Banet-Noach, C., Simanov, L., Grinfeld, N., Aizenberg, Z., Levi, O., Lahav, D., Malkinson, M., Perk, S., and Shpigel, N. Y. (2006). Experimental infection of common garter snakes (Thamnophis sirtalis) with West Nile virus. *Vector Borne Zoonotic Dis* **6**(4)**,** 361-368.

Stramer, S. L. (2007). Current risks of transfusion-transmitted agents: a review. *Arch Pathol Lab Med* **131**(5)**,** 702-707.

Styer, L. M., Bernard, K. A., and Kramer, L. D. (2006). Enhanced early West Nile virus infection in young chickens infected by mosquito bite: effect of viral dose. *Am J Trop Med Hyg* **75**(2)**,** 337-345.

Styer, L. M., Kent, K. A., Albright, R. G., Bennett, C. J., Kramer, L. D., and Bernard, K. A. (2007). Mosquitoes inoculate high doses of West Nile virus as they probe and feed on live hosts. *PLoS Pathog* **3**(9)**,** 1262-1270.

Su, H. L., Liao, C. L., and Lin, Y. L. (2002). Japanese encephalitis virus infection initiates endoplasmic reticulum stress and an unfolded protein response. *J Virol* **76**(9)**,** 4162-4171.

Sumiyoshi, H., Hoke, C. H., and Trent, D. W. (1992). Infectious Japanese encephalitis virus RNA can be synthesized from in vitro-ligated cDNA templates. *J Virol* **66**(9)**,** 5425-5431.

Sumpter, R., Jr., Loo, Y. M., Foy, E., Li, K., Yoneyama, M., Fujita, T., Lemon, S. M., and Gale, M., Jr. (2005). Regulating intracellular antiviral defense and permissiveness to hepatitis C virus RNA replication through a cellular RNA helicase, RIG-I. *J Virol* **79**(5)**,** 2689-2699.

Sumpter, R., Jr., Wang, C., Foy, E., Loo, Y. M., and Gale, M., Jr. (2004). Viral evolution and interferon resistance of hepatitis C virus RNA replication in a cell culture model. *J Virol* **78**(21)**,** 11591-11604.

Swayne, D. E., Beck, J. R., Smith, C. S., Shieh, W. J., and Zaki, S. R. (2001). Fatal encephalitis and myocarditis in young domestic geese (Anser anser domesticus) caused by West Nile virus. *Emerg Infect Dis* **7**(4)**,** 751-753.

Takeda, K., and Akira, S. (2005). Toll-like receptors in innate immunity. *Int Immunol* **17**(1)**,** 1-14.

Tan, B. H., Fu, J., Sugrue, R. J., Yap, E. H., Chan, Y. C., and Tan, Y. H. (1996). Recombinant dengue type 1 virus NS5 protein expressed in Escherichia coli exhibits RNA-dependent RNA polymerase activity. *Virology* **216**(2)**,** 317-325.

Taylor, R. M., Work, T. H., Hurlbut, H. S., and Rizk, F. (1956). A study of the ecology of West Nile virus in Egypt. *Am J Trop Med Hyg* **5**(4)**,** 579-620.

Tesh, R. B. (1980). Experimental studies on the transovarial transmission of Kunjin and San Angelo viruses in mosquitoes. *Am J Trop Med Hyg* **29**(4)**,** 657-666.

Tesh, R. B., Siirin, M., Guzman, H., Travassos da Rosa, A. P., Wu, X., Duan, T., Lei, H., Nunes, M. R., and Xiao, S. Y. (2005). Persistent West Nile virus infection in the golden hamster: studies on its mechanism and possible implications for other flavivirus infections. *J Infect Dis* **192**(2)**,** 287-295.

Theiler, M., and Smith, H. H. (1937). The use of yellow fever virus modified by in vitro cultivation for human immunization. *Journal of Experimental Medicine* **65,** 787-800.

Tiawsirisup, S., Platt, K. B., Tucker, B. J., and Rowley, W. A. (2005). Eastern cottontail rabbits (Sylvilagus floridanus) develop West Nile virus viremias sufficient for infecting select mosquito species. *Vector Borne Zoonotic Dis* **5**(4)**,** 342-350.

Tonry, J. H., Brown, C. B., Cropp, C. B., Co, J. K., Bennett, S. N., Nerurkar, V. R., Kuberski, T., and Gubler, D. J. (2005a). West Nile virus detection in urine. *Emerg Infect Dis* **11**(8)**,** 1294-1296.

Tonry, J. H., Xiao, S. Y., Siirin, M., Chen, H., da Rosa, A. P., and Tesh, R. B. (2005b). Persistent shedding of West Nile virus in urine of experimentally infected hamsters. *Am J Trop Med Hyg* **72**(3)**,** 320-324.

Travanty, E. A., Adelman, Z. N., Franz, A. W., Keene, K. M., Beaty, B. J., Blair, C. D., James, A. A., and Olson, K. E. (2004). Using RNA interference to develop dengue virus resistance in genetically modified Aedes aegypti. *Insect Biochem Mol Biol* **34**(7)**,** 607-613.

Tsai, T. F., Popovici, F., Cernescu, C., Campbell, G. L., and Nedelcu, N. I. (1998). West Nile encephalitis epidemic in southeastern Romania. *Lancet* **352**(9130)**,** 767-771.

Ubeda, M., Wang, X. Z., Zinszner, H., Wu, I., Habener, J. F., and Ron, D. (1996). Stress-induced binding of the transcriptional factor CHOP to a novel DNA control element. *Mol Cell Biol* **16**(4)**,** 1479-1489.

Umareddy, I., Chao, A., Sampath, A., Gu, F., and Vasudevan, S. G. (2006). Dengue virus NS4B interacts with NS3 and dissociates it from single-stranded RNA. *J Gen Virol* **87**(Pt 9)**,** 2605-2614.

Umrigar, M. D., and Pavri, K. M. (1977). Comparative biological studies on Indian strains of West Nile virus isolated from different sources. *Indian J Med Res* **65**(5)**,** 596-602.

Vaidyanathan, R., and Scott, T. W. (2006). Apoptosis in mosquito midgut epithelia associated with West Nile virus infection. *Apoptosis* **11**(9)**,** 1643-1651.

van Regenmortel, M. H. V., Fauquet, C. M., Bishop, D. H. L., Carstens, E. B., Estes, M. K., Lemon, S. M., Maniloff, J., Mayo, M. A., McGeoch, D. J., Pringle, C. R., and Wickner, R. B. (2000). Family Flaviviridae. 7 ed. *In* "Virus Taxonomy" (M. H. V. van Regenmortel, C. M. Fauquet, D. H. L. Bishop, E. B. Carstens, M. K. Estes, S. M. Lemon, J. Maniloff, M. A. Mayo, D. J. McGeoch, C. R. Pringle, and R. B. Wickner, Eds.), pp. 859-878. Academic Press, San Diego.

Vanlandingham, D. L., McGee, C. E., Klinger, K. A., Vessey, N., Fredregillo, C., and Higgs, S. (2007). Relative susceptibilties of South Texas mosquitoes to infection with west nile virus. *Am J Trop Med Hyg* **77**(5)**,** 925-928.

Vanlandingham, D. L., Schneider, B. S., Klingler, K., Fair, J., Beasley, D., Huang, J., Hamilton, P., and Higgs, S. (2004). Real-time reverse transcriptase-polymerase chain reaction quantification of West Nile virus transmitted by Culex pipiens quinquefasciatus. *Am J Trop Med Hyg* **71**(1)**,** 120-123.

Wakita, T., Pietschmann, T., Kato, T., Date, T., Miyamoto, M., Zhao, Z., Murthy, K., Habermann, A., Krausslich, H. G., Mizokami, M., Bartenschlager, R., and Liang, T. J. (2005). Production of infectious hepatitis C virus in tissue culture from a cloned viral genome. *Nat Med* **11**(7)**,** 791-796.

Wang, J., Chun, H. J., Wong, W., Spencer, D. M., and Lenardo, M. J. (2001). Caspase-10 is an initiator caspase in death receptor signaling. *Proc Natl Acad Sci U S A* **98**(24)**,** 13884-13888.

Wang, T., Scully, E., Yin, Z., Kim, J. H., Wang, S., Yan, J., Mamula, M., Anderson, J. F., Craft, J., and Fikrig, E. (2003). IFN-gamma-producing gamma delta T cells help control murine West Nile virus infection. *J Immunol* **171**(5)**,** 2524-2531.

Wang, T., Town, T., Alexopoulou, L., Anderson, J. F., Fikrig, E., and Flavell, R. A. (2004). Toll-like receptor 3 mediates West Nile virus entry into the brain causing lethal encephalitis. *Nat Med* **10**(12)**,** 1366-1373.

Wang, X. Z., and Ron, D. (1996). Stress-induced phosphorylation and activation of the transcription factor CHOP (GADD153) by p38 MAP Kinase. *Science* **272**(5266)**,** 1347-1349.

Weber, A. N., Tauszig-Delamasure, S., Hoffmann, J. A., Lelievre, E., Gascan, H., Ray, K. P., Morse, M. A., Imler, J. L., and Gay, N. J. (2003). Binding of the Drosophila cytokine Spatzle to Toll is direct and establishes signaling. *Nat Immunol* **4**(8)**,** 794-800.

Wei, M. C., Zong, W. X., Cheng, E. H., Lindsten, T., Panoutsakopoulou, V., Ross, A. J., Roth, K. A., MacGregor, G. R., Thompson, C. B., and Korsmeyer, S. J. (2001). Proapoptotic BAX and BAK: a requisite gateway to mitochondrial dysfunction and death. *Science* **292**(5517)**,** 727-730.

Weiner, L. P., Cole, G. A., and Nathanson, N. (1970). Experimental encephalitis following peripheral inoculation of West Nile virus in mice of different ages. *J Hyg (Lond)* **68**(3)**,** 435-446.

Wengler, G., and Wengler, G. (1993). The NS 3 nonstructural protein of flaviviruses contains an RNA triphosphatase activity. *Virology* **197**(1)**,** 265-273.

Wengler, G., Wengler, G., and Gross, H. J. (1978). Studies on virus-specific nucleic acids synthesized in vertebrate and mosquito cells infected with flaviviruses. *Virology* **89**(2)**,** 423-437.

Werme, K., Wigerius, M., and Johansson, M. (2008). Tick-borne encephalitis virus NS5 associates with membrane protein scribble and impairs interferon-stimulated JAK-STAT signalling. *Cell Microbiol* **10**(3):696-712.

Westaway, E. G. (1977). Strategy of the flavivirus genome: evidence for multiple internal initiation of translation of proteins specified by Kunjin virus in mammalian cells. *Virology* **80**(2)**,** 320-335.

Westaway, E. G., Khromykh, A. A., Kenney, M. T., Mackenzie, J. M., and Jones, M. K. (1997a). Proteins C and NS4B of the flavivirus Kunjin translocate independently into the nucleus. *Virology* **234**(1)**,** 31-41.

Westaway, E. G., Mackenzie, J. M., Kenney, M. T., Jones, M. K., and Khromykh, A. A. (1997b). Ultrastructure of Kunjin virus-infected cells: colocalization of NS1 and NS3 with double-stranded RNA, and of NS2B with NS3, in virus-induced membrane structures. *J Virol* **71**(9)**,** 6650-6661.

Wicker, J. A., Whiteman, M. C., Beasley, D. W., Davis, C. T., Zhang, S., Schneider, B. S., Higgs, S., Kinney, R. M., and Barrett, A. D. (2006). A single amino acid substitution in the central portion of the West Nile virus NS4B protein confers a highly attenuated phenotype in mice. *Virology* **349**(2)**,** 245-253.

Winkler, G., Heinz, F. X., and Kunz, C. (1987). Studies on the glycosylation of flavivirus E proteins and the role of carbohydrate in antigenic structure. *Virology* **159**(2)**,** 237-243.

Wu, S. F., Liao, C. L., Lin, Y. L., Yeh, C. T., Chen, L. K., Huang, Y. F., Chou, H. Y., Huang, J. L., Shaio, M. F., and Sytwu, H. K. (2003). Evaluation of protective efficacy and immune mechanisms of using a non-structural protein NS1 in DNA vaccine against dengue 2 virus in mice. *Vaccine* **21**(25-26)**,** 3919-3929.

Xiao, S. Y., Guzman, H., Zhang, H., Travassos da Rosa, A. P., and Tesh, R. B. (2001). West Nile virus infection in the golden hamster (Mesocricetus auratus): a model for West Nile encephalitis. *Emerg Infect Dis* **7**(4)**,** 714-721.

Xu, L. G., Wang, Y. Y., Han, K. J., Li, L. Y., Zhai, Z., and Shu, H. B. (2005). VISA is an adapter protein required for virus-triggered IFN-beta signaling. *Mol Cell* **19**(6)**,** 727-740.

Xue, Y., Daly, A., Yngvadottir, B., Liu, M., Coop, G., Kim, Y., Sabeti, P., Chen, Y., Stalker, J., Huckle, E., Burton, J., Leonard, S., Rogers, J., and Tyler-Smith, C. (2006). Spread of an inactive form of caspase-12 in humans is due to recent positive selection. *Am J Hum Genet* **78**(4)**,** 659-670.

Yamamoto, M., Sato, S., Mori, K., Hoshino, K., Takeuchi, O., Takeda, K., and Akira, S. (2002). Cutting edge: a novel Toll/IL-1 receptor domain-containing adapter that preferentially activates the IFN-beta promoter in the Toll-like receptor signaling. *J Immunol* **169**(12)**,** 6668-6672.

Yamshchikov, V. F., Wengler, G., Perelygin, A. A., Brinton, M. A., and Compans, R. W. (2001). An infectious clone of the West Nile flavivirus. *Virology* **281**(2)**,** 294-304.

Yang, J.-S., Ramanathan, M. P., Muthumani, K., Choo, A. Y., Jin, S.-H., Yu, Q.-C., Hwang, D. S., Choo, D. K., Lee, M. D., Dang, K., WaixingTang, Kim, J. J., and Weiner, D. B. (2002). Induction of inflammation by West Nile virus capsid through the caspase-9 apoptotic pathway. *Emerging Infectious Diseases* **8**(12)**,** 1379-1384.

Yi, M., Bodola, F., and Lemon, S. M. (2002). Subgenomic hepatitis C virus replicons inducing expression of a secreted enzymatic reporter protein. *Virology* **304**(2)**,** 197-210.

Yon, C., Teramoto, T., Mueller, N., Phelan, J., Ganesh, V. K., Murthy, K. H., and Padmanabhan, R. (2005). Modulation of the nucleoside triphosphatase/RNA helicase and 5'-RNA triphosphatase activities of Dengue virus type 2 nonstructural protein 3 (NS3) by interaction with NS5, the RNA-dependent RNA polymerase. *J Biol Chem* **280**(29)**,** 27412-27419.

Yoneda, T., Imaizumi, K., Oono, K., Yui, D., Gomi, F., Katayama, T., and Tohyama, M. (2001). Activation of caspase-12, an endoplastic reticulum (ER) resident caspase, through tumor necrosis factor receptor-associated factor 2-dependent mechanism in response to the ER stress. *J Biol Chem* **276**(17)**,** 13935-13940.

Yoneyama, M., Kikuchi, M., Natsukawa, T., Shinobu, N., Imaizumi, T., Miyagishi, M., Taira, K., Akira, S., and Fujita, T. (2004). The RNA helicase RIG-I has an essential function in double-stranded RNA-induced innate antiviral responses. *Nat Immunol* **5**(7)**,** 730-737.

Yu, C. Y., Hsu, Y. W., Liao, C. L., and Lin, Y. L. (2006). Flavivirus Infection Activates XBP1 Pathway of the Unfolded Protein Response to Cope with Endoplasmic Reticulum Stress. *J Virol* **80**(23), 11868-11880.

Zhang, Y., Corver, J., Chipman, P. R., Zhang, W., Pletnev, S. V., Sedlak, D., Baker, T. S., Strauss, J. H., Kuhn, R. J., and Rossmann, M. G. (2003). Structures of immature flavivirus particles. *Embo J* **22**(11)**,** 2604-2613.

Zhong, J., Gastaminza, P., Cheng, G., Kapadia, S., Kato, T., Burton, D. R., Wieland, S. F., Uprichard, S. L., Wakita, T., and Chisari, F. V. (2005). Robust hepatitis C virus infection in vitro. *Proc Natl Acad Sci U S A* **102**(26)**,** 9294-9299.

Zhu, N., Ware, C. F., and Lai, M. M. (2001). Hepatitis C virus core protein enhances FADD-mediated apoptosis and suppresses TRADD signaling of tumor necrosis factor receptor. *Virology* **283**(2)**,** 178-187.

Zinszner, H., Kuroda, M., Wang, X., Batchvarova, N., Lightfoot, R. T., Remotti, H., Stevens, J. L., and Ron, D. (1998). CHOP is implicated in programmed cell death in response to impaired function of the endoplasmic reticulum. *Genes Dev* **12**(7)**,** 982-995.

APPENDIX

Abbreviations

Ab	antibody
abx	antibiotics
BHK	baby hamster kidney
BSA	bovine serum albumin
C	capsid (flavivirus-encoded protein)
CHOP	C/EBP homologous protein
CNS	central nervous system
CO_2	carbon dioxide
DENV	dengue virus
DNA	deoxyribonucleic acid
dpi	day post infection
dsRNA	double-stranded RNA
E	envelope (flavivirus-encoded protein)
eGFP	enhanced green fluorescent protein
ER	endoplasmic reticulum
FBS	fetal bovine serum
ffu	focus-forming units
FLIC	full-length infectious cDNA clone
f.p.	footpad
GFP	green fluorescent protein
HCV	hepatitis C virus
hpe-	hours post electroporation
hpi	hours post infection
hrs	hours
IFA	immunofluorescence assay
IFN	interferon
IHC	immunohistochemical assay

i.c.	intracranial
i.n.	intranasal
i.p.	intraperioneal
i.u.	infectious unit
JEV	Japanese encephalitis virus
kD	kilodalton
KUNV	Kunjin virus
LD_{50}	Lethal dose-50 value
M	membrane (flavivirus-encoded protein)
MEF	mouse embryo fibroblast
MEM	modified eagle's media
MEM+++	MEM with 1% FBS, abx and HEPES
MeOH	methanol
MHIAF	murine hyperimmune ascitic fluid
MODV	Modoc virus
MOI	multiplicity of infection
NaPyr	sodium pyruvate
NEAA	nonessential amino acids
NHS	normal horse serum
NIH	National Institute of Health
nm	nanometers
NMS	normal mouse serum
NS	nonstructural (flavivirus-encoded proteins)
ORF	open reading frame
PBS	phosphate buffered saline
PCR	polymerase chain reaction
pfu	plaque-forming unit
p.i.	post infection
prM	preMembrane (flavivirus-encoded precursor protein)
RNA	ribonucleic acid
rpm	revolutions per minute
rRNA	ribosomal RNA
RTPCR	reverse transcription polymerase chain reaction
s.c.	subcutaneous

ssRNA	single-stranded RNA
TBEV	tick-borne encephalitis virus
TUNEL	Terminal deoxynucleotidyl Transferase Biotin-dUTP Nick End Labeling
U	unit (refers specifically to IFN quantification)
UV	ultraviolet
VEER	Venezuelan equine encephalitis replicon
VEEV	Venezuelan equine encephalitis virus
VLP	virus-like particle
VLP^{HS}	heparan sulfate binding virus-like particle
VP	vesicle packet
WNR	West Nile virus replicon
WNV	West Nile virus
YFV	yellow fever virus
Δ	deletion
μg	microgram
μl	microliter
μm	micrometer
°C	degrees Celsius
°F	degrees Fahrenheit

Glossary

Figure 32: Replicon Genomes

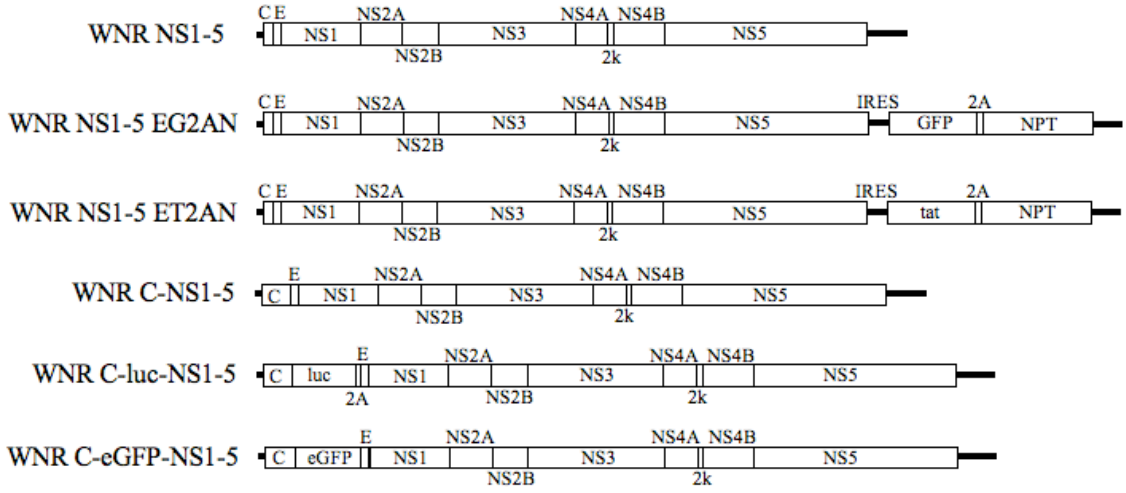

Figure 32: A schematic diagram of the wt replicon genomes used during this study.

Table 7: List of sequencing primers used

Primer Name	Orientation	Position in Gene	Position in WNV	Sequence 5' → 3'
U1n	Sense	5' UTR	1-20	AGTAGTTCGCCTGTGTGAGC
U57	Sense	NS1	2503-2521	GAGCTGAGATGTGGAAGTG
U25	Sense	NS1	2635-2652	GGTCTACGATCAGTTTCC
U20	Anti-sense	NS1	2950-2967	CCGAGTGCTGGTGAGACC
U129	Sense	NS1	3303-3321	TTACTGCCCAGGAACTACG
U26	Anti-sense	NS1	3382-3399	GGGTGTCACAACACTCAG
U5	Sense	NS2A	3944-3941	GGATGATACTGAGAGCCA
U4	Anti-sense	NS2A	4073-4090	CCCTGATCAAGCTGCCTA
U27	Sense	NS2B	4376-4393	GGATTGAGAGAACGGCGG
U28	Anti-sense	NS3	5329-5346	TGTCTGGTACCGGATGGG
U12n	Anti-sense	NS3	5888-5903	TTCACACTCTTCCGGC
U29	Sense	NS3	5991-6008	ACGTATCGGTAGAAATCC
U127	Sense	NS4A	6700-6719	GGAAAGATAGGTTTGGGAGG
U139	Sense	NS4B	7355-7373	AGAACGCTGTAGTGGATGG
U30	Anti-sense	NS4B	7609-7626	ACATGACAACCAACCCCC
U7	Sense	NS5	7883-7900	GGAGGTTTCTCGAACCGG
U6	Anti-sense	NS5	8090-8107	GGGTGTCACAACACTCAG
U31	Sense	NS5	8292-8309	GGGACTGGTCAGAAACCC
U130	Sense	NS5	8645-8664	TGGTCAATGGAGTGGTCAGG
U48	Anti-sense	NS5	9661-9678	ACTGACAGCCATGCGGCT
U37	Sense	NS5	10099-10116	GAGTGGATGACAACAGAG
U46	Anti-sense	NS5	10152-10169	TCCATCCATTCATTCTCC
U106	Anti-sense	* IRES	8303-8322	TGCTCGTCAAGAAGACAGGG
U171	Sense	* tat	8553-8571	GTGGAAAGAGTCAAATGGC
U172	Anti-sense	* tat	8582-8599	AGCCCCTTGTTGAATACG
U173	Sense	* NPT	9133-9151	CTATTCGGCTATGACTGGG
U174	Anti-sense	* NPT	9159-9177	ATCAGAGCAGCCGATTGTC
U52	Anti-sense	3' UTR	10506-10525	CGGGAACTTCCCGGCCTGAC
U32	Anti-sense	3' UTR	10514-10531	CGGTGGCGGGAACTTCCC
U8n	Anti-sense	3' UTR	11010-11029	AGATCCTGTGTTCTCGCACC

* located in the minipolyprotein of WNR genomes. The position of the primer annealing is based on the WNR genome, not the WVN genome for these oligos.

VITA

Shannan L. Rossi was born in Nyack, NY in 1980. She was the first-born child of Deborah M. Vinski and Fred Rossi. She grew up in Pearl River, NY and graduated from Pearl River High School in 1998. She matriculated into Cornell University where she majored in general biological sciences and earned her B.S. in 2001. After graduation, she worked at Wyeth Ayerst for a year where she helped to develop and characterize persistent alphavirus vectors. She started her graduate work at the University of Texas Medical Branch in 2002 and joined the lab of Dr. Peter W. Mason in May of 2003. Her dissertation research was focused on describing the virus and host cell interactions during a persistent WNV infection.

Education

B.S., May 2001, Cornell Unviersity, Ithaca, NY

Publications

S.L. Rossi, Q. Zhao, V. O'Donnell, and P.M. Mason. (2005) Adaptation of West Nile virus replicons to cells in culture and use of replicon-bearing cells to probe antiviral action. Virology, 331(2): 457-470.

S.L. Rossi, R.Z. Fayzulin, N. Dewsbury, N. Bourne, and P.M. Mason. (2007) Mutations in West Nile Virus Nonstructural Proteins That Facilitate Replicon Persistence In Vitro Attenuate Virus Replication In Vitro and In Vivo. Virology, 364(1): 184-195.

N. Bourne, F. Scholle, M. Silva, S.L. Rossi, N. Dewsbury, B. Judy, J.B. De Aguiar, M.A. Leon, D.M. Estes, R. Fayzulin, and P.M. Mason. (2007) Early Production of Type I Interferon During West Nile Virus Infection: Role for Lymphoid Tissues in IRF3-Independent Pathway in Interferon Production. Journal of Virology, 81(17): 9100-9108.

S.L. Rossi and P.M. Mason. (2008) Persistent Infections of Mammals and Mammalian Cell Cultures with West Nile Virus. Future Virology, 3(1): 25-34.

Abstracts

A. Mo, N. Vasilakis**,** A. Cupo, C. Shi, S. Rossi, S. Bhargava, T. Zamb, and G. Kovacs. Venezuelan Equine Encephalitis Virus (VEEV) Replicons that Express Parainfluenza Virus Type 3 HN and F are a Potential Subunit Vaccine: Hamster Immunogenicity and Virus Challenge Studies. Presentation at the XIIth International Congress of Virology. Paris, France; July 27 August 1, 2002

S.L. Rossi, Q. Zhao, V. O'Donnell and P. W. Mason. Adaptation of West Nile virus replicons to cells in culture; selection of stable cell lines and their use to screen drugs to treat flavivirus infections. Presented at the 23rd annual meeting of the American Society of Virology. Montréal, Canada; July 10-14, 2004.

S.L. Rossi, Q. Zhao, V. O'Donnell and P. W. Mason. Adaptation of West Nile virus replicons in cell culture: selection of stable transfected cells and their application for antiviral drug screening. Presented at the 53rd annual meeting of the American Society of Tropical Medicine and Hygiene, Miami Beach, Florida, November 7-11, 2004.

S.L. Rossi, Q. Zhao, V. O'Donnell and P. W. Mason. Use of West Nile virus replicons in cell culture for antiviral drug screening. Presented at the Mc Laughlin Symposium for Translating Vaccines for Emerging Diseases and Biodefense to the Marketplace. Galveston, Texas. November 12-14, 2004.

S.L. Rossi, F. Scholle and P.W. Mason. Multiple Mutations in NS2A Confer a Cell-Adapted Phenotype in West Nile Virus Replicons. Orally presented at the 24th annual meeting of the American Society of Virology. University Park, Pennsylvania. June 18-22, 2005.

S.L. Rossi, R. Fayzulin, F. Scholle and P.W. Mason. In Vitro Persistence of WNV Replicons Correlates with a Reduction in Genome Replication and Cytopathic Effects.

Orally presented at the 25th annual meeting of the American Society of Virology. Madison, Wisconsin. July 15-19, 2006.

S.L. Rossi, N. Bourne, R. Fayzulin and P.W.Mason. West Nile Viruses with Mutations in NS2A Are Attenuated In Vivo. Presented at the Sealy Center for Vaccine Development for The Changing Landscape of Vaccine Development- Vaccines for Global Health. Galveston, Texas. November 8-10, 2006.

S.L. Rossi, R.Z. Fazulin, N. Dewsbury, N. Bourne, and P.W. Mason. Mutations within NS2A of West Nile virus lead to attenuation in vivo. Orally presented at the 26th annual meeting of the American Society of Virology. Corvallis, Oregon. July 14-18, 2007.